



UNIVERSIDADE ESTADUAL DE CAMPINAS
INSTITUTO DE BIOLOGIA

DANIELLE GOUVÊA JUNQUEIRA

PERFIL PROTEÔMICO DE CÉLULAS PROGENITORAS NEURAIS E
NEUROESFERAS INFECTADAS COM CEPAS DE ZIKA VÍRUS E DENGUE VÍRUS

PROTEOMIC PROFILE OF NEURAL STEM CELLS AND NEUROSPHERES
INFECTED WITH DENGUE AND ZIKA VIRUS STRAINS

CAMPINAS

2021

DANIELLE GOUVÊA JUNQUEIRA

**PERFIL PROTEÔMICO DE CÉLULAS PROGENITORAS NEURAIS E
NEUROESFERAS INFECTADAS COM CEPAS DE ZIKA VÍRUS E DENGUE
VÍRUS**

**PROTEOMIC PROFILE OF NEURAL STEM CELLS AND NEUROSPHERES
INFECTED WITH DENGUE AND ZIKA VIRUS STRAINS**

Dissertação apresentada ao Instituto de Biologia da Universidade Estadual de Campinas como parte dos requisitos exigidos para a obtenção do título Mestra em Biologia Funcional e Molecular, na área de bioquímica

Dissertation presented to the Institute of Biology of the University of Campinas in partial fulfillment of the requirements for the degree of Master's degree in Functional and Molecular Biology in the area of Biochemistry

Orientador: Prof. Dr. Daniel Martins de Souza

ESTE ARQUIVO DIGITAL CORRESPONDE À
VERSÃO FINAL DA DISSERTAÇÃO DEFENDIDA PELA
ALUNA DANIELLE GOUVÊA JUUNQUEIRA, E ORIENTADA
PELO PROF. DR. DANIEL MARTINS DE SOUZA

CAMPINAS

2021

Ficha catalográfica
Universidade Estadual de Campinas
Biblioteca do Instituto de Biologia
Mara Janaina de Oliveira - CRB 8/6972

Gouvêa-Junqueira, Danielle, 1997-
G745p Perfil proteômico de células progenitoras neurais e neuroesferas infectadas com cepas de zika vírus e dengue vírus / Danielle Gouvêa Junqueira. – Campinas, SP : [s.n.], 2021.

Orientador: Daniel Martins de Souza.
Dissertação (mestrado) – Universidade Estadual de Campinas, Instituto de Biologia.

1. Transtornos do neurodesenvolvimento. 2. Microcefalia. 3. Flavivírus. I. Martins-de-Souza, Daniel, 1979-. II. Universidade Estadual de Campinas. Instituto de Biologia. III. Título.

Informações para Biblioteca Digital

Título em outro idioma: Proteomic profile of neural stem cells and neurospheres infected with dengue and zikva virus strains

Palavras-chave em inglês:

Neurodevelopmental disorders

Microcephaly

Flaviviruses

Área de concentração: Bioquímica

Titulação: Mestra em Biologia Funcional e Molecular

Banca examinadora:

Daniel Martins de Souza [Orientador]

Lucilene Delazari dos Santos

José Luiz Proença Modena

Data de defesa: 11-05-2021

Programa de Pós-Graduação: Biologia Funcional e Molecular

Identificação e informações acadêmicas do(a) aluno(a)

- ORCID do autor: <https://orcid.org/0000-0002-2534-4112>

- Currículo Lattes do autor: <http://lattes.cnpq.br/5325255456438131>

Campinas, 11 de Maio de 2021.

COMISSÃO EXAMINADORA

Prof. Dr. Daniel Martins de Souza

Dra. Lucilene Delazari dos Santos

Prof. Dr. José Luiz Proença Modena

Os membros da Comissão Examinadora acima assinaram a Ata de Defesa, que se encontram no processo de vida acadêmica do aluno.

A Ata da defesa com as respectivas assinaturas dos membros encontra-se no SIGA/Sistema de Fluxo de Dissertação/Tese e na Secretaria do Programa de Pós Graduação em Biologia Funcional e Molecular da Unidade do Instituto de Biologia da Universidade Estadual de Campinas.

DEDICATÓRIA

Dedico essa dissertação aos meus pais, que sempre me apoiaram e me incentivaram. Também dedico essa dissertação ao meu namorado, Guilherme Serradilha Gonçalves, que me deu força e suporte nos momentos mais difíceis. Espero conseguir retribuir a todos tudo aquilo que vocês já fizeram e fazem por mim.

AGRADECIMENTOS

O presente trabalho foi realizado com apoio da Coordenação de Aperfeiçoamento de Pessoal de Nível Superior - Brasil (CAPES) - Código de Financiamento 001.

Agradeço o apoio financeiro da Fundação de Amparo à Pesquisa do Estado de São Paulo – FAPESP pelo apoio financeiro (Processo 2018/25439-9).

Ao meu orientador, prof. Dr. Daniel Martins de Souza, por toda orientação e oportunidades que me proporcionou ao longo do desenvolvimento dos 02 projetos de iniciação científica e do mestrado no Laboratório de Neuroproteômica (LNP). Sou extremamente grata por ter tido a oportunidade de fazer parte do time do LNP.

Aos meus colegas do Laboratório de Neuroproteômica, pela companhia e ajuda profissional. Agradeço em especial à Dra. Fernanda Crunfli pelas orientações em relação ao desenvolvimento dos experimentos, bem como no desenvolvimento do artigo de revisão que publicamos; à Dra. Valéria de Almeida por todo apoio científico ao longo do mestrado, por toda orientação e suporte. Val e Fer, vocês são minhas inspirações, exemplos incríveis de cientistas, profissionais. À Giuliana Zuccoli por toda ajuda, apoio e suporte desde os meus projetos de iniciação científica até os momentos finais do mestrado.

A todos, minha eterna gratidão, sem vocês nada disso seria possível.

RESUMO

Em 2015, o surto brasileiro do Zika vírus foi acompanhado por um aumento no número de casos de microcefalia, que envolve graves alterações no desenvolvimento cerebral, indicando uma possível associação da infecção viral com essas malformações cerebrais. Os mecanismos moleculares que promovem essas modificações ainda não se encontram totalmente elucidados. Assim, a investigação dos processos envolvendo o neurodesenvolvimento desencadeados pela infecção viral e as vias bioquímicas que ela afeta é de extrema importância. Para tanto, modelos de estudo utilizando células tronco de pluripotência induzida diferenciadas em células neurais podem ser empregados como modelo de neurodesenvolvimento. Neste trabalho, células tronco neurais foram infectadas com cepas de vírus Zika e Dengue. A infecção também foi realizada em neuroesferas, geradas a partir do cultivo em suspensão das células tronco neurais, visando analisar *in vitro* as modificações causadas pela infecção viral nesses modelos, que são um dos tipos celulares mais afetados pelo vírus Zika. As amostras, infectadas ou não com uma cepa dos diferentes vírus, foram submetidas à análise proteômica quantitativa em larga escala, com o objetivo de analisar diferenças e semelhanças em relação aos efeitos das cepas virais do Zika brasileiro e africano, bem como ao perfil molecular causado pela infecção do vírus da Dengue. A análise quantitativa do proteoma celular permitiu a identificação de diferenças em processos biológicos incluindo transporte celular, metabolismo de RNA e neurogênese, além de proteínas, como DCX, SEPHS1 e DYNC2H1, que podem estar relacionadas aos mecanismos e desenvolvimento da infecção viral em células neurais. Portanto, com este trabalho foi possível investigar potenciais distinções em relação às respostas celulares induzidas pela infecção com cepas de Zika e Dengue, proporcionando avanços em relação à compreensão das alterações celulares induzidas pelos flavivírus.

ABSTRACT

The Brazilian Zika virus outbreak in 2015 was accompanied by an increased in the number of cases of microcephaly, which involves severe changes in brain development, indicating a possible association between the viral infection with these brain malformations. The molecular mechanisms that promote these changes are not yet fully understood. Thus, investigating the processes involving neurodevelopment triggered by viral infection and the biochemical pathways it affects is extremely important. Therefore, models using induced pluripotent stem cells differentiated into neural cells can be used as a neurodevelopment model. Here, neural stem cells have been infected with strains of Zika and Dengue virus. The infection was also carried out in neurospheres, generated from the suspension culture of neural stem cells, to analyze *in vitro* the changes caused by viral infection in these models, which are one of the cell types most affected by the Zika virus. The samples, infected or not with a strain of the virus, were subjected to quantitative proteomic analysis on a large scale, with the aim of analyzing differences and similarities regarding the effects of the Brazilian and African viral strains, as well as comparing Zika virus infection with the Dengue. The quantitative analysis of the cellular proteome allowed the identification of biological processes, including altered cellular transport, RNA metabolism, and proteins, such as DCX, SEPHS1 and DYNC2H1, that may be related to the mechanisms and development of viral infection in neural cells. Thus, we were able to point out potential differences between the cellular response to the different strains of Zika virus and Dengue, gathering relevant information regarding the comprehension of the molecular mechanisms induced by flaviviruses.

ÍNDICE DE FIGURAS

CAPÍTULO I

Figure 1. The three different viral strains infected NSCs for two hours. Then, two different protocols were performed: the culture of NSCs for three days and the protocol for NSCs cultivated in suspension, as neurospheres, for three days. The cells were harvested and the samples were prepared for proteomic analysis, followed by *in silico* analysis.

Figure 2. Comparison of regulated proteins found in neural stem cells (NSC) and neurospheres infected by ZIKV (Br and MR766 strains) and DENV. A. Overlap of proteins differentially regulated in NSCs, represented by chord diagram lines in purple (ZIKV MR766 and DENV), green (Br ZIKV and DENV), pink (Br ZIKV and MR766) and black for commonly found in all three viral strains. Light gray lines on the background are relative to the overlap of pathways and GO terms enriched by regulated proteins in NSCs. B. Pearson correlation of the effects of ZIKV strains and DENV on NSCs. C. Overlap of proteins differentially regulated in neurospheres, represented by chord diagram lines in purple (ZIKV MR766 and DENV), green (Br ZIKV and DENV), pink (Br ZIKV and MR766) and black for commonly found in all three virus strains. Light gray lines on the background are relative to the overlap of pathways and GO terms enriched by regulated proteins in neurospheres. D. Pearson correlation of the effects of ZIKV strains and DENV on neurospheres.

Figure 3. Comparison of pathways and proteins associated with NSCs and neurospheres infected by ZIKV (Br and MR766 strains) and DENV. Heatmap hierarchical clustering of enriched ontology terms and pathways altered due to differentially regulated proteins in A. NSCs and B. neurospheres. C. Differential expression data of commonly deregulated proteins among the ZIKV MR766, Br ZIKV and DENV infections in NSCs and neurospheres.

Figure 4. Regulation of pathways enriched in NSCs and neurospheres infected by ZIKV (Br and MR766 strains) and DENV. Heatmap showing the regulation of enriched pathways in A. NSCs and B. neurospheres, where colors represent the median fold change of proteins within the pathway.

Figure 5. Protein-protein interaction network from the differentially regulated proteins infected by ZIKV in NSCs. **A.** Clustered interactions of proteins modulated by ZIKV MR766 in comparison to MOCK. In red, SRP-dependent cotranslational protein targeting the membrane ($\text{Log}_{10}(P)$ -16.3) and ribosome activity ($\text{Log}_{10}(P)$ -12.9). In blue, cytoplasmic

translational initiation ($\text{Log}_{10}(P) -6.3$) and RNA transport ($\text{Log}_{10}(P) -6.0$). In green, RNA splicing, via transesterification reactions with bulged adenosine as a nucleophile ($\text{Log}_{10}(P) -11.2$), mRNA splicing, via spliceosome ($\text{Log}_{10}(P) -11.2$). In purple, proton transmembrane transport ($\text{Log}_{10}(P) -6.1$). **B.** Clustered interactions of proteins modulated by Br ZIKV in comparison to MOCK. The cluster in red represents the enrichment of biosynthesis of amino acids ($\text{Log}_{10}(P) -9.1$) and glucose metabolism ($\text{Log}_{10}(P) -6.2$); in green, mRNA splicing ($\text{Log}_{10}(P) - 6.6$).

Figure 6. Protein-protein interaction network identified in the differentially regulated proteins infected by ZIKV in Neurospheres. **A.** Clustered interaction of proteins modulated by ZIKV MR766 in comparison to MOCK. The red cluster was enriched for L13a-mediated translational silencing of Ceruloplasmin expression ($\text{Log}_{10}(P) -25.3$), eukaryotic translation initiation ($\text{Log}_{10}(P) -24.9$) and Cap-dependent translation initiation ($\text{Log}_{10}(P) -24.9$). The blue cluster was enriched for the role of GTSE1 in G2/M progression after G2 checkpoint ($\text{Log}_{10}(P) -22.0$), separation of sister chromatids ($\text{Log}_{10}(P) -17.9$) and G2/M transition ($\text{Log}_{10}(P) -17.9$). The green one was enriched for RAB GEFs exchange GTP for GDP on RABs ($\text{Log}_{10}(P) -5.3$). And the orange one for COPI-mediated anterograde transport ($\text{Log}_{10}(P) -7.3$), Golgi-to-ER retrograde transport ($\text{Log}_{10}(P) -7.0$) and ER to Golgi Anterograde Transport ($\text{Log}_{10}(P) -6.8$).

B. Clustered interaction of proteins modulated by Br ZIKV in comparison to MOCK. The cluster in red was enriched for the cellular amino acid metabolic process ($\text{Log}_{10}(P) -19$), the role of GTSE1 in G2/M progression after G2 checkpoint ($\text{Log}_{10}(P) -17.6$) and proteasome ($\text{Log}_{10}(P) -17.1$). The cluster in blue was enriched for the HSP90 chaperone cycle for steroid hormone receptors (SHR) ($\text{Log}_{10}(P) -5.6$), mitochondrial protein import ($\text{Log}_{10}(P) -5.4$) and cellular responses to stress ($\text{Log}_{10}(P) -5.2$). The cluster in green was enriched for SRP-dependent cotranslational protein targeting to the membrane ($\text{Log}_{10}(P) -16.6$), influenza Viral RNA Transcription and Replication ($\text{Log}_{10}(P) -15.9$) and influenza Infection ($\text{Log}_{10}(P) -15.4$).

MATERIAL SUPLEMENTAR

FIGURA

Figure S1. Heatmap of differentially expressed proteins related to RNA processing and metabolism in A. NSCs and B. neurospheres.

LISTAS DE TABELAS

CAPÍTULO I

MATERIAL SUPLEMENTAR

Table S1. List of proteins identified, quantified, differentially regulated, upregulated, and downregulated in neural progenitor cells infected with Br ZIKV, ZIKV 766 and DENV.

Table S2. List of proteins identified, quantified, differentially regulated, upregulated, and downregulated in neurospheres infected with Br ZIKV, ZIKV 766 and DENV.

SUMÁRIO

1	INTRODUÇÃO	14
1.1	Zika Vírus	14
1.2	Dengue Vírus	16
1.3	O estudo de células neurais <i>in vitro</i>	17
1.4	Proteômica	18
1.5	Espectrometria de Massas (MS)	19
1.5.1	Empregando a proteômica na compreensão da infecção por ZIKV	20
2	OBJETIVOS	22
3	MATERIAIS E MÉTODOS	23
3.1	Cultivo e infecção das células tronco neurais	23
3.2	Preparo das Amostras para Análise proteômica	23
3.3	Análise proteômica.....	24
4	CAPÍTULO I	25
5	CONCLUSÃO	50
6	REFERÊNCIAS BIBLIOGRÁFICAS (INTRODUÇÃO E CONCLUSÃO) ...	52
7	MATERIAL SUPLEMENTAR	58
8	ANEXOS	156
8.1	DECLARAÇÃO DE BIOÉTICA E BIOSSEGURANÇA.....	156
8.2	DECLARAÇÃO DE DIREITOS AUTORAIS	157

1 INTRODUÇÃO

1.1 Zika Vírus

O Zika vírus (ZIKV) é um arbovírus pertencente à família Flaviviridae, que compreende vírus causadores de doenças em humanos, incluindo o vírus da Dengue (DENV) e o da hepatite C. Em 1947, o ZIKV foi isolado a partir do sangue de macacos Rhesus infectados, havendo poucos indícios de infecções em humanos durante décadas desde o isolamento viral. O registro de novos casos de infecção em humanos ocorreu nos anos de 2013 e 2014, na Polinésia Francesa e em algumas ilhas do Pacífico (Dick et al., 1952; Fauci et al., 2016; Petersen et al., 2016).

Com a dispersão do vírus pela América, nos anos 2014 e 2015, houve uma alarmante mobilização, em função das severas alterações no desenvolvimento cerebral que foram então relacionadas com essa doença infecciosa (Gulland 2016). No Brasil, o surto do ZIKV foi acompanhado pelo aumento no número de casos de microcefalia em neonatos de mães infectadas pela cepa brasileira do Zika vírus, doença relacionada ao neurodesenvolvimento a qual o vírus foi associado como agente causador. Esta grave doença neurológica prejudica o neurodesenvolvimento, sendo que sua fisiopatologia se relaciona principalmente com alterações nos processos proliferativos das células progenitoras neurais e em processos migratórios durante o neurodesenvolvimento (Woods et al., 2005; Woods et al., 2013).

De acordo com a Organização Mundial da Saúde (OMS), a microcefalia caracteriza-se por um perímetro encefálico com desvios de 2 níveis abaixo do padrão da mediana para determinada idade e sexo, resultando em complicações neurológicas, como retardo no desenvolvimento, convulsões, bem como quadros de deficiência auditiva e visual (Miranda-Filho et al., 2016). Sendo assim, diversos estudos buscam compreender a relação entre a infecção do ZIKV e o desenvolvimento de alterações neurológicas e malformações cerebrais (Calvet et al., 2016; Bayer et al., 2016; Cugola et al., 2016; Garcez et al., 2016; Qian et al., 2016; Tang et al., 2016).

Atualmente, sabe-se que o ZIKV é capaz de promover alterações no sistema nervoso em função de sua capacidade de invadir o tecido neural e de sua neurovirulência, ou seja, é capaz de infectar e proliferar em células nervosas (Calvet et al., 2016). Sabe-se que células progenitoras neurais derivadas de células tronco de pluripotência induzida (iPSCs), quando

infectadas com o ZIKV, apresentam alterações no ciclo celular, desregulando-o, e são induzidas à morte celular (Cugola et al., 2016; Tang et al., 2016; Garcez et al., 2017). Cabe ressaltar que dentre os tipos de mortes celulares, a indução da apoptose mediado pela atividade da caspase 3 (Tang et al., 2016; Garcez et al., 2017). Estudos utilizando células progenitoras neurais derivadas de iPSCs, permitiram comparar como o vírus pode afetar esses tipos celulares, provindos de diferentes cepas do ZIKV circulante, asiático, africano ou brasileiro, assim como em comparação destes com o DENV em níveis de expressão gênica (Zhang et al., 2016).

Em recente estudo, o ZIKV circulante no Brasil foi avaliado em nível celular e molecular, comparando as alterações no transcriptoma e no proteoma de neuroesferas e organoides derivados de células tronco neurais (Garcez et al., 2017). O estudo mostra o início das alterações derivadas da infecção, bem como a indicação de instabilidade cromossômica e interrupção do programa neurogênico. Este estudo corrobora e complementa informações que haviam sido apontadas por outros trabalhos envolvendo análise do transcriptoma de células progenitoras neurais infectadas com ZIKV asiático e africano, promovendo alterações como o retardamento da proliferação celular, levando à morte celular (Zhang et al., 2016).

Em relação às diferentes cepas do ZIKV circulante, foi observado que as linhagens africana e asiática promoveram alterações específicas nas células progenitoras infectadas. O ZIKV asiático provoca alterações em mecanismos de replicação e reparo de DNA, bem como genes relacionados a sinalização de IFN (Zhang et al., 2016). Já o ZIKV africano, apresentou genes alterados mais especificamente relacionadas como processo de divisão e ciclo celular (Zhang et al., 2016). Na análise da cepa circulante no Brasil, foram identificadas proteínas diferencialmente expressas relacionadas a replicação viral, a retenção do ciclo celular, como CDKN1A, a resposta ao estresse e danos e falhas no reparo de DNA (Garcez et al., 2017). Porém a comparação direta dos efeitos das linhagens do ZIKV africano e brasileiro não se encontra totalmente elucidada, havendo a necessidade de estudos analisando as diferenças moleculares entre os processos de infecção dessas cepas.

Em relação à infecção por ZIKV utilizando modelos *in vitro* 3D, foram observadas alterações morfológicas em neuroesferas e redução do crescimento em organoides cerebrais em comparação ao controle (MOCK), não sendo evidenciadas alterações morfológicas em neuroesferas infectadas pelo DENV (Cugola et al., 2016; Garcez et al., 2016). Tais dados evidenciam que as alterações no desenvolvimento cerebral se relacionam aos mecanismos de

atuação do ZIKV, não sendo alterações gerais causadas por vírus da família Flaviviridae (Garcez et al., 2016). Ademais, foi demonstrado que as diferenças temporais e geográficas do ZIKV podem alterar diferencialmente aspectos específicos no processo de infecção, modificando diferentes vias metabólicas. Sendo imprescindível a investigação dos distintos mecanismos moleculares envolvidos com a infecção de diferentes flavivírus, incluindo ZIKV e DENV.

1.2 Dengue Vírus

O Dengue vírus (DENV), como mencionado anteriormente, também se trata de um arbovírus pertencente à família Flaviviridae, havendo quatro sorotipos distintos (DENV 1–4) (Guzman et al., 2015). De acordo com a OMS, o DENV é endêmico em mais de centenas de países, sendo que sua incidência tem aumentado nos últimos 50 anos, constituindo um importante problema de saúde pública (WHO 2012).

A maioria dos indivíduos acometidos são assintomáticos, porém pode ocorrer o desenvolvimento de quadros clínicos mais severos incluindo hepatite e alterações neurológicas (Acevedo et al., 1982; Guzman et al., 2015). Sendo que infecções secundárias, principalmente em adultos, aumentam os riscos para o desenvolvimento de alterações de permeabilidade vascular, levando a graves sangramentos (Thu et al., 2012).

Investigando os mecanismos moleculares por trás das alterações induzidas por DENV, estudos revelaram a modulação de proteínas e vias metabólicas relacionadas com a cascata de coagulação, adesão celular, autofagia e metabolismo lipídico (Han et al., 2019; Heaton et al., 2010; Koraka et al., 2004). Em comparação com à infecção por ZIKV, células infectadas por DENV apresentaram maiores alterações no transcriptoma, predominando genes relacionados com processos inflamatórios (Zhang et al., 2016). Ademais, como mencionado no tópico anterior, neuroesferas infectadas por ZIKV apresentaram alterações morfológicas, já em DENV tais alterações não foram observadas (Cugola et al., 2016; Garcez et al., 2016).

Sendo assim, novos estudos focados nestas diferenças de infecção pelo ZIKV e DENV podem auxiliar na compreensão das alterações induzidas pelas infecções virais e no desenvolvimento de possíveis abordagens terapêuticas relacionadas com a infecção por ZIKV, e as consequentes malformações cerebrais desencadeadas, bem como em relação à DENV.

1.3 O estudo de células neurais *in vitro*

Nos anos 1990, células tronco neurais (NSCs) foram isoladas a partir do tecido cerebral de mamíferos, possibilitando a investigação de aspectos relacionados ao neurodesenvolvimento (Reynolds et al., 1992). Desde então, avanços significativos ocorreram em relação ao cultivo de células neurais, incluindo o desenvolvimento de células de pluripotência induzida (iPSCs) a partir da reprogramação de células somáticas (Takahashi et al., 2006; Takahashi et al., 2007).

Nesses modelos, células tronco embrionárias e/ou iPSCs são diferenciadas para linhagens celulares específicas, sendo capazes de representar diferentes regiões cerebrais, bem como sistemas neurais tridimensionais, que resultam em neuroesferas ou até em organóides cerebrais (Dang et al., 2016). Tais modelos estruturais 3D podem se diferenciar, constituindo estruturas complexas. Portanto, mesmo não contemplando todos os aspectos mecânicos e fisiológicos observados nos modelos *in vivo*, os modelos *in vitro* tridimensionais têm proporcionado importantes avanços na comunicação e na interação celular, contribuindo para o estudo dos mecanismos de doenças e aspectos essenciais do neurodesenvolvimento em humanos e outros mamíferos (Dang et al., 2016; Lancaster et al., 2013).

Diferentes estudos e pesquisas em modelos *in vivo*, bem como em modelos *in vitro*, como os que utilizam células progenitoras neurais e organoides, estão em desenvolvimento a fim de investigar os mecanismos do ZIKV responsáveis pelas alterações e malformações cerebrais, estudando também a relação da infecção viral com a microcefalia (Cugola et al., 2016; Martines et al., 2016).

Os modelos *in vitro* são estratégias reprodutíveis e capazes de englobar os complexos processos iniciais do neurodesenvolvimento, permitindo a análise e compreensão dos mecanismos de atuação do ZIKV, bem como as alterações provocadas nas células nervosas, que resultam em quadros graves de malformações, como a microcefalia (Dang et al., 2016; Garcez et al. 2016). Ademais, os modelos *in vitro* possibilitam a comparação entre o processo de infecção nas células progenitoras e nas estruturas 3D de neuroesferas e organoides cerebrais, uma vez que o ZIKV tem como alvo principal as células progenitoras (Garcez et al. 2017).

Com os modelos 2D de células progenitoras neurais é possível obter informações sobre a infecção direta de uma monocamada de cultura. Já os modelos estruturais 3D, neuroesferas e organoides cerebrais, constituem estruturas mais complexas, permitindo o estudo da infecção do tecido, bem como da comunicação celular e outros mecanismos durante o neurodesenvolvimento, em associação ao que é observado *in vivo*. Dessa forma, a investigação das alterações celulares induzidas pela infecção viral, associadas às análises moleculares de larga escala, como a técnica da proteômica, podem contribuir para a identificação dos principais processos celulares e vias metabólicas afetadas pelo processo de infecção do ZIKV.

1.4 Proteômica

A proteômica é a ciência que estuda o proteoma, o qual corresponde ao conjunto de proteínas expressas em um indivíduo, um tecido ou uma célula, em um dado momento e/ou condição fisiológica (mod. Wilkins et al., 1996). Análises proteômicas permitem a identificação de proteínas diferencialmente reguladas nas amostras estudadas, sendo possível identificar os processos biológicos associados a essas proteínas por análises *in silico* (Martins-de-Souza et al., 2011; Martins-de-Souza et al., 2015). Ademais, também possibilita a busca por proteínas que sirvam como possíveis candidatos a biomarcadores, que podem auxiliar no diagnóstico de doenças, bem como predição de resposta a tratamentos.

Inserida no contexto da era pós-genômica, a proteômica consiste em uma área de estudo capaz de fornecer informações que vão além do produto da expressão gênica, caracterizando um fenótipo. Dessa forma, com a identificação e quantificação de proteínas, engloba-se aspectos envolvidos na regulação da tradução, interações proteína-proteína, bem como modificações pós-traducionais. Atualmente, o método mais comumente utilizado consiste na combinação da cromatografia líquida (LC) com a espectrometria de massas (MS). Em geral, sistemas de LC-MS são empregados em estudos de *shotgun proteomics*, abordagem que se refere à análise de uma mistura complexa de proteínas. Geralmente, estudo de *shotgun proteomics* são do tipo *bottom-up proteomics*, no qual o proteoma de interesse é submetido a uma digestão proteolítica. Os produtos (peptídeos) são separados por LC e as frações diretamente injetadas no espectrômetro de massas (Yates 2013). A principal alternativa a esta estratégia, consiste no emprego de *top-down proteomics*, em que proteínas intactas são submetidas à análise proteômica, permitindo a identificação de proteoformas e de

modificações pós-traducionais (Scheffler 2014). *Shotgun proteomics* consiste em um método de análise proteômica não direcionada por hipótese, ou seja, sua aplicação está focada na cobertura total do proteoma, identificando e, eventualmente quantificando, de maneira relativa, milhares de proteínas. Outra possível abordagem consiste em *targeted proteomics*, a qual permite a identificação de alvos específicos, de maneira mais precisa e sensível (Gillette et al., 2013).

1.5 Espectrometria de Massas (MS)

A MS consiste em uma técnica com elevada precisão qualitativa e quantitativa, que identifica moléculas a partir de suas razões massa/carga (m/z). Para tanto, a etapa de ionização é essencial. Diferentes técnicas estão disponíveis, sendo as principais aplicadas à proteômica, a ionização e dessorção a laser auxiliada por matriz (Matrix Assisted Laser Desorption/Ionization, MALDI) e a ionização por *eletrospray* (ESI) (Karas et al., 1988; Fenn et al., 1989).

Após a ionização dos analitos, obtém-se íons em estado gasoso, que são então separados de acordo com sua relação m/z . Tal processo de separação ocorre nos analisadores de massa, que utilizam energia elétrica estática ou dinâmica e campos magnéticos isolados ou combinados para a distinção e separação dos íons (Porter et al., 1981). Exemplos de analisadores amplamente utilizados na proteômica são quadrupolo (Q, quadrupole mass filters), TOF (time of flight mass analyzers) e Orbitrap. Nos analisadores quadrupolo, são utilizados campos elétricos oscilantes, estabilizando ou seletivamente desestabilizando os íons, o que permite sua separação de acordo com os seus valores de m/z (Hoffmann et al., 2007). Já nos analisadores TOF, a relação m/z de um íon é obtida a partir do seu tempo de “vôo” no vácuo através de um tubo (Andrews et al., 2011). Já o analisador Orbitrap consiste num *trap* no qual os íons se deslocam a partir de um campo eletrostático ao redor de um eletrodo central, movimentando-se em um complexo padrão espiral. A corrente dos íons aprisionados é detectada individualmente e convertida em um espectro de massa usando a transformada de Fourier do sinal de frequência (Scigelova et al., 2006).

Assim, um espectrômetro de massas apresenta uma fonte de ionização, um ou mais analisadores, e possui também um detector, responsável por detectar e amplificar a informação fornecida pelo analisador, havendo a conversão de feixes de íons em sinais elétricos, gerando espectros de massas (Porter et al., 1981). Ademais, o acoplamento da LC

ao espectrômetro de massas (LC-MS) permite uma eficiente separação de misturas complexas, como peptídeos, melhorando a sensibilidade analítica e ampliando a cobertura do proteoma (Pitt 2009).

Os conjuntos de dados gerados por LC-MS são extraídos por meio de diferentes ferramentas computacionais automatizadas. Para proteômica, algumas utilizadas são MASCOT®, MaxQuant (Cox et al., 2008), PLGS® e Progenesis®. Tais ferramentas realizam a comparação com um banco de dados de espectros teoricamente obtidos, que são gerados com base no genoma do organismo estudado, permitindo a identificação das proteínas obtidas experimentalmente.

1.5.1 Empregando a proteômica na compreensão da infecção por ZIKV

Em relação aos estudos com o ZIKV, a análise do proteoma possibilita uma comparação entre as células tronco neurais controle (MOCK) e as infectadas pelo ZIKV. Primeiramente, foram investigados os efeitos da cepa brasileira do ZIKV em neuroesferas infectadas (Garcez et al. 2017). Porém, muitas perguntas ainda estão sem resposta em relação aos efeitos da infecção de diferentes cepas do ZIKV e seus efeitos em células neurais. Assim como pouco foi estudado na comparação de proteínas diferencialmente expressas entre o ZIKV e outros vírus da família Flaviviridae, como o DENV (Garcez et al., 2016; Garcez et al. 2017). Para auxiliar na interpretação do proteoma em relação às alterações desencadeadas por essas infecções virais, pode-se empregar ferramentas de análise de biologia de sistemas, que possibilitam estudos em larga escala de um amplo volume de dados, gerando informações sobre processos biológicos associadas às proteínas diferencialmente reguladas (Sherman et al., 2017).

Diante do grande volume de dados oriundos de experimentos empregando técnicas de genômica e proteômica, a existência de ferramentas e programas, que utilizam algoritmos e a informação biológica acumulada até então, permite a análise e a interpretação desse grande volume de dados (Sherman et al., 2007). Dentre tais programas e ferramentas, podemos citar o STRING, Reactome Knowledgebase e DAVID - Functional Annotation Bioinformatics Microarray Analysis. Cada uma dessas ferramentas apresenta diferentes métodos de análise e sua utilização combinada permite uma melhor interpretação dos dados que se deseja analisar.

Em relação ao STRING, tal ferramenta permite estabelecer uma correlação entre genes situados próximos entre si no genoma e a funcionalidade das proteínas que os codificam. Diante disso, trata-se de uma ferramenta de pesquisa para instâncias recorrentes de genes vizinhos (Snel et al., 2000). Possibilita a busca e interpretação de padrões na organização do genoma, permitindo explorar associações funcionais de um gene em questão (Snel et al., 2000).

Já a ferramenta de análise DAVID - Functional Annotation Bioinformatics Microarray Analysis, utiliza o banco de dados do Biocarta, constituindo uma base integrativa de conhecimentos biológicos. Possibilita a interpretação das funções de listas de genes e proteínas, além de apresentar ferramentas capazes de relacionar e comparar os genes inseridos na lista, bem como gerar mapas e figuras das vias metabólicas que envolvem as proteínas que se deseja analisar (Huang et al., 2009). Além disso, possibilita uma referência cruzada entre identificadores de genes e proteínas, como o UniProt e NCBI, sendo uma ferramenta capaz de ampliar e integrar as informações dessas diferentes fontes, resultando em uma melhor compreensão das funções e associações para um determinado gene (Huang et al., 2009).

Outra ferramenta de análise é o Reactome Knowledgebase, que reúne informações sobre diversos processos celulares, como transdução de sinal, transporte celular, reparo de DNA, gerando mapas metabólicos. As vias geradas no Reactome são organizadas hierarquicamente, agrupando vias específicas e detalhadas, como tradução e modificações pós-traducionais. E também agrupando funções e aspectos mais amplos como metabolismo proteico, gerando uma via gráfica (Jassal et al., 2020).

2 OBJETIVOS

A presente dissertação teve como objetivo contribuir para a compreensão de mecanismos moleculares por trás das alterações induzidas por ZIKV em células neurais humanas em desenvolvimento, dada a potencial associação do ZIKV com o processo de microcefalia observado em neonatos de mães infectadas.

Para isso, realizamos análise proteômica em larga escala de células tronco neurais e neuroesferas infectadas com diferentes cepas do Zika vírus (ZIKV 766 e Br ZIKV) e do vírus dengue (DENV), investigando aspectos comparativos em ambos os modelos *in vitro* em resposta à infecção viral.

3 MATERIAIS E MÉTODOS

3.1 Cultivo e infecção das células tronco neurais

O cultivo das células tronco neurais (NSCs), bem como o cultivo de neuroesferas foi realizado em parceria com o grupo do Prof. Stevens K. Rehen no Instituto D'Or de Pesquisa e Ensino (IDOR) e Instituto de Ciências Biomédicas ICB-UFRJ. As células foram cultivadas em monocamadas, assim como foi realizado o cultivo em suspensão, possibilitando a formação das neuroesferas, como previamente descrito em Garcez et al. 2017. Estas células foram infectadas pelas cepas brasileiras (Br ZIKV- KU497555), africana (ZIKV MR766), e pelo vírus da dengue (DENV2). Para realizar a infecção, o ZIKV foi propagado em células Vero (ATCC #CCL-81), cultivadas com DMEM e 5% de soro fetal bovino¹⁴. Então, o vírus foi submetido à titulação e congelado em alíquotas, bem como o meio condicionado em células Vero, porém não contendo o vírus, constituindo a condição MOCK.

As células das linhagens CF1CL10, CF2CL2 e GM23679A foram infectadas com *Multiplicity of infection* (MOI) 0.025, sendo incubadas por 2h. Após esse processo, foi realizada a troca para o meio de cultivo de NSCs, que consiste em advanced DMEM/F12 e neurobasal (1:1), suplementado com o fator de indução neural, sendo mantidas em cultivo por 3 dias após a infecção, para então prosseguir com as análises¹⁴. As amostras já em tampão de lise (descrito a seguir) foram então encaminhadas para o Laboratório de Neuroproteômica (LNP) de acordo com o protocolo de preparo amostra para proteômica.

3.2 Preparo das Amostras para Análise proteômica

Após o processo de infecção, as células foram lavadas em PBS gelado, raspadas da placa de cultura e coletadas em um tubo. Em seguida, as células foram centrifugadas (200g por 5 min), o PBS removido e o tampão de lise RIPA (300 mM NaCl; 50mM Tris, pH 7.4; 0.5% Triton X-100), contendo cocktail de inibidores de proteases cOMPLETE (Roche) foi adicionado. Após a lise por aproximadamente 30 min em gelo, as amostras foram mantidas congeladas a -80°C e transportadas para o Laboratório de Neuroproteômica. Para a realização das etapas de quantificação e digestão, foram centrifugadas a 10,000g por 10 min para separação dos debris. Finalizando o preparo e a extração das proteínas das amostras. Assim, as proteínas obtidas no processo de extração foram quantificadas por fluorescência no Qubit®3.0 Fluorometer (Thermo Fisher Scientific), e 50µg de proteína de cada amostra foi submetida ao protocolo de digestão em gel de poliacrilamida SDS-PAGE. As amostras foram

reduzidas com 100 mM de DTT (30 min a 60°C) e alquiladas com 200 mM de iodoacetamida (30 min à temperatura ambiente). Finalmente, as amostras foram digeridas a uma razão de 1:100 (tripsina: proteína m/m), em tampão e temperaturas ótimos (50 mM bicarbonato de amônio, a 37 o C) por 16h. As amostras foram mantidas congeladas (-20°C a -80°C) até a realização da análise de espectrometria de massas.

3.3 Análise proteômica

Foram injetados 500 pg/ μ L de peptídeos resultantes da digestão das proteínas, em um sistema nano-LC (ACQUITY UPLC (2D-RP/RP), que está acoplado ao espectrômetro de massas com fonte ionizadora nano-electrospray (ESI) instalada em um Synapt G2-Si (Waters). Na cromatografia líquida HSS T3 Column (1.8 μ m, 75 μ m \times 150 mm; Waters Corporation, USA), a eluição se deu com um gradiente de acetonitrila de 7% a 40% (v/v) por 95 minutos a uma taxa de fluxo de 0,4 μ L/min diretamente no Synapt G2-Si. Havendo a eluição dos peptídeos, que foram analisados online em ESI-MS e ESI-MS/MS em modo positivo. Os espectros de fragmentação (modo MS/MS) foram obtidos através do modo independente de coleta de dados (data independent analysis - DIA), mais especificamente com a otimização das energias de colisão dos precursores iônicos através de seus drift-time (UDMSE, Waters Co.). Tal método apresenta elevada eficiência na fragmentação dos peptídeos, havendo a fragmentação dos íons precursores, independentemente de seu pico de intensidade, obtendo um espectro mais complexo, porém favorecendo a identificação das proteínas (Cassoli, et al.2017). Os espectros foram deconvoluídos através do algoritmo Ion Accounting pelo Progenesis QI for Proteomics 3.0 (Waters Co.).

Para a atribuição dos espectros, utilizamos o banco de dados Homo sapiens do Uniprot (revisado, Outubro de 2019), com 1% de taxa de falsa descoberta (FDR), 2 fragmentos/peptídeo, 5 fragmentos/proteína, 1 peptídeo/proteína. Como método de quantificação, utilizamos os 3 peptídeos mais intensos de cada proteína (High-3). Finalmente, os peptídeos com erro de massa maior de 20 ppm foram descartados, juntamente com eventuais proteínas contaminantes inerentes da prática de proteômica (ex. queratina).

4 CAPÍTULO I

Zika Strains and Dengue Virus Induce Different Proteomic Changes in Neural Stem Cells and Neurospheres

Danielle Gouvêa-Junqueira^{1*}, Juliana Minardi Nascimento^{1,2,3*}, Giuliana S. Zuccoli¹,
 Erick Correia Loiola², Juliana S. Cassoli¹, Luiza M. Higa⁴, Amilcar Tanuri⁴,
 Patricia Garcez^{2,5}, Stevens K. Rehen^{2,5@}, Daniel Martins-de-Souza^{1,2,6,7@}

¹Laboratory of Neuroproteomics, Department of Biochemistry and Tissue Biology, Institute of Biology, University of Campinas, Campinas, Brazil.

²D’Or Institute for Research and Education (IDOR), Rio de Janeiro, Brazil.

³Department of Biosciences, Federal University of São Paulo, Santos, Brazil.

⁴Institute of Biology, Federal University of Rio de Janeiro (UFRJ), Rio de Janeiro, Brazil.

⁵Institute of Biomedical Sciences, Federal University of Rio de Janeiro (UFRJ), Rio de Janeiro, Brazil.

⁶Experimental Medicine Research Cluster (EMRC), University of Campinas, Brazil.

⁷Instituto Nacional de Biomarcadores em Neuropsiquiatria (INBION), Conselho Nacional de Desenvolvimento Científico e Tecnológico, São Paulo, Brazil.

* These authors contributed equally.

Correspondence:

Daniel Martins-de-Souza, Department of Biochemistry and Tissue Biology, Institute of Biology, University of Campinas (UNICAMP), Rua Monteiro Lobato, 255, 13083-862, Campinas, SP, Brazil, dmsouza@unicamp.br, +55-19-3521-6129; and Stevens K. Rehen, D’Or Institute for Research and Education (IDOR), Rua Diniz Cordeiro, 30, 22281-100, Rio de Janeiro, RJ, Brazil, +55-21-3883-6000, srehen@lance-ufrj.org.

Keywords neurodevelopment, microcephaly, Flaviviridae.

Abstract

The Brazilian Zika virus outbreak in 2015 was accompanied by an increased in the number of cases of microcephaly, which involves severe changes in brain development, indicating a possible association between the viral infection with these brain malformations. The molecular mechanisms that promote these changes are not yet fully understood. Thus, investigating the processes involving neurodevelopment triggered by viral infection and the biochemical pathways it affects is extremely important. Therefore, models using induced pluripotent stem cells differentiated into neural cells can be used as a neurodevelopment model. Here, neural stem cells have been infected with strains of Zika and Dengue virus. The infection was also carried out in neurospheres, generated from the suspension culture of neural stem cells, to analyze *in vitro* the changes caused by viral infection in these models, which are one of the cell types most affected by the Zika virus. The samples, infected or not with a strain of the virus, were subjected to quantitative proteomic analysis on a large scale, with the aim of analyzing differences and similarities regarding the effects of the Brazilian and African viral strains, as well as comparing Zika virus infection with the Dengue. The quantitative analysis of the cellular proteome allowed the identification of biological processes, including altered cellular transport, RNA metabolism, and proteins, such as DCX, SEPHS1 and DYNC2H1, that may be related to the mechanisms and development of viral infection in neural cells. Thus, we were able to point out potential differences between the cellular response to the different strains of Zika virus and Dengue, gathering relevant information regarding the comprehension of the molecular mechanisms induced by flaviviruses.

Introduction

The Zika virus (ZIKV) outbreak in 2015, which in Brazil and other American countries peaked in 2016, was an international concern due to the increased number of cases of congenital brain abnormalities such as microcephaly ('WHO | Zika epidemiology update', 2019). Microcephaly is a developmental disease and the virus is considered to be a causative agent (Bayer *et al.*, 2016; Calvet *et al.*, 2016; 'WHO | Zika epidemiology update', 2019); it severely impairs neurodevelopment and its virus-independent pathophysiology is mainly related to changes in the proliferative processes of neural progenitor cells (NPCs) and migratory processes during neurodevelopment (Woods *et al.*, 2005; Woods and Parker, 2013). This results in neurological complications, such as delayed development, seizures, as well as hearing and visual impairment (Miranda-Filho *et al.*, 2016). Therefore, several studies sought to understand the relationship between ZIKV infection and the development of neurological changes and brain malformations using animal models, human neurospheres and brain organoids (Cugola *et al.*, 2016; Dang *et al.*, 2016; Garcez *et al.*, 2016; Li *et al.*, 2016; Qian *et al.*, 2016; Tang *et al.*, 2016; Ledur *et al.*, 2020).

Previous studies have used pluripotent stem cell models to understand mechanistic effects of ZIKV on neurodevelopment, which includes deregulation of cell cycle and proliferation, oxidative damage and neural cell death (Cugola *et al.*, 2016; Tang *et al.*, 2016; Garcez *et al.*, 2017; Ledur *et al.*, 2020). In these models, pluripotent stem cells differentiated into 2D or 3D neural systems to represent different brain regions (Dang *et al.*, 2016). While 2D models of neural stem cells provide insight into the direct infection of a culture monolayer, 3D structural models, neurospheres and brain organoids, constitute more complex structures, allowing the study of tissue infection and essential cell communication and other mechanisms during neurodevelopment, closer to that which is observed *in vivo* (Lancaster *et al.*, 2013; Dang *et al.*, 2016; Garcez *et al.*, 2017). ZIKV-infected neurospheres revealed impaired growth and disrupted pathways, affecting neurogenesis during brain development (Garcez *et al.*, 2017; Garcez *et al.*, 2016).

Two major family strains of the Zika virus, the African and the Asian, are distinguished by sequencing analysis. Those found circulating in Brazil were matched to the Asian strains (Calvet *et al.*, 2016). Comparisons between African and Asian ZIKV strains have shown specific, unique changes in infected neural progenitors. While the African ZIKV strain induced gene alterations leading to impairments related to the cell cycle and cell death (Garcez *et al.*, 2016; Zhang *et al.*, 2016), the Asian ZIKV strains, including those circulating in Brazil, are connected to changes in oxidative stress, DNA replication and repair

mechanisms, chromosome instability and interruption of the neurogenic program, additionally affecting genes related to IFN signaling (Zhang *et al.*, 2016; Garcez *et al.*, 2017; Ledur *et al.*, 2020). Moreover, it has been reported that the Brazilian strain can induce a delayed innate immune response unlike the African and other Asian strains (Esser-Nobis *et al.*, 2019).

The more the temporal and geographical differences of ZIKV strains are studied, the more is understood about how specific aspects of the infection process can be altered by modifying different metabolic pathways. Nonetheless, the molecular mechanisms behind such differences remain largely unexplored. Here we investigated the molecular responses to two ZIKV strains (Br and MR766) in iPS-derived neural stem cells and neurospheres using label-free, mass-spectrometry based proteomics, and compared them to another mosquito-borne flavivirus, a Dengue virus strain. Here, we observe altered patterns of expression when comparing both ZIKV strains and DENV, with the modulation of pathways involved with cellular transport, glucose metabolism, neurogenesis, mRNA metabolism. Thus, molecular differences between the infection processes of these strains were focused on gathering data for the discovery of potential biomarkers, as well as to help understand and treat brain malformations triggered by the viral infection.

Methods

2.1 Ethics Statement

The experimental protocols and procedures were carried out in partnership with the Rehen Lab at the D'Or Institute for Research and Education (IDOR) and the Institute of Biomedical Sciences ICB-UFRJ. The experimental procedures were approved by the Institutional Research Ethics Committee of Hospital Copa D'Or (CEPCOPADOR) under protocols #727.269 and #1.269.816. All experiments were performed following relevant guidelines and regulations.

2.2 Culture of neural stem cells and neurospheres

Three different control iPS cell lines (CF1CL10, CF2CL2, and GM23679A) were differentiated into neural stem cells (NSC) using PSC neural induction medium (Thermo Fisher Scientific, USA), containing Neurobasal medium and PSC supplement, according to the manufacturer's protocol, and as previously described in (Garcez *et al.*, 2017). NSCs were

cultured in monolayers on neural induction medium (Advanced DMEM/F12 and Neurobasal medium (1:1), supplemented with PSC supplement, Thermo Fisher Scientific, USA), and media was changed every other day, and maintained at 37 °C in humidified air with 5% CO₂. Neurospheres were differentiated from NSCs cultured until 80% confluence and split with Accutase (Merck-Millipore, Germany). Resuspended cells were then grown under a 90 rpm rotation on Advanced DMEM/F12 and Neurobasal medium (1:1), supplemented with 1x N2 and 1x B27 supplements (Thermo Fisher Scientific, USA), and maintained at 37 °C in humidified air with 5% CO₂.

2.3 NSC infection with ZIKV and DENV

DENV (DENV2 16681) and ZIKV (BrZIKV (KU497555) and MR766) strains were propagated in C6/36 or Vero (ATCC #CCL-81) cells, respectively. Briefly, cells were cultured in mock or virus-infected medium supplemented with 2% FBS, collected, titred, and frozen in aliquots, as previously described in (Garcez *et al.*, 2016, 2017). NSCs were then infected with 0.025 MOI ZIKV (Br or MR766) or DENV2. After incubation for 2 hours, the medium was replaced with advanced DMEM/F12 and neurobasal media (1:1), supplemented with PSC supplement in NSCs, or suspended and cultured according to the neurosphere protocol. Cells were then maintained in culture for 3 days after infection, the same for both monoculture and suspended culture, enabling the formation of neurospheres.

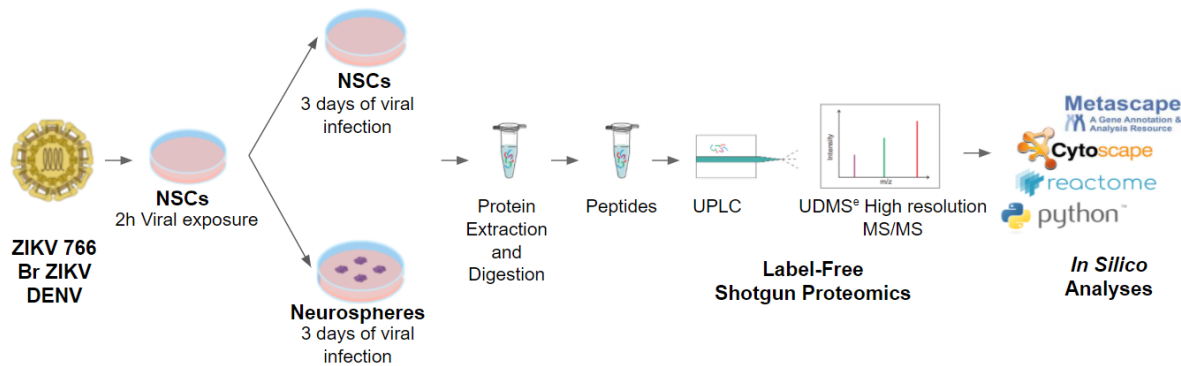


Figure 1. The three different viral strains infected NSCs for two hours. Then, two different protocols were performed: the culture of NSCs for three days and the protocol for NSCs cultivated in suspension, as neurospheres, for three days. The cells were harvested, and the samples were prepared for proteomic analysis, followed by *in silico* analysis.

2.4 Protein Extraction and Digestion

After viral infection and incubation, cells were washed with ice-cold PBS, scraped, and collected into a tube. Then, cells were centrifuged (200xg for 5 min), and PBS was removed and fresh RIPA lysis buffer (300 mM NaCl; 50 mM Tris, pH 7.4; 0.5% Triton X-100) containing cOMPLETE protease inhibitor cocktail (Roche) was added. After lysis for approximately 30 min on ice, samples were kept frozen at -80°C.

Just prior to the quantification and digestion steps, cells were thawed and centrifuged at 10,000xg for 10 min to separate debris. The proteins obtained during the extraction were quantified by fluorescence in a Qubit® 3.0 Fluorometer (Thermo Fisher Scientific), and 50 µg of protein from each sample was submitted to SDS-PAGE polyacrylamide gel digestion (Shevchenko *et al.*, 2006). Briefly, SDS-gel slices containing protein samples were reduced with 100 mM DTT (30 min at 60 °C) and alkylated with 200 mM iodoacetamide (30 min at room temperature). Finally, the samples were digested at a ratio of 1:100 (trypsin:protein w/w), in Ambic buffer and optimal temperatures (50 mM ammonium bicarbonate, at 37°C) for 16h. Extracted peptides were kept frozen (-20°C to -80°C) until mass spectrometry analyses were carried out.

2.5 Proteomic Analysis

Peptide loads (500 pg/µL) were injected into a nano-LC system (ACQUITY UPLC; 2D-RP/RP) coupled to the mass spectrometer (Synapt G2-Si, Waters Corporation), ionized with a nano-electrospray ionization source in positive mode (ESI+). Chromatographic separation was performed on a HSS T3 Column (1.8 µm, 75 µm × 150 mm, Waters Corporation, USA), eluted with an acetonitrile gradient from 7% to 40% (v/v) for 95 min at a flow rate of 0.4 µL/min directly into a Synapt G2-Si. The fragmentation spectra (MS/MS mode) were obtained through data-independent acquisition (DIA), with the optimization of collision energies of ionic precursors across their drift-time (UDMS^E, Waters Co.). This method results in a more complex spectrum but favoring the identification of proteins, with high efficiency in the fragmentation of peptide precursor ions, regardless of peak intensity (Cassoli *et al.* 2017). The mass spectrometer operated in resolution mode with an m/z resolving power of about 40 000 FWHM, using ion mobility with a cross-section resolving power at least 40 Ω/ΔΩ. Injection was performed by nano-electrospray ionization in positive ion mode nanoESI (+) and a NanoLock Spray (Waters, UK) ionization source. The lock mass channel was sampled every 30 sec. The MS/MS spectrum of [Glu1]-Fibrinopeptide B human

(Glu-Fib) from the NanoLock Spray source was used for calibration of the mass spectrometer. Biological samples were run in triplicates.

The spectra were deconvolved using the Ion Accounting algorithm by Progenesis QI for Proteomics version 3.0 (Waters Co.). For the assignment of spectra, we used the *Homo sapiens* database from Uniprot (revised, October 2019), and identified and quantified proteins using the following parameters: 1% false discovery rate (FDR), 2 fragments/peptide, 5 fragments/protein, and 1 peptide/protein. The 3 most intense peptides of each protein were used for relative quantitation (Hi-3). Finally, peptides with a mass error greater than 20 ppm were discarded, along with any contaminating proteins common in shotgun proteomics (e.g. keratin). Proteins were considered to be differentially expressed when one-way analysis of variance (ANOVA) returned a p-value < 0.05.

2.6 In Silico Analysis

Protein data were then submitted to bioinformatic analysis using tools, databases, and predictions in systems biology for *in silico* evaluation of protein interactions and altered metabolic pathways, including Metascape (Zhou *et al.*, 2019). The protein-protein interaction enrichment analysis was performed using the Molecular Complex Detection (MCODE) algorithm to identify network components and connections (Bader and Hogue, 2003). All the Metascape analyses were carried out with the update of 2020-09-16.

Other bioinformatic tools and databases include String (Szklarczyk *et al.*, 2018), Reactome Knowledgebase (Jassal *et al.*, 2019), CORUM (Giurgiu *et al.*, 2019), and the KEGG and KO (KEGG ORTHOLOGY) Databases (Kanehisa *et al.*, 2016).

Results and Discussion

NSCs and neurospheres are two different steps in cell organization and differentiation. Using those human iPSC-derived brain cells in different stages, we could explore and compare different molecular aspects of ZIKVs and DENV infection. While NSCs, which are one of the main targets of ZIKV (Tang *et al.*, 2016), are cultured and infected in monolayers, neurospheres are the 3D-derivations of those infected NSCs which were allowed to differentiate further due to cell-cell contact communication. Thus, the proteomic analyses of those NSCs and neurospheres by ZIKV and DENV resulted in a total of 792 differentially regulated proteins (p value < 0.05).

The whole-cell proteomic analyses of NSCs identified and quantified a total of 1265 proteins (Supplementary Table 1), of which 149 were differentially regulated (p value < 0.05) in ZIKV MR766, 53 in Br ZIKV and 121 in DENV, a combined modulation of 323 different proteins, as shown in Figure 2A. A comparative analysis of those proteins revealed 10 proteins in common between Br ZIKV and MR766, 7 between Br ZIKV and DENV and 28 between MR766 and DENV (Figure 2A), and several biological pathways are shared among the viruses. A Pearson correlation of total protein changes in NSCs shows differences of ZIKV strains in comparison to DENV. While Br ZIKV has a higher correlation with ZIKV MR766 (0.33) (Figure 2B) than DENV (0.04), ZIKV MR766 has a similar correlation between Br ZIKV and DENV (0.33 and 0.39, respectively).

As neural stem cells differentiated into neurospheres, we observed a shift in the effects of the viruses on neural cell proteomes. In neurospheres, we identified and quantified a total of 1068 proteins (Supplementary Table 2), 127 of which were differentially regulated (p value < 0.05) in ZIKV MR766, 182 in Br ZIKV and 160 in DENV. Analysis of proteins common among different strains revealed that Br ZIKV had 25 proteins in common with ZIKV MR766 and 34 in common with DENV, while DENV and ZIKV MR766 had 25 other proteins in common, with a total of 469 differentially regulated proteins in comparison to mock-treated cells (Figure 2C). Despite having few proteins in common, several pathways are shared. In contrast with NSCs, the correlation between both ZIKV strains was higher (0.65) than those with DENV, with a correlation of 0.33 for Br ZIKV and 0.18 for ZIKV MR766 (Figure 2D). Given that neurospheres represent later neurodevelopmental and organizational stages than NSCs, the proteomic differences observed may reflect the complexity of the models that can be affected by these viruses.

The proteomic data thus revealed that ZIKV strains, though similar in some regards, have a distinct signature that can change in response to neurodevelopmental cell conditions. The similarities and differences observed among the strains -- comparing the two ZIKV strains as well as ZIKV vs. DENV -- will be further explored in the following sections.

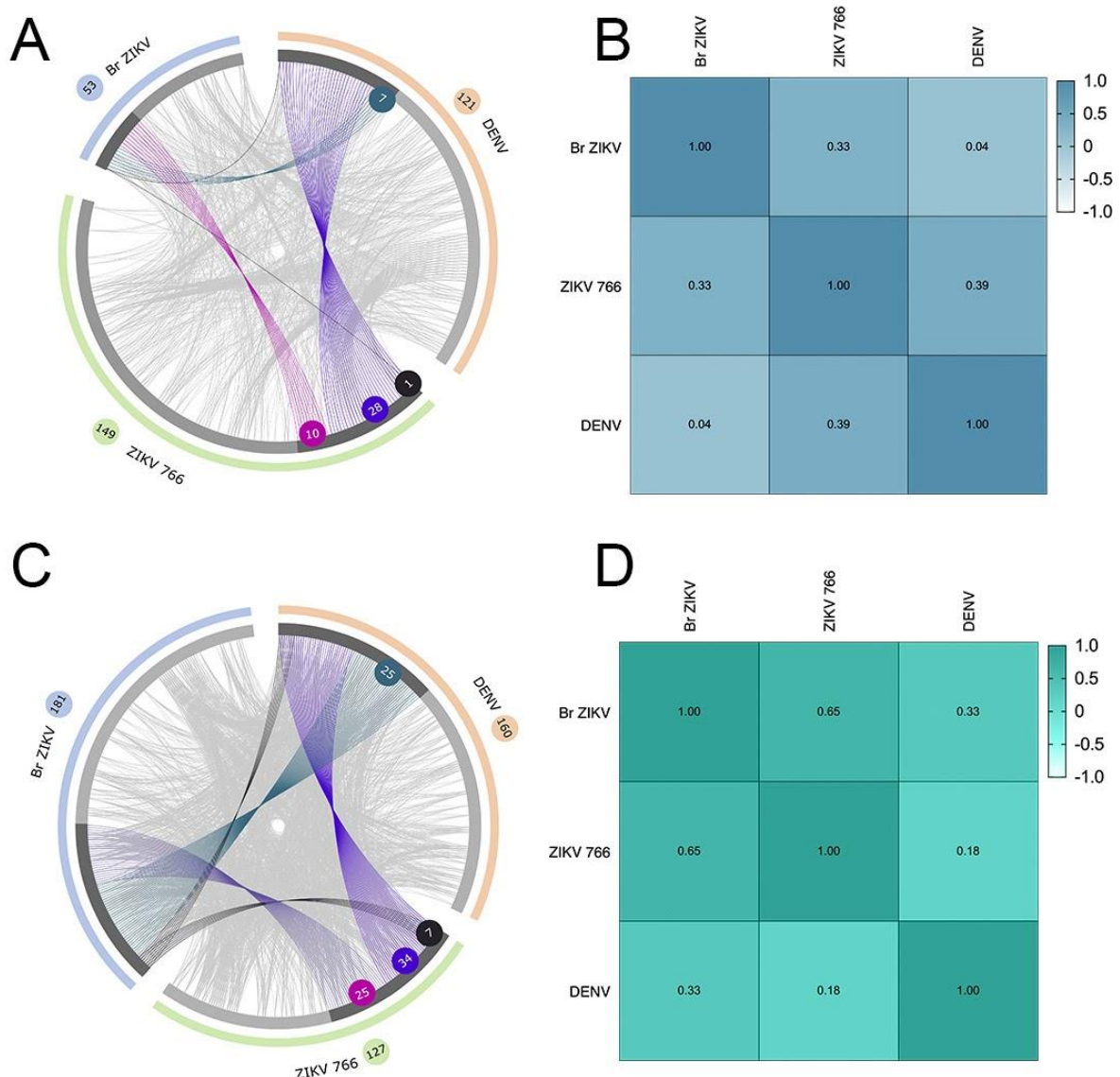


Figure 2. Comparison of regulated proteins found in neural stem cells (NSC) and neurospheres infected by ZIKV (Br and MR766 strains) and DENV. A. Overlap of proteins differentially regulated in NSCs, represented by chord diagram lines in purple (ZIKV MR766 and DENV), green (Br ZIKV and DENV), pink (Br ZIKV and MR766) and black for commonly found in all three viral strains. Light gray lines on the background are relative to the overlap of pathways and GO terms enriched by regulated proteins in NSCs. **B.** Pearson correlation of the effects of ZIKV strains and DENV on NSCs. **C.** Overlap of proteins differentially regulated in neurospheres, represented by chord diagram lines in purple (ZIKV MR766 and DENV), green (Br ZIKV and DENV), pink (Br ZIKV and MR766) and black for commonly found in all three virus strains. Light gray lines on the background are relative to the overlap of pathways and GO terms enriched by regulated

proteins in neurospheres. **D.** Pearson correlation of the effects of ZIKV strains and DENV on neurospheres.

3.1 ZIKV hijacks multiple pathways of cellular maintenance in NSCs and neurospheres

When exploring how different ZIKV virus strains can target neural cells and what some of their phenotypic consequences might be (Qian *et al.*, 2016; Gabriel *et al.*, 2017; Esser-Nobis *et al.*, 2019), several of the molecular dysregulations were varied among different models, strains and cell types. Previous indications that Br ZIKV effects could deplete neural stem cells (Garcez *et al.*, 2017) left unanswered questions regarding when the molecular effects of infections leading to major phenotypic changes first appear: in neural progenitor cells, or when those cells start to differentiate. Therefore, we looked deeper into the modulation occurring in neural cells by exploring affected proteins and pathways.

We identified a series of pathways enriched in both NSCs and neurospheres which revealed that a major target effect of ZIKV MR766 and Br ZIKV is to hijack the cellular machinery to perform viral transcription and replication. Beginning at the NSC stage, mRNA splicing, metabolism of RNA, nuclear transport, RNA degradation, protein folding, translation, protein processing in the endoplasmic reticulum (ER) and destabilizing microtubule-based movement are pathways constituting the main targets of ZIKVs (Figures 3A). These effects are essential for cell proliferation and growth and dysregulation culminates in cell cycle arrest of progenitor cells (Qian *et al.*, 2016; Tang *et al.*, 2016; Garcez *et al.*, 2017). During the neurosphere differentiation process, defects in cellular maintenance are enhanced, leading to a major cellular response to stress, including mitochondrial permeabilization, apoptosis and DNA change and repair, among other pathways (Figure 3B).

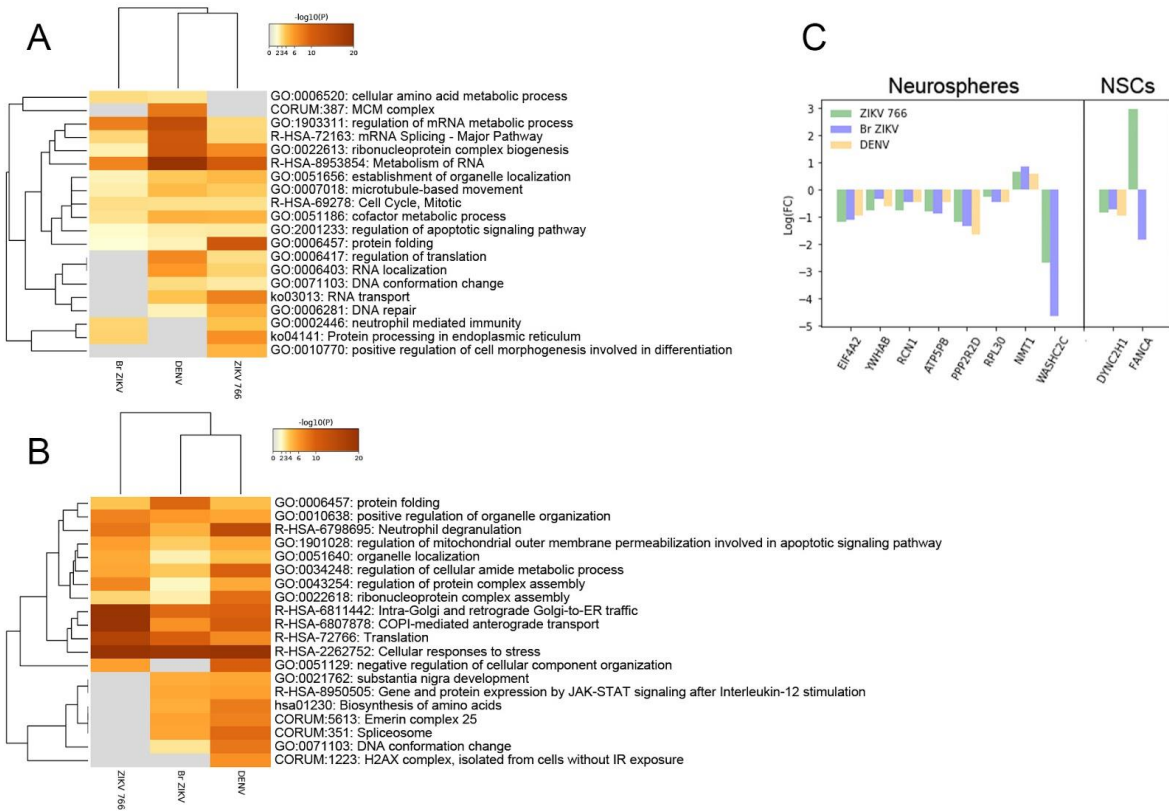


Figure 3. Comparison of pathways and proteins associated with NSCs and neurospheres infected by ZIKV (Br and MR766 strains) and DENV. Heatmap hierarchical clustering of enriched ontology terms and pathways altered due to differentially regulated proteins in **A.** NSCs and **B.** neurospheres. **C.** Differential expression data of commonly deregulated proteins among the ZIKV MR766, Br ZIKV and DENV infections in NSCs and neurospheres.

Although ZIKV and DENV infections shared several pathways, there were few differentially regulated proteins common to all three treatments. In NSCs, the only protein in common was cytoplasmic dynein 2, heavy chain 1 (DYNC2H1) (Figure 3C), a cellular motor protein with ATP binding activity that plays an important role in cell transport and division. DYNC2H1 showed consistent, downregulated expression in all viral strains compared to MOCK infected cells. DYNC2H1 variants have been associated with a lethal perinatal skeletal disorder (Chen et al., 2016) and a congenital malformation known as hypothalamic hamartoma (Fujita et al., 2019). Hence, those studies are in line with the association between DYNC2H1 and fetal malformations as a possible role in brain abnormalities induced by the Flaviviridae viruses, such as the congenital malformations, including microcephaly, caused by ZIKV (Calvet *et*

al., 2016; Cugola *et al.*, 2016), and neurological alterations linked to DENV (reviewed in Li *et al.*, 2017)

Regarding the neurospheres, 7 proteins were differentially regulated in both ZIKVs and DENV (Figure 3C), all of which showed a similar regulation in response to the viruses. Downregulated proteins were eukaryotic initiation factor 4A-II (EIF4A2), ribosomal protein L30 (RPL30), mostly when related to RNA metabolism, and 14-3-3 protein beta/alpha (YWHAB), ATP synthase peripheral stalk-membrane subunit B (ATP5PB), Reticulocalbin-1 (RCN1), and serine/threonine-protein phosphatase 2A (PPP2R2D), involved in ATP synthesis, cell signaling, and proliferation. These proteins are associated with the Hippo signaling pathway, which promotes the inactivation of YAP/TAZ transcription factors modulating the expression of genes related to cell growth, proliferation and apoptosis (Buttitta and Edgar, 2007). Previous studies have already linked ZIKV infection to the Hippo signaling (Garcia *et al.*, 2020), specifically regarding the control of cell proliferation, responses to stress, differentiation and renewal of stem cells in development and the apoptosis signaling pathway (Mo, Park and Guan, 2014). In contrast, the only protein that was found to be upregulated in all strains was glycylpeptide N-tetradecanoyltransferase 1 (NMT1; also known as N-myristoyltransferase 1), as shown in Figure 3C. NMT1 is a protein that performs N-terminal protein modifications (Rajala *et al.*, 2000) and is thought to be associated with mechanisms affecting viral replication of flaviviruses, as its inhibition impaired DENV replication (Suwanmanee *et al.*, 2019).

Although modulation of viral replication cellular machinery was present in ZIKVs and DENV, the direction of modulation diverged among the viruses. Our results revealed increased levels of FANCA (FA Complementation Group A) in ZIKV MR766-infected NSCs (Figure 3C), indicating a possible association between this strain and DNA damage, as FANCA activation is associated with the blockade of replication due to DNA damage (Deans and West, 2011). In Br ZIKV, however, this protein was observed downregulated. Downregulation of FA Complementation Group proteins have been associated with ZIKV infection, as a mechanism involved with viral replication and selective autophagy (Tiwari *et al.*, 2020).

In NSCs, the neuronal migration protein doublecortin, encoded by the gene DCX, was identified as downregulated in both ZIKV strains. This microtubule-associated protein is a key player in neuronal differentiation and migration (Gleeson *et al.*, 1999) and its downregulation, in both ZIKV MR766 and Br ZIKV, supports the evidence that these strains impact neurogenesis (Tang *et al.*, 2016; Gabriel *et al.*, 2017). DCX has been previously linked

to ZIKV infection and was also reported downregulated in transcriptomic and proteomic analyses of NPCs (Jiang et al., 2018). This shows that ZIKV infection is able to disrupt and reorganize signaling regulation throughout the infected cell.

In neurospheres, the main divergent protein between the two ZIKV strains is already known to be essential for viral replication and intracellular transport of viruses. WASHC2C (WASH Complex Subunit 2C) (Figure 3C) is associated with the endolysosomal system, lysosomal degradation and receptor recycling (Bartuzzi *et al.*, 2016; Hashimoto *et al.*, 2020) and was strongly downregulated in both ZIKV strains. WASH-depleted cells have been shown to display a collapsed endolysosomal system (Gomez *et al.*, 2012). Modifications in the aforementioned pathways suggest impaired cellular trafficking, affecting viral replication (Hashimoto *et al.*, 2020). Potentially aiming to escape from these host-cell mechanisms, the ZIKV-induced downregulation of WAHS2C might be associated with assured viral replication. These changes in turn deplete progenitors and disrupt the neuronal differentiation program due to interference in important pathways in NSCs and neurospheres by ZIKV infection.

3.2 The divergent modulation of pathways by ZIKV strains

ZIKV and DENV have shown distinct alterations on NSCs and neurospheres. ZIKV MR766 and DENV revealed a common modulated pattern of downregulated pathways in NSCs, whereas Br ZIKV revealed upregulated pathways (Figure 4A). This pattern, however, was not observed in neurospheres, where Br ZIKV was found to downregulate several pathways similarly to ZIKV MR766 and DENV in this 3D model (Figure 4B).

Despite being common to the three viruses, proteins involved in mRNA processes were, on average, upregulated in Br ZIKV infection of NSCs (Figure 4A); though DENV and ZIKV MR766 had major downregulation of proteins in this pathway. Another interesting aspect is the regulation of mRNA splicing, which was found upregulated in both ZIKV strains in NSCs and downregulated in DENV. However, in neurospheres, mRNA splicing was found upregulated in DENV (Figure 4A), indicating potential differences due to the distinct complexity of the models evaluated.

In addition to the previously mentioned dynein subunit DYNC2H1, in regards to cellular transport-related pathways, we also highlight biological processes of retrograde vesicle-mediated transport, Golgi to ER transport and Golgi organization, which might signal altered

protein conformation from the ER and have been observed in the ZIKV strains in NSCs and neurospheres. Moreover, NSCs showed downregulation of Ras-related protein Rab-6A (RAB6A) and RAB6B which are involved with cellular transport and secretory and endocytic pathways (Martinez and Goud, 1998) and RAB6B also plays a role in retrograde transport in neuronal cells (Wanschers *et al.*, 2007). RAB GTPases have been linked with viral replication mechanisms, especially within the late stages of viral replication (Spearman, 2018)

NSCs showed an upregulation of Ras-related protein Rap-1B (RAP1B), which exhibits GTPase activity (Scrima *et al.*, 2008) and is involved in biological processes such as the interleukin-12-mediated signaling pathway, neutrophil degranulation and negative regulation of synaptic vesicle exocytosis. Furthermore, RAP1B variants have been associated with congenital malformations (Niemann *et al.*, 2020). This might indicate a potential association involving ZIKV-induced altered expression of Ras GTPase and the development of congenital malformations.

Also regarding cellular transport alterations in NSCs, AKAP9 was found upregulated in ZIKV MR766 and downregulated in Br ZIKV (Supplementary Table 1), suggesting the existence of different mechanisms involving cellular transport in these viral strains. AKAP9 is a protein from the family of A-kinase anchor proteins (AKAPs), which are known for binding to the regulatory subunit of protein kinase A (PKA), arresting the holoenzyme to determined locations within the cell (Colledge and Scott, 1999). This gene encodes for proteins localized to the centrosome and the Golgi apparatus and its products interact with various signaling molecules from multiple signal transduction pathways (Witczak *et al.*, 1999; Larocca *et al.*, 2004). These results are in line with the fact that ZIKV and other flaviviruses are known to replicate in the ER (Reid, Airo and Hobman, 2015); however, the specifics regarding viral assembly within the ER remain elusive (Sirohi and Kuhn, 2017).

In the ZIKV MR766-infected NSCs, the differentially regulated proteins highlighted the following biological processes: translation initiation, viral transcription, nuclear-transcribed mRNA catabolic process, SRP-dependent cotranslational protein targeting membrane and nonsense-mediated decay (NMD). We also identified pathways involving the ribosome and RNA transport as shown in Figure 5A. Moreover, the downregulated proteins were mostly involved in L13a-mediated translational silencing of Ceruloplasmin expression, GTP hydrolysis and joining of the 60S ribosomal subunit (Supplementary Figure 1), evidencing potential alterations regarding translation and associated processes.

Concerning the pathways related to Br ZIKV in infected NSCs, we observed the deregulation of mRNA metabolic processes, RNA stability processes and mRNA splicing (Figure 5B), all with the majority of proteins in each pathway found to be upregulated (Supplementary Figure 1). In both NSCs and neurospheres infected with Br ZIKV, mRNA stability and binding were enriched pathways, including AUF1 (hnRNP D0). Moreover, we also observed pathways related to metabolic alterations including biosynthesis of amino acids and glucose metabolism, as observed in Figure 5B. Altered glucose metabolism has been previously associated with ZIKV infection in relation to important aspects involving viral replication (Sanchez and Lagunoff, 2015; Gilbert-Jaramillo *et al.*, 2019). The L-lactate dehydrogenase-like protein LDHAL6A, for instance, was found upregulated in ZIKV MR766-infected NSCs, indicating increased pyruvate metabolism; though it was downregulated in Br ZIKV-infected NSCs, evidencing potential metabolic differences caused by ZIKV strains.

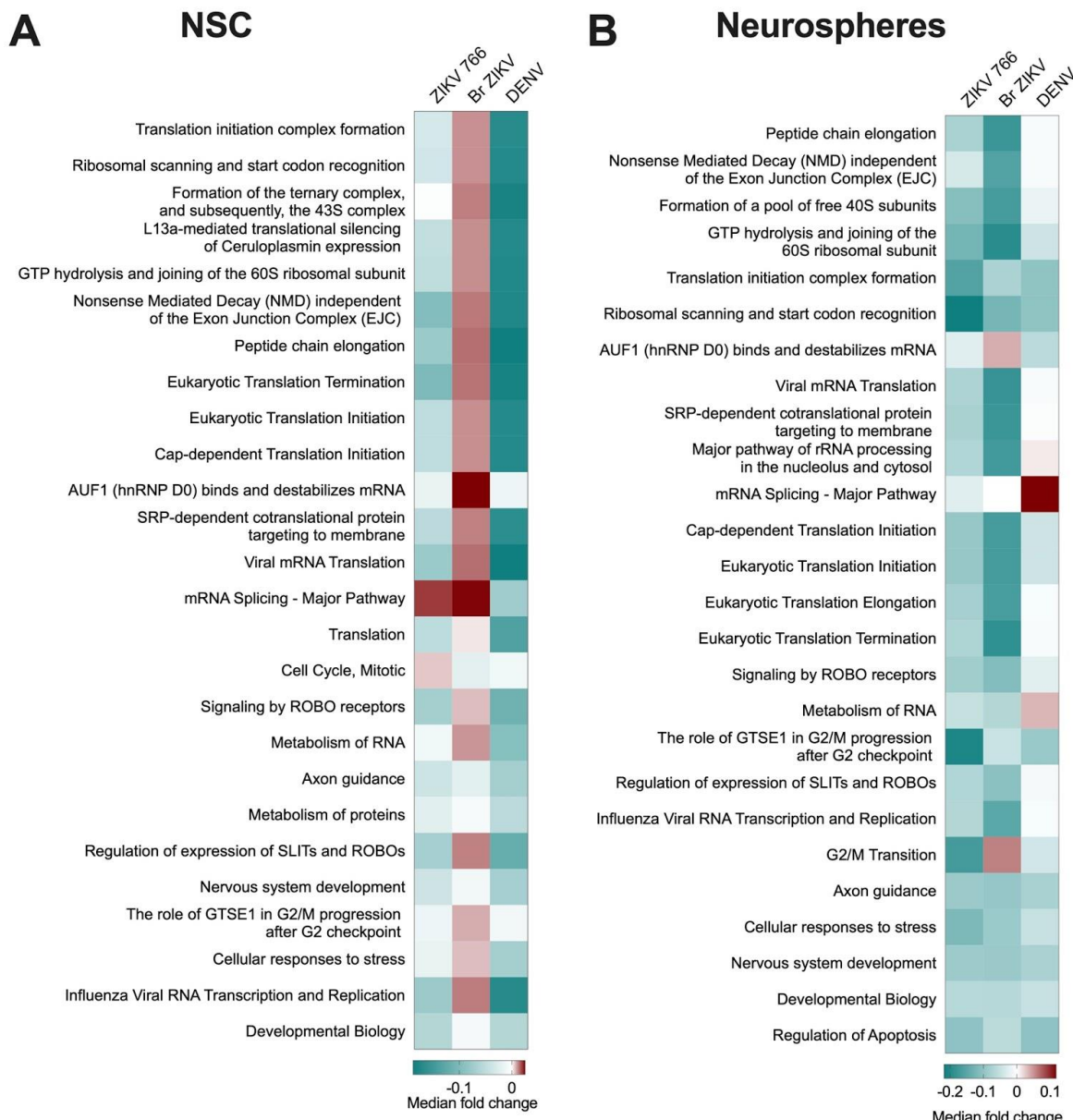


Figure 4. Regulation of pathways enriched in NSCs and neurospheres infected by ZIKV (Br and MR766 strains) and DENV. Heatmap showing the regulation of enriched pathways in **A.** NSCs and **B.** neurospheres, where colors represent the median fold change of proteins within the pathway.

Between NSCs and neurospheres, there are shared pathways involved with neurodevelopment, such as regulation of expression of SLITs and ROBO receptors. In NSCs, SLITs and ROBO signaling, along with transcription regulation mediated by RUNX3, presented the majority of proteins identified to be upregulated. SLITs and ROBO signaling play a role in axonal guidance, cell migration and proliferation (Dickson and Gilestro, 2006),

and RUNX3 acts in nervous system development, including the development of sensory neurons (Dykes *et al.*, 2010; Wang and Stifani, 2017).

Neurospheres infection by ZIKV MR766 affected pathways related to cell cycle regulation, as well as signaling involving NMDA receptors (NMDAr), metabolism of proteins, selective autophagy, cellular response to stress and nervous system development (Figure 6A). Regarding the NMDAr, its blockade has been shown to prevent neuronal death induced by ZIKV infection and as such, modulation of pathways involving NMDAr may be associated with neuronal damage induced by ZIKV (Costa *et al.*, 2017). Br ZIKV infection, however, showed cell cycle regulation to be enriched by the role of GTSE1 in G2/M progression after G2 checkpoint (Figure 6B) in a balance with the regulation of apoptosis. In neurospheres, ZIKV infection had effects on the metabolism of RNA, and differentially regulated proteins related to proteasomes -- which presented opposite patterns of expression when comparing ZIKV MR766 with Br ZIKV (Supplementary Figure 1) -- are a major cellular response to stress. These biological pathways can lead to effects on proteins controlling growth and proliferation, such as selenophosphate synthetase 1 (SEPHS1), found downregulated in both strains of ZIKV-infected neurospheres. SEPHS1 is essential for cellular proliferation and differentiation, and its gene knockout in Drosophila resulted in reduced brain size (Serras *et al.*, 2001). This evidence strengthens the association between ZIKV and congenital malformations.

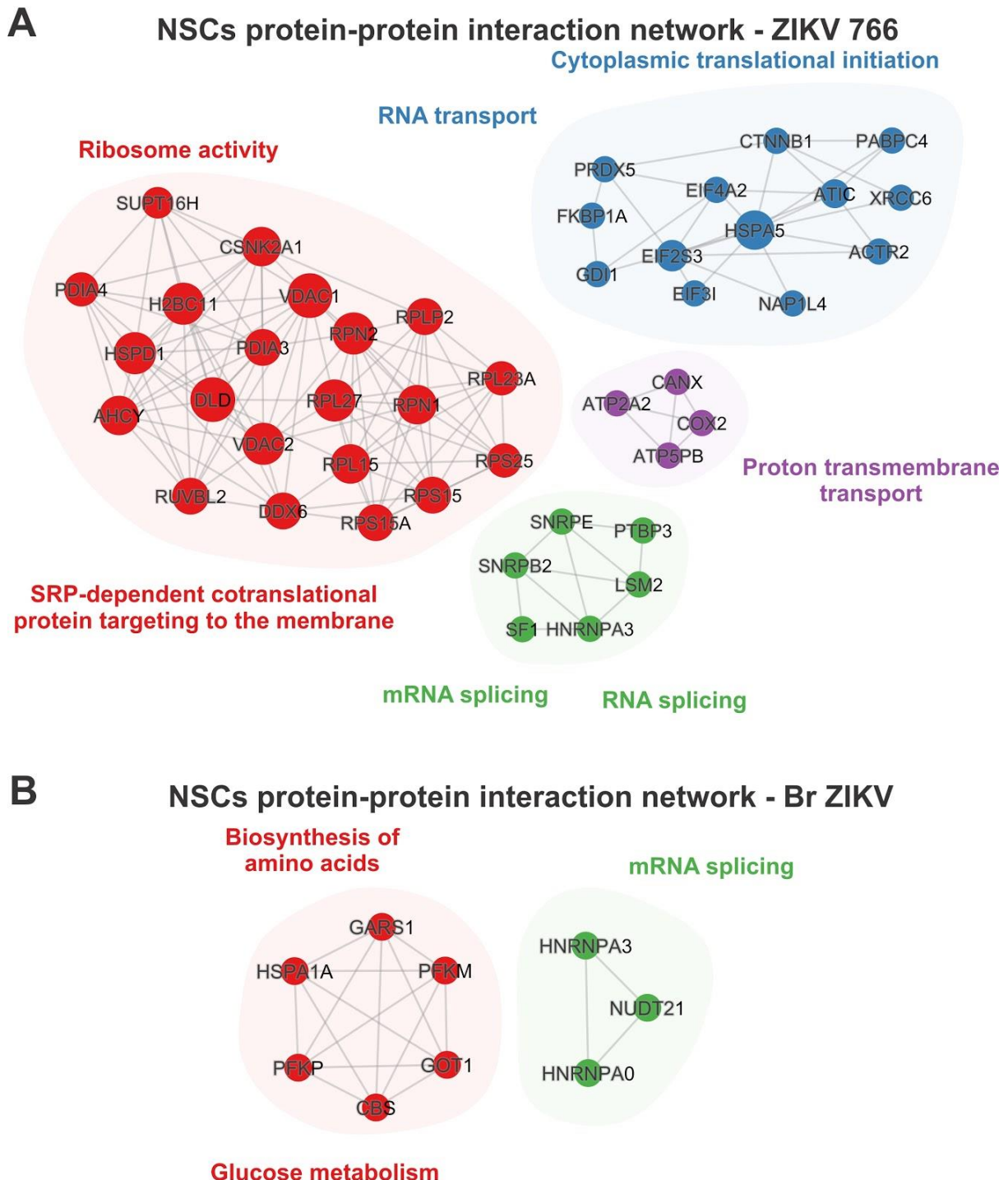


Figure 5 Protein-protein interaction network from the differentially regulated proteins infected by ZIKV in NSCs. A. Clustered interactions of proteins modulated by ZIKV MR766 in comparison to MOCK. In red, SRP-dependent cotranslational protein targeting the membrane ($\text{Log}_{10}(P) - 16.3$) and ribosome activity ($\text{Log}_{10}(P) - 12.9$). In blue, cytoplasmic translational initiation ($\text{Log}_{10}(P) - 6.3$) and RNA transport ($\text{Log}_{10}(P) - 6.0$). In green, RNA splicing, via transesterification reactions with bulged adenosine as a nucleophile ($\text{Log}_{10}(P) - 11.2$), mRNA splicing, via spliceosome ($\text{Log}_{10}(P) - 11.2$). In purple, proton transmembrane

transport ($\text{Log}_{10}(P) - 6.1$). **B.** Clustered interactions of proteins modulated by Br ZIKV in comparison to MOCK. The cluster in red represents the enrichment of biosynthesis of amino acids ($\text{Log}_{10}(P) - 9.1$) and glucose metabolism ($\text{Log}_{10}(P) - 6.2$); in green, mRNA splicing ($\text{Log}_{10}(P) - 6.6$).

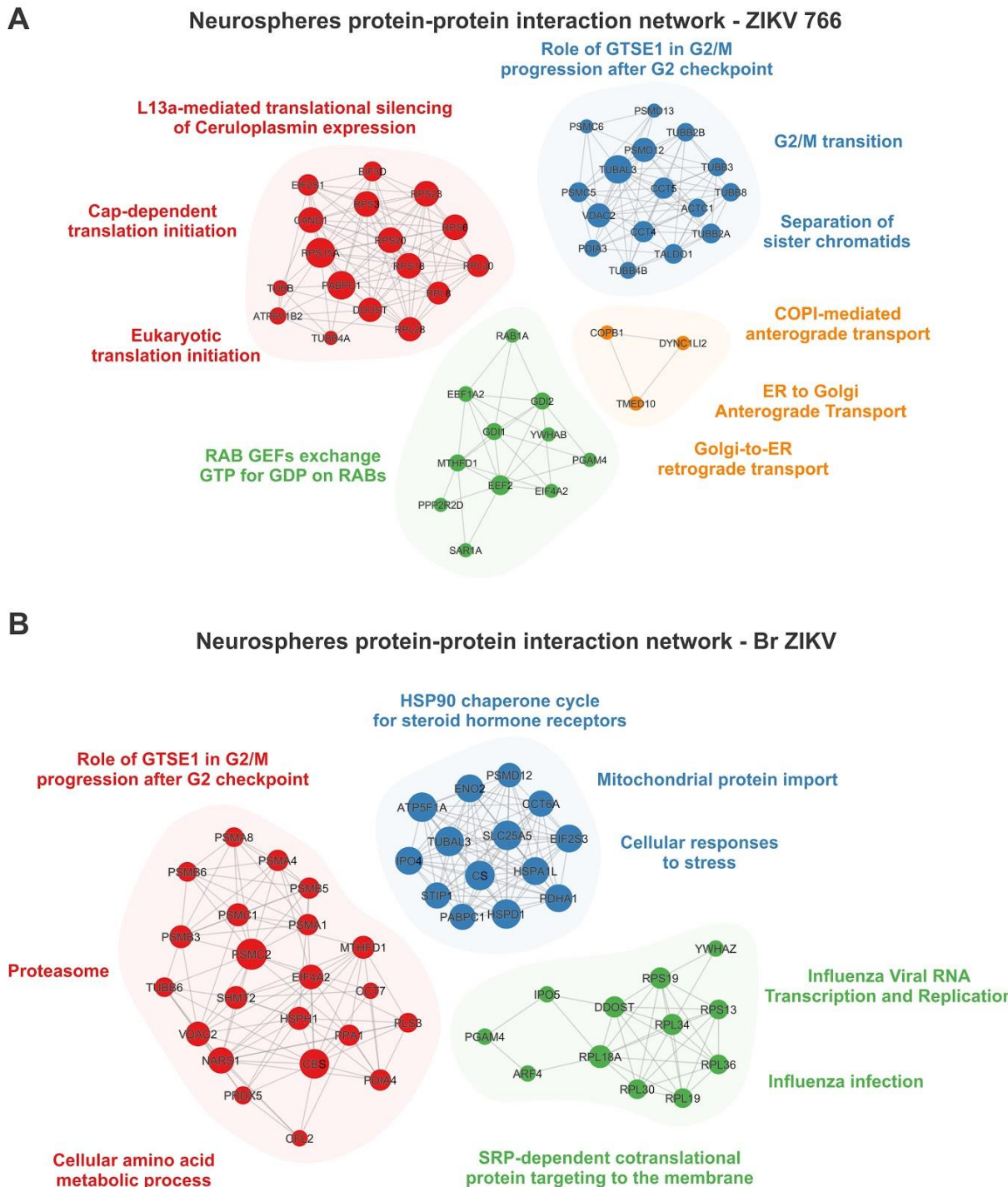


Figure 6. Protein-protein interaction network identified in the differentially regulated proteins infected by ZIKV in Neurospheres. A. Clustered interaction of proteins

modulated by ZIKV MR766 in comparison to MOCK. The red cluster was enriched for L13a-mediated translational silencing of Ceruloplasmin expression ($\text{Log}_{10}(P) -25.3$), eukaryotic translation initiation ($\text{Log}_{10}(P) -24.9$) and Cap-dependent translation initiation ($\text{Log}_{10}(P) -24.9$). The blue cluster was enriched for the role of GTSE1 in G2/M progression after G2 checkpoint ($\text{Log}_{10}(P) -22.0$), separation of sister chromatids ($\text{Log}_{10}(P) -17.9$) and G2/M transition ($\text{Log}_{10}(P) -17.9$). The green one was enriched for RAB GEFs exchange GTP for GDP on RABs ($\text{Log}_{10}(P) -5.3$). And the orange one for COPI-mediated anterograde transport ($\text{Log}_{10}(P) -7.3$), Golgi-to-ER retrograde transport ($\text{Log}_{10}(P) -7.0$) and ER to Golgi Anterograde Transport ($\text{Log}_{10}(P) -6.8$).

B. Clustered interaction of proteins modulated by Br ZIKV in comparison to MOCK. The cluster in red was enriched for the cellular amino acid metabolic process ($\text{Log}_{10}(P) -19$), the role of GTSE1 in G2/M progression after G2 checkpoint ($\text{Log}_{10}(P) -17.6$) and proteasome ($\text{Log}_{10}(P) -17.1$). The cluster in blue was enriched for the HSP90 chaperone cycle for steroid hormone receptors (SHR) ($\text{Log}_{10}(P) -5.6$), mitochondrial protein import ($\text{Log}_{10}(P) -5.4$) and cellular responses to stress ($\text{Log}_{10}(P) -5.2$). The cluster in green was enriched for SRP-dependent cotranslational protein targeting to the membrane ($\text{Log}_{10}(P) -16.6$), influenza Viral RNA Transcription and Replication ($\text{Log}_{10}(P) -15.9$) and influenza Infection ($\text{Log}_{10}(P) -15.4$).

Conclusion

Despite not reaching the point of being an epidemic emergency, understanding ZIKV strains and their divergent and similar mechanisms is important not only for the development of treatment strategies but also for the comprehension of congenital syndromes associated with the Br ZIKV in the outbreak of 2015. We compared the ZIKV infection in two different models, a two-dimensional (2D) NSC culture and a 3D neurosphere culture. This allowed us to gather information regarding differentially regulated proteins and biochemical pathways shared between ZIKV strains and DENV, as well as pathways exclusive to each. These results show that the proteomic fingerprint of ZIKV infection differs greatly depending on the developmental state of neural cells, in addition to the viral strain.

Conflict of Interest

The authors declare no competing financial interests.

Author Contributions

DMS, SKR, JMN and PPG conceived and designed the study. DJG and JMN performed *in silico* proteomic analyses. JMN and JSC performed mass spectrometry experiments. GSZ performed pathway analysis and interpretation. ECL and PPG cultured, infected and differentiated iPS-derived cells. DJG and JMN interpreted the data, wrote, edited and revised the manuscript. DMS and SKR coordinated the study. All authors contributed to the final version of the manuscript.

Funding

DGJ, JMN, GSZ and DMS are supported by the São Paulo Research Foundation (FAPESP, grant numbers 2018/25439-9; 2017/25055-3; 2014/21035-0; 2018/14666-4; 2017/25588-1.

Acknowledgments

The authors thank Gabriela Vitoria, Ismael Gomes, and Paulo Baldasso for their excellent technical support and Bradley Smith, MSc for critical comments and English review support during the process.

References

- Bader, G. D. and Hogue, C. W. V. (2003) ‘An automated method for finding molecular complexes in large protein interaction networks’, *BMC bioinformatics*, 4, p. 2.
- Bartuzi, P. *et al.* (2016) ‘CCC- and WASH-mediated endosomal sorting of LDLR is required for normal clearance of circulating LDL’, *Nature communications*, 7, p. 10961.
- Bayer, A. *et al.* (2016) ‘Type III Interferons Produced by Human Placental Trophoblasts Confer Protection against Zika Virus Infection’, *Cell Host & Microbe*, pp. 705–712. doi: 10.1016/j.chom.2016.03.008.
- Buttitta, L. A. and Edgar, B. A. (2007) ‘How size is controlled: from Hippos to Yorkies’, *Nature Cell Biology*, pp. 1225–1227. doi: 10.1038/ncb1107-1225.
- Calvet, G. *et al.* (2016) ‘Detection and sequencing of Zika virus from amniotic fluid of fetuses with microcephaly in Brazil: a case study’, *The Lancet Infectious Diseases*, pp. 653–660. doi: 10.1016/s1473-3099(16)00095-5.

- Costa, V. V. *et al.* (2017) ‘N-Methyl-d-Aspartate (NMDA) Receptor Blockade Prevents Neuronal Death Induced by Zika Virus Infection’, *mBio*, 8(2). doi: 10.1128/mBio.00350-17.
- Cugola, F. R. *et al.* (2016) ‘The Brazilian Zika virus strain causes birth defects in experimental models’, *Nature*, pp. 267–271. doi: 10.1038/nature18296.
- Dang, J. *et al.* (2016) ‘Zika Virus Depletes Neural Progenitors in Human Cerebral Organoids through Activation of the Innate Immune Receptor TLR3’, *Cell Stem Cell*, pp. 258–265. doi: 10.1016/j.stem.2016.04.014.
- Dickson, B. J. and Gilestro, G. F. (2006) ‘Regulation of commissural axon pathfinding by slit and its Robo receptors’, *Annual review of cell and developmental biology*, 22, pp. 651–675.
- Dykes, I. M. *et al.* (2010) ‘Brn3a regulates neuronal subtype specification in the trigeminal ganglion by promoting Runx expression during sensory differentiation’, *Neural development*, 5, p. 3.
- Esser-Nobis, K. *et al.* (2019) ‘Comparative Analysis of African and Asian Lineage-Derived Zika Virus Strains Reveals Differences in Activation of and Sensitivity to Antiviral Innate Immunity’, *Journal of virology*, 93(13). doi: 10.1128/JVI.00640-19.
- Gabriel, E. *et al.* (2017) ‘Recent Zika Virus Isolates Induce Premature Differentiation of Neural Progenitors in Human Brain Organoids’, *Cell stem cell*, 20(3), pp. 397–406.e5.
- Garcez, P. P. *et al.* (2016) ‘Zika virus impairs growth in human neurospheres and brain organoids’, *Science*, pp. 816–818. doi: 10.1126/science.aaf6116.
- Garcez, P. P. *et al.* (2017) ‘Zika virus disrupts molecular fingerprinting of human neurospheres’, *Scientific Reports*. doi: 10.1038/srep40780.
- Garcia, G. *et al.* (2020) ‘Hippo Signaling Pathway Has a Critical Role in Zika Virus Replication and in the Pathogenesis of Neuroinflammation’, *The American Journal of Pathology*, pp. 844–861. doi: 10.1016/j.ajpath.2019.12.005.
- Gilbert-Jaramillo, J. *et al.* (2019) ‘The potential contribution of impaired brain glucose metabolism to congenital Zika syndrome’, *Journal of anatomy*, 235(3), pp. 468–480.
- Giurgiu, M. *et al.* (2019) ‘CORUM: the comprehensive resource of mammalian protein complexes—2019’, *Nucleic Acids Research*, pp. D559–D563. doi: 10.1093/nar/gky973.

- Gomez, T. S. *et al.* (2012) ‘Trafficking defects in WASH-knockout fibroblasts originate from collapsed endosomal and lysosomal networks’, *Molecular biology of the cell*, 23(16), pp. 3215–3228.
- Hashimoto, Y. *et al.* (2020) ‘Temporal dynamics of protein complex formation and dissociation during human cytomegalovirus infection’, *Nature communications*, 11(1), p. 806.
- Jassal, B. *et al.* (2019) ‘The reactome pathway knowledgebase’, *Nucleic Acids Research*. doi: 10.1093/nar/gkz1031.
- Jiang, X *et al.* (2018). ‘Proteomic Analysis of Zika Virus Infected Primary Human Fetal Neural Progenitors Suggests a Role for Doublecortin in the Pathological Consequences of Infection in the Cortex’, *Frontiers in Microbiology*, 9, 1067.
- Kanehisa, M. *et al.* (2016) ‘KEGG as a reference resource for gene and protein annotation’, *Nucleic acids research*, 44(D1), pp. D457–62.
- Lancaster, M. A. *et al.* (2013) ‘Cerebral organoids model human brain development and microcephaly’, *Nature*, pp. 373–379. doi: 10.1038/nature12517.
- Larocca, M. C. *et al.* (2004) ‘AKAP350 interaction with cdc42 interacting protein 4 at the Golgi apparatus’, *Molecular biology of the cell*, 15(6), pp. 2771–2781.
- Ledur, P. F. *et al.* (2020) ‘Zika virus infection leads to mitochondrial failure, oxidative stress and DNA damage in human iPSC-derived astrocytes’, *Scientific reports*, 10(1), p. 1218.
- Li, G.-H. *et al.* (2017) ‘Neurological Manifestations of Dengue Infection’, *Frontiers in cellular and infection microbiology*, 7, p. 449.
- Li, H. *et al.* (2016) ‘Zika Virus Infects Neural Progenitors in the Adult Mouse Brain and Alters Proliferation’, *Cell stem cell*, 19(5), pp. 593–598.
- Miranda-Filho, D. de B. *et al.* (2016) ‘Initial Description of the Presumed Congenital Zika Syndrome’, *American Journal of Public Health*, pp. 598–600. doi: 10.2105/ajph.2016.303115.
- Mo, J.-S., Park, H. W. and Guan, K.-L. (2014) ‘The Hippo signaling pathway in stem cell biology and cancer’, *EMBO reports*, 15(6), pp. 642–656.

- Niemann, J. H. *et al.* (2020) ‘De novo missense variants in the RAP1B gene identified in two patients with syndromic thrombocytopenia’, *Clinical genetics*. doi: 10.1111/cge.13807.
- Qian, X. *et al.* (2016) ‘Brain-Region-Specific Organoids Using Mini-bioreactors for Modeling ZIKV Exposure’, *Cell*, 165(5), pp. 1238–1254.
- Rajala, R. V. *et al.* (2000) ‘N-myristoyltransferase’, *Molecular and cellular biochemistry*, 204(1-2), pp. 135–155.
- Sanchez, E. L. and Lagunoff, M. (2015) ‘Viral activation of cellular metabolism’, *Virology*, 479-480, pp. 609–618.
- Scrima, A. *et al.* (2008) ‘The Rap–RapGAP complex: GTP hydrolysis without catalytic glutamine and arginine residues’, *The EMBO journal*, 27(7), pp. 1145–1153.
- Serras, F. *et al.* (2001) ‘The Drosophila selenophosphate synthetase (selD) gene is required for development and cell proliferation’, *BioFactors*, pp. 143–149. doi: 10.1002/biof.5520140119.
- Shevchenko, A. *et al.* (2006) ‘In-gel digestion for mass spectrometric characterization of proteins and proteomes’, *Nature protocols*, 1(6), pp. 2856–2860.
- Sirohi, D. and Kuhn, R. J. (2017) ‘Zika Virus Structure, Maturation, and Receptors’, *The Journal of infectious diseases*, 216(suppl_10), pp. S935–S944.
- Spearman, P. (2018) ‘Viral interactions with host cell Rab GTPases’, *Small GTPases*, 9(1-2), pp. 192–201.
- Suwanmanee, S. *et al.* (2019) ‘Inhibition of N -myristoyltransferase1 affects dengue virus replication’, *MicrobiologyOpen*, 8(9), p. e52065.
- Szklarczyk, D. *et al.* (2018) ‘STRING v11: protein–protein association networks with increased coverage, supporting functional discovery in genome-wide experimental datasets’, *Nucleic acids research*, 47(D1), pp. D607–D613.
- Tang, H. *et al.* (2016) ‘Zika Virus Infects Human Cortical Neural Progenitors and Attenuates Their Growth’, *Cell Stem Cell*, pp. 587–590. doi: 10.1016/j.stem.2016.02.016.
- Tiwari, S. K. *et al.* (2020) ‘Zika virus depletes neural stem cells and evades selective autophagy by suppressing the Fanconi anemia protein FANCC’, *EMBO reports*, p. e49183.

- Wang, J. W. and Stifani, S. (2017) ‘Roles of Runx Genes in Nervous System Development’, *Advances in experimental medicine and biology*, 962, pp. 103–116.
- Wanschers, B. F. J. *et al.* (2007) ‘A role for the Rab6B Bicaudal-D1 interaction in retrograde transport in neuronal cells’, *Experimental cell research*, 313(16), pp. 3408–3420.
- ‘WHO | Zika epidemiology update’ (2019). Available at: <https://www.who.int/emergencies/diseases/zika/epidemiology-update/en/> (Accessed: 19 November 2020).
- Witczak, O. *et al.* (1999) ‘Cloning and characterization of a cDNA encoding an A-kinase anchoring protein located in the centrosome, AKAP450’, *The EMBO journal*, 18(7), pp. 1858–1868.
- Woods, C. G. *et al.* (2005) ‘Autosomal Recessive Primary Microcephaly (MCPH): A Review of Clinical, Molecular, and Evolutionary Findings’, *The American Journal of Human Genetics*, pp. 717–728. doi: 10.1086/429930.
- Woods, C. G. and Parker, A. (2013) ‘Investigating microcephaly’, *Archives of Disease in Childhood*, pp. 707–713. doi: 10.1136/archdischild-2012-302882.
- Zhang, F. *et al.* (2016) ‘Molecular signatures associated with ZIKV exposure in human cortical neural progenitors’, *Nucleic Acids Research*, pp. 8610–8620. doi: 10.1093/nar/gkw765.
- Zhou, Y. *et al.* (2019) ‘Metascape provides a biologist-oriented resource for the analysis of systems-level datasets’, *Nature communications*, 10(1), p. 1523.

5 CONCLUSÃO

O Zika vírus é um arbovírus pertencente à família Flaviviridae. Apesar de não constituir uma atual emergência de saúde pública, casos de infecção continuam sendo reportados e ainda existe a necessidade de se compreender as alterações causadas por tal infecção viral, incluindo as diferenças entre as cepas circulantes, de modo a desvendar as relações entre a infecção e as alterações neurológicas decorrentes, destacando o desenvolvimento da síndrome congênita, incluindo os quadros de microcefalia em neonatos de mães infectadas pela cepa brasileira de ZIKV.

Ademais, dentro do cenário atual em que estamos inseridos, com a pandemia do novo coronavírus, observa-se a importância do estudo dos vírus, a compreensão de seus mecanismos, buscando o desenvolvimento de medidas profiláticas, como as vacinas, além de tratamentos. Para tanto, modelos *in vitro* utilizando iPSCs e organoides, possibilitam a investigação relacionada com diferentes estágios do desenvolvimento.

Neste trabalho foi realizada a análise proteômica de células tronco neurais e neuroesferas infectadas com cepas brasileira e africana do ZIKV (Br ZIKV e MR766) em comparação ao DENV. Em nossas análises foi possível observar padrões distintos de alterações não só entre as cepas estudadas, mas também em relação aos modelos *in vitro*. Tais distinções podem se vincular à própria diferença em complexidade dos modelos avaliados, uma vez que as neuroesferas consistem um estágio do neurodesenvolvimento mais avançado em relação às células tronco neurais.

Com os dados obtidos, evidenciamos a presença de alterações em proteínas e processos biológicos relacionados à neurogênese, transporte celular, metabolismo de energia, ciclo celular e processamento de RNA, tanto nas NSCs como nas neuroesferas. No tocante às NSCs, cabe ressaltar as vias de sinalização envolvendo a regulação do ciclo celular e a sinalização apoptótica, além da proteína DCX, que atua na migração e diferenciação neural (Jiang et al., 2018), sendo identificada negativamente reguladas em ambas as cepas de ZIKV (ZIKV 766 e Br ZIKV), constituindo um potencial mecanismo associado às alterações neurológicas induzidas pela infecção por ZIKV.

Já em relação às neuroesferas, foram identificadas proteínas relacionadas à via de sinalização Hippo, reportada como sendo essencial para aspectos de replicação viral. Ademais, também relacionada com mecanismos envolvidos com a replicação viral (Garcia et al., 2020), foi identificada a proteína NMT1, apresentando-se positivamente regulada nas três cepas virais

(ZIKV 766, Br ZIKV e DENV) (Suwanmanee et al., 2019). Outra proteína potencialmente relevante identificada nas neuroesferas corresponde à SEPHS1, negativamente regulada em ambas as cepas de ZIKV (ZIKV 766 e Br ZIKV). De acordo com a literatura, o *knockout* desse gene *in vivo* foi associado à redução do volume cerebral (Serras et al., 2001). Deste modo a investigação de SEPHS1 em relação à infecção por ZIKV pode fornecer informações acerca das alterações neurais induzidas por tais flavivírus, especialmente no que se refere ao desenvolvimento do quadro da microcefalia.

Ademais, observamos um padrão distinto de expressão especialmente focado na modulação das vias pela cepa do Br ZIKV, que pode se relacionar com potenciais alterações relacionadas com o neurodesenvolvimento, contribuindo para a compreensão das alterações moleculares induzidas pelo ZIKV, às quais resultam em distúrbios congênitos.

Portanto, neste trabalho, com os dados de proteômica gerados, foi possível corroborar informações previamente conhecidas acerca da infecção por ZIKV e DENV, bem como a identificação de outras proteínas e processos biológicos que podem contribuir para a elucidação dos mecanismos moleculares desencadeados pela infecção por tais cepas.

6 REFERÊNCIAS BIBLIOGRÁFICAS (INTRODUÇÃO E CONCLUSÃO)

- Acevedo, J., Casanova, M. F., Antonini, A. C., & Morales, H. (1982). Acute polyneuritis associated with dengue. *The Lancet*, 1(8285), 1357.
- Andrews, G. L., Simons, B. L., Young, J. B., Hawkridge, A. M., & Muddiman, D. C. (2011). Performance characteristics of a new hybrid quadrupole time-of-flight tandem mass spectrometer (TripleTOF 5600). *Analytical Chemistry*, 83(13), 5442–5446.
- Bayer, A., Lennemann, N. J., Ouyang, Y., Bramley, J. C., Morosky, S., Marques, E. T. D. A., Jr, Cherry, S., Sadovsky, Y., & Coyne, C. B. (2016). Type III Interferons Produced by Human Placental Trophoblasts Confer Protection against Zika Virus Infection. *Cell Host & Microbe*, 19(5), 705–712.
- Calvet, G., Aguiar, R. S., Melo, A. S. O., Sampaio, S. A., de Filippis, I., Fabri, A., Araujo, E. S. M., de Sequeira, P. C., de Mendonça, M. C. L., de Oliveira, L., Tschoeke, D. A., Schrago, C. G., Thompson, F. L., Brasil, P., Dos Santos, F. B., Nogueira, R. M. R., Tanuri, A., & de Filippis, A. M. B. (2016). Detection and sequencing of Zika virus from amniotic fluid of fetuses with microcephaly in Brazil: a case study. *The Lancet Infectious Diseases*, 16(6), 653–660.
- Cox, J., & Mann, M. (2008). MaxQuant enables high peptide identification rates, individualized p.p.b.-range mass accuracies and proteome-wide protein quantification. *Nature Biotechnology*, 26(12), 1367–1372.
- Cugola, F. R., Fernandes, I. R., Russo, F. B., Freitas, B. C., Dias, J. L. M., Guimarães, K. P., Benazzato, C., Almeida, N., Pignatari, G. C., Romero, S., Polonio, C. M., Cunha, I., Freitas, C. L., Brandão, W. N., Rossato, C., Andrade, D. G., Faria, D. de P., Garcez, A. T., Buchpigel, C. A., ... Beltrão-Braga, P. C. B. (2016). The Brazilian Zika virus strain causes birth defects in experimental models. *Nature*, 534(7606), 267–271.
- Dang, J., Tiwari, S. K., Lichinchi, G., Qin, Y., Patil, V. S., Eroshkin, A. M., & Rana, T. M. (2016). Zika Virus Depletes Neural Progenitors in Human Cerebral Organoids through Activation of the Innate Immune Receptor TLR3. *Cell Stem Cell*, 19(2), 258–265.
- Dick, G. W. A., Kitchen, S. F., & Haddow, A. J. (1952). Zika Virus (I). Isolations and serological specificity. In *Transactions of the Royal Society of Tropical Medicine and Hygiene* (Vol. 46, Issue 5, pp. 509–520). [https://doi.org/10.1016/0035-9203\(52\)90042-4](https://doi.org/10.1016/0035-9203(52)90042-4)

- Fauci, A. S., & Morens, D. M. (2016). Zika virus in the Americas — yet another arbovirus threat. *The New England Journal of Medicine*, 374(7), 601–604.
- Fenn, J. B., Mann, M., Meng, C. K., Wong, S. F., & Whitehouse, C. M. (1989). Electrospray ionization for mass spectrometry of large biomolecules. *Science*, 246(4926), 64–71.
- Garcez, P. P., Loiola, E. C., Madeiro da Costa, R., Higa, L. M., Trindade, P., Delvecchio, R., Nascimento, J. M., Brindeiro, R., Tanuri, A., & Rehen, S. K. (2016). Zika virus impairs growth in human neurospheres and brain organoids. *Science*, 352(6287), 816–818.
- Garcez, P. P., Nascimento, J. M., de Vasconcelos, J. M., Madeiro da Costa, R., Delvecchio, R., Trindade, P., Loiola, E. C., Higa, L. M., Cassoli, J. S., Vitória, G., Sequeira, P. C., Sochacki, J., Aguiar, R. S., Fuzii, H. T., de Filippis, A. M. B., da Silva Gonçalves Vianez Júnior, J. L., Tanuri, A., Martins-de-Souza, D., & Rehen, S. K. (2017). Zika virus disrupts molecular fingerprinting of human neurospheres. *Scientific Reports*, 7, 40780.
- Garcia, G., Jr, Paul, S., Beshara, S., Ramanujan, V. K., Ramaiah, A., Nielsen-Saines, K., Li, M. M. H., French, S. W., Morizono, K., Kumar, A., & Arumugaswami, V. (2020). Hippo Signaling Pathway Has a Critical Role in Zika Virus Replication and in the Pathogenesis of Neuroinflammation. *The American Journal of Pathology*, 190(4), 844–861.
- Giles, K., Pringle, S. D., Worthington, K. R., Little, D., Wildgoose, J. L., & Bateman, R. H. (2004). Applications of a travelling wave-based radio-frequency-only stacked ring ion guide. *Rapid Communications in Mass Spectrometry: RCM*, 18(20), 2401–2414.
- Gillette, M. A., & Carr, S. A. (2013). Quantitative analysis of peptides and proteins in biomedicine by targeted mass spectrometry. *Nature Methods*, 10(1), 28–34.
- Gulland, A. (2016). Zika virus is a global public health emergency, declares WHO. *BMJ* , 352, i657.
- Guzman, M. G., & Harris, E. (2015). Dengue. *The Lancet*, 385(9966), 453–465.
- Han, L., Ao, X., Lin, S., Guan, S., Zheng, L., Han, X., & Ye, H. (2019). Quantitative Comparative Proteomics Reveal Biomarkers for Dengue Disease Severity. *Frontiers in Microbiology*, 10, 2836.
- Heaton, N. S., & Randall, G. (2010). Dengue virus-induced autophagy regulates lipid metabolism. *Cell Host & Microbe*, 8(5), 422–432.

- Hoffmann, E. de, & Stroobant, V. (2007). Mass spectrometry: principles and applications. *Mass Spectrometry Reviews*, 29. https://research.usc.edu.au/discovery/fulldisplay/ alma996377002621/61USC_INST:Resear chRepository
- Huang, D. W., Sherman, B. T., & Lempicki, R. A. (2009). Systematic and integrative analysis of large gene lists using DAVID bioinformatics resources. *Nature Protocols*, 4(1), 44–57.
- Jassal, B., Matthews, L., Viteri, G., Gong, C., Lorente, P., Fabregat, A., Sidiropoulos, K., Cook, J., Gillespie, M., Haw, R., Loney, F., May, B., Milacic, M., Rothfels, K., Sevilla, C., Shamovsky, V., Shorser, S., Varusai, T., Weiser, J., ... D'Eustachio, P. (2020). The reactome pathway knowledgebase. *Nucleic Acids Research*, 48(D1), D498–D503.
- Jiang, X., Dong, X., Li, S.-H., Zhou, Y.-P., Rayner, S., Xia, H.-M., Gao, G. F., Yuan, H., Tang, Y.-P., & Luo, M.-H. (2018). Proteomic Analysis of Zika Virus Infected Primary Human Fetal Neural Progenitors Suggests a Role for Doublecortin in the Pathological Consequences of Infection in the Cortex. *Frontiers in Microbiology*, 9, 1067.
- Karas, M., & Hillenkamp, F. (1988). Laser desorption ionization of proteins with molecular masses exceeding 10,000 daltons. *Analytical Chemistry*, 60(20), 2299–2301.
- Keller, J. M., & Frega, M. (2019). Past, Present, and Future of Neuronal Models In Vitro. *Advances in Neurobiology*, 22, 3–17.
- Koraka, P., Murgue, B., Deparis, X., Van Gorp, E. C. M., Setiati, T. E., Osterhaus, A. D. M. E., & Groen, J. (2004). Elevation of soluble VCAM-1 plasma levels in children with acute dengue virus infection of varying severity. *Journal of Medical Virology*, 72(3), 445–450.
- Lancaster, M. A., Renner, M., Martin, C.-A., Wenzel, D., Bicknell, L. S., Hurles, M. E., Homfray, T., Penninger, J. M., Jackson, A. P., & Knoblich, J. A. (2013). Cerebral organoids model human brain development and microcephaly. *Nature*, 501(7467), 373–379.
- Levin, Y., Hradetzky, E., & Bahn, S. (2011). Quantification of proteins using data-independent analysis (MSE) in simple and complex samples: a systematic evaluation. *Proteomics*, 11(16), 3273–3287.
- Li, G.-Z., Vissers, J. P. C., Silva, J. C., Golick, D., Gorenstein, M. V., & Geromanos, S. J. (2009). Database searching and accounting of multiplexed precursor and product ion spectra

from the data independent analysis of simple and complex peptide mixtures. *Proteomics*, 9(6), 1696–1719.

Martines, R. B., Bhatnagar, J., Kelly Keating, M., Silva-Flannery, L., Muehlenbachs, A., Gary, J., Goldsmith, C., Hale, G., Ritter, J., Rollin, D., Shieh, W.-J., Luz, K. G., de Oliveira Ramos, A. M., Davi, H. P. F., de Oliveria, W. K., Lanciotti, R., Lambert, A., & Zaki, S. (2016). Notes from the Field: Evidence of Zika Virus Infection in Brain and Placental Tissues from Two Congenitally Infected Newborns and Two Fetal Losses — Brazil, 2015. In *MMWR. Morbidity and Mortality Weekly Report* (Vol. 65, Issue 06, pp. 1–2). <https://doi.org/10.15585/mmwr.mm6506e1er>

Martins-de-Souza, D. (2011). Proteomics as a tool for understanding schizophrenia. *Clinical Psychopharmacology and Neuroscience: The Official Scientific Journal of the Korean College of Neuropsychopharmacology*, 9(3), 95–101.

Martins-de-Souza, D., Cassoli, J. S., Nascimento, J. M., Hensley, K., Guest, P. C., Pinzon-Velasco, A. M., & Turck, C. W. (2015). The protein interactome of collapsin response mediator protein-2 (CRMP2/DPYSL2) reveals novel partner proteins in brain tissue. *PROTEOMICS--Clinical Applications*, 9(9-10), 817–831.

Miranda-Filho, D. de B., de Barros Miranda-Filho, D., Martelli, C. M. T., de Alencar Ximenes, R. A., Araújo, T. V. B., Rocha, M. A. W., Ramos, R. C. F., Dhalia, R., de Oliveira França, R. F., de Azevedo Marques Júnior, E. T., & Rodrigues, L. C. (2016). Initial Description of the Presumed Congenital Zika Syndrome. In *American Journal of Public Health* (Vol. 106, Issue 4, pp. 598–600). <https://doi.org/10.2105/ajph.2016.303115>

Oliveira, B. M., Coorssen, J. R., & Martins-de-Souza, D. (2014). 2DE: the phoenix of proteomics. *Journal of Proteomics*, 104, 140–150.

Organization, W. H., & Others. (2012). Global strategy for dengue prevention and control 2012-2020.

https://apps.who.int/iris/bitstream/handle/10665/75303/9789241504034_eng.pdf

Petersen, L. R., Jamieson, D. J., Powers, A. M., & Honein, M. A. (2016). Zika Virus. In *New England Journal of Medicine* (Vol. 374, Issue 16, pp. 1552–1563). <https://doi.org/10.1056/nejmra1602113>

- Pitt, J. J. (2009). Principles and applications of liquid chromatography-mass spectrometry in clinical biochemistry. *The Clinical Biochemist. Reviews / Australian Association of Clinical Biochemists*, 30(1), 19–34.
- Porter, C. J., Beynon, J. H., & Ast, T. (1981). The modern mass spectrometer—a complete chemical laboratory. *Journal of Mass Spectrometry: JMS*, 16(3), 101–114.
- Qian, X., Nguyen, H. N., Song, M. M., Hadiono, C., Ogden, S. C., Hammack, C., Yao, B., Hamersky, G. R., Jacob, F., Zhong, C., Yoon, K.-J., Jeang, W., Lin, L., Li, Y., Thakor, J., Berg, D. A., Zhang, C., Kang, E., Chickering, M., ... Ming, G.-L. (2016). Brain-Region-Specific Organoids Using Mini-bioreactors for Modeling ZIKV Exposure. *Cell*, 165(5), 1238–1254.
- Reynolds, B. A., & Weiss, S. (1992). Generation of neurons and astrocytes from isolated cells of the adult mammalian central nervous system. *Science*, 255(5052), 1707–1710.
- Scheffler, K. (2014). Top-down proteomics by means of Orbitrap mass spectrometry. *Methods in Molecular Biology* , 1156, 465–487.
- Scigelova, M., & Makarov, A. (2006). Orbitrap Mass Analyzer – Overview and Applications in Proteomics. In *PROTEOMICS* (Vol. 6, Issue S2, pp. 16–21). <https://doi.org/10.1002/pmic.200600528>
- Serras, F., Morey, M., Alsina, B., Baguna, J., & Corominas, M. (2001). The Drosophila selenophosphate synthetase (selD) gene is required for development and cell proliferation. *BioFactors* , 14(1-4), 143–149.
- Sherman, B. T., Huang, D. W., Tan, Q., Guo, Y., Bour, S., Liu, D., Stephens, R., Baseler, M. W., Lane, H. C., & Lempicki, R. A. (2007). DAVID Knowledgebase: a gene-centered database integrating heterogeneous gene annotation resources to facilitate high-throughput gene functional analysis. *BMC Bioinformatics*, 8(1), 426.
- Snel, B., Lehmann, G., Bork, P., & Huynen, M. A. (2000). STRING: a web-server to retrieve and display the repeatedly occurring neighbourhood of a gene. *Nucleic Acids Research*, 28(18), 3442–3444.
- Suwanmanee, S., Mahakhunkijcharoen, Y., Ampawong, S., Leaungwutiwong, P., Missé, D., & Luplertlop, N. (2019). Inhibition of N-myristoyltransferase1 affects dengue virus replication. In *MicrobiologyOpen* (Vol. 8, Issue 9). <https://doi.org/10.1002/mbo3.831>

- Takahashi, K., Tanabe, K., Ohnuki, M., Narita, M., Ichisaka, T., Tomoda, K., & Yamanaka, S. (2007). Induction of pluripotent stem cells from adult human fibroblasts by defined factors. *Cell*, 131(5), 861–872.
- Takahashi, K., & Yamanaka, S. (2006). Induction of pluripotent stem cells from mouse embryonic and adult fibroblast cultures by defined factors. *Cell*, 126(4), 663–676.
- Thu, T. L. T., Minh, D. N., Van, N. T., Tinh, H. T., Van Vinh, C. N., Wolbers, M., Hoai, T. D. T., Farrar, J., Simmons, C., Wills, B., & Others. (2012). Clinical features of dengue in a large Vietnamese cohort: intrinsically lower platelet counts and greater risk for bleeding in adults than children. *PLoS Neglected Tropical Diseases*, 6(6), e1679.
- Wilkins, M. R., Sanchez, J.-C., Gooley, A. A., Appel, R. D., Humphery-Smith, I., Hochstrasser, D. F., & Williams, K. L. (1996). Progress with Proteome Projects: Why all Proteins Expressed by a Genome Should be Identified and How To Do It. *Biotechnology & Genetic Engineering Reviews*, 13(1), 19–50.
- Woods, C. G., Geoffrey Woods, C., Bond, J., & Enard, W. (2005). Autosomal Recessive Primary Microcephaly (MCPH): A Review of Clinical, Molecular, and Evolutionary Findings. In *The American Journal of Human Genetics* (Vol. 76, Issue 5, pp. 717–728). <https://doi.org/10.1086/429930>
- Woods, C. G., & Parker, A. (2013). Investigating microcephaly. *Archives of Disease in Childhood*, 98(9), 707–713.
- Yates, J. R., 3rd. (2013). The revolution and evolution of shotgun proteomics for large-scale proteome analysis. *Journal of the American Chemical Society*, 135(5), 1629–1640.
- Zhang, F., Hammack, C., Ogden, S. C., Cheng, Y., Lee, E. M., Wen, Z., Qian, X., Nguyen, H. N., Li, Y., Yao, B., Xu, M., Xu, T., Chen, L., Wang, Z., Feng, H., Huang, W.-K., Yoon, K.-J., Shan, C., Huang, L., ... Jin, P. (2016). Molecular signatures associated with ZIKV exposure in human cortical neural progenitors. *Nucleic Acids Research*, 44(18), 8610–8620.

7 MATERIAL SUPPLEMENTAR

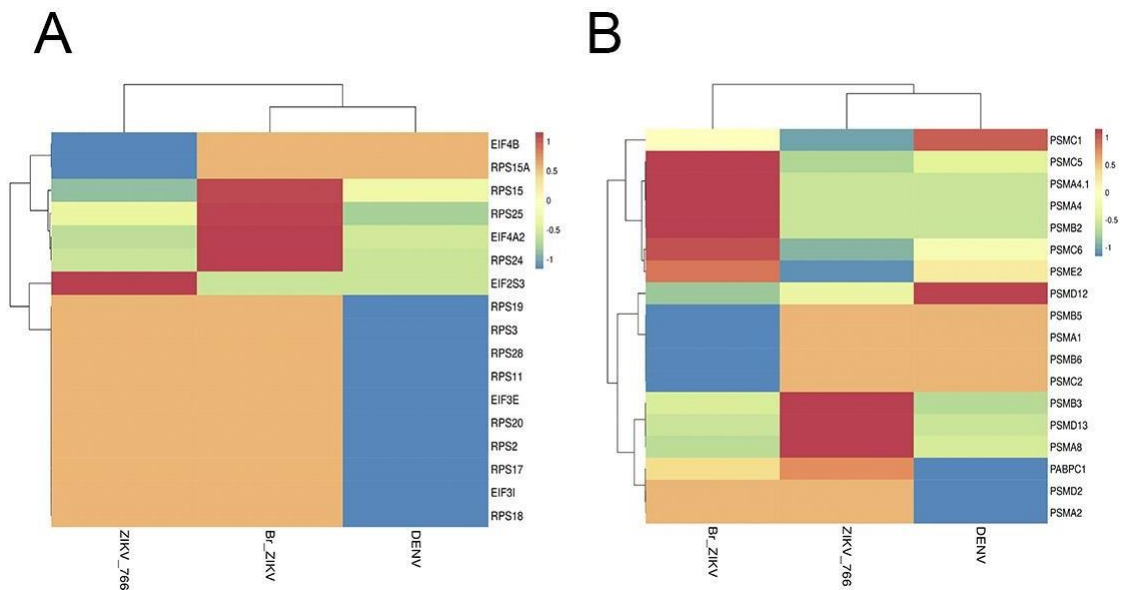


Figure S1. Heatmap of differentially expressed proteins related to RNA processing and metabolism in A. NSCs and B. neurospheres.

Table S1. List of proteins identified, quantified, differentially regulated, upregulated, and downregulated in neural progenitor cells infected with BrZIKV, ZIKV 766 and DENV.

Accession	Description	Anova (p) ZIKV 766	Log Fold Change ZIKV 766	Anova (p) Br ZIKV	Log Fold Change Br ZIKV	Anova (p) DENV	Log Fold Change DENV
A0A075B759	Peptidyl-prolyl cis-trans isomerase A-like 4E	0.018050241	-1.132982107	0.061075398	-1.014230795	0.172306640	-0.399812919
A0A1B0GUS4	Ubiquitin-conjugating enzyme E2 L5	0.751949989	0.030223795	0.469367389	-0.285418088	0.608223708	-0.216553658
A1A5D9	BICD family-like cargo adapter 2	0.737586594	-0.064296191	0.102784185	-3.742812712	0.990599942	-0.048428457
A1L0T0	Acetolactate synthase-like protein	0.286590533	5.613911297	0.514048272	-0.634989963	0.805206101	0.239084406
A2RUR9	Coiled-coil domain-containing protein 144A	0.771146874	0.039498131	0.850444655	-0.110148321	0.941680034	0.002119785
A2VDJ0	Transmembrane protein 131-like	0.101170397	3.466445739	0.345934156	-1.160245690	0.319137367	-1.302695046
A3KMH1	von Willebrand factor A domain-containing protein 8	0.455334478	-0.174203570	0.525747637	0.202078848	0.078381845	-0.463006003
A4UGR9	Xin actin-binding repeat-containing protein 2	0.681613224	0.102645760	0.854313008	0.430602762	0.430979085	-0.172689939
A6NCM1	IQ and AAA domain-containing protein 1-like	0.554002405	0.530996383	0.300392337	0.683545469	0.848081532	-0.685207106
A6NEC2	Puromycin-sensitive aminopeptidase-like protein	0.313827764	1.609737077	0.561862180	0.678277636	0.584682753	0.240103626
A6NHL2	Tubulin alpha chain-like 3	0.564790224	-0.053337506	0.220382556	-0.381249272	0.394218438	-0.586851484
A6NHQ2	rRNA/tRNA 2'-O-methyltransferase fibrillarin-like protein 1	0.127016371	-0.346393082	0.135710726	-0.484219994	0.266201503	-0.227765509
A8MTJ3	Guanine nucleotide-binding protein G(t) subunit alpha-3	0.291360022	2.248370770	0.071766211	-1.278481539	0.377190948	1.528614775
B2RPK0	Putative high mobility group protein B1-like 1	0.123484140	0.456737132	0.447263992	0.244880489	0.910964008	-0.018152778
B5MCN3	Putative SEC14-like protein 6	0.221689456	-0.309868451	0.422346278	0.429457242	0.208038861	-0.344911205
B5ME19	Eukaryotic translation initiation factor 3 subunit C-like protein	0.700059393	-0.144492801	0.592684733	0.721797913	0.931783452	-0.019865114
E7EW31	Proline-rich basic protein 1	0.565291514	0.400566580	0.694439445	0.212868138	0.214578369	0.597868301
E9PAV3	Nascent polypeptide-associated complex subunit alpha_muscle-specific form	0.682290792	0.010629276	0.834705063	-0.018870371	0.923768232	-0.125529376
O00154	Cytosolic acyl coenzyme A thioester hydrolase	0.960554888	0.002465070	0.435142958	-0.101720257	0.045161049	-0.245337013
O00231	26S proteasome non-ATPase regulatory subunit 11	0.442713951	-0.451007363	0.670086620	0.084434780	0.718413050	-0.261188613
O00232	26S proteasome non-ATPase regulatory subunit 12	0.102721365	0.362887865	0.559594801	0.085068360	0.914718903	-0.023561233

O00255	Menin	0.304640384	0.881759160	0.076204031	1.688079588	0.931859273	-0.165553731
O00264	Membrane-associated progesterone receptor component 1	0.832535989	0.129668361	0.895554690	0.030129643	0.041262736	-0.306140806
O00299	Chloride intracellular channel protein 1	0.030876051	-0.341764576	0.125209817	-0.201979153	0.145388651	-0.157858688
O00410	Importin-5	0.925810962	-0.062873332	0.862995264	0.058746997	0.189382889	-0.325108114
O00425	Insulin-like growth factor 2 mRNA-binding protein 3	0.710960441	0.029127146	0.730185220	-0.187090647	0.906987081	0.115187166
O00429	Dynamin-1-like protein	0.814150252	-0.344726277	0.635323326	-0.312427122	0.802243739	-0.256227363
O00463	TNF receptor-associated factor 5	0.023056391	0.647003726	0.035800406	-0.714106847	0.891445729	-0.033124869
O00487	26S proteasome non-ATPase regulatory subunit 14	0.136822318	-0.460266542	0.484602779	-0.214954003	0.519035937	0.288434924
O00505	Importin subunit alpha-4	0.212733483	0.761356628	0.754355617	-0.392841581	0.630689063	0.490827495
O00567	Nucleolar protein 56	0.983646411	-0.158312781	0.771490563	-0.234940872	0.991778968	-0.072804009
O00571	ATP-dependent RNA helicase DDX3X	0.755793733	0.024087128	0.109030655	0.386574847	0.659961923	-0.063374992
O14531	Dihydropyrimidinase-related protein 4	0.645689707	-0.405213359	0.779279723	0.024893982	0.453922104	-0.547365598
O14556	Glyceraldehyde-3-phosphate dehydrogenase_testis-specific	0.586041381	-0.276158196	0.614260587	0.230935816	0.989263019	-0.017534665
O14579	Coatomer subunit epsilon	0.445888755	-0.364375876	0.326013291	-0.389170972	0.438878855	-0.246625029
O14737	Programmed cell death protein 5	0.002496449	-0.486650312	0.831164538	0.017218885	0.036305854	-0.465324297
O14744	Protein arginine N-methyltransferase 5	0.914078911	-0.046556477	0.268141898	-0.318631437	0.554011682	0.101207111
O14745	Na(+)/H(+) exchange regulatory cofactor NHE-RF1	0.599348185	-4.190119712	0.488826989	0.343060560	0.671492923	-0.027723311
O14782	Kinesin-like protein KIF3C	0.203313756	-1.564990521	0.813667383	-0.087929184	0.193660879	-1.327230589
O14818	Proteasome subunit alpha type-7	0.719085045	0.129149055	0.389456041	0.254501139	0.122503278	-0.186403810
O14929	Histone acetyltransferase type B catalytic subunit	0.840223081	-1.681287668	0.747663014	-0.831817330	0.815692261	-1.134216114
O14950	Myosin regulatory light chain 12B	0.138305512	-0.243283520	0.393203714	-0.710454994	0.407801967	0.311741677
O14979	Heterogeneous nuclear ribonucleoprotein D-like	0.152667313	-0.519087303	0.676097403	0.044590113	0.199023844	-0.422201043
O14980	Exportin-1	0.330015108	0.203133033	0.747462767	0.119275041	0.371128646	-0.249146802
O14983	Sarcoplasmic/endoplasmic reticulum calcium ATPase 1	0.401274691	0.219262440	0.928219671	-0.003965623	0.079183650	-0.263339911

O15067	Phosphoribosylformylglycinamide synthase	0.512746561	0.195732449	0.101251909	1.163520315	0.914271573	-0.038143967
O15075	Serine/threonine-protein kinase DCLK1	0.159956275	-0.563898175	0.135538515	-0.871821967	0.699988199	-0.144692897
O15144	Actin-related protein 2/3 complex subunit 2	0.246638011	1.053025761	0.762244961	-0.023598060	0.075660536	-0.313406962
O15145	Actin-related protein 2/3 complex subunit 3	0.714304478	0.015804469	0.753265949	0.066717954	0.427763990	0.202084150
O15173	Membrane-associated progesterone receptor component 2	0.291755903	0.995216928	0.164440836	0.864419719	0.757106858	-0.068355576
O15260	Surfeit locus protein 4	0.953509286	0.050628854	0.248388504	-0.513864652	0.616960644	0.211859944
O15347	High mobility group protein B3	0.912294495	-0.448556790	0.669830275	0.387941286	0.428201453	0.569599224
O15355	Protein phosphatase 1G	0.855270712	-0.115654874	0.618650309	0.280852870	0.502273381	-0.388250148
O15360	Fanconi anemia group A protein	0.004290794	2.950193205	0.038519662	-1.850614354	0.196986441	1.913487271
O15371	Eukaryotic translation initiation factor 3 subunitD	0.144854035	-0.547648500	0.537863409	0.558968481	0.943282668	0.003570946
O15372	Eukaryotic translation initiation factor 3 subunitH	0.387342321	0.543479271	0.653805264	-0.073879566	0.648660021	0.254554175
O15523	ATP-dependent RNA helicase DDX3Y	0.224057992	0.300649658	0.044496900	0.604750658	0.750339864	-0.059039738
O43143	Pre-mRNA-splicing factor ATP-dependent RNA helicase DHX15	0.974812643	-0.023667561	0.794107762	-0.049751292	0.331220458	-0.180360974
O43150	Arf-GAP with SH3 domain_ ANK repeat and PH domain-containing protein 2	0.282727934	-1.398627372	0.070627425	-1.834262311	0.594686583	0.725190789
O43169	Cytochrome b5 type B	0.630216054	1.404434181	0.720636350	-0.237229418	0.163490933	1.449894983
O43175	D-3-phosphoglycerate dehydrogenase	0.501737487	0.140347606	0.956947676	0.020025733	0.023771579	-0.352126140
O43182	Rho GTPase-activating protein 6	0.920767312	-0.402727506	0.159331455	-1.460230600	0.442895204	-0.988312019
O43237	Cyttoplasmic dynein 1 light intermediate chain 2	0.340004433	0.178798603	0.280499565	0.357161988	0.570969022	-0.101816755
O43242	26S proteasome non-ATPase regulatory subunit3	0.061754575	-0.411092162	0.157816997	-0.238842185	0.071556864	-0.299738343
O43252	Bifunctional 3'-phosphoadenosine 5'-phosphosulfate synthase 1	0.407912500	-0.375260199	0.245137875	-0.424606118	0.634757442	-0.225103600
O43347	RNA-binding protein Musashi homolog 1	0.561649198	-0.469623838	0.232252306	-1.375745114	0.785940032	0.264024437
O43390	Heterogeneous nuclear ribonucleoprotein R	0.438867360	0.128388837	0.204322506	0.498732857	0.703805826	-0.083733872
O43396	Thioredoxin-like protein 1	0.575817653	-0.125580644	0.342507854	-0.204390917	0.088832437	-0.369611446

O43423	Acidic leucine-rich nuclear phosphoprotein 32 family member C	0.977880185	-0.010849058	0.156793461	0.658809885	0.078446461	-0.393748720
O43432	Eukaryotic translation initiation factor 4 gamma3	0.924150174	-0.027512162	0.103645506	-0.714370374	0.043139318	-0.356490289
O43602	Neuronal migration protein doublecortin	0.030931792	-0.972502360	0.038102051	-0.851084516	0.450370179	0.708984313
O43684	Mitotic checkpoint protein BUB3	0.205235207	0.371845259	0.163077335	0.525570004	0.775256758	-0.098997493
O43707	Alpha-actinin-4	0.105666899	-0.206047632	0.190636665	-0.206216025	0.034051492	-0.268152746
O43765	Small glutamine-rich tetratricopeptide repeat-containing protein alpha	0.585738517	-0.260152649	0.421081373	-0.309617428	0.964380754	-0.054222151
O43809	Cleavage and polyadenylation specificity factor subunit 5	0.397773442	-0.173748439	0.045405848	-0.634022666	0.838977795	0.001426571
O43852	Calumenin	0.369698564	-0.291380128	0.401867919	-0.230261816	0.215920803	-0.389941679
O43865	S-adenosylhomocysteine hydrolase-like protein 1	0.800265097	0.014916800	0.515216562	0.413401952	0.726460008	-0.064109629
O60256	Phosphoribosyl pyrophosphate synthase-associated protein 2	0.726145424	-0.091536763	0.120662742	-0.396925054	0.998395196	0.003961775
O60282	Kinesin heavy chain isoform 5C	0.213718714	-0.305215574	0.073583456	-0.965395621	0.279501160	0.300041752
O60361	Putative nucleoside diphosphate kinase	0.698197927	0.127594851	0.209319459	0.704750895	0.549081406	-0.241118459
O60506	Heterogeneous nuclear ribonucleoprotein Q	0.655624290	-0.124039742	0.896131592	0.157639472	0.251408010	-0.261793549
O60522	Tudor domain-containing protein 6	0.057442422	-2.466129146	0.241238418	-0.888059636	0.342074485	-1.129442391
O60664	Perilipin-3	0.089278297	-0.479198107	0.822890715	-0.015355739	0.472199067	-0.146431670
O60701	UDP-glucose 6-dehydrogenase	0.000140460	0.968446837	0.988360514	0.040901516	0.149364998	-0.201724167
O60884	DnaJ homolog subfamily A member 2	0.105483057	0.477104366	0.288961494	1.856367190	0.992748697	0.017638421
O60888	Protein CutA	0.420433111	-0.109027482	0.214772314	0.514111927	0.897369622	-0.009840611
O75051	Plexin-A2	0.943786262	0.050294680	0.783918681	0.106505830	0.623862505	0.156553925
O75083	WD repeat-containing protein 1	0.510990304	-0.112090397	0.587509108	0.553077239	0.041144938	-0.540732676
O75106	Retina-specific copper amine oxidase	0.813714282	3.407392314	0.618106952	-0.078205912	0.439372241	1.187054314
O75131	Copine-3	0.478458869	-0.189858973	0.203795627	-1.042095987	0.685840020	0.276080241
O75340	Programmed cell death protein 6	0.274529804	0.125276794	0.052636989	0.786147151	0.090744848	0.156354415
O75347	Tubulin-specific chaperone A	0.226406740	-0.164849754	0.844088746	0.066892140	0.002851671	-0.238213488

O75367	Core histone macro-H2A.1	0.029519031	0.634159827	0.827838812	-0.047862876	0.689002063	0.148460853
O75368	SH3 domain-binding glutamic acid-rich-like protein	0.105394946	-0.351720527	0.846178796	0.005310860	0.105233341	-0.352003950
O75369	Filamin-B	0.864610560	0.031541886	0.466812632	-0.135952254	0.202026362	-0.211629979
O75390	Citrate synthase_ mitochondrial	0.960944798	-0.232281037	0.087040037	-1.111553280	0.484229302	0.309784330
O75436	Vacuolar protein sorting-associated protein 26A	0.372940598	-0.518926770	0.973517544	-0.055063908	0.503396587	0.303367326
O75475	PC4 and SFRS1-interacting protein	0.775570374	-0.063175310	0.330602874	-0.174301248	0.184454841	-0.217430191
O75477	Erlin-1	0.830569845	-0.048874881	0.159172921	-0.756749334	0.814380458	-0.365681791
O75489	NADH dehydrogenase [ubiquinone] iron-sulfur protein 3_mitochondrial	0.639643819	-0.176088363	0.131643015	-0.849143043	0.917776059	-0.022765120
O75526	RNA-binding motif protein_X-linked-like-2	0.026232796	1.472124701	0.665426074	0.064014189	0.474495506	0.547469580
O75531	Barrier-to-autointegration factor	0.234498447	-0.724445503	0.042695394	-1.160734000	0.647976524	0.023163480
O75533	Splicing factor 3B subunit 1	0.440098377	0.139796121	0.121403752	0.274728527	0.208414350	-0.136599303
O75534	Cold shock domain-containing protein E1	0.066114753	-0.637378186	0.001433824	-1.586462849	0.062181415	-0.481744691
O75569	Interferon-inducible double-stranded RNA-dependent protein kinase activator A	0.101855714	-0.410700910	0.112179632	-0.481804646	0.031714423	-0.408424660
O75643	U5 small nuclear ribonucleoprotein 200 kDa helicase	0.645361776	0.092009112	0.363032781	0.477624509	0.880958090	-0.061603031
O75694	Nuclear pore complex protein Nup155	0.499969983	0.167580303	0.545527209	0.124519319	0.769621676	-0.081587809
O75821	Eukaryotic translation initiation factor 3 subunitG	0.231360579	0.541394926	0.288367800	-0.249868229	0.859774818	0.062212017
O75874	Isocitrate dehydrogenase [NADP] cytoplasmic	0.779916926	-0.081538172	0.967294440	-0.052121315	0.483881834	-0.223606951
O75937	DnaJ homolog subfamily C member 8	0.431828335	0.130109373	0.400369239	0.155182995	0.728503739	-0.035577473
O75947	ATP synthase subunit d_mitochondrial	0.309342886	-0.152123704	0.372653956	-0.147188659	0.164598218	-0.212544494
O75964	ATP synthase subunit g_mitochondrial	0.788447654	-0.063784401	0.246005608	-0.433859934	0.880841021	-0.082191016
O76003	Glutaredoxin-3	0.537776360	-0.230933428	0.640603094	0.226133549	0.923095130	0.136882225
O76021	Ribosomal L1 domain-containing protein 1	0.789773775	-0.169418522	0.165993363	-0.708712674	0.554766631	0.190885347
O94887	FERM_ARHGEF and pleckstrin domain-containing protein 2	0.135852924	-0.617528536	0.424070556	0.063542562	0.168548367	-0.518880566
O94923	D-glucuronyl C5-epimerase	0.740922981	-0.723815410	0.523209998	-0.665387832	0.647870269	-0.572211951

O95336	6-phosphogluconolactonase	0.954785113	-0.070864126	0.422613326	-0.599316976	0.929359102	-0.158087790
O95373	Importin-7	0.345020781	-0.330898984	0.249180243	-0.370232654	0.212241284	-0.394126510
O95433	Activator of 90 kDa heat shock protein ATPase homolog 1	0.922205003	-0.009284892	0.434062207	0.276744178	0.928991189	-0.067320493
O95573	Long-chain-fatty-acid--CoA ligase 3	0.265286830	-0.341546743	0.448366444	-0.184160036	0.020974538	-0.731181731
O95678	Keratin_type II cytoskeletal 75	0.670476281	-0.064146370	0.259430578	0.281147337	0.829346098	0.121448690
O95716	Ras-related protein Rab-3D	0.320395934	-0.322874925	0.400609952	0.092266094	0.228888533	-0.362272310
O95747	Serine/threonine-protein kinaseR1	0.934618872	0.068183406	0.100022056	-0.614438162	0.161844033	-0.313837598
O95757	Heat shock 70 kDa protein 4L	0.468243785	1.632487837	0.473405103	0.161664762	0.215975370	1.331935894
O95758	Polypyrimidine tract-binding protein 3	0.009277923	2.336052086	0.507436834	0.332969142	0.043729480	-0.511406940
O95782	AP-2 complex subunit alpha-1	0.550117610	0.133382215	0.076678810	-1.185614898	0.867442557	-0.167510075
O95822	Malonyl-CoA decarboxylase_mitochondrial	0.011430100	2.783197703	0.439845893	-0.116490556	0.815430753	1.220855859
O95831	Apoptosis-inducing factor 1_mitochondrial	0.796509904	-0.139305789	0.874332162	-0.042605467	0.435341945	-0.272681959
O95865	N(G)_N(G)-dimethylarginine dimethylaminohydrolase 2	0.589652335	-0.050746530	0.543975355	0.082528622	0.383966476	-0.190067797
O95881	Thioredoxin domain-containing protein 12	0.804631442	-0.324773857	0.869637864	0.264020150	0.681819844	0.387235462
O96019	Actin-like protein 6A	0.890751073	0.033591653	0.934613194	0.050159975	0.807502731	-0.062086848
P00338	L-lactate dehydrogenase A chain	0.981587600	0.024174224	0.239142794	-0.418908966	0.409693339	0.512396293
P00367	Glutamate dehydrogenase 1_mitochondrial	0.464750875	0.355689673	0.192949754	0.785222973	0.328058307	-0.301985695
P00374	Dihydrofolate reductase	0.487420514	0.173623753	0.247921020	0.843709222	0.005904313	-0.235283669
P00387	NADH-cytochrome b5 reductase 3	0.023978536	1.310007319	0.098971121	1.095401206	0.172251655	0.236545717
P00403	Cytochrome c oxidase subunit 2	0.043534489	0.792977997	0.468182849	0.142720187	0.149714235	0.253576152
P00441	Superoxide dismutase [Cu-Zn]	0.469338494	0.289524790	0.160925161	1.428189164	0.100987407	0.361453637
P00505	Aspartate aminotransferase_mitochondrial	0.995852395	-0.035623259	0.272615196	0.642362837	0.505775354	-0.162922608
P00558	Phosphoglycerate kinase 1	0.427427269	-0.235113641	0.819593866	0.146251447	0.377014204	-0.242865330
P00568	Adenylate kinase isoenzyme 1	0.658871140	0.061447332	0.524362380	-0.174639033	0.790819767	-0.082160971
P01266	Thyroglobulin	0.078751980	0.884386967	0.658989431	-0.065524106	0.235221155	0.981187503
P02768	Serum albumin	0.537222212	1.580830810	0.886940576	-0.294177519	0.152189487	1.525760244

P02787	Serotransferrin	0.850383976	0.146835994	0.103324405	-0.403872746	0.500054095	0.878465036
P04075	Fructose-bisphosphate aldolase A	0.747803419	-0.086028921	0.325875638	-0.217343491	0.447930349	-0.165653040
P04080	Cystatin-B	0.123958215	-0.343105002	0.546083263	0.257355210	0.198844372	-0.262304720
P04083	Annexin A1	0.508057805	-0.301791144	0.110997840	-1.007976378	0.849257450	0.539776406
P04114	Apolipoprotein B-100	0.319953579	0.141390413	0.417481697	0.481666288	0.060378844	-0.351604429
P04259	Keratin_type II cytoskeletal 6B	0.052417223	-2.137590626	0.079860868	-0.590766207	0.630595464	-0.121275544
P04264	Keratin_type II cytoskeletal 1	0.229740894	0.761495930	0.242390508	1.408100484	0.746488025	-0.452856122
P04350	Tubulin beta-4A chain	0.890892433	-0.006187002	0.568339265	-0.153307597	0.412365109	-0.214180713
P04406	Glyceraldehyde-3-phosphate dehydrogenase	0.455649865	-0.149325887	0.292116440	0.676851335	0.543148440	-0.111926094
P04632	Calpain small subunit 1	0.225171797	-0.474124864	0.052156019	-1.459548005	0.129684390	-0.771566654
P04792	Heat shock protein beta-1	0.980543953	0.125451401	0.683324393	-0.073308161	0.888546784	0.038359909
P04818	Thymidylate synthase	0.144498531	-0.783375598	0.931094658	-0.125260435	0.192582726	-0.635453568
P04843	Dolichyl-diphosphooligosaccharide--protein glycosyltransferase subunit 1	0.024836552	0.586823382	0.246957049	0.352034370	0.662814887	0.044062615
P04844	Dolichyl-diphosphooligosaccharide--protein glycosyltransferase subunit 2	0.024244090	0.638232716	0.239802814	0.426877098	0.722993145	0.132963772
P04899	Guanine nucleotide-binding protein G(i) subunit alpha-2	0.983200788	0.028183764	0.383148290	0.364167408	0.489146123	-0.188967844
P05023	Sodium/potassium-transporting ATPase subunit alpha-1	0.322189312	0.120754793	0.693441186	0.057529860	0.795955855	-0.042032848
P05091	Aldehyde dehydrogenase_mitochondrial	0.149916651	-0.444619973	0.430437561	-0.227053837	0.192139606	-0.374436754
P05129	Protein kinase C gamma type	0.090471587	0.365669003	0.215770472	0.932129814	0.088837445	-0.409369334
P05141	ADP/ATP translocase 2	0.242606933	0.503171659	0.678032889	0.177036916	0.976541997	-0.075359078
P05161	Ubiquitin-like protein ISG15	0.316415713	0.202411581	0.310912576	0.225860162	0.000034788	2.666788102
P05164	Myeloperoxidase	0.824515500	0.039491703	0.014978942	-0.380762162	0.019040206	-0.260933126
P05198	Eukaryotic translation initiation factor 2 subunit 1	0.176063979	-0.465099591	0.997598787	0.097828572	0.296912612	-0.204403488
P05204	Non-histone chromosomal protein HMG-17	0.179845635	-1.436775460	0.363342947	-1.136459478	0.253923784	-1.344673296
P05386	60S acidic ribosomal protein P1	0.620382495	-0.043096521	0.627439553	0.105188017	0.000002871	-0.449207301

P05387	60S acidic ribosomal protein P2	0.022928858	-0.454593716	0.770972836	0.255515458	0.001846889	-0.755793895
P05388	60S acidic ribosomal protein P0	0.109294403	-0.461035676	0.056217621	-0.582729065	0.098469908	-0.452740722
P05455	Lupus La protein	0.995983547	-0.056772776	0.507587230	-0.157429160	0.703470399	-0.108629674
P05556	Integrin beta-1	0.380201217	-0.192598578	0.219520411	-0.270327473	0.182924375	-0.288199995
P05787	Keratin_type II cytoskeletal 8	0.215553331	0.141686913	0.214326506	-0.132084257	0.573669993	-0.073602247
P06396	Gelsolin	0.429094582	0.116769942	0.524314896	0.177568770	0.372282375	-0.110170195
P06454	Prothymosin alpha	0.004067061	-0.651904242	0.784073916	0.334043285	0.007868377	-0.835722293
P06493	Cyclin-dependent kinase 1	0.133266197	0.546081921	0.790152277	-0.025538080	0.857347378	0.058476109
P06576	ATP synthase subunit beta_mitochondrial	0.182621735	0.259461285	0.415836897	0.268102920	0.236801457	-0.219469216
P06730	Eukaryotic translation initiation factor 4E	0.704165404	0.044509921	0.431547067	-0.172125183	0.802448918	-0.047959981
P06732	Creatine kinase M-type	0.055395427	-1.058947757	0.252260471	-0.429478335	0.075701311	-0.902347080
P06733	Alpha-enolase	0.831151120	-0.062414254	0.380356417	0.504202135	0.287743159	-0.246290534
P06737	Glycogen phosphorylase_liver form	0.060819898	-3.407419421	0.270831878	-0.416908593	0.959957370	0.128811711
P06744	Glucose-6-phosphate isomerase	0.093554648	-0.270857642	0.127846091	-0.573513380	0.196370118	0.135833484
P06748	Nucleophosmin	0.214737075	0.282975278	0.151576498	0.973619221	0.396829989	-0.197565668
P06753	Tropomyosin alpha-3 chain	0.569178844	-0.088527106	0.284591188	1.092693637	0.072115496	-0.324955446
P06899	Histone H2B type 1-J	0.028586176	0.683320587	0.508905329	-0.039560364	0.831779160	0.113777988
P07195	L-lactate dehydrogenase B chain	0.897370567	0.093528596	0.406280055	0.247029719	0.725314005	0.082525600
P07196	Neurofilament light polypeptide	0.486464873	-1.020836370	0.500830761	-0.934505319	0.637223917	1.867027119
P07197	Neurofilament medium polypeptide	0.612892381	0.065426862	0.326878173	0.256237424	0.759073017	0.103190906
P07205	Phosphoglycerate kinase 2	0.049949827	0.719014181	0.289478062	0.562695128	0.334443015	0.200384690
P07237	Protein disulfide-isomerase	0.314783768	0.458934202	0.354926219	0.746989598	0.938050534	-0.030765460
P07305	Histone H1.0	0.087642084	-2.121688941	0.456514236	-0.911034525	0.343755357	0.139880863
P07339	Cathepsin D	0.595513030	-0.238312746	0.622071161	0.365793633	0.546684758	0.613727593
P07355	Annexin A2	0.748410295	-0.046141946	0.811998199	0.100987650	0.053244161	-0.277890482
P07437	Tubulin beta chain	0.928468884	-0.047056554	0.850930657	0.040485546	0.411622016	-0.187480403
P07602	Prosaposin	0.285853527	-0.232271764	0.823402270	0.312840141	0.473858361	0.884731558

P07737	Profilin-1	0.798268375	0.027448487	0.838498928	0.087087567	0.572556843	-0.169457553
P07741	Adenine phosphoribosyltransferase	0.732480380	-0.169118309	0.112698235	-0.842672266	0.228483747	0.344767750
P07814	Bifunctional glutamate/proline-tRNA ligase	0.542617030	-0.239469928	0.589651935	0.157061914	0.842734797	-0.112207958
P07864	L-lactate dehydrogenase C chain	0.450101011	0.792235392	0.123172270	1.709179721	0.711321997	0.065027597
P07900	Heat shock protein HSP 90-alpha	0.984308853	-0.037412710	0.623620994	0.170149190	0.305750786	-0.319530900
P07910	Heterogeneous nuclear ribonucleoproteins C1/C2	0.434963076	-0.360759864	0.327227738	0.750045239	0.268867838	-0.434875989
P07948	Tyrosine-protein kinase Lyn	0.119873820	-1.581308379	0.931198404	-1.032448048	0.166660099	-1.427543306
P07951	Tropomyosin beta chain	0.066357454	-0.903003488	0.417456291	0.599225406	0.861821937	-0.152607032
P07954	Fumarate hydratase_mitochondrial	0.150287889	-0.325789547	0.998471283	0.034872897	0.301209056	-0.235568759
P08133	Annexin A6	0.870422479	-0.017027371	0.455449740	0.386793376	0.302275145	-0.235393767
P08134	Rho-related GTP-binding protein RhoC	0.730967980	0.028284393	0.379700499	0.243243738	0.842713464	0.071746162
P08237	ATP-dependent 6-phosphofructokinase_muscle type	0.098681318	-0.167124014	0.021512469	-0.323223424	0.074962581	-0.181033623
P08238	Heat shock protein HSP 90-beta	0.702539251	-0.223454587	0.738495350	0.152668468	0.350837551	-0.382401432
P08243	Asparagine synthetase [glutamine-hydrolyzing]	0.004536854	1.717414758	0.727443436	0.211937122	0.701315520	0.033498341
P08397	Porphobilinogen deaminase	0.023527370	-0.753660398	0.053698071	-0.794819012	0.011612408	-0.532641989
P08559	Pyruvate dehydrogenase E1 component subunit alpha_somatic form_mitochondrial	0.318182065	-2.221108056	0.917200683	-1.231223856	0.652636468	-0.893424539
P08574	Cytochrome c1_heme protein_mitochondrial	0.420351498	1.251076395	0.582226303	0.839766562	0.390098193	0.384836759
P08579	U2 small nuclear ribonucleoprotein B"	0.017883684	2.502262960	0.407063614	0.611574297	0.099701960	2.268076233
P08621	U1 small nuclear ribonucleoprotein 70 kDa	0.869371460	0.061965413	0.572300773	0.111404456	0.000069705	-0.454304318
P08670	Vimentin	0.606158669	0.073823145	0.558339043	0.119952877	0.660424339	-0.049945669
P08708	40S ribosomal protein S17	0.766616998	-0.101517938	0.141439346	0.880359661	0.039534904	-0.903928279
P08729	Keratin_type II cytoskeletal 7	0.023729945	-0.568671503	0.050344897	-0.446760805	0.389540461	-0.162356911
P08754	Guanine nucleotide-binding protein G(i) subunit alpha	0.371780641	-0.259456940	0.858760691	0.017251424	0.945405421	-0.040397341
P08758	Annexin A5	0.876966795	-0.061798456	0.117511424	-0.396084499	0.742009288	0.148016017
P08779	Keratin_type I cytoskeletal 16	0.219480680	-0.416050656	0.076393733	-0.859645371	0.967828833	0.025418816

P08865	40S ribosomal protein SA	0.606340266	-0.125792421	0.638980469	0.193248221	0.156344679	-0.318692980
P09012	U1 small nuclear ribonucleoprotein A	0.608151520	0.066425317	0.559158451	0.161468737	0.950197036	-0.010460498
P09104	Gamma-enolase	0.765815291	-0.732987176	0.643064073	0.077547079	0.501627513	-0.909203815
P09132	Signal recognition particle 19 kDa protein	0.183997251	-0.859596235	0.340936481	-0.162323284	0.407838859	2.110127671
P09211	Glutathione S-transferase P	0.727398365	0.034902224	0.784303335	0.160742904	0.722935823	-0.146488161
P09417	Dihydropteridine reductase	0.617520825	0.041654061	0.527261942	-0.077326400	0.029168662	-0.280681577
P09429	High mobility group protein B1	0.123484261	0.456737132	0.447264987	0.244880489	0.910964278	-0.018152778
P09471	Guanine nucleotide-binding protein G(o) subunit alpha	0.482662208	0.190417925	0.057237896	-0.612051306	0.816915997	-0.008390253
P09488	Glutathione S-transferase Mu 1	0.158300158	-0.499838847	0.387351961	-1.230731504	0.187935927	-1.345733720
P09493	Tropomyosin alpha-1 chain	0.517063797	-0.076355781	0.400003596	0.946583812	0.375390085	-0.114859487
P09622	Dihydrolipoyl dehydrogenase_ mitochondrial	0.011173013	0.487018665	0.184596685	0.900060588	0.079739767	-0.292157427
P09651	Heterogeneous nuclear ribonucleoprotein A1	0.620546984	-0.011829826	0.021209814	0.699681449	0.308110934	-0.139206829
P09661	U2 small nuclear ribonucleoprotein A'	0.295265862	-0.419793979	0.769296760	0.018496974	0.362473208	-0.339632963
P09874	Poly [ADP-ribose] polymerase 1	0.050430353	0.410181067	0.212328661	0.963414328	0.812780910	0.031992159
P09936	Ubiquitin carboxyl-terminal hydrolase isozyme L1	0.850142887	-0.280376694	0.655458218	0.119660900	0.795454297	-0.032163071
P09960	Leukotriene A-4 hydrolase	0.239433760	-0.694845096	0.974414726	0.133908606	0.382401663	0.249079537
P09972	Fructose-bisphosphate aldolase C	0.927238586	0.085258690	0.228466895	-0.458911710	0.852269198	-0.078444302
P0C0S5	Histone H2A.Z	0.309389039	0.383230630	0.479086595	0.273002890	0.457801680	0.428519537
P0CG47	Polyubiquitin-B	0.927486947	0.008172035	0.158888776	1.304648586	0.294938158	-0.392182319
P0DKB5	Trophoblast glycoprotein-like	0.651646098	-0.126599471	0.148498558	-0.672120007	0.955994905	0.188299983
P0DMV8	Heat shock 70 kDa protein 1A	0.518572696	0.439314326	0.007603373	0.618917066	0.416771232	0.200344921
P0DN79	Cystathionine beta-synthase-like protein	0.062176635	1.241144617	0.005763703	-0.754730122	0.002237689	-0.776829370
P0DP24	Calmodulin-2	0.901720542	0.026256929	0.219967831	1.477132351	0.272034648	-0.174817812
P0DPH8	Tubulin alpha-3D chain	0.258374239	-0.827642853	0.333586493	-0.757158137	0.537178013	0.097029844
P10155	60 kDa SS-A/Ro ribonucleoprotein	0.727024919	-0.078314763	0.900462796	0.064223524	0.922811582	-0.047055928

P10266	Endogenous retrovirus group K member 10 Pol protein	0.868358201	-0.831721986	0.460717248	-0.400757313	0.722712836	0.145150412
P10412	Histone H1.4	0.345731492	0.273363977	0.600872546	0.243716917	0.782985419	0.046748549
P10599	Thioredoxin	0.058030066	-0.335530224	0.471419687	0.435574648	0.000371370	-0.464130416
P10620	Microsomal glutathione S-transferase 1	0.565365978	-0.149540974	0.129392214	1.279747979	0.561984949	-0.766600610
P10644	cAMP-dependent protein kinase type I-alpha regulatory subunit	0.367289988	-0.378555053	0.047250038	-1.121983631	0.565769837	-0.261157096
P10768	S-formylglutathione hydrolase	0.064363767	-0.625911431	0.546520325	0.606997791	0.598900494	-0.148192072
P10809	60 kDa heat shock protein_mitochondrial	0.016604093	0.615735516	0.173466928	1.416545934	0.112971075	-0.167827047
P11021	Endoplasmic reticulum chaperone BiP	0.018160885	0.697474509	0.292130407	0.669698814	0.399401480	0.124910659
P11137	Microtubule-associated protein 2	0.194324957	0.580124594	0.104078576	-0.632833554	0.088388517	0.911145840
P11142	Heat shock cognate 71 kDa protein	0.881609855	0.068822292	0.323969249	0.505140298	0.371759839	-0.175119082
P11166	Solute carrier family 2_facilitated glucose transporter member 1	0.449137000	0.376810186	0.278866160	0.429058920	0.309481890	-0.547934944
P11177	Pyruvate dehydrogenase E1 component subunit beta_mitochondrial	0.000000000	0.000000000	0.457004379	-3.328015699	0.695732512	-0.757125569
P11216	Glycogen phosphorylase_brain form	0.000000000	0.000000000	0.612361985	0.453348250	0.029583386	-0.297760055
P11217	Glycogen phosphorylase_muscle form	0.539092499	0.063720896	0.156170932	-0.333557196	0.461776170	-0.103134563
P11233	Ras-related protein Ral-A	0.036624204	-2.597623530	0.629920181	-0.129980484	0.590303575	-0.681263076
P11279	Lysosome-associated membrane glycoprotein 1	0.629740902	-0.149991424	0.625429563	0.292620830	0.383630854	-0.234131077
P11310	Medium-chain specific acyl-CoA dehydrogenase_mitochondrial	0.792405663	-0.353053237	0.249026645	0.428660134	0.419200502	0.557024549
P11387	DNA topoisomerase 1	0.536004408	0.032039224	0.894777037	-0.375498663	0.947596759	-0.288890133
P11413	Glucose-6-phosphate 1-dehydrogenase	0.318542791	-0.498995399	0.261634515	-0.510546729	0.384116456	-0.405528162
P11586	C-1-tetrahydrofolate synthase_cytoplasmic	0.068419153	-0.261299054	0.511755351	0.199487488	0.011481716	-0.278789109
P11766	Alcohol dehydrogenase class-3	0.362049731	0.160296783	0.853432768	-0.035501102	0.856204633	-0.061567563
P11940	Polyadenylate-binding protein 1	0.371640383	0.183058655	0.288372428	0.246347977	0.959733347	-0.037967042
P12004	Proliferating cell nuclear antigen	0.378185548	-0.251833788	0.910656083	0.063524536	0.145385423	-0.374400331
P12035	Keratin_type II cytoskeletal 3	0.917512309	-0.202187556	0.302384360	1.470429386	0.550474641	-0.432371923

P12036	Neurofilament heavy polypeptide	0.031434225	-0.566475373	0.069696849	-0.426349430	0.462778811	-0.114498073
P12236	ADP/ATP translocase 3	0.363047854	-0.359136274	0.807284984	-0.800238046	0.703320317	-0.040162436
P12268	Inosine-5'-monophosphate dehydrogenase 2	0.064390604	-0.582908513	0.110500739	1.147868130	0.388896222	0.229089021
P12270	Nucleoprotein TPR	0.244859504	0.550111079	0.136531362	0.904969421	0.657700331	-0.096364758
P12277	Creatine kinase B-type	0.297990532	0.575084901	0.130977551	1.515488634	0.506746465	-0.055808571
P12814	Alpha-actinin-1	0.569331762	-0.230495141	0.971543536	0.015426280	0.384997829	-0.281965124
P12956	X-ray repair cross-complementing protein 6	0.005658790	0.831028260	0.560108864	0.094815107	0.998820214	-0.023840865
P13010	X-ray repair cross-complementing protein 5	0.160367396	0.221891582	0.300392374	-0.251834497	0.257383944	0.172598967
P13073	Cytochrome c oxidase subunit 4 isoform 1_mitochondrial	0.715067683	0.327723316	0.485583041	-0.109513272	0.134749932	-0.416952576
P13473	Lysosome-associated membrane glycoprotein 2	0.057007976	0.475292689	0.163805865	0.828691541	0.239550519	0.453414385
P13489	Ribonuclease inhibitor	0.085494890	-0.311772001	0.186691971	-0.257593989	0.019886169	-0.519770468
P13639	Elongation factor 2	0.396996267	-0.108019450	0.379186962	-0.099080988	0.999131171	0.004172438
P13645	Keratin_type I cytoskeletal 10	0.411224348	0.192118121	0.344782826	-0.551398670	0.944187814	0.163704332
P13647	Keratin_type II cytoskeletal 5	0.434639236	-0.260879961	0.690065832	-0.122266929	0.338405182	-0.321426614
P13667	Protein disulfide-isomerase A4	0.000520607	1.104963154	0.082326758	0.972328384	0.245057866	0.356758705
P13796	Plastin-2	0.726230880	-0.208475359	0.725784561	0.410025584	0.622245494	0.346870064
P13798	Acylamino-acid-releasing enzyme	0.938704065	-0.004168854	0.652236639	0.233529937	0.588869273	-0.163157797
P13804	Electron transfer flavoprotein subunit alpha_mitochondrial	0.230095667	0.328512429	0.433727451	-0.112578318	0.801548345	0.037335664
P14136	Glial fibrillary acidic protein	0.053486520	0.931235116	0.598255230	0.199878966	0.766698186	-0.064211513
P14174	Macrophage migration inhibitory factor	0.326991763	-0.130536484	0.725258997	0.081445573	0.651466266	0.141451814
P14314	Glucosidase 2 subunit beta	0.443662386	0.462445416	0.262534074	0.851108982	0.114505843	-0.294683705
P14324	Farnesyl pyrophosphate synthase	0.671461774	0.082403024	0.499775171	-0.177899726	0.318724262	-0.281762140
P14550	Aldo-keto reductase family 1 member A1	0.262051976	-0.442442765	0.601125007	-0.218797088	0.815862061	-0.095845386
P14618	Pyruvate kinase PKM	0.284036009	0.477684401	0.126602268	1.280557778	0.520405741	-0.142231193
P14625	Endoplasmin	0.206644134	0.337552891	0.682825288	0.095117670	0.816856029	0.029803374
P14866	Heterogeneous nuclear ribonucleoprotein L	0.389546874	0.209286875	0.496807363	-0.109385720	0.932330192	-0.012520697

P14868	Aspartate--tRNA ligase_ cytoplasmic	0.865022287	-0.099711183	0.248585094	0.325002441	0.598705105	-0.299700560
P14923	Junction plakoglobin	0.260327348	0.336987299	0.251373862	1.561023496	0.351198460	-0.188956888
P15121	Aldo-keto reductase family 1 member B1	0.937602547	-0.022718741	0.546491147	-0.154627401	0.818100177	-0.068024858
P15170	Eukaryotic peptide chain release factor GTP-binding subunit ERF3A	0.217020442	0.504687428	0.793492978	0.072893927	0.957645041	0.032765229
P15259	Phosphoglycerate mutase 2	0.555617766	0.059663113	0.536840889	0.309000027	0.175935442	-0.211231166
P15311	Ezrin	0.238396878	-0.257091065	0.788935172	0.134279584	0.818129089	-0.041407547
P15531	Nucleoside diphosphate kinase A	0.183412304	-0.613040867	0.527981080	0.336196220	0.269854063	-0.450702520
P15880	40S ribosomal protein S2	0.861334745	-0.032491444	0.507745726	0.142008374	0.017505951	-0.399745503
P15927	Replication protein A 32 kDa subunit	0.966909924	-0.051582861	0.191023008	0.392763971	0.521287276	0.183485890
P16104	Histone H2AX	0.487717886	-0.216621687	0.769439094	-0.300222426	0.841763775	0.155239618
P16234	Platelet-derived growth factor receptor alpha	0.656511058	0.220923986	0.060357949	-2.365499954	0.406446500	0.885477936
P16401	Histone H1.5	0.336167765	0.445279231	0.586590024	0.200697268	0.983006029	-0.119241369
P16403	Histone H1.2	0.345727593	0.273363977	0.600869712	0.243716917	0.782982382	0.046748549
P16435	NADPH--cytochrome P450 reductase	0.502832997	-0.337032090	0.199326221	-0.521116198	0.776018700	0.135915264
P16615	Sarcoplasmic/endoplasmic reticulum calcium ATPase 2	0.040658190	1.431714147	0.663229328	-0.059665969	0.751750882	-0.043138774
P16949	Stathmin	0.496644029	0.126654208	0.294375481	1.137127007	0.056402889	-0.298042279
P16989	Y-box-binding protein 3	0.713486556	-0.075914585	0.049842348	0.859757802	0.597611667	-0.154306412
P17066	Heat shock 70 kDa protein 6	0.660855422	-0.478442917	0.801422929	-0.190325204	0.984190625	-0.069511560
P17174	Aspartate aminotransferase_ cytoplasmic	0.062552074	1.357192308	0.008168184	1.661638835	0.849713608	0.133649348
P17480	Nucleolar transcription factor 1	0.216753649	-0.614998277	0.947033912	-0.031745204	0.382046706	-0.395837349
P17661	Desmin	0.628744253	0.134836800	0.060357025	-0.885609145	0.641287056	0.101280279
P17677	Neuromodulin	0.287119252	-0.281104083	0.234920442	1.610723437	0.072484061	0.398060569
P17812	CTP synthase 1	0.811852672	-0.022021031	0.831743410	-0.017167556	0.167534450	-0.170740758
P17844	Probable ATP-dependent RNA helicase DDX5	0.863899627	-0.036652616	0.308951364	0.407000940	0.007710450	-0.429749414
P17858	ATP-dependent 6-phosphofructokinase_ liver type	0.671892260	0.040160360	0.339585365	-0.176528535	0.337095709	-0.185769291

P17948	Vascular endothelial growth factor receptor 1	0.748364263	0.123049742	0.100610677	0.434877868	0.161442747	-0.133342477
P17980	26S proteasome regulatory subunit 6A	0.931477881	0.007520862	0.284595815	-0.219790690	0.695425757	-0.079170508
P17987	T-complex protein 1 subunit alpha	0.931389721	0.057094856	0.354782151	-0.151295778	0.874755235	0.044004896
P18085	ADP-ribosylation factor 4	0.703536106	0.197489423	0.240024636	0.794394844	0.448374821	-0.193134020
P18124	60S ribosomal protein L7	0.329700034	0.342637087	0.177307718	0.315592291	0.100103282	-0.213178129
P18206	Vinculin	0.979348390	-0.058517252	0.141621428	-0.588712472	0.893797044	-0.012184743
P18621	60S ribosomal protein L17	0.817750194	0.016195459	0.376864354	0.208544551	0.005214884	-0.561491066
P18669	Phosphoglycerate mutase 1	0.528833055	-0.155305118	0.602267028	0.323897820	0.676737821	-0.078079011
P18754	Regulator of chromosome condensation	0.697685489	0.351555633	0.969677487	-0.102682522	0.449638278	0.225381662
P18858	DNA ligase 1	0.198495365	-0.570596491	0.197366299	-0.501047359	0.580065575	0.544238530
P19012	Keratin_type I cytoskeletal 15	0.013786870	0.666949652	0.207458393	2.037724276	0.956371609	0.115989630
P19013	Keratin_type II cytoskeletal 4	0.360746146	1.131289493	0.248256433	-0.638723241	0.183998715	1.066762667
P19022	Cadherin-2	0.230528605	-0.314604940	0.678614045	0.049344694	0.395321796	-0.141580170
P19087	Guanine nucleotide-binding protein G(t) subunit alpha-2	0.000715865	-0.694550352	0.102002233	-0.512273136	0.474401082	-0.080635296
P19338	Nucleolin	0.108929209	0.686660110	0.088499993	1.456739451	0.007965403	-0.304375365
P19793	Retinoic acid receptor RXR-alpha	0.296126476	-0.634700848	0.301774715	-0.534070712	0.653516064	-0.279674290
P20290	Transcription factor BTF3	0.001097488	-1.672067074	0.449585735	-0.084657352	0.034092869	-0.393119282
P20338	Ras-related protein Rab-4A	0.228813902	-1.408191087	0.497078977	0.531764089	0.621396994	-0.220923946
P20340	Ras-related protein Rab-6A	0.041487662	-0.534171231	0.033669944	-0.616210069	0.230387942	-0.269845281
P20591	Interferon-induced GTP-binding protein Mx1	0.117912239	-0.395773589	0.044416268	-0.608795972	0.009065833	0.647492933
P20592	Interferon-induced GTP-binding protein Mx2	0.407462989	1.574626550	0.749198891	0.249565324	0.156979091	1.487944249
P20618	Proteasome subunit beta type-1	0.228998056	-0.334898315	0.755327405	-0.076601859	0.197776188	-0.350781216
P20674	Cytochrome c oxidase subunit 5A_mitochondrial	0.685719191	0.055944525	0.365592655	-0.472858995	0.378395505	0.245594348
P20700	Lamin-B1	0.286469324	-0.628563751	0.407274084	-0.454312415	0.235631582	-0.613610863
P20839	Inosine-5'-monophosphate dehydrogenase 1	0.944030738	0.033539722	0.808745202	-0.057630972	0.481110299	-0.410911610
P21281	V-type proton ATPase subunit B_brain isoform	0.725833552	0.419033338	0.137259906	-0.868658322	0.477776519	0.870641917

P21333	Filamin-A	0.248865949	-0.191018922	0.767161583	0.155265978	0.390187254	-0.141941771
P21399	Cytoplasmic aconitate hydratase	0.211452222	-0.822295192	0.068868155	-1.350354356	0.509839515	-0.433667310
P21741	Midkine	0.294642051	4.749742585	0.473463804	-0.143642499	0.010330227	3.786447466
P21796	Voltage-dependent anion-selective channel protein 1	0.016518562	0.592352318	0.261758631	0.390756906	0.556755267	0.117432047
P21802	Fibroblast growth factor receptor 2	0.110240238	-4.092340185	0.532788562	-0.912893058	0.821345385	-0.326640414
P22090	40S ribosomal protein S4_Y isoform 1	0.564351357	-0.632500957	0.899795931	0.250161141	0.734579952	-0.033248145
P22102	Trifunctional purine biosynthetic protein adenosine-3	0.067805098	-0.268648391	0.106670871	-0.266291477	0.065075421	-0.243215858
P22105	Tenascin-X	0.046981374	2.015192142	0.912737888	0.106687084	0.516879071	0.709982516
P22234	Multifunctional protein ADE2	0.247230463	-0.279407290	0.843696208	-0.049334077	0.136412034	-0.327167197
P22307	Non-specific lipid-transfer protein	0.068981373	0.323890827	0.586139832	0.110340343	0.007902605	0.854921816
P22314	Ubiquitin-like modifier-activating enzyme 1	0.715590780	0.032949700	0.813082006	-0.244203660	0.802459080	0.201165080
P22392	Nucleoside diphosphate kinase B	0.642632512	-0.190951141	0.394433145	0.550353298	0.327353411	-0.319446188
P22455	Fibroblast growth factor receptor 4	0.722428025	3.927251651	0.261155301	-2.264191744	0.090256167	2.783689812
P22492	Histone H1t	0.243917549	0.380458563	0.333586708	0.698576167	0.838889426	0.037556459
P22570	NADPH:adrenodoxin oxidoreductase_mitochondrial	0.888588301	0.101770273	0.742221067	0.160087650	0.698578543	-0.074490162
P22626	Heterogeneous nuclear ribonucleoproteins A2/B1	0.710150587	0.081455000	0.091992385	0.315955441	0.000530640	-0.200353123
P22695	Cytochrome b-c1 complex subunit 2_mitochondrial	0.062027536	-0.594543160	0.055540235	-0.801724014	0.693902183	-0.085078376
P23193	Transcription elongation factor A protein 1	0.809491864	-0.250602660	0.217385647	-0.355146825	0.954694008	0.028886589
P23246	Splicing factor_proline- and glutamine-rich	0.475958372	0.179277232	0.461630021	0.169368030	0.817128568	0.055365184
P23284	Peptidyl-prolyl cis-trans isomerase B	0.026363383	0.611115595	0.210529008	0.407873561	0.112516470	0.090441883
P23368	NAD-dependent malic enzyme_mitochondrial	0.165965607	-0.484948635	0.021859701	-0.776233977	0.043821748	-0.690156310
P23381	Tryptophan--tRNA ligase_cytoplasmic	0.345043082	0.285586361	0.955753967	-0.130754944	0.530516159	0.388880612
P23396	40S ribosomal protein S3	0.565042723	-0.131823199	0.902405750	-0.008016664	0.002988307	-0.757796888
P23497	Nuclear autoantigen Sp-100	0.131734535	0.369403869	0.250359552	0.426936194	0.674108713	0.136634322
P23526	Adenosylhomocysteinase	0.041878517	-0.417472502	0.525739321	0.271597709	0.156425516	-0.296130569

P23528	Cofilin-1	0.372088497	0.374847345	0.105287075	0.625643645	0.948018802	0.023902969
P23588	Eukaryotic translation initiation factor 4B	0.029867427	-0.836749882	0.620542441	0.175282297	0.062695969	-0.604895879
P23786	Carnitine O-palmitoyltransferase 2_mitochondrial	0.297736665	0.835640711	0.557632976	-0.619980627	0.861158686	-0.051774557
P23921	Ribonucleoside-diphosphate reductase large subunit	0.871119459	-0.217311510	0.767822569	0.116472859	0.369271464	-0.492939969
P24468	COUP transcription factor 2	0.630375820	0.056176382	0.306714694	0.362389769	0.843331884	-0.032240883
P24534	Elongation factor 1-beta	0.723633463	-0.168262829	0.576811678	0.299850590	0.353135705	-0.371997325
P24539	ATP synthase F(0) complex subunit B1_mitochondrial	0.046838013	-0.574558408	0.174309205	-0.554433161	0.891673008	0.092392933
P24666	Low molecular weight phosphotyrosine protein phosphatase	0.441270724	0.144055526	0.845762222	0.120331678	0.064138283	-0.403603798
P24752	Acetyl-CoA acetyltransferase_ mitochondrial	0.800845332	-0.213324158	0.831240624	0.326855646	0.749300889	-0.158343234
P24941	Cyclin-dependent kinase 2	0.069944044	0.549283078	0.950797240	0.199759731	0.345577374	0.511602266
P25205	DNA replication licensing factor MCM3	0.085077608	0.292997853	0.350839267	0.315813622	0.367069005	-0.174303827
P25325	3-mercaptopyruvate sulfurtransferase	0.000005130	3.555338749	0.268040978	-0.299688436	0.340009986	-0.258353459
P25398	40S ribosomal protein S12	0.376068244	0.195650363	0.306026820	1.005032676	0.346665654	-0.232025187
P25705	ATP synthase subunit alpha_ mitochondrial	0.203727711	0.540901975	0.211396543	0.669382106	0.853083353	0.037446583
P25786	Proteasome subunit alpha type-1	0.798393398	-0.021238828	0.218454137	0.532898013	0.734739876	0.015395795
P25787	Proteasome subunit alpha type-2	0.441377115	0.359920748	0.293248852	0.859816882	0.986628595	-0.028918940
P25788	Proteasome subunit alpha type-3	0.212005294	-0.807475980	0.732744550	-0.165572105	0.423114183	-0.219792158
P25789	Proteasome subunit alpha type-4	0.581069635	-0.133440402	0.250408746	0.516878256	0.403400655	-0.184468119
P26038	Moesin	0.699637332	-0.030012962	0.244929037	0.629974397	0.873300490	0.010147982
P26196	Probable ATP-dependent RNA helicase DDX6	0.019160634	1.017946913	0.059805844	1.123626594	0.112013525	0.342315631
P26232	Catenin alpha-2	0.636567519	0.114287980	0.159439202	0.952360544	0.207869274	0.277857982
P26368	Splicing factor U2AF 65 kDa subunit	0.299607020	-0.314503391	0.224412386	-0.486167361	0.433158402	-0.225970528
P26373	60S ribosomal protein L13	0.779877104	-0.017388169	0.878922049	-0.022626526	0.128916843	-0.269650434
P26583	High mobility group protein B2	0.714308816	0.126558881	0.107660527	0.695317675	0.738181356	0.127530916
P26599	Polypyrimidine tract-binding protein 1	0.572612660	0.071888799	0.192905458	0.470448032	0.572463130	-0.122589546

P26639	Threonine--tRNA ligase_ cytoplasmic	0.163273187	-0.913246353	0.315811300	-0.451207373	0.319448780	-0.598704474
P26640	Valine--tRNA ligase	0.460548703	1.475351348	0.630064389	0.067168506	0.180354497	1.197112262
P26641	Elongation factor 1-gamma	0.066714836	-0.614491726	0.612999565	0.130796095	0.458585191	-0.194837388
P27348	14-3-3 protein theta	0.310391665	-0.369155348	0.699814862	-0.147354959	0.286424024	-0.353649111
P27361	Mitogen-activated protein kinase 3	0.813243040	0.389961054	0.874635759	0.040980375	0.631253123	-0.272985237
P27635	60S ribosomal protein L10	0.772895499	-0.172871220	0.404821279	-0.291368015	0.529093673	-0.190492835
P27694	Replication protein A 70 kDa DNA-binding subunit	0.292859118	0.673566417	0.151929171	0.710189546	0.546200213	-0.114125090
P27695	DNA-(apurinic or apyrimidinic site) lyase	0.927276099	0.011926138	0.177288668	-0.342074819	0.304941916	0.109853832
P27708	CAD protein	0.096223602	0.880047473	0.603181989	0.339171240	0.103986411	0.869587857
P27797	Calreticulin	0.069908363	0.514918767	0.271863320	0.726120862	0.998171656	0.014943603
P27816	Microtubule-associated protein 4	0.348154365	0.111492210	0.192105746	-0.193300534	0.008015889	-0.133668763
P27824	Calnexin	0.017335147	0.608523183	0.232597918	0.543957182	0.761300319	0.033632882
P28066	Proteasome subunit alpha type-5	0.965576145	-0.025194117	0.424053795	0.577150707	0.142582974	-0.453647726
P28070	Proteasome subunit beta type-4	0.633216659	-0.202843883	0.372691335	0.466160950	0.275654010	-0.496543191
P28072	Proteasome subunit beta type-6	0.780875038	-0.030539243	0.218398843	0.281154818	0.980106144	-0.005560165
P28074	Proteasome subunit beta type-5	0.409141092	-0.110309554	0.064145717	-0.224858311	0.066580945	0.159198755
P28161	Glutathione S-transferase Mu 2	0.139721643	-0.681065487	0.146279211	-1.220751087	0.846930553	0.492300525
P28482	Mitogen-activated protein kinase 1	0.768651725	0.140082157	0.955571844	-0.028339601	0.267105125	-0.519284341
P28838	Cytosol aminopeptidase	0.226924716	0.608423038	0.538019477	0.051835250	0.156810715	0.668160553
P29373	Cellular retinoic acid-binding protein 2	0.130771859	-0.655016809	0.603622656	-0.167798126	0.491070625	-0.204144387
P29401	Transketolase	0.299188121	0.203198058	0.172854028	0.831082827	0.951355482	0.005326581
P29692	Elongation factor 1-delta	0.991978611	0.079624098	0.248567026	0.515204096	0.385142467	-0.280674155
P29762	Cellular retinoic acid-binding protein 1	0.828185160	-0.038456769	0.792483529	0.253702924	0.880379880	-0.070850460
P29966	Myristoylated alanine-rich C-kinase substrate	0.003440102	-1.632938360	0.496816973	-0.160323355	0.122094115	-0.632041814
P30040	Endoplasmic reticulum resident protein 29	0.569875011	0.165289423	0.045062909	-0.397888053	0.992097193	-0.003442728
P30041	Peroxiredoxin-6	0.195532045	0.453381065	0.108902477	0.817146769	0.408614960	0.174405007

P30044	Peroxiredoxin-5_mitochondrial	0.021367408	0.449100383	0.266042630	0.698501273	0.062964718	-0.239624876
P30046	D-dopachrome decarboxylase	0.058289876	-1.110154974	0.229939259	-0.606629333	0.958437352	0.052128374
P30048	Thioredoxin-dependent peroxide reductase_mitochondrial	0.818892402	-0.033969781	0.859980124	0.059136657	0.921249825	0.014671546
P30049	ATP synthase subunit delta_mitochondrial	0.030727173	0.465768416	0.473585418	-0.141364249	0.033131773	0.327117546
P30050	60S ribosomal protein L12	0.674313875	0.049576720	0.767673860	0.146369712	0.132382945	-0.273015243
P30084	Enoyl-CoA hydratase_mitochondrial	0.404025490	0.196460196	0.683099358	0.094705839	0.972712745	-0.085544098
P30085	UMP-CMP kinase	0.852671719	-0.163488562	0.377371693	-0.452235910	0.830112512	-0.172309235
P30086	Phosphatidylethanolamine-binding protein 1	0.778180774	0.208235351	0.130080917	1.500917521	0.444204553	-0.210807136
P30101	Protein disulfide-isomerase A3	0.035998808	0.616239208	0.420194209	0.212903421	0.905646577	0.012510227
P30153	Serine/threonine-protein phosphatase 2A 65 kDa regulatory subunit A alpha isoform	0.933379114	0.007891533	0.430805911	0.153258840	0.214496366	-0.252210027
P30154	Serine/threonine-protein phosphatase 2A 65 kDa regulatory subunit A beta isoform	0.604319913	0.127292770	0.591040034	0.912984125	0.629712922	-0.554778038
P30613	Pyruvate kinase PKLR	0.014004979	1.491059789	0.913889743	-0.104600467	0.954308231	-0.181540514
P30626	Sorcin	0.134333557	-0.491121265	0.844895135	-0.055928577	0.231999130	-0.375588463
P31150	Rab GDP dissociation inhibitor alpha	0.000041504	2.968590000	0.164768259	0.686099101	0.434112309	0.153857720
P31153	S-adenosylmethionine synthase isoform type-2	0.056266699	-0.659589153	0.675572832	-0.128396767	0.205065968	-0.419295055
P31350	Ribonucleoside-diphosphate reductase subunit M2	0.237026017	-2.088244330	0.560246204	0.487587208	0.749544412	-0.070018462
P31483	Nucleolysin TIA-1 isoform p40	0.572090621	0.080314603	0.113202537	-1.117712884	0.493120224	0.283792467
P31689	DnaJ homolog subfamily A member 1	0.975871452	-0.136981397	0.181145863	0.488446566	0.999549489	-0.042512959
P31930	Cytochrome b-c1 complex subunit 1_mitochondrial	0.616982540	0.113855940	0.327428382	0.461467394	0.486050048	-0.107262135
P31939	Bifunctional purine biosynthesis protein PURH	0.005478862	0.424461574	0.936960910	0.032411256	0.116277767	-0.132205958
P31942	Heterogeneous nuclear ribonucleoprotein H3	0.528523698	0.108811336	0.311603395	0.369353181	0.713257916	-0.078414336
P31943	Heterogeneous nuclear ribonucleoprotein H	0.261529571	0.416678168	0.126817143	0.861166475	0.057627171	-0.263202242
P31946	14-3-3 protein beta/alpha	0.811532810	-0.082674562	0.977607784	-0.018292308	0.558729707	-0.150709611
P31948	Stress-induced-phosphoprotein 1	0.336580024	-0.213948543	0.403431732	-0.177300002	0.233612001	-0.254483736

P32119	Peroxiredoxin-2	0.653027947	0.057716795	0.312388434	0.507222719	0.468425602	-0.095716979
P32969	60S ribosomal protein L9	0.073276822	0.349067822	0.080982939	0.847820818	0.321061711	-0.209530152
P33176	Kinesin-1 heavy chain	0.943745769	-0.031246982	0.890837007	-0.023792869	0.148112517	-0.276176962
P33316	Deoxyuridine 5'-triphosphate nucleotidohydrolase_ mitochondrial	0.262413351	-0.544176160	0.345414322	-0.369611218	0.422873874	-0.340705033
P33991	DNA replication licensing factor MCM4	0.251687686	-0.181908796	0.904308018	-0.003193620	0.007249447	-0.407697156
P33992	DNA replication licensing factor MCM5	0.675444705	-0.052409375	0.205222472	-0.298796125	0.044468658	-0.310776996
P33993	DNA replication licensing factor MCM7	0.115961485	-0.369838982	0.200950302	-0.407549741	0.668908606	-0.082473252
P34897	Serine hydroxymethyltransferase_ mitochondrial	0.325535854	0.365235628	0.317477803	0.481137376	0.053941091	-0.246565762
P34925	Tyrosine-protein kinase RYK	0.741964930	-0.655125218	0.757807746	-1.525553402	0.488348237	0.255154283
P34931	Heat shock 70 kDa protein 1-like	0.254163634	0.215253331	0.223551913	0.527227213	0.327883481	-0.182352728
P34932	Heat shock 70 kDa protein 4	0.759394655	-0.106395266	0.452080326	0.345161164	0.252433267	-0.268388262
P35221	Catenin alpha-1	0.155077577	-0.322207209	0.074333288	0.453780920	0.166914666	0.329709682
P35222	Catenin beta-1	0.001142682	-0.292691710	0.191283928	-0.389496577	0.369869864	0.102449225
P35232	Prohibitin	0.255036847	0.165671083	0.883223095	-0.004016400	0.674547235	-0.037686053
P35241	Radixin	0.264914444	-0.221570215	0.429857605	0.416107225	0.823019925	-0.017745472
P35244	Replication protein A 14 kDa subunit	0.369070662	-0.093135144	0.909100272	0.016029183	0.377467719	-0.107951903
P35268	60S ribosomal protein L22	0.353765301	-0.184030532	0.181486522	0.358701315	0.006343292	-0.508475230
P35527	Keratin_ type I cytoskeletal 9	0.625748032	-0.078044069	0.342264597	0.202799473	0.547693389	-0.084711589
P35579	Myosin-9	0.987587575	-0.036581553	0.580138915	-0.128146962	0.751106579	-0.069795677
P35580	Myosin-10	0.079869167	0.362377170	0.606809031	-0.045093771	0.042317646	-0.126458314
P35606	Coatomer subunit beta'	0.718551212	-0.030170410	0.038063931	-0.521232437	0.032434611	-0.195472929
P35609	Alpha-actinin-2	0.178077384	0.402509346	0.247436590	0.473314778	0.917759499	-0.008595349
P35611	Alpha-adducin	0.471154736	-0.412330614	0.349151163	-0.465729397	0.991200427	-0.075289431
P35613	Basigin	0.819303872	0.049035982	0.885705919	-0.017512871	0.345990156	-0.344764428
P35637	RNA-binding protein FUS	0.453601702	0.184189683	0.058120469	0.342783366	0.200053070	-0.312073218
P35659	Protein DEK	0.044141632	0.610150055	0.496848901	0.701391523	0.782254598	-0.095368087

P35749	Myosin-11	0.553935919	0.090255461	0.123230427	-0.758960831	0.958191682	-0.051227509
P35908	Keratin_type II cytoskeletal 2 epidermal	0.749857049	0.592474660	0.342837013	-0.945597156	0.192200263	-1.237485566
P35998	26S proteasome regulatory subunit 7	0.882712572	0.000720995	0.923453589	0.038969585	0.311800081	-0.172358736
P36405	ADP-ribosylation factor-like protein 3	0.210473243	-0.144512356	0.226953662	0.730002648	0.018903798	-0.295687970
P36507	Dual specificity mitogen-activated protein kinase kinase 2	0.416346507	0.396115705	0.709823984	0.503280233	0.341879256	0.589017426
P36542	ATP synthase subunit gamma_mitochondrial	0.236674779	0.163829947	0.950451678	-0.001717244	0.392654090	-0.115059346
P36578	60S ribosomal protein L4	0.628311053	-0.094331447	0.474800088	-0.123145380	0.098367867	-0.340041991
P36873	Serine/threonine-protein phosphatase PP1-gamma catalytic subunit	0.183497626	0.813594149	0.208224783	0.541955923	0.337395422	-0.582428161
P36957	Dihydrolipoyllysine-residue succinyltransferase component of 2-oxoglutarate dehydrogenase complex_mitochondrial	0.186095437	-0.398817680	0.331232658	-0.312610453	0.992282586	-0.036284563
P37108	Signal recognition particle 14 kDa protein	0.133449154	0.291237831	0.091352375	0.957020637	0.991107411	0.048587976
P37235	Hippocalcin-like protein 1	0.006292510	2.486174402	0.392987033	0.159169002	0.007255635	0.412601480
P37268	Squalene synthase	0.536801113	0.324132687	0.706338909	0.601941512	0.136804199	-0.636926690
P37802	Transgelin-2	0.532286920	0.055725329	0.668087566	0.246106656	0.894579103	-0.260354768
P37837	Transaldolase	0.510830666	-0.240673912	0.779803070	0.215692703	0.325465157	-0.314682446
P38159	RNA-binding motif protein_X chromosome	0.439418506	0.141835903	0.119701627	0.499456376	0.551306299	-0.190864765
P38606	V-type proton ATPase catalytic subunit A	0.751478418	-0.142344226	0.855798924	-0.101710455	0.353029378	-0.322848685
P38646	Stress-70 protein_mitochondrial	0.460345569	0.125348901	0.858596846	-0.073232306	0.681493473	-0.137417385
P38919	Eukaryotic initiation factor 4A-III	0.972748993	-0.123311937	0.968215812	-0.070668071	0.466780657	0.426761198
P39019	40S ribosomal protein S19	0.114602604	-0.258066771	0.843440686	-0.005383550	0.000462097	-0.489078102
P39023	60S ribosomal protein L3	0.541222230	0.258487434	0.102279661	0.443259969	0.016244702	-0.463273653
P39656	Dolichyl-diphosphooligosaccharide-protein glycosyltransferase 48 kDa subunit	0.140109905	0.167263485	0.216950479	0.208020279	0.894904909	-0.012621744
P39687	Acidic leucine-rich nuclear phosphoprotein 32 family member A	0.890792898	-0.026784798	0.417548076	0.258681686	0.342604267	-0.288844792
P39748	Flap endonuclease 1	0.099007262	0.342328000	0.094393173	0.797271417	0.207295829	-0.309347036
P40227	T-complex protein 1 subunit zeta	0.350477285	0.295330412	0.132760539	0.551236716	0.703330663	-0.110267274

P40429	60S ribosomal protein L13a	0.626123300	-0.149243934	0.387666426	-0.294749289	0.222824617	-0.422813336
P40925	Malate dehydrogenase_ cytoplasmic	0.720720359	0.099030013	0.694752770	0.192212123	0.337375342	-0.245297512
P40926	Malate dehydrogenase_ mitochondrial	0.757634652	0.023007221	0.327068972	0.765702338	0.386534000	-0.191013102
P40939	Trifunctional enzyme subunit alpha_ mitochondrial	0.107906485	0.232000017	0.695931306	0.097516555	0.780631283	-0.050742124
P41091	Eukaryotic translation initiation factor 2 subunit3	0.011976810	0.664508743	0.169263331	-0.420047776	0.146111383	0.345858936
P41219	Peripherin	0.002087058	-1.330866826	0.118598428	-0.462751149	0.391651705	-0.227490842
P41250	Glycine--tRNA ligase	0.074798125	-0.438194760	0.046046369	-0.663199445	0.286620370	-0.126880166
P41252	Isoleucine--tRNA ligase_ cytoplasmic	0.088681735	0.435030589	0.093942054	0.715921700	0.344379360	0.174919635
P42025	Beta-centractin	0.318188196	-0.623986228	0.188648660	-0.727580128	0.157770186	-0.775204092
P42166	Lamina-associated polypeptide 2_ isoform alpha	0.087055445	0.593975735	0.433042480	0.186076411	0.184575879	-0.128851368
P42167	Lamina-associated polypeptide 2_ isoforms beta/gamma	0.087055445	0.593975735	0.433042481	0.186076411	0.184575878	-0.128851368
P42224	Signal transducer and activator of transcription 1-alpha/beta	0.947409973	0.088306279	0.431209573	0.193280668	0.719035670	-0.021612231
P42263	Glutamate receptor 3	0.003629490	-1.385444120	0.606093508	0.944860219	0.182898763	-0.570861050
P42356	Phosphatidylinositol 4-kinase alpha	0.398561256	0.161426919	0.634281204	0.422111902	0.613028677	-0.135082182
P42704	Leucine-rich PPR motif-containing protein_mitochondrial	0.174006414	-0.138683882	0.060354232	-0.194808443	0.019971108	-0.174597070
P42785	Lysosomal Pro-X carboxypeptidase	0.808000546	0.008763578	0.799272615	0.121771683	0.105082471	0.824219511
P43034	Platelet-activating factor acetylhydrolase IB subunit alpha	0.093907617	-0.176025483	0.657862159	-0.033893157	0.073297769	-0.119572089
P43243	Matrin-3	0.829085775	-0.013103613	0.352591507	0.493147568	0.871273269	0.091012278
P43246	DNA mismatch repair protein Msh2	0.925344127	0.072685755	0.277265156	0.728905372	0.246219647	-0.264042916
P43487	Ran-specific GTPase-activating protein	0.643674677	0.306181999	0.130403837	0.533243211	0.984263328	0.041996995
P43686	26S proteasome regulatory subunit 6B	0.133746017	-0.140182743	0.142921231	-0.381497250	0.232091827	0.197336034
P45880	Voltage-dependent anion-selective channel protein 2	0.011639952	0.815740812	0.131451037	1.538004473	0.224807653	0.280663704
P45973	Chromobox protein homolog 5	0.315189092	0.234858160	0.231306677	0.282308742	0.503642008	-0.188440903

P45974	Ubiquitin carboxyl-terminal hydrolase 5	0.997224288	-0.012661728	0.337218010	-0.135757382	0.831678998	-0.000782710
P45985	Dual specificity mitogen-activated protein kinase kinase 4	0.873632272	-0.208490687	0.596336277	-0.033137540	0.927716521	-0.109589315
P46060	Ran GTPase-activating protein 1	0.356723168	-0.456379664	0.617558332	-0.242895203	0.860785715	0.194003005
P46109	Crk-like protein	0.020375151	0.710032686	0.407036079	0.260782712	0.995521360	-0.044176111
P46776	60S ribosomal protein L27a	0.860848943	0.011305940	0.129125715	0.280717493	0.206608905	-0.244710208
P46777	60S ribosomal protein L5	0.294962762	0.259549625	0.278271315	0.648131794	0.532328473	-0.315590359
P46778	60S ribosomal protein L21	0.233461522	-0.874516812	0.134496942	-0.902881846	0.734276017	-0.126623869
P46779	60S ribosomal protein L28	0.083813703	-0.193188334	0.940374284	0.020330062	0.127531951	-0.191670181
P46781	40S ribosomal protein S9	0.743168091	0.082331408	0.564286721	0.089435357	0.246522890	-0.230156150
P46782	40S ribosomal protein S5	0.647787408	-0.075751327	0.081629027	-0.352218581	0.167065892	-0.213873218
P46783	40S ribosomal protein S10	0.105451848	-0.559858632	0.174160365	0.251279494	0.309852788	-0.294493958
P46821	Microtubule-associated protein 1B	0.452055744	0.170783095	0.454999645	0.492214957	0.147153314	-0.233507229
P46926	Glucosamine-6-phosphate isomerase 1	0.657162306	0.227674023	0.241666475	0.556490806	0.378569090	-0.303794795
P46937	Transcriptional coactivator YAP1	0.552106024	0.566495773	0.032466294	2.134187660	0.217087884	-0.345759525
P46940	Ras GTPase-activating-like protein IQGAP1	0.732385810	0.056890445	0.952457066	0.033323315	0.758360179	-0.130896632
P47736	Rap1 GTPase-activating protein 1	0.484976052	0.614911197	0.033184912	-3.167080151	0.913955325	0.026363375
P47755	F-actin-capping protein subunit alpha-2	0.682264479	0.061318146	0.988240159	-0.001691804	0.867966609	-0.048120028
P47756	F-actin-capping protein subunit beta	0.774742792	-0.097108005	0.867689891	0.087489173	0.599640748	-0.133307766
P47813	Eukaryotic translation initiation factor 1A_X-chromosomal	0.421384760	0.670460195	0.995601994	-0.218696157	0.832552197	0.252765680
P47897	Glutamine--tRNA ligase	0.884648089	0.016537950	0.730807319	0.165102622	0.041714199	-0.481403800
P48047	ATP synthase subunit O_mitochondrial	0.904952309	-0.002338102	0.478670216	0.247258913	0.056486546	-0.337137943
P48444	Coatomer subunit delta	0.934078731	0.387124955	0.166516841	0.457647672	0.236676259	-0.488196859
P48643	T-complex protein 1 subunit epsilon	0.948612801	0.040562587	0.337878531	0.372129273	0.605083649	-0.140182958
P48681	Nestin	0.892612266	-0.063521286	0.272138874	-0.364532425	0.957404527	0.051354051
P48735	Isocitrate dehydrogenase [NADP]_mitochondrial	0.420658470	0.119326861	0.531404884	-0.083332941	0.030638108	-0.305741793

P49006	MARCKS-related protein	0.120141723	-0.657926343	0.205099404	1.189934414	0.100889120	-0.730319136
P49207	60S ribosomal protein L34	0.106889589	-2.022550746	0.126209771	-0.792394287	0.693749083	-0.465516218
P49257	Protein ERGIC-53	0.138367434	1.114179632	0.885493885	0.278583455	0.278579017	0.374594176
P49321	Nuclear autoantigenic sperm protein	0.985273132	0.032693591	0.255537559	0.462906645	0.406893847	-0.159348982
P49327	Fatty acid synthase	0.481804022	-0.047835639	0.679275178	0.082445880	0.001744281	-0.294838781
P49368	T-complex protein 1 subunit gamma	0.706901210	-0.082966401	0.443935957	-0.150522611	0.086765843	-0.318063744
P49411	Elongation factor Tu_ mitochondrial	0.646151824	0.122477887	0.071543407	0.373896313	0.938512164	0.019306125
P49419	Alpha-aminoacidic semialdehyde dehydrogenase	0.586842941	0.587160697	0.406211923	0.278977172	0.307650872	0.567968013
P49448	Glutamate dehydrogenase 2_ mitochondrial	0.545795918	0.296231047	0.230149256	0.685986146	0.284078545	-0.317495222
P49458	Signal recognition particle 9 kDa protein	0.713021742	0.169700385	0.103008635	0.747141441	0.010791405	-0.203207704
P49588	Alanine-tRNA ligase_ cytoplasmic	0.238171933	0.275197300	0.281878611	1.358859941	0.956264799	0.021705202
P49591	Serine-tRNA ligase_ cytoplasmic	0.290835379	0.311723820	0.169029971	0.353089508	0.285201414	-0.298474667
P49720	Proteasome subunit beta type-3	0.051566261	0.791569928	0.484758885	0.269340113	0.791940415	-0.068798776
P49721	Proteasome subunit beta type-2	0.137926224	-0.680506633	0.131008077	-0.607445267	0.538890594	-0.247695905
P49736	DNA replication licensing factor MCM2	0.354351864	0.589346753	0.177448446	0.312079408	0.043208097	1.649593245
P49755	Transmembrane emp24 domain-containing protein 10	0.079356142	0.689058778	0.111459164	0.382402251	0.053756309	0.339263122
P49773	Histidine triad nucleotide-binding protein 1	0.074578388	0.607353367	0.195858267	1.515779544	0.264806268	-0.169741760
P49841	Glycogen synthase kinase-3 beta	0.366619374	-1.122066700	0.736720401	0.048388740	0.563428407	-0.662789747
P49903	Selenide_water dikinase 1	0.666687910	-0.142214829	0.163953470	0.414461088	0.555915996	-0.194194129
P49915	GMP synthase [glutamine-hydrolyzing]	0.333577694	0.159779361	0.925759729	0.025055143	0.208748819	-0.150950246
P50222	Homeobox protein MOX-2	0.362854130	1.734455699	0.889102825	0.745458014	0.805128286	0.051520223
P50395	Rab GDP dissociation inhibitor beta	0.296365566	-0.232598776	0.146295210	-0.399619048	0.936515167	0.024799924
P50454	Serpin H1	0.868799009	0.092843895	0.490244865	0.739956333	0.986515084	0.107222895
P50502	Hsc70-interacting protein	0.669900411	-0.082977149	0.248698123	0.476018046	0.307224342	-0.269508429
P50897	Palmitoyl-protein thioesterase 1	0.566606178	0.112656504	0.843757159	0.261734604	0.505381751	0.081580760
P50914	60S ribosomal protein L14	0.954625641	0.011012403	0.130410688	0.459442763	0.007586782	-0.406799332

P50990	T-complex protein 1 subunit theta	0.735247033	0.283243589	0.317491051	0.478421187	0.420109948	-0.286195281
P50991	T-complex protein 1 subunit delta	0.946833367	-0.001502905	0.195348827	0.484419370	0.960226435	-0.069798978
P51148	Ras-related protein Rab-5C	0.121447920	-0.455815418	0.878076925	0.065385579	0.252977218	-0.203301885
P51149	Ras-related protein Rab-7a	0.743639126	0.057041637	0.421069434	0.330512615	0.467498245	-0.216415454
P51153	Ras-related protein Rab-13	0.906872810	0.669540397	0.973982060	0.275857425	0.934055853	-0.091768035
P51451	Tyrosine-protein kinase Blk	0.010357487	0.726959865	0.346896903	0.758528866	0.222466191	-0.306342792
P51571	Translocon-associated protein subunit delta	0.273902037	-0.911117732	0.100630647	-1.684252605	0.334030906	-1.073723866
P51659	Peroxisomal multifunctional enzyme type 2	0.438356971	0.663886034	0.426337079	0.255108429	0.323862162	0.359974604
P51665	26S proteasome non-ATPase regulatory subunit7	0.206644202	-0.277378385	0.357034479	-0.147639814	0.093382333	-0.246500658
P51668	Ubiquitin-conjugating enzyme E2 D1	0.928031895	0.020051537	0.906869567	-0.033450704	0.547971193	-0.134314531
P51805	Plexin-A3	0.001848053	0.961398420	0.543408414	0.257317514	0.082473920	-0.286027418
P51858	Hepatoma-derived growth factor	0.331709507	-1.084912748	0.674330330	-0.588209590	0.523473770	-0.681026637
P51991	Heterogeneous nuclear ribonucleoprotein A3	0.046456167	0.501908462	0.021783613	0.507431380	0.239731042	0.163197553
P52209	6-phosphogluconate dehydrogenase_decarboxylating	0.689312284	0.294504155	0.659627628	0.116143207	0.737626276	-0.121527653
P52272	Heterogeneous nuclear ribonucleoprotein M	0.604220191	0.136505762	0.138903722	0.716882692	0.001630498	-0.409846729
P52292	Importin subunit alpha-1	0.054348930	-0.884466637	0.720996341	-0.114957729	0.599708690	-0.256728824
P52565	Rho GDP-dissociation inhibitor 1	0.274406843	0.111912314	0.222238187	1.207403191	0.704131948	0.061762247
P52597	Heterogeneous nuclear ribonucleoprotein F	0.352368067	0.376076462	0.104791818	1.145540668	0.251966822	-0.310381698
P52701	DNA mismatch repair protein Msh6	0.353977362	-0.429433867	0.111906175	-0.904713581	0.822993752	0.189694830
P52788	Spermine synthase	0.318287464	0.306306830	0.491134511	-0.281043865	0.778592607	-0.117138507
P52907	F-actin-capping protein subunit alpha-1	0.418927005	0.188096699	0.596323078	0.187863260	0.318114131	-0.185542745
P52926	High mobility group protein HMGI-C	0.124300822	-1.137290745	0.498440390	-0.526315297	0.185536310	-0.912387554
P52943	Cysteine-rich protein 2	0.685860814	-0.259858022	0.650116850	-0.367371087	0.851333500	-0.015097992
P53041	Serine/threonine-protein phosphatase 5	0.070296636	-1.479232711	0.349953373	-0.446724497	0.928054906	-0.021198262
P53396	ATP-citrate synthase	0.204314745	0.645938238	0.991298721	-0.037865259	0.506711273	0.599529431
P53618	Coatomer subunit beta	0.690523773	0.422886563	0.074160011	-0.538785147	0.835561970	-0.032918717

P53621	Coatomer subunit alpha	0.127004801	0.199861848	0.143667122	-0.218773341	0.667741851	-0.057336601
P53675	Clathrin heavy chain 2	0.174447448	0.773091965	0.191406412	0.932875998	0.874342356	-0.066303286
P53992	Protein transport protein Sec24C	0.614910638	-0.168949139	0.523038508	0.442646399	0.886852396	-0.050769849
P53999	Activated RNA polymerase II transcriptional coactivator p15	0.919374628	0.001361834	0.200447085	0.405987569	0.031210624	-0.330680645
P54136	Arginine--tRNA ligase_ cytoplasmic	0.853141381	-0.034951933	0.844075921	0.005550397	0.627224121	-0.185589710
P54577	Tyrosine--tRNA ligase_ cytoplasmic	0.244733292	-0.612990860	0.816372880	0.018777295	0.751284603	-0.164260719
P54578	Ubiquitin carboxyl-terminal hydrolase 14	0.503005506	-0.926087208	0.226315404	-0.955801080	0.601181744	-0.558123166
P54652	Heat shock-related 70 kDa protein 2	0.267800127	0.691467911	0.458930450	0.381037445	0.604085886	-0.096882080
P54687	Branched-chain-amino-acid aminotransferase_ cytosolic	0.569837674	-0.247831712	0.795574189	-0.054790217	0.428070460	-0.238212707
P54727	UV excision repair protein RAD23 homolog B	0.000125283	2.267305446	0.187167719	1.075138856	0.179478670	-0.350100725
P54760	Ephrin type-B receptor 4	0.545627565	0.808190948	0.185089384	0.630492819	0.827674638	-1.774614576
P54802	Alpha-N-acetylglucosaminidase	0.667301253	-0.227928512	0.621517541	-0.105400225	0.497499123	-0.249480025
P54819	Adenylate kinase 2_ mitochondrial	0.236356827	0.455148655	0.317513439	-0.638418121	0.844720723	-0.029952043
P54886	Delta-1-pyrroline-5-carboxylate synthase	0.083064424	0.254022839	0.599046322	-0.045371375	0.903989651	0.020890545
P54920	Alpha-soluble NSF attachment protein	0.237479305	-0.482237187	0.800019323	-0.127997101	0.668259341	-0.189669299
P55010	Eukaryotic translation initiation factor 5	0.010855543	-0.211403410	0.517300204	-0.082027411	0.047100201	-0.180089805
P55036	26S proteasome non-ATPase regulatory subunit4	0.346968708	0.249118858	0.261689139	0.459381594	0.326804461	-0.167168034
P55060	Exportin-2	0.266265647	-0.323588148	0.814093669	-0.073055890	0.312294771	-0.271766089
P55072	Transitional endoplasmic reticulum ATPase	0.061467565	0.294002596	0.294947013	0.401543172	0.478776585	0.099737927
P55145	Mesencephalic astrocyte-derived neurotrophic factor	0.214313227	-0.353309544	0.349493830	0.794489792	0.710879747	0.031048648
P55209	Nucleosome assembly protein 1-like 1	0.729272956	0.163219895	0.056513330	0.299348899	0.018337283	-0.119472132
P55210	Caspase-7	0.060836180	0.566173610	0.112732124	1.312736933	0.423682868	-0.150353570
P55263	Adenosine kinase	0.194111837	0.430376922	0.577074572	0.182722860	0.312061942	-0.344914473
P55786	Puromycin-sensitive aminopeptidase	0.244854368	-0.258727737	0.150458914	-0.330384978	0.341550097	-0.198392605
P55795	Heterogeneous nuclear ribonucleoprotein H2	0.096459705	0.516516282	0.085694188	0.852719592	0.347580657	-0.108052635

P55884	Eukaryotic translation initiation factor 3 subunitB	0.448042077	0.490071398	0.540552603	0.139064763	0.892814627	0.003998662
P56192	Methionine--tRNA ligase_ cytoplasmic	0.607579759	-0.170474870	0.646820816	0.227549566	0.363498371	-0.272271728
P56470	Galectin-4	0.356111758	-0.735120759	0.600860583	-0.523522050	0.662471029	-0.165807641
P56537	Eukaryotic translation initiation factor 6	0.298909695	0.147086965	0.531460498	0.436960888	0.793156085	-0.018288112
P56545	C-terminal-binding protein 2	0.704538124	0.131268414	0.348168014	0.262525103	0.237315801	-0.173277919
P57721	Poly(rC)-binding protein 3	0.526224513	-0.331950083	0.964568521	0.047205962	0.494292562	-0.307922616
P57723	Poly(rC)-binding protein 4	0.189062787	-0.760528904	0.132559483	-0.690838267	0.964036750	-0.132280285
P58546	Myotrophin	0.837366885	-0.120233551	0.358179022	-0.340931292	0.682928726	-0.173052971
P59190	Ras-related protein Rab-15	0.593438051	0.096096065	0.830052223	-0.097877856	0.271594904	-0.505073404
P59998	Actin-related protein 2/3 complex subunit 4	0.342128335	-0.430853087	0.700649819	-0.083393807	0.055172605	-0.850243960
P60174	Triosephosphate isomerase	0.307963884	0.218153702	0.210800496	1.378094833	0.271107380	-0.170147679
P60228	Eukaryotic translation initiation factor 3 subunitE	0.240284135	-0.564772877	0.601327328	0.886647103	0.023435592	-1.110122673
P60510	Serine/threonine-protein phosphatase 4 catalytic subunit	0.198810127	0.345987344	0.124982078	1.635655995	0.535633517	-0.130326714
P60660	Myosin light polypeptide 6	0.647258743	-0.117037737	0.594265829	-0.117863574	0.684057208	-0.080308612
P60842	Eukaryotic initiation factor 4A-I	0.993650354	-0.018519008	0.445302240	0.279958516	0.493068530	-0.243540812
P60866	40S ribosomal protein S20	0.349642552	0.141492003	0.342103090	-0.105580034	0.001119356	-0.344570669
P60900	Proteasome subunit alpha type-6	0.225261717	0.260397285	0.310513303	0.594544136	0.958663179	-0.006473588
P60953	Cell division control protein 42 homolog	0.423292128	0.126402654	0.008163326	-0.622624175	0.894823201	0.023188056
P60981	Destrin	0.169929412	-0.212686238	0.049163287	-0.393411090	0.292993601	-0.162216330
P61006	Ras-related protein Rab-8A	0.023167647	-1.892351581	0.276766350	-0.493125351	0.087761308	-1.084277143
P61018	Ras-related protein Rab-4B	0.529964984	0.101061211	0.185574708	-0.256298520	0.508240238	0.233021754
P61019	Ras-related protein Rab-2A	0.474915452	0.156035864	0.949257131	-0.028554625	0.924594978	-0.092104283
P61026	Ras-related protein Rab-10	0.284936542	0.172115473	0.634554297	-0.063580919	0.108709052	0.243116109
P61077	Ubiquitin-conjugating enzyme E2 D3	0.790698945	-0.159159462	0.875962961	-0.053212978	0.340254266	0.189711947
P61081	NEDD8-conjugating enzyme Ubc12	0.257681330	0.299520346	0.302380293	0.380367829	0.648099617	0.219456372

P61088	Ubiquitin-conjugating enzyme E2 N	0.975489017	0.100165278	0.510930454	0.180572871	0.319740059	-0.290039274
P61106	Ras-related protein Rab-14	0.172681164	0.278082128	0.355947939	-0.233750467	0.766531567	-0.062830600
P61158	Actin-related protein 3	0.433841854	-0.240146751	0.273993335	-0.308796023	0.565368422	-0.158984077
P61160	Actin-related protein 2	0.012245817	-0.359242433	0.488196283	0.105054315	0.629057425	-0.054356162
P61163	Alpha-centractin	0.836235597	-0.016123818	0.893779921	0.070396306	0.457672252	-0.145196760
P61201	COP9 signalosome complex subunit 2	0.157624012	-1.500096992	0.170100462	-1.356168155	0.113238447	0.861150154
P61204	ADP-ribosylation factor 3	0.667008121	0.193146625	0.207156490	0.930343007	0.721869763	-0.127935929
P61221	ATP-binding cassette sub-family E member 1	0.022630137	-0.676370777	0.244467232	-0.307118675	0.620289855	0.172644609
P61224	Ras-related protein Rap-1b	0.037072487	0.931604796	0.045445435	0.786620758	0.911910272	0.050397021
P61247	40S ribosomal protein S3a	0.510606325	-0.417259442	0.213099091	-0.736496153	0.773483785	0.039696066
P61254	60S ribosomal protein L26	0.030832776	-1.295644722	0.670285505	0.571604582	0.051468056	-1.099547149
P61313	60S ribosomal protein L15	0.038811208	-0.722409463	0.285060375	-0.307723313	0.028429166	-0.796209295
P61326	Protein mago nashi homolog	0.896195782	0.109717962	0.407628066	0.312701834	0.503539673	-0.446780538
P61353	60S ribosomal protein L27	0.020600569	-0.400688067	0.419942813	0.138217673	0.016807790	-0.511946352
P61586	Transforming protein RhoA	0.245905134	0.375600432	0.238357932	1.125668866	0.755278623	-0.104980834
P61604	10 kDa heat shock protein_mitochondrial	0.599460789	0.198453502	0.258063202	0.679112187	0.186591777	-0.307986971
P61619	Protein transport protein Sec61 subunit alpha isoform 1	0.595378626	1.492315527	0.350049943	0.440683168	0.963573226	-0.362237652
P61758	Prefoldin subunit 3	0.006702298	-0.705136748	0.492971983	-0.129241083	0.873494910	0.052382412
P61916	NPC intracellular cholesterol transporter 2	0.554259260	-0.194600735	0.229736972	1.315263742	0.693272463	0.129054651
P61970	Nuclear transport factor 2	0.814835624	-0.116037800	0.803056241	0.142225998	0.826378340	-0.066914075
P61978	Heterogeneous nuclear ribonucleoprotein K	0.549300106	0.206143926	0.137935424	0.752384324	0.118018917	-0.198472525
P61981	14-3-3 protein gamma	0.000005976	-0.793622699	0.079673807	-0.515944350	0.655479861	-0.035504920
P62081	40S ribosomal protein S7	0.262508238	0.223342968	0.514866431	0.080062216	0.358519805	-0.264964148
P62136	Serine/threonine-protein phosphatase PP1-alpha catalytic subunit	0.275539099	-0.246075885	0.156838910	0.337356860	0.666363680	0.090889630
P62191	26S proteasome regulatory subunit 4	0.442408472	-0.148815060	0.726759804	-0.058525118	0.008909699	-0.591904917
P62195	26S proteasome regulatory subunit 8	0.992045490	-0.008176666	0.291929848	-0.239074291	0.341089542	0.209843879

P62241	40S ribosomal protein S8	0.382279220	0.224103211	0.087786048	0.318722136	0.056615298	-0.375165769
P62244	40S ribosomal protein S15a	0.014220642	-1.069295395	0.177937283	-0.466269671	0.387721207	-0.260978025
P62249	40S ribosomal protein S16	0.137405962	-0.356220269	0.659661305	-0.094026541	0.163198704	-0.389981619
P62258	14-3-3 protein epsilon	0.878001816	0.030104963	0.498877305	-0.146515288	0.668231216	-0.096525125
P62263	40S ribosomal protein S14	0.540206769	-0.194416910	0.548879896	0.157961447	0.069262641	-0.592790268
P62266	40S ribosomal protein S23	0.333310965	-0.101463116	0.111470274	0.308394268	0.052865952	-0.391631160
P62269	40S ribosomal protein S18	0.140932283	-0.208599851	0.167660390	-0.219857454	0.012976410	-0.466761082
P62273	40S ribosomal protein S29	0.587058769	-0.558978062	0.578689315	-0.425327958	0.141623603	-1.122517336
P62277	40S ribosomal protein S13	0.194091067	-0.200474451	0.138031202	-0.235903377	0.070177120	-0.369784940
P62280	40S ribosomal protein S11	0.217892896	-0.135052220	0.141319236	-0.161890041	0.002891210	-0.339752351
P62304	Small nuclear ribonucleoprotein E	0.041105642	-0.391778711	0.372410474	0.284509149	0.455998825	-0.089752980
P62306	Small nuclear ribonucleoprotein F	0.345860368	-0.344289773	0.172270837	0.523981814	0.211681768	-0.432497379
P62308	Small nuclear ribonucleoprotein G	0.176668913	-0.529416063	0.893254741	0.488418787	0.209038433	-0.571321984
P62310	U6 snRNA-associated Sm-like protein LSm3	0.996825484	-0.029066180	0.414525368	-0.445874834	0.431312835	0.267046314
P62314	Small nuclear ribonucleoprotein Sm D1	0.247841013	-0.305644220	0.585104051	-0.137313630	0.961246375	-0.009128379
P62316	Small nuclear ribonucleoprotein Sm D2	0.437995315	-0.130236203	0.435670089	0.228403610	0.115648063	-0.247800922
P62318	Small nuclear ribonucleoprotein Sm D3	0.355080924	0.178241531	0.256436469	0.550417476	0.014234487	-0.198236711
P62328	Thymosin beta-4	0.607333987	-0.475862237	0.395370462	1.190382308	0.848745436	0.002481957
P62333	26S proteasome regulatory subunit 10B	0.621159150	-0.132147264	0.916144462	-0.013989576	0.960850484	-0.020910970
P62424	60S ribosomal protein L7a	0.471939983	-0.289100148	0.297530321	0.274249124	0.499505673	-0.197558558
P62491	Ras-related protein Rab-11A	0.771927996	-0.077041003	0.124757289	-0.923799485	0.000007485	3.150576388
P62495	Eukaryotic peptide chain release factor subunit 1	0.004822062	-1.780700802	0.173426193	-0.503625706	0.439383775	-0.136656940
P62633	Cellular nucleic acid-binding protein	0.339646781	0.407163843	0.620954001	-0.402597665	0.794480411	-0.122366141
P62701	40S ribosomal protein S4_X isoform	0.211305946	0.608754617	0.426408631	0.590533675	0.756107696	0.317372463
P62736	Actin_ aortic smooth muscle	0.217732479	-1.349573657	0.328842941	-1.140448178	0.988887481	-0.631228532
P62750	60S ribosomal protein L23a	0.027320746	-0.896874989	0.734680045	0.022845205	0.012156681	-0.657378241
P62753	40S ribosomal protein S6	0.829823508	-0.003725970	0.328597035	0.244358240	0.003333069	-0.447107357

P62805	Histone H4	0.250440641	0.530849238	0.542368058	0.328191761	0.767310726	0.065092996
P62820	Ras-related protein Rab-1A	0.312150851	-0.172576290	0.653151983	0.084152773	0.206360451	-0.210946019
P62826	GTP-binding nuclear protein Ran	0.811215307	0.098178261	0.281282225	0.289181640	0.502305832	-0.146521801
P62829	60S ribosomal protein L23	0.171826464	-0.297992695	0.267225763	0.247089290	0.122738178	-0.388223352
P62841	40S ribosomal protein S15	0.023652979	-1.242983749	0.059375430	-1.109348145	0.012567219	-0.847961592
P62847	40S ribosomal protein S24	0.687210935	0.088961830	0.017723264	0.536426525	0.157402965	-0.403729869
P62851	40S ribosomal protein S25	0.022046702	-0.499055528	0.169672096	-0.239267040	0.003102615	-0.651295142
P62857	40S ribosomal protein S28	0.183868121	-0.423609828	0.985059859	0.044604059	0.048187134	-0.627801459
P62873	Guanine nucleotide-binding protein G(I)/G(S)/G(T) subunit beta-1	0.587920707	-0.265666642	0.037629531	0.939584574	0.425906260	-0.275474141
P62879	Guanine nucleotide-binding protein G(I)/G(S)/G(T) subunit beta-2	0.086219485	-0.326191444	0.091810313	0.538642716	0.219211485	0.102411027
P62888	60S ribosomal protein L30	0.701582734	0.085844352	0.069383498	0.451353496	0.223998878	-0.247069256
P62899	60S ribosomal protein L31	0.455135181	0.215696563	0.440288673	0.150471323	0.085903426	-0.296701741
P62906	60S ribosomal protein L10a	0.280240265	0.288069618	0.080966952	1.730124717	0.031973539	-0.300318100
P62910	60S ribosomal protein L32	0.146596271	-0.462780740	0.126671365	-0.551903632	0.135231292	-0.430393101
P62913	60S ribosomal protein L11	0.218369100	-0.336460080	0.197478815	-0.351792757	0.195196329	-0.248846795
P62917	60S ribosomal protein L8	0.869804447	0.037162957	0.911855472	0.036795219	0.051028314	-0.525045121
P62937	Peptidyl-prolyl cis-trans isomerase A	0.896134946	-0.026556180	0.924255279	-0.021207019	0.341129180	-0.254546525
P62942	Peptidyl-prolyl cis-trans isomerase FKBP1A	0.047140133	-0.756768104	0.500318842	0.616974368	0.073599219	-0.478230332
P62979	Ubiquitin-40S ribosomal protein S27a	0.927491103	0.008172035	0.158888032	1.304648586	0.294938909	-0.392182319
P62995	Transformer-2 protein homolog beta	0.284033030	-0.216638293	0.377778441	-0.149332916	0.030444557	-0.495183850
P63000	Ras-related C3 botulinum toxin substrate 1	0.030161034	0.611911083	0.089810821	0.750396737	0.088753000	0.225058218
P63010	AP-2 complex subunit beta	0.453945365	-0.395520544	0.060218537	-1.381929283	0.790161419	0.036859901
P63104	14-3-3 protein zeta/delta	0.858667880	-0.109837931	0.857464902	-0.055060954	0.833882273	-0.055267463
P63151	Serine/threonine-protein phosphatase 2A 55 kDa regulatory subunit B alpha isoform	0.686806248	-0.056757370	0.195462228	-0.387302070	0.071482010	0.299816585
P63162	Small nuclear ribonucleoprotein-associated protein N	0.259782036	-0.277405192	0.195041018	0.599912499	0.140677474	-0.468340791

P63167	Dynein light chain 1_ cytoplasmic	0.932062954	-0.009217980	0.270530572	0.420138325	0.355453521	-0.118267663
P63208	S-phase kinase-associated protein 1	0.132476179	-1.695455879	0.564361057	-0.555372129	0.833079982	-0.475700272
P63241	Eukaryotic translation initiation factor 5A-1	0.475337417	0.337986409	0.140245875	1.120284467	0.715173949	-0.143257531
P63244	Receptor of activated protein C kinase 1	0.555180828	0.300588897	0.132372522	1.069792840	0.142301100	-0.464116927
P63261	Actin_ cytoplasmic 2	0.409931704	-0.236077685	0.572476567	0.318116166	0.709301340	-0.076902484
P63279	SUMO-conjugating enzyme UBC9	0.022487890	-0.804269454	0.052885577	-0.710225739	0.093041907	-0.487546073
P67775	Serine/threonine-protein phosphatase 2A catalytic subunit alpha isoform	0.276040544	-0.313834350	0.412887199	0.341777371	0.231948089	-0.319102076
P67809	Nuclease-sensitive element-binding protein 1	0.083144444	-0.566300534	0.212038034	0.758119407	0.015652228	-0.891572185
P67812	Signal peptidase complex catalytic subunit SEC11A	0.753102781	-0.000455370	0.815796892	0.191530420	0.907393255	0.388840865
P67936	Tropomyosin alpha-4 chain	0.745874540	0.142811274	0.318178425	1.057847798	0.038371154	-0.319980950
P68036	Ubiquitin-conjugating enzyme E2 L3	0.855102195	-0.089147642	0.542192886	-0.169028763	0.482841640	-0.198241618
P68366	Tubulin alpha-4A chain	0.056738738	1.227776166	0.224224717	0.727714559	0.763686830	-0.064463814
P68371	Tubulin beta-4B chain	0.890892457	-0.006187002	0.568339255	-0.153307597	0.412365133	-0.214180713
P68400	Casein kinase II subunit alpha	0.015715020	0.504532882	0.368828069	0.032016008	0.007481654	0.646834158
P68402	Platelet-activating factor acetylhydrolase IB subunit beta	0.505879692	-0.220318508	0.089881720	0.535934498	0.220914190	0.307405203
P68431	Histone H3.1	0.334946044	0.296369386	0.257229828	1.773374851	0.857518479	0.534293704
P78344	Eukaryotic translation initiation factor 4 gamma2	0.982806380	0.012210732	0.069410469	-0.412634851	0.051126459	-0.294270018
P78347	General transcription factor II-I	0.029645858	-0.599502183	0.222270270	-0.338255753	0.336423362	-0.204822764
P78371	T-complex protein 1 subunit beta	0.283677133	0.483415617	0.144644220	1.188708827	0.489081448	-0.170548878
P78385	Keratin_ type II cuticular Hb3	0.440577252	0.942222681	0.483604422	2.433936076	0.678207551	-2.177521796
P78527	DNA-dependent protein kinase catalytic subunit	0.282049571	-0.269347404	0.264060706	-0.257148017	0.156731932	-0.293088902
P78559	Microtubule-associated protein 1A	0.625493780	1.818487831	0.095586717	-3.518073033	0.926561943	-0.938859432
P80404	4-aminobutyrate aminotransferase_mitochondrial	0.880960446	0.098895435	0.572676762	0.088461895	0.379897342	0.258272191
P80723	Brain acid soluble protein 1	0.916713767	0.116609468	0.099425268	1.548228414	0.949650369	-0.001673240

P82979	SAP domain-containing ribonucleoprotein	0.307075375	-0.265505576	0.711052026	0.061537617	0.230326428	-0.279660316
P83731	60S ribosomal protein L24	0.277309435	0.166994222	0.036096592	0.434347043	0.071809333	-0.290004666
P83916	Chromobox protein homolog 1	0.531828721	-0.217347668	0.770738669	0.087768995	0.790382881	-0.102712539
P84074	Neuron-specific calcium-binding protein hippocalcin	0.076617699	0.655736388	0.550140843	0.157841784	0.622866061	0.143096653
P84085	ADP-ribosylation factor 5	0.703536131	0.197489423	0.240024653	0.794394844	0.448374822	-0.193134020
P84095	Rho-related GTP-binding protein RhoG	0.108505314	1.252933235	0.853745591	-0.060544013	0.762566520	0.024208552
P84098	60S ribosomal protein L19	0.111161516	-0.790427764	0.254708494	-0.477118632	0.558746776	-0.265326628
P84103	Serine/arginine-rich splicing factor 3	0.423715112	0.212811297	0.231475382	0.403173716	0.740625486	-0.091254598
P84243	Histone H3.3	0.251491154	0.514730423	0.580407422	0.476022536	0.658352447	0.788337403
P98179	RNA-binding protein 3	0.361388676	-0.290443963	0.585216378	0.140054338	0.207021726	-0.437183644
P99999	Cytochrome c	0.019975480	-1.024612384	0.043607998	-0.753278697	0.213847492	-0.393994893
Q00005	Serine/threonine-protein phosphatase 2A 55 kDa regulatory subunit B beta isoform	0.940605418	0.384709157	0.131791028	-0.674465883	0.708547044	0.137166247
Q00325	Phosphate carrier protein_ mitochondrial	0.245891426	0.165870008	0.500069967	-0.082792460	0.310598994	-0.174258292
Q00341	Vigilin	0.158014696	0.618278932	0.301565902	-0.742639034	0.981320517	-0.190838373
Q00526	Cyclin-dependent kinase 3	0.878464172	0.085236716	0.134491623	-0.428160653	0.639218715	-0.104025482
Q00534	Cyclin-dependent kinase 6	0.467738296	0.265589856	0.156720905	-0.677472833	0.222909214	1.136083249
Q00536	Cyclin-dependent kinase 16	0.584490751	0.540464769	0.216220776	0.302591596	0.077573506	-0.292413166
Q00610	Clathrin heavy chain 1	0.516321293	-0.077437682	0.736205437	-0.029325579	0.116386867	0.146440497
Q00688	Peptidyl-prolyl cis-trans isomerase FKBP3	0.040340979	-1.309336889	0.067082858	-1.392784855	0.164331062	-0.579244127
Q00796	Sorbitol dehydrogenase	0.668153548	0.219206047	0.360244722	0.148164642	0.311731062	-0.262627541
Q00839	Heterogeneous nuclear ribonucleoprotein U	0.802560938	0.026135920	0.328379380	0.117115276	0.359481016	-0.163109036
Q01081	Splicing factor U2AF 35 kDa subunit	0.144695935	0.652919942	0.214523238	-0.350686317	0.684028269	-0.053619277
Q01082	Spectrin beta chain_ non-erythrocytic 1	0.181987686	-0.765420817	0.638995196	-0.289798895	0.623368667	0.044083423
Q01105	Protein SET	0.830571429	0.164447109	0.111766482	0.728198366	0.226442501	-0.202328462
Q01130	Serine/arginine-rich splicing factor 2	0.097936315	-0.575986469	0.722262742	0.116561027	0.092561638	-0.530242529
Q01469	Fatty acid-binding protein 5	0.947444933	0.059011406	0.599321181	0.254323660	0.519928599	-0.271800886

Q01518	Adenylyl cyclase-associated protein 1	0.935541077	0.010258449	0.831112178	0.116729384	0.457808708	-0.186087906
Q01546	Keratin_type II cytoskeletal 2 oral	0.003611454	-0.816482780	0.384409270	0.514066660	0.030297880	-0.396498180
Q01581	Hydroxymethylglutaryl-CoA synthase_cytoplasmic	0.632151872	-0.357770005	0.311849859	-0.509959425	0.171700651	-0.681165536
Q01638	Interleukin-1 receptor-like 1	0.868194922	0.787298291	0.246108026	-0.156323822	0.563117023	0.541861487
Q01813	ATP-dependent 6-phosphofructokinase_platelet type	0.074189532	1.071363748	0.020743800	-0.666354111	0.930309653	0.071763802
Q01844	RNA-binding protein EWS	0.778756215	0.238650366	0.243782960	0.358190543	0.491248589	-0.155344567
Q01995	Transgelin	0.276175478	-0.714579332	0.237787000	-0.638521086	0.336399086	-0.502345095
Q02224	Centromere-associated protein E	0.497821995	0.121789882	0.077479897	-1.071346619	0.010700322	-1.563168275
Q02543	60S ribosomal protein L18a	0.154892502	1.012801665	0.522428076	0.401116649	0.950165929	-0.090897653
Q02750	Dual specificity mitogen-activated protein kinase kinase 1	0.753693235	-0.418971793	0.971651320	0.231795203	0.553629383	-0.111351382
Q02779	Mitogen-activated protein kinase kinase kinase10	0.125649925	-1.043303341	0.279580848	-0.758903119	0.422019539	0.182118179
Q02790	Peptidyl-prolyl cis-trans isomerase FKBP4	0.231911374	0.523634525	0.689482493	0.150492366	0.716046361	0.134677078
Q02878	60S ribosomal protein L6	0.065607048	-0.169467536	0.202868947	0.126919836	0.040865946	-0.319988382
Q02952	A-kinase anchor protein 12	0.150406706	-1.010255105	0.398805626	-0.470617070	0.809197608	0.604705579
Q03113	Guanine nucleotide-binding protein subunit alpha-12	0.846395490	-0.414051672	0.410455176	-0.388489722	0.863868545	-0.291036532
Q03252	Lamin-B2	0.904954921	0.071479673	0.813751741	0.224554077	0.818149323	-0.120516889
Q04637	Eukaryotic translation initiation factor 4 gamma1	0.305994934	-0.423299373	0.319401396	-0.404837407	0.746753651	-0.120119995
Q04760	Lactoylglutathione lyase	0.798558402	-0.101511386	0.234708018	0.925546561	0.959845512	-0.030268946
Q04837	Single-stranded DNA-binding protein_mitochondrial	0.138950381	-0.492809110	0.154439099	1.049804038	0.348333525	-0.224387033
Q04917	14-3-3 protein eta	0.181504534	-0.843506176	0.565183520	-0.328238253	0.436938284	-0.424611020
Q05682	Caldesmon	0.007446592	-2.048641634	0.944028138	0.343121933	0.126157314	-0.852626164
Q06830	Peroxiredoxin-1	0.071768135	-0.351702121	0.175467673	0.901806243	0.201070454	-0.252714195
Q07020	60S ribosomal protein L18	0.243768269	-0.269699354	0.968570080	0.003326504	0.035596495	-0.476370382

Q07021	Complement component 1 Q subcomponent-binding protein_mitochondrial	0.759525427	-0.067241964	0.119474660	0.653024188	0.421788000	-0.143182677
Q07065	Cytoskeleton-associated protein 4	0.028334827	0.323894529	0.891582773	0.031209468	0.202699909	-0.215037709
Q07666	KH domain-containing_RNA-binding_signal transduction-associated protein 1	0.481700511	0.486641766	0.411234741	0.200271113	0.281759331	-0.285349261
Q07812	Apoptosis regulator BAX	0.573764567	0.545070926	0.197401685	1.020848305	0.024110614	-0.318552131
Q07866	Kinesin light chain 1	0.002148995	-4.321490296	0.191291394	-0.220623963	0.326421313	-0.183106015
Q07955	Serine/arginine-rich splicing factor 1	0.600200653	0.177508129	0.124958618	0.790534042	0.451417690	-0.226994513
Q08043	Alpha-actinin-3	0.285737259	0.612962899	0.320634398	-0.827696874	0.711742286	-0.130024210
Q08170	Serine/arginine-rich splicing factor 4	0.025085584	0.710186699	0.072330603	-0.328909925	0.907691833	0.229609491
Q08211	ATP-dependent RNA helicase A	0.143973161	0.229752402	0.529574246	0.152097384	0.143932875	-0.253191447
Q08257	Quinone oxidoreductase	0.920607012	-0.009057502	0.147122541	-0.639720409	0.617314885	-0.189386367
Q08945	FACT complex subunit SSRP1	0.048513740	0.534472872	0.712215049	0.017298546	0.299654775	0.374564641
Q08AG5	Zinc finger protein 844	0.920126441	-0.007980795	0.285726763	0.361209970	0.006974574	4.931374878
Q09028	Histone-binding protein RBBP4	0.007935479	-0.646965301	0.772262605	0.084739354	0.063567818	-0.385537515
Q09161	Nuclear cap-binding protein subunit 1	0.294930761	-0.388620019	0.380447793	-0.336459437	0.336451950	-0.313814962
Q0VDD8	Dynein heavy chain 14_axonemal	0.263333933	-0.227828942	0.397319325	0.584165611	0.019261892	-0.561501703
Q12765	Secernin-1	0.210215126	0.650279083	0.949340842	0.079374429	0.342447172	0.228880630
Q12840	Kinesin heavy chain isoform 5A	0.008390165	-0.894764220	0.079791208	-0.606506210	0.006629263	-0.910667361
Q12849	G-rich sequence factor 1	0.205859398	-0.488228141	0.080344089	-0.815340027	0.941031923	0.000943676
Q12873	Chromodomain-helicase-DNA-binding protein 3	0.801963671	0.805146843	0.730094026	-0.460112469	0.205301381	1.616330899
Q12874	Splicing factor 3A subunit 3	0.811499397	-0.013099027	0.809469768	0.107789291	0.032303685	-0.221388050
Q12904	Aminoacyl tRNA synthase complex-interacting multifunctional protein 1	0.261812732	-0.238193895	0.153273182	-0.341943912	0.305338697	-0.109954295
Q12905	Interleukin enhancer-binding factor 2	0.957404162	0.005712337	0.208414214	0.732291589	0.610207269	-0.073672842
Q12906	Interleukin enhancer-binding factor 3	0.519674033	0.166456984	0.249395026	0.263797093	0.862316258	-0.038328128
Q12907	Vesicular integral-membrane protein VIP36	0.145032854	-0.891903250	0.009142385	-1.647414198	0.708109504	0.026321284
Q12931	Heat shock protein 75 kDa_mitochondrial	0.319547498	0.935175778	0.696537728	-0.078166624	0.312888658	0.707783290

Q13011	Delta(3_5)-Delta(2_4)-dienoyl-CoA isomerase_mitochondrial	0.775344640	1.091727577	0.403828219	0.044584272	0.564483415	1.748317109
Q13098	COP9 signalosome complex subunit 1	0.045674801	-0.655092138	0.195896647	-0.429787239	0.826403664	-0.073313215
Q13148	TAR DNA-binding protein 43	0.702697392	0.089731352	0.111509158	0.685942870	0.908225277	-0.092461883
Q13151	Heterogeneous nuclear ribonucleoprotein A0	0.245487402	0.344589979	0.044632017	1.235497338	0.664785570	-0.058193788
Q13155	Aminoacyl tRNA synthase complex-interacting multifunctional protein 2	0.375475199	0.303303152	0.136412842	0.863642845	0.490780785	-0.050055006
Q13162	Peroxiredoxin-4	0.647673332	0.103430506	0.348891922	0.973703419	0.196139071	-0.359506318
Q13177	Serine/threonine-protein kinase PAK 2	0.252559657	0.319307588	0.199436410	0.328826217	0.887136525	0.151459723
Q13185	Chromobox protein homolog 3	0.843098558	0.108622644	0.564926858	0.095582002	0.023656308	-0.384418585
Q13200	26S proteasome non-ATPase regulatory subunit2	0.405868749	0.321855512	0.093249384	0.580972513	0.629643749	0.043276529
Q13242	Serine/arginine-rich splicing factor 9	0.537573688	-0.066466273	0.566731900	-0.053818491	0.000007567	-0.442602582
Q13243	Serine/arginine-rich splicing factor 5	0.152777695	0.391317082	0.301377096	-0.208611937	0.468659615	-0.120282041
Q13247	Serine/arginine-rich splicing factor 6	0.391991248	1.134869028	0.111273037	-0.974446818	0.413590535	1.589129628
Q13263	Transcription intermediary factor 1-beta	0.324559353	-0.382310049	0.384396225	-0.314824013	0.290865792	-0.376862926
Q13283	Ras GTPase-activating protein-binding protein 1	0.114557931	-0.308279258	0.409961404	-0.167326266	0.237461806	-0.259116443
Q13310	Polyadenylate-binding protein 4	0.003036172	0.302674117	0.550403559	0.305643532	0.001570007	-0.272484592
Q13347	Eukaryotic translation initiation factor 3 subunit I	0.000003676	2.037411256	0.748920917	-0.033826523	0.006728013	-0.439530952
Q13367	AP-3 complex subunit beta-2	0.523029116	-0.596639467	0.948249262	-0.300657489	0.863912129	-0.507597562
Q13404	Ubiquitin-conjugating enzyme E2 variant 1	0.150279539	-0.365537647	0.530220154	-0.155316344	0.128727302	-0.364193419
Q13409	Cytoplasmic dynein 1 intermediate chain 2	0.059165329	0.586035838	0.149878556	2.314882708	0.607268075	-0.142103518
Q13435	Splicing factor 3B subunit 2	0.083201875	-0.359349923	0.801202150	0.062096935	0.263863628	-0.193021086
Q13442	28 kDa heat- and acid-stable phosphoprotein	0.896865552	-1.445250622	0.138103887	1.352040638	0.231929338	0.897860355
Q13509	Tubulin beta-3 chain	0.364621812	0.218634607	0.223441507	0.279952180	0.485884349	-0.123115146
Q13557	Calcium/calmodulin-dependent protein kinase type II subunit delta	0.804354407	0.015043447	0.463629724	-0.207175057	0.642009279	0.146109028
Q13561	Dynactin subunit 2	0.786332975	-0.282956916	0.244575836	-0.603221747	0.492843168	-0.349466663
Q13564	NEDD8-activating enzyme E1 regulatory subunit	0.701838385	-0.174765739	0.219186764	-0.478959690	0.241180810	-0.399035886

Q13595	Transformer-2 protein homolog alpha	0.595471747	-0.469282792	0.165473869	-1.095004877	0.457053372	0.397920054
Q13642	Four and a half LIM domains protein 1	0.076074427	-0.714125671	0.952136928	0.172834903	0.034755336	-0.767903035
Q13813	Spectrin alpha chain_ non-erythrocytic 1	0.756280569	-0.003576625	0.821764737	-0.175152570	0.979480250	-0.052088038
Q13838	Spliceosome RNA helicase DDX39B	0.830754130	0.162153920	0.269616509	0.381264960	0.290058237	-0.379917925
Q13867	Bleomycin hydrolase	0.629903843	-0.145857092	0.061334981	-0.529944474	0.889006714	-0.002780687
Q13885	Tubulin beta-2A chain	0.850165785	-0.090760824	0.695932828	-0.117838040	0.504013594	-0.152729779
Q13907	Isopentenyl-diphosphate Delta-isomerase 1	0.466403828	0.180701722	0.475756583	0.242413297	0.535444079	-0.139398170
Q14004	Cyclin-dependent kinase 13	0.397689244	-0.243859234	0.596694395	0.127661679	0.785071294	-0.085346246
Q14019	Coactosin-like protein	0.656900229	0.233501984	0.725083848	0.084194697	0.533770719	-0.206320405
Q14103	Heterogeneous nuclear ribonucleoprotein D0	0.137475829	-0.501047680	0.067454948	-0.420329030	0.096343892	-0.576768361
Q14118	Dystroglycan	0.698180182	0.289693859	0.461200277	0.226303859	0.540953566	0.308818631
Q14141	Septin-6	0.000019606	3.194811180	0.123960858	1.285542723	0.872887894	0.060544790
Q14151	Scaffold attachment factor B2	0.149657210	0.521795203	0.165759222	0.524498365	0.448046753	0.165187619
Q14152	Eukaryotic translation initiation factor 3 subunit A	0.328785970	-0.350942840	0.826183343	-0.069772763	0.248905639	-0.373250653
Q14194	Dihydropyrimidinase-related protein 1	0.198504452	0.221078285	0.183894866	0.606250578	0.703433762	0.054268487
Q14195	Dihydropyrimidinase-related protein 3	0.074756710	-0.348715620	0.604197269	0.147878864	0.903612541	-0.007172392
Q14204	Cytoplasmic dynein 1 heavy chain 1	0.633089825	0.129186659	0.665747636	-0.231527145	0.831970373	-0.129119186
Q14240	Eukaryotic initiation factor 4A-II	0.035370446	-0.675453336	0.713724516	0.112619756	0.023379191	-0.630809834
Q14257	Reticulocalbin-2	0.954679266	-0.036151766	0.288555044	-0.409088430	0.743667364	0.172174037
Q14315	Filamin-C	0.008019813	-1.669052349	0.127239385	-0.791504025	0.344705582	-0.307209664
Q14344	Guanine nucleotide-binding protein subunit alpha-13	0.604754340	2.093275562	0.517969111	-0.352902789	0.950998845	-0.299043712
Q14444	Caprin-1	0.093298037	-0.574551621	0.861506279	-0.041447768	0.394133654	-0.279728264
Q14498	RNA-binding protein 39	0.158086307	0.773945391	0.019765184	0.938367959	0.651085078	-0.088430887
Q14562	ATP-dependent RNA helicase DHX8	0.563960577	-0.076017684	0.274268236	-0.216366880	0.153798995	0.165293351
Q14566	DNA replication licensing factor MCM6	0.244622534	-0.201950103	0.061372413	-0.254001371	0.000947320	-0.581448412
Q14696	LRP chaperone MESD	0.011849338	1.173998758	0.129908590	-0.497317221	0.749639746	-0.045300151

Q14697	Neutral alpha-glucosidase AB	0.917182950	-0.000677540	0.167619677	0.953928050	0.956530637	-0.030827952
Q14739	Delta(14)-sterol reductase LBR	0.645181344	0.065278060	0.432683626	-0.175841246	0.931291332	-0.029288673
Q14839	Chromodomain-helicase-DNA-binding protein 4	0.927205130	0.034379233	0.118538217	-0.639573505	0.470295499	1.392495510
Q14847	LIM and SH3 domain protein 1	0.005552706	-1.569686140	0.064884930	-0.984751713	0.097316905	-0.954053759
Q14964	Ras-related protein Rab-39A	0.357876215	-0.210092578	0.359929181	0.880712417	0.338721731	-0.217952517
Q14974	Importin subunit beta-1	0.000145067	0.835246495	0.081327680	-0.220280095	0.157748546	-0.150002086
Q14980	Nuclear mitotic apparatus protein 1	0.999592288	-0.072274249	0.497026359	0.122042406	0.865931790	0.030083235
Q15003	Condensin complex subunit 2	0.317795635	0.329658756	0.017008960	-0.471877865	0.790233562	-0.019701431
Q15008	26S proteasome non-ATPase regulatory subunit6	0.551145894	-0.096482316	0.002441673	-0.778783706	0.069109662	-0.443748784
Q15019	Septin-2	0.402644436	-0.203369149	0.588047180	-0.121514491	0.230496275	-0.266536154
Q15020	Squamous cell carcinoma antigen recognized by T-cells 3	0.115868704	-0.517323818	0.064123199	-0.680286760	0.643990544	-0.110007890
Q15029	116 kDa U5 small nuclear ribonucleoprotein component	0.618916235	0.239813773	0.534085768	0.431383214	0.041145009	-0.484456545
Q15046	Lysine--tRNA ligase	0.082283170	1.988003806	0.140071009	1.010470190	0.211399798	-0.202805061
Q15056	Eukaryotic translation initiation factor 4H	0.131911836	-0.581438455	0.065702910	-0.648215382	0.538100909	-0.197509968
Q15084	Protein disulfide-isomerase A6	0.050624321	0.455797968	0.466668478	0.193026979	0.317426593	0.131987181
Q15102	Platelet-activating factor acetylhydrolase IB subunit gamma	0.336515699	1.011069343	0.346680262	0.655871162	0.280551403	0.793773395
Q15121	Astrocytic phosphoprotein PEA-15	0.006061997	-1.398513535	0.605407309	-0.114218653	0.371706863	-0.399048043
Q15181	Inorganic pyrophosphatase	0.579557109	0.228416971	0.537521885	0.180791067	0.670128373	-0.120162738
Q15185	Prostaglandin E synthase 3	0.736697630	0.198386925	0.573216294	0.195031924	0.598232468	-0.226668578
Q15233	Non-POU domain-containing octamer-binding protein	0.925969128	-0.149513614	0.680865310	-0.144015571	0.456105979	0.221211907
Q15257	Serine/threonine-protein phosphatase 2A activator	0.216761061	0.447269609	0.412537925	0.625484152	0.488024647	0.424092146
Q15274	Nicotinate-nucleotide pyrophosphorylase [carboxylating]	0.028897507	-0.265714347	0.101606295	-0.351407429	0.123038014	0.274891331
Q15293	Reticulocalbin-1	0.129217357	0.478346319	0.088021100	0.707077167	0.301306584	-0.179699915

Q15334	Lethal(2) giant larvae protein homolog 1	0.421956244	-2.035653705	0.161679290	-2.516194389	0.303399508	-2.256764690
Q15365	Poly(rC)-binding protein 1	0.097120734	-0.261686485	0.340848697	-0.134486567	0.259908957	-0.160851667
Q15366	Poly(rC)-binding protein 2	0.599438348	-0.149175258	0.404575325	-0.204441268	0.435127617	-0.193691435
Q15369	Elongin-C	0.399738031	-0.324870375	0.213040230	0.651144862	0.970226178	-0.057446137
Q15392	Delta(24)-sterol reductase	0.077328732	1.623300169	0.468605522	0.327698587	0.999301534	-0.048117997
Q15393	Splicing factor 3B subunit 3	0.582430007	0.069770251	0.844191643	0.040053030	0.510740764	-0.135041087
Q15417	Calponin-3	0.449588089	-0.143595917	0.195397929	-0.243247978	0.868255632	0.130619171
Q15424	Scaffold attachment factor B1	0.308086975	0.365497214	0.181157354	0.429125601	0.006443305	-0.345456855
Q15435	Protein phosphatase 1 regulatory subunit 7	0.614456540	-0.298484238	0.074462566	-1.312765503	0.405787395	0.351434255
Q15436	Protein transport protein Sec23A	0.000547839	-1.195602540	0.054789319	-0.642041592	0.021935682	-0.498855851
Q15459	Splicing factor 3A subunit 1	0.838138711	-0.071643351	0.426291511	-0.202876919	0.570117037	-0.137350760
Q15637	Splicing factor 1	0.010133049	-1.228863232	0.124224395	-0.399267436	0.051696505	-0.765608244
Q15691	Microtubule-associated protein RP/EB family member 1	0.128311541	-0.348316906	0.973598094	0.021812806	0.091991364	-0.267639900
Q15717	ELAV-like protein 1	0.628282655	-0.110748420	0.616527006	-0.106425590	0.117091045	-0.331511337
Q15738	Sterol-4-alpha-carboxylate 3-dehydrogenase_decarboxylating	0.288264839	-0.504952879	0.253413047	-0.756828341	0.771482381	-0.331928094
Q15772	Striated muscle preferentially expressed protein kinase	0.624405632	0.063472436	0.945464502	-0.022572665	0.964393769	-0.066567975
Q15819	Ubiquitin-conjugating enzyme E2 variant 2	0.198398796	-0.569411759	0.859761838	-0.108994308	0.277666651	-0.437124815
Q15833	Syntaxin-binding protein 2	0.729439755	-0.365074876	0.442895695	-0.386810925	0.416234918	-0.564535461
Q16181	Septin-7	0.589764915	0.401334178	0.993694907	-0.072487898	0.410559368	0.267799700
Q16186	Proteasomal ubiquitin receptor ADRM1	0.960274934	0.105925910	0.310693219	-0.385223527	0.976332915	-0.030764775
Q16281	Cyclic nucleotide-gated cation channel alpha-3	0.452173821	-1.029158839	0.720665880	-1.014127787	0.953903128	-0.485350120
Q16352	Alpha-internexin	0.789525955	-0.066884356	0.060876760	0.324976356	0.677247845	0.383291377
Q16531	DNA damage-binding protein 1	0.785074558	-0.042730605	0.657947110	-0.033075682	0.169485193	-0.394013809
Q16543	Hsp90 co-chaperone Cdc37	0.173272051	-0.349624940	0.244309567	-0.277885976	0.475688189	-0.159353345
Q16555	Dihydropyrimidinase-related protein 2	0.905408511	0.102453268	0.103577998	0.699448625	0.744040451	-0.109695789

Q16576	Histone-binding protein RBBP7	0.739349184	-0.088981836	0.196931677	1.595235763	0.084824628	-0.455860813
Q16629	Serine/arginine-rich splicing factor 7	0.807765123	-0.012125533	0.365972241	0.376530104	0.002149804	-0.307995492
Q16630	Cleavage and polyadenylation specificity factor subunit 6	0.814263699	0.028932242	0.778231847	0.092607034	0.838093944	-0.022150910
Q16643	Drebrin	0.246584746	-0.195770747	0.441542235	0.189186800	0.032623171	-0.374313309
Q16658	Fascin	0.595128222	0.430150980	0.055702205	1.020367923	0.992504361	-0.105226958
Q16695	Histone H3.1t	0.136014418	0.585104805	0.888903265	-0.086766189	0.627686349	0.205285250
Q16698	2_4-dienoyl-CoA reductase_mitochondrial	0.812904934	0.057181341	0.178273796	1.769276523	0.231035975	-0.349365837
Q16822	Phosphoenolpyruvate carboxykinase [GTP]_mitochondrial	0.058978903	-1.436223590	0.266150722	-0.099656770	0.489517677	-0.172353452
Q16836	Hydroxyacyl-coenzyme A dehydrogenase_mitochondrial	0.111428702	-0.609337321	0.064232226	-0.707213438	0.738390761	-0.035244746
Q16851	UTP--glucose-1-phosphate uridylyltransferase	0.586887420	0.081496575	0.885126106	-0.061172912	0.371918853	0.214939608
Q16891	MICOS complex subunit MIC60	0.715071796	0.323172099	0.287093363	0.541500467	0.758125848	-0.057797879
Q1KMD3	Heterogeneous nuclear ribonucleoprotein U-like protein 2	0.133064668	-0.285908270	0.542657491	0.278809496	0.160472844	-0.250220229
Q2TAC2	Coiled-coil domain-containing protein 57	0.592503475	-0.248634197	0.231227081	-0.384378490	0.903779962	0.331275657
Q2VIR3	Eukaryotic translation initiation factor 2 subunit 3B	0.362734813	-1.333231184	0.201555626	-1.438539092	0.912499080	-0.183216953
Q2VPB7	AP-5 complex subunit beta-1	0.871705340	-0.057218477	0.225551902	-0.203792698	0.050150692	0.755185555
Q3V6T2	Girdin	0.593827454	-0.259970756	0.444912642	0.325702997	0.636007640	-0.201885147
Q3ZCM7	Tubulin beta-8 chain	0.292211098	0.197516691	0.565299740	-0.098013910	0.141931312	-0.278572411
Q4G0J3	La-related protein 7	0.873651572	-0.786060160	0.447842315	0.400005006	0.816378342	-0.586678743
Q4VNC1	Probable cation-transporting ATPase 13A4	0.027700342	-0.342529963	0.171002645	0.654173607	0.427748401	-0.113753945
Q4VXU2	Polyadenylate-binding protein 1-like	0.998253084	-0.025272041	0.816707702	-0.055735372	0.386094189	-0.252756903
Q52LJ0	Protein FAM98B	0.399921789	0.558089250	0.094090627	-0.772782318	0.267028485	0.694981515
Q53EV4	Leucine-rich repeat-containing protein 23	0.629020521	0.139159423	0.468342699	5.493401319	0.576957202	-0.486502014
Q53GQ0	Very-long-chain 3-oxoacyl-CoA reductase	0.654253230	-0.192124451	0.613488422	-0.215733960	0.680541167	0.241293716
Q53GS9	U4/U6.U5 tri-snRNP-associated protein 2	0.086877997	-0.486612322	0.142366481	-0.557639990	0.773536075	-0.070545597

Q53HC0	Coiled-coil domain-containing protein 92	0.037803859	-1.819177910	0.621341550	-0.083908438	0.233877309	0.488936366
Q562R1	Beta-actin-like protein 2	0.871563538	0.006383954	0.810076658	0.078715121	0.555186555	-0.095485930
Q58FF3	Putative endoplasmin-like protein	0.099529102	-0.814092119	0.073289264	-0.715159579	0.693882966	-0.087677607
Q58FF6	Putative heat shock protein HSP 90-beta 4	0.000096204	-2.849453590	0.115417669	-0.593166339	0.140132509	-0.555551007
Q58FF7	Putative heat shock protein HSP 90-beta-3	0.822053383	-0.007255093	0.827973883	0.119926443	0.414058810	-0.156352493
Q58FF8	Putative heat shock protein HSP 90-beta 2	0.304282693	-0.526116098	0.716422748	-0.082298134	0.645356148	-0.049455286
Q58FG0	Putative heat shock protein HSP 90-alpha A5	0.416789404	0.420546225	0.487627598	-0.279742544	0.634152786	0.090620374
Q58FG1	Putative heat shock protein HSP 90-alpha A4	0.822741690	-0.122102269	0.086909113	-0.531036562	0.499368835	-0.226767747
Q5JWF2	Guanine nucleotide-binding protein G(s) subunit alpha isoforms XLAs	0.000004172	4.297145949	0.234919456	0.952769457	0.013960254	-0.321766724
Q5JX69	Protein FAM209B	0.384692261	0.646814641	0.144054903	1.128190740	0.405990366	0.558769473
Q5QNW6	Histone H2B type 2-F	0.288638196	0.522740507	0.616962426	0.294968932	0.804548550	0.023133337
Q5SSJ5	Heterochromatin protein 1-binding protein 3	0.303420854	0.130739625	0.408965346	0.173008366	0.473173229	-0.095189891
Q5SW79	Centrosomal protein of 170 kDa	0.093307044	-0.671811073	0.058084928	-0.946523150	0.221522807	-0.165125502
Q5T4T6	Synaptonemal complex protein 2-like	0.006309878	-2.568708759	0.532583072	-0.483779882	0.030484187	-1.778685721
Q5T6S3	PHD finger protein 19	0.297153365	0.336593278	0.662768847	0.207294262	0.746721271	-0.142725960
Q5TCY1	Tau-tubulin kinase 1	0.240436642	1.086809851	0.084131136	1.995112976	0.560723825	-0.192111346
Q5TZA2	Rootletin	0.433649276	1.094982870	0.208613715	-0.453834141	0.177361437	1.786917801
Q5VTE0	Putative elongation factor 1-alpha-like 3	0.020157375	-0.495272397	0.620503468	-0.096922700	0.225604609	-0.220030731
Q5VWN6	Protein TASOR 2	0.810124973	-0.533978504	0.585840862	-1.065724276	0.863756791	-0.046317861
Q5VZ46	Uncharacterized protein KIAA1614	0.492318130	-1.218097428	0.559647779	-0.960778954	0.478611262	-1.036812885
Q5XKE5	Keratin_ type II cytoskeletal 79	0.342997981	-0.315944181	0.787675844	0.001935492	0.845868654	-0.057446513
Q66LE6	Serine/threonine-protein phosphatase 2A 55 kDa regulatory subunit B delta isoform	0.599798629	-0.470190529	0.348732972	-0.421796034	0.795179457	-0.296890711
Q68CZ1	Protein fantom	0.691367444	-0.129724891	0.099099849	0.675794806	0.385466464	-0.242407683
Q6BDS2	UHRF1-binding protein 1	0.714363957	-0.447668454	0.375289178	-1.016835607	0.465715376	0.176269808
Q6DKJ4	Nucleoredoxin	0.413031248	-0.154331737	0.398325705	0.380621920	0.936695889	-0.016535916
Q6DN03	Putative histone H2B type 2-C	0.420319025	0.195293445	0.443220534	0.067958988	0.547477068	0.239112600

Q6IQ22	Ras-related protein Rab-12	0.169070336	0.515637925	0.725948431	-0.149294843	0.556441571	0.767456548
Q6NUK1	Calcium-binding mitochondrial carrier protein SCaMC-1	0.916278497	-0.104811509	0.892122810	0.252749111	0.779331938	-0.160004483
Q6P158	Putative ATP-dependent RNA helicase DHX57	0.922107208	-0.039142478	0.671312375	0.325753997	0.165288838	-0.583015790
Q6P1J9	Parafibromin	0.243491428	-0.679391253	0.224460419	-0.535740713	0.127917842	0.676385302
Q6P2Q9	Pre-mRNA-processing-splicing factor 8	0.687466737	-0.082846696	0.856623875	0.030092930	0.237927963	-0.219930766
Q6PCT2	F-box/LRR-repeat protein 19	0.085447130	-0.534372626	0.151642324	-0.591190876	0.472511738	-0.184090302
Q6S8J3	POTE ankyrin domain family member E	0.004335525	-1.672420995	0.100549438	-0.485927787	0.074050002	-0.845435021
Q6UB98	Ankyrin repeat domain-containing protein 12	0.447948550	-0.666124117	0.319993839	0.814405822	0.649378831	-0.572222904
Q6UB99	Ankyrin repeat domain-containing protein 11	0.068972403	0.348565638	0.316117660	0.733732693	0.480653446	-0.116416613
Q6UXK5	Leucine-rich repeat neuronal protein 1	0.657904568	0.134971521	0.585280012	-0.790855630	0.324985318	0.520199276
Q6UXN9	WD repeat-containing protein 82	0.000632039	-2.648462066	0.929732942	0.029914423	0.192263828	-0.429326362
Q6ZMR3	L-lactate dehydrogenase A-like 6A	0.000001851	1.868782549	0.038970824	-0.356606942	0.385209216	0.253346640
Q6ZQQ6	WD repeat-containing protein 87	0.005254102	-1.874115840	0.071735271	-0.705336562	0.020778149	-1.554315935
Q6ZU15	Septin-14	0.669098281	1.423962152	0.998173389	-0.168205516	0.319704725	0.916603022
Q6ZVD7	Storkhead-box protein 1	0.878356504	0.003007018	0.704861908	0.085783999	0.521287326	-0.197784081
Q70Z35	Phosphatidylinositol 3_4_5-trisphosphate-dependent Rac exchanger 2 protein	0.622444833	-0.564281075	0.459786251	0.186105473	0.284671553	0.487615112
Q71DI3	Histone H3.2	0.265189244	0.446013296	0.434724313	1.190686075	0.953094104	0.439998100
Q7KZF4	Staphylococcal nuclease domain-containing protein 1	0.293302798	-0.152074707	0.343361120	-0.163999784	0.504184040	0.414172517
Q7L014	Probable ATP-dependent RNA helicase DDX46	0.402796356	0.222494412	0.235495295	-0.392186146	0.406740003	0.150777936
Q7L1Q6	Basic leucine zipper and W2 domain-containing protein 1	0.022335390	-0.691643574	0.056689042	-0.489631921	0.982068360	0.016315079
Q7L2H7	Eukaryotic translation initiation factor 3 subunitM	0.706001760	-0.381418750	0.726886325	-0.013238283	0.521057191	-0.510439483
Q7Z2T5	TRMT1-like protein	0.280440536	-3.756374006	0.944659413	-0.277179939	0.797790552	0.163235101
Q7Z406	Myosin-14	0.309348762	-0.337773008	0.046448563	-0.920592501	0.986914004	0.121787203
Q7Z6Z7	E3 ubiquitin-protein ligase HUWE1	0.082799636	0.779177671	0.073751655	0.772269758	0.485204090	0.315688301

Q7Z794	Keratin_type II cytoskeletal 1b	0.597254557	-2.253498992	0.831571116	-1.169350339	0.852448743	-0.902009398
Q7Z7K6	Centromere protein V	0.780509926	0.024359407	0.682183903	-0.095388873	0.801054646	0.171985791
Q86SE5	RNA-binding Raly-like protein	0.227922945	2.282067045	0.789122278	0.093890624	0.223703315	-0.441213761
Q86TJ2	Transcriptional adapter 2-beta	0.375538703	-0.686621573	0.734004987	-0.478427537	0.662337479	-0.204685395
Q86U42	Polyadenylate-binding protein 2	0.232547047	-0.275541759	0.444744666	0.358642025	0.012923955	-0.597947912
Q86UU0	B-cell CLL/lymphoma 9-like protein	0.715877085	1.055808290	0.284432160	2.246146906	0.227747374	-1.777832439
Q86V81	THO complex subunit 4	0.990133843	-0.622396987	0.171570200	1.815277029	0.670943713	-0.320884426
Q86VP6	Cullin-associated NEDD8-dissociated protein 1	0.421630069	-0.200624833	0.169667727	-0.427686338	0.761457741	-0.069338680
Q86W28	NACHT_LRR and PYD domains-containing protein 8	0.773331394	-0.128926961	0.050701084	-0.873124438	0.666690738	-0.164327177
Q86W56	Poly(ADP-ribose) glycohydrolase	0.392751679	1.233465873	0.027159681	-0.771675984	0.203311379	1.330475343
Q86X55	Histone-arginine methyltransferase CARM1	0.146932354	0.453516690	0.160333787	0.285614245	0.528415586	0.103719431
Q86XE0	Sorting nexin-32	0.868331268	0.333913429	0.725350794	0.483526116	0.814130980	0.246166979
Q86YS6	Ras-related protein Rab-43	0.369809442	1.529433269	0.764149509	-0.173472011	0.176248604	1.108769897
Q8IUE6	Histone H2A type 2-B	0.619573299	-0.073851160	0.823200890	-0.173609263	0.733223528	0.201346524
Q8IWP9	Coiled-coil domain-containing protein 28A	0.187733422	-0.460473764	0.433861259	0.331311620	0.034110589	-0.721935825
Q8IWS0	PHD finger protein 6	0.201787632	1.452516603	0.275500386	-0.432799681	0.246692073	0.577209230
Q8IX03	Protein KIBRA	0.553532309	-0.412243116	0.520509166	0.198923027	0.895323119	-0.126571281
Q8IYA2	Putative coiled-coil domain-containing protein 144C	0.842417006	-0.002313548	0.861621707	-0.103462469	0.950737901	0.000166399
Q8IYS4	Uncharacterized protein C16orf71	0.246107258	-0.313380552	0.270108285	-0.296048446	0.625313831	-0.118351696
Q8IYT4	Katanin p60 ATPase-containing subunit A-like 2	0.495407193	-2.125979082	0.622723781	-0.613875348	0.618911283	-0.727709324
Q8IZP2	Putative protein FAM10A4	0.210569953	-0.356591448	0.794652995	-0.050275980	0.279450910	-0.285789835
Q8IZS8	Voltage-dependent calcium channel subunit alpha-2/delta-3	0.753120834	-0.263264232	0.322077891	0.286336959	0.613351871	-0.314860467
Q8N0Y7	Probable phosphoglycerate mutase 4	0.127598186	-0.557312608	0.884358272	-0.006102262	0.746649696	-0.100061515
Q8N163	Cell cycle and apoptosis regulator protein 2	0.807327687	-0.093104553	0.393696106	0.297052571	0.401854728	-0.349362153
Q8N1F7	Nuclear pore complex protein Nup93	0.411643571	-0.412580628	0.227889329	-0.705373819	0.617107410	-0.259360606

Q8N1G4	Leucine-rich repeat-containing protein 47	0.243813863	0.190261646	0.726032876	-0.077598172	0.815068418	-0.044649296
Q8N1N4	Keratin_type II cytoskeletal 78	0.000114642	-7.130109158	0.066172121	-1.474000333	0.445540852	0.246694295
Q8N568	Serine/threonine-protein kinase DCLK2	0.152535220	-0.412924162	0.042813799	-0.707617486	0.836548973	0.110707550
Q8N684	Cleavage and polyadenylation specificity factor subunit 7	0.500530056	-0.431605402	0.580015052	0.088139629	0.635875393	0.061845547
Q8N7X1	RNA-binding motif protein_X-linked-like-3	0.115217144	-1.329657077	0.113304162	-1.218977623	0.499308749	-0.379588003
Q8N8S7	Protein enabled homolog	0.041436580	-1.223503922	0.088873657	-1.003338862	0.963603139	0.111913565
Q8NB90	ATPase family protein 2 homolog	0.216505271	-0.401793462	0.129269551	-0.561090712	0.666745736	-0.118871700
Q8NBS9	Thioredoxin domain-containing protein 5	0.702935216	0.050663935	0.255565946	0.926515901	0.539121653	-0.093599222
Q8NC51	Plasminogen activator inhibitor 1 RNA-binding protein	0.000563296	-1.185451963	0.058987440	-0.445723967	0.019152334	-0.796472072
Q8NCI6	Beta-galactosidase-1-like protein 3	0.858840463	-0.357895537	0.723090876	1.760992993	0.131434006	2.152035581
Q8NCM8	Cytoplasmic dynein 2 heavy chain 1	0.000583791	-0.832798650	0.001168745	-0.723530871	0.000104184	-0.941243633
Q8NDA2	Hemicentin-2	0.349263661	0.281239799	0.472009303	1.022433256	0.844256674	-0.048267733
Q8NFP9	Neurobeachin	0.317350042	0.599864025	0.209483671	3.261064500	0.189963645	-1.492858102
Q8NHQ8	Ras association domain-containing protein 8	0.419323976	-0.197284632	0.127765772	-0.536227783	0.383031402	0.356757563
Q8TAA3	Proteasome subunit alpha-type 8	0.408645479	1.022430932	0.116412567	0.670264789	0.530163106	0.488489915
Q8TBY8	Polyamine-modulated factor 1-binding protein 1	0.522083344	0.188281011	0.456539716	-0.136589438	0.116614153	-0.524229840
Q8TD43	Transient receptor potential cation channel subfamily M member 4	0.660736158	-0.082630627	0.165334705	-0.657062008	0.840932178	-0.145602253
Q8TD47	40S ribosomal protein S4_Y isoform 2	0.343456358	-1.294039909	0.924614475	0.077551548	0.688413368	-0.173661464
Q8TE49	OTU domain-containing protein 7A	0.180948471	0.664497933	0.299257900	1.984943335	0.539901591	0.011778398
Q8TEA8	D-aminoacyl-tRNA deacylase 1	0.531645095	0.077121308	0.013300774	-0.347282163	0.001133755	-0.411387057
Q8TEX9	Importin-4	0.309301486	-0.661122107	0.700125115	0.095756202	0.415328818	-0.500318195
Q8WU76	Sec1 family domain-containing protein 2	0.407616152	-1.114380367	0.526635283	0.175674937	0.315880503	-1.390366933
Q8WUD1	Ras-related protein Rab-2B	0.315336535	0.177848476	0.881101730	0.067327787	0.903472270	-0.035136167
Q8WUM4	Programmed cell death 6-interacting protein	0.289472470	-0.690196647	0.226254131	-0.718010785	0.739541970	-0.359446138
Q8WVV9	Heterogeneous nuclear ribonucleoprotein L-like	0.650918877	0.132780997	0.189458389	1.041581808	0.725115896	-0.065613680

Q8WX94	NACHT_LRR and PYD domains-containing protein 7	0.114375780	-1.149048045	0.085104542	-1.692381369	0.435187795	0.142907001
Q8WXE0	Caskin-2	0.472347189	0.189124638	0.544154353	-0.350554668	0.528896285	0.761948832
Q8WXF1	Paraspeckle component 1	0.135208969	0.338128035	0.956699500	-0.038205992	0.604345243	0.148537043
Q8WXG1	Radical S-adenosyl methionine domain-containing protein 2	0.729240513	-0.070090023	0.361746418	-0.270258588	0.560354870	-0.119434687
Q92499	ATP-dependent RNA helicase DDX1	0.549014827	0.341163626	0.116300298	0.750469788	0.455719687	-0.209172170
Q92522	Histone H1x	0.831043306	0.032471514	0.047219696	1.118000883	0.652831158	0.443971645
Q92598	Heat shock protein 105 kDa	0.834080884	0.036523723	0.724869794	0.131550734	0.832045093	-0.106211208
Q92688	Acidic leucine-rich nuclear phosphoprotein 32 family member B	0.447810275	-0.312921403	0.263332654	-0.444819799	0.289233831	-0.422794883
Q92734	Protein TFG	0.986751226	-0.089337287	0.721646083	-0.145350640	0.771229693	0.038552484
Q92769	Histone deacetylase 2	0.246249181	-0.291293237	0.305755086	0.234946968	0.312000637	-0.256923947
Q92804	TATA-binding protein-associated factor 2N	0.035977343	-0.359468201	0.111693168	-0.361375062	0.017007018	-0.387040602
Q92841	Probable ATP-dependent RNA helicase DDX17	0.332669991	0.204619850	0.102677299	0.361751522	0.119099026	-0.174315189
Q92900	Regulator of nonsense transcripts 1	0.397281638	-0.220806413	0.139773388	-0.504885545	0.396572019	-0.248685440
Q92901	60S ribosomal protein L3-like	0.005764989	1.158695781	0.072871671	-0.962114317	0.299013246	-0.282767788
Q92945	Far upstream element-binding protein 2	0.681597330	-0.011207163	0.893257137	0.015050124	0.037926814	-0.376380704
Q92973	Transportin-1	0.082601836	-0.344853602	0.049786514	-0.526257336	0.031642631	-0.249279365
Q93009	Ubiquitin carboxyl-terminal hydrolase 7	0.003057255	0.395413359	0.835339764	0.047366841	0.902497977	0.024182832
Q93084	Sarcoplasmic/endoplasmic reticulum calcium ATPase 3	0.958690989	-0.193221966	0.765372837	-0.084945612	0.983939586	-0.205809241
Q96AC1	Fermitin family homolog 2	0.026045672	1.900352016	0.216964144	-0.229859203	0.360273779	0.099092601
Q96AE4	Far upstream element-binding protein 1	0.523394456	0.126239661	0.202638250	0.595536033	0.782241416	0.029702839
Q96AG4	Leucine-rich repeat-containing protein 59	0.842997794	-0.309770455	0.106885199	-2.060398662	0.617041820	-0.121890284
Q96AX2	Ras-related protein Rab-37	0.179718102	-5.309656075	0.272371772	-3.172290964	0.563802520	-3.423831139
Q96AY3	Peptidyl-prolyl cis-trans isomerase FKBP10	0.608311652	0.113105938	0.269517145	1.057192189	0.704297470	-0.091401204
Q96C45	Serine/threonine-protein kinase ULK4	0.390543432	0.472210124	0.326314548	0.963239587	0.335357093	-0.282518411
Q96DA2	Ras-related protein Rab-39B	0.361224087	-0.593217803	0.980868003	0.700943139	0.420801303	-0.486788947

Q96DH6	RNA-binding protein Musashi homolog 2	0.377868198	0.433958841	0.468312616	-0.126955518	0.373799595	0.319993007
Q96DI7	U5 small nuclear ribonucleoprotein 40 kDa protein	0.733118387	-0.287848586	0.829587929	-0.057256998	0.150225686	-1.194902138
Q96DY7	Mdm2-binding protein	0.738591137	0.037230936	0.189370955	0.656417913	0.253282921	0.268832295
Q96E17	Ras-related protein Rab-3C	0.849205079	-3.043935918	0.877443186	-1.436026106	0.938930543	-1.236020699
Q96E39	RNA binding motif protein_X-linked-like-1	0.404135747	0.274995904	0.058119744	0.528024183	0.996252718	-0.006245710
Q96FJ2	Dynein light chain 2_cytoplasmic	0.419279172	0.148827119	0.263516260	0.246144055	0.474647580	0.064423046
Q96FW1	Ubiquitin thioesterase OTUB1	0.318678575	0.186865406	0.502760396	-0.106209079	0.404138509	-0.118677286
Q96G03	Phosphoglucomutase-2	0.195751097	0.125134166	0.543527986	0.219242938	0.003324442	-0.529799267
Q96HN2	Adenosylhomocysteinase 3	0.594213027	0.068642618	0.605564395	0.247191218	0.380950044	-0.219169493
Q96I24	Far upstream element-binding protein 3	0.125424010	-0.872861817	0.228844226	-0.604327519	0.918582521	-0.092882662
Q96IX5	ATP synthase membrane subunit DAPIT_mitochondrial	0.344164449	0.298553274	0.842690310	0.076249626	0.037816279	-0.426488410
Q96IX9	Putative ankyrin repeat domain-containing protein 26-like 1	0.236195042	0.677083783	0.867438228	0.018666082	0.653831936	-0.128242889
Q96JN2	Coiled-coil domain-containing protein 136	0.564951555	-0.101202059	0.620160679	0.108388392	0.135443257	-0.410420250
Q96KP4	Cytosolic non-specific dipeptidase	0.529228944	0.127443467	0.678942677	0.117389485	0.343628934	-0.221469128
Q96P70	Importin-9	0.052830798	-0.204757860	0.002448279	-0.337591458	0.531040359	-0.070146124
Q96PK6	RNA-binding protein 14	0.319998896	-0.290899399	0.364800250	0.302170873	0.455582863	0.377030719
Q96PP8	Guanylate-binding protein 5	0.054178361	-0.430971651	0.918069164	-0.026934968	0.514942763	-0.127396826
Q96PU8	Protein quaking	0.039246831	-0.382076825	0.164912933	-0.324055302	0.417967015	-0.103072790
Q96PZ0	Pseudouridylate synthase 7 homolog	0.001363475	4.819262939	0.144142696	2.887004118	0.444833653	0.133761827
Q96QK1	Vacuolar protein sorting-associated protein 35	0.774797738	-0.137815772	0.241900294	-0.352553949	0.201782074	-0.373610041
Q96SI9	Spermatid perinuclear RNA-binding protein	0.213961072	0.492902686	0.492401576	0.303010374	0.646729672	0.292188000
Q96T58	Msx2-interacting protein	0.133642589	-1.063929118	0.216336961	-0.793667146	0.534428959	-0.256132693
Q99426	Tubulin-folding cofactor B	0.684502286	-0.090837994	0.149252689	-0.254661520	0.623700855	-0.095302448
Q99436	Proteasome subunit beta type-7	0.301990878	0.281177990	0.017951937	1.183717801	0.115700102	0.336817293
Q99439	Calponin-2	0.000288294	-2.076078504	0.072394990	-0.655388706	0.054246000	-1.061463659

Q99459	Cell division cycle 5-like protein	0.866541765	0.056821265	0.417481205	-0.122000657	0.011989968	-0.411437420
Q99460	26S proteasome non-ATPase regulatory subunit1	0.174388181	-0.320638997	0.707056448	0.062607106	0.783963752	-0.067711725
Q99497	Protein/nucleic acid deglycase DJ-1	0.969120255	0.009276357	0.222169812	1.238517694	0.420402847	-0.164441418
Q99536	Synaptic vesicle membrane protein VAT-1 homolog	0.016369830	1.177842458	0.151812325	2.083293468	0.732176313	0.165143948
Q99623	Prohibitin-2	0.186656942	0.784310966	0.057544528	1.179114700	0.466493679	-0.149869052
Q99627	COP9 signalosome complex subunit 8	0.105982170	-0.241788077	0.537355070	0.673242889	0.005400700	-0.426891489
Q99714	3-hydroxyacyl-CoA dehydrogenase type-2	0.596560986	0.156205484	0.233697233	0.543192074	0.140197515	-0.247742645
Q99729	Heterogeneous nuclear ribonucleoprotein A/B	0.142457516	-1.961006739	0.206291689	-1.668367252	0.769280805	-0.576513168
Q99733	Nucleosome assembly protein 1-like 4	0.018254849	1.831915586	0.891061206	0.068878064	0.041590738	-0.631792916
Q99798	Aconitate hydratase_ mitochondrial	0.331734115	0.278823236	0.722929536	0.043196262	0.227669585	-0.403622149
Q99829	Copine-1	0.237045565	1.180019153	0.646233446	-0.083109717	0.220858539	0.993774191
Q99832	T-complex protein 1 subunit eta	0.217480300	0.192425145	0.131450153	0.909639602	0.450261339	-0.087800648
Q99873	Protein arginine N-methyltransferase 1	0.911512525	-0.113384724	0.703832439	-0.158311714	0.955881107	-0.046907198
Q99878	Histone H2A type 1-J	0.503680487	0.062637281	0.946535913	-0.595191086	0.844283645	-0.032821270
Q99996	A-kinase anchor protein 9	0.000037434	4.053108556	0.022827817	-1.270910857	0.326671439	0.579270172
Q9BPU6	Dihydropyrimidinase-related protein 5	0.231421875	0.467067605	0.681116700	0.173003688	0.849154563	-0.107595865
Q9BPW8	Protein NipSnap homolog 1	0.073941641	0.623512544	0.108318583	0.843977829	0.789742918	-0.047141528
Q9BQ39	ATP-dependent RNA helicase DDX50	0.893915539	-0.240343830	0.182522438	-0.768861917	0.673836132	-0.229709071
Q9BQ67	Glutamate-rich WD repeat-containing protein 1	0.397457957	-1.005141997	0.285050593	-0.968463146	0.766338895	0.064897392
Q9BQE3	Tubulin alpha-1C chain	0.768324841	0.039547960	0.562886244	-0.121609807	0.565930309	-0.095751912
Q9BQS8	FYVE and coiled-coil domain-containing protein 1	0.462322867	-0.109487202	0.115095672	-2.470566294	0.609536000	-0.001639825
Q9BRL6	Serine/arginine-rich splicing factor 8	0.105874548	-0.512704783	0.705692982	0.136829531	0.125375049	-0.452158990
Q9BRP8	Partner of Y14 and mago	0.797412004	0.174622201	0.445174203	0.327955825	0.795912756	0.042136660
Q9BRX5	DNA replication complex GINS protein PSF3	0.078111289	-0.697320973	0.154515306	-0.568001811	0.164755886	-0.527945800
Q9BRX8	Peroxiredoxin-like 2A	0.857489783	-0.043431160	0.468720405	1.147708981	0.830046605	0.218248694

Q9BSH5	Haloacid dehalogenase-like hydrolase domain-containing protein 3	0.038117835	-0.609709089	0.094199388	-0.590108684	0.534488463	0.119985748
Q9BSJ8	Extended synaptotagmin-1	0.906418352	0.007108370	0.745392810	0.083838048	0.525469186	0.252672589
Q9BT78	COP9 signalosome complex subunit 4	0.782321725	0.022645924	0.122656498	-0.508770151	0.251755308	-0.249335811
Q9BTT0	Acidic leucine-rich nuclear phosphoprotein 32 family member E	0.101085382	0.398156351	0.053841238	-0.506840151	0.152746401	0.967255912
Q9BUF5	Tubulin beta-6 chain	0.203785137	0.263846428	0.066364724	0.290060108	0.837821298	0.221096281
Q9BUJ2	Heterogeneous nuclear ribonucleoprotein U-like protein 1	0.220359203	0.186052548	0.392602740	0.395425527	0.684442681	-0.061507585
Q9BVA1	Tubulin beta-2B chain	0.830166791	-0.073520371	0.899827414	-0.036269649	0.489152242	-0.140980119
Q9BWD1	Acetyl-CoA acetyltransferase_cytosolic	0.265637862	-0.369426877	0.495902283	0.302183343	0.305944903	-0.291270302
Q9BWF3	RNA-binding protein 4	0.668614837	-0.591040427	0.555821499	-0.422345165	0.684367142	0.038582450
Q9BXJ9	N-alpha-acetyltransferase 15_NatA auxiliary subunit	0.928116425	-0.018012237	0.327367277	0.255132273	0.179998159	-0.213635535
Q9BXP5	Serrate RNA effector molecule homolog	0.333587834	0.806714232	0.286313529	-0.364298368	0.300122025	0.875629746
Q9BXT5	Testis-expressed protein 15	0.713613435	1.444731370	0.055147538	0.901212168	0.554255075	0.827058069
Q9BYD6	39S ribosomal protein L1_mitochondrial	0.408772923	0.234339650	0.163350883	-0.692193856	0.767346779	0.118321004
Q9BYZ2	L-lactate dehydrogenase A-like 6B	0.141101252	-0.666288871	0.298354387	-0.423866551	0.282790065	-0.443961368
Q9BZ23	Pantothenate kinase 2_mitochondrial	0.087589229	-0.606993037	0.040187003	-1.578265961	0.095231395	-0.759597562
Q9BZZ5	Apoptosis inhibitor 5	0.972025758	-0.072194075	0.862079193	-0.066307896	0.549470837	-0.206291019
Q9C005	Protein dpy-30 homolog	0.057460203	-1.453916582	0.086722745	-0.986296307	0.180312260	-0.796355420
Q9C0A0	Contactin-associated protein-like 4	0.822337077	-0.055448823	0.635502423	0.399803625	0.726076547	0.056127874
Q9GZT3	SRA stem-loop-interacting RNA-binding protein_mitochondrial	0.148345111	-0.874250835	0.073748324	-0.995127463	0.172446680	-0.624246630
Q9GZV4	Eukaryotic translation initiation factor 5A-2	0.645653170	0.095892894	0.471359269	0.222810751	0.626048337	-0.140839643
Q9H0C2	ADP/ATP translocase 4	0.344030611	0.191720634	0.173515743	0.222243689	0.661675309	-0.066793702
Q9H0D6	5'-3' exoribonuclease 2	0.518629994	0.076630702	0.017624366	-0.984287595	0.107000638	-0.326372083
Q9H0M0	NEDD4-like E3 ubiquitin-protein ligase WWP1	0.546466879	0.139462944	0.276363064	1.268110305	0.296840029	-0.277931895
Q9H0U4	Ras-related protein Rab-1B	0.777255386	-0.130321705	0.389377073	-0.448496327	0.729198181	0.004124204

Q9H1E3	Nuclear ubiquitous casein and cyclin-dependent kinase substrate 1	0.021703251	-1.110828926	0.749923100	0.846804019	0.154919658	-0.486393563
Q9H299	SH3 domain-binding glutamic acid-rich-like protein 3	0.240476693	-0.228666082	0.654054169	-0.066262272	0.007087193	-0.481377881
Q9H307	Pinin	0.902280451	-0.104738932	0.958535304	-0.016850819	0.569750506	-0.194715103
Q9H3N1	Thioredoxin-related transmembrane protein 1	0.226275254	0.236440123	0.907056726	-0.035717244	0.646072103	0.048568863
Q9H4B7	Tubulin beta-1 chain	0.408492738	0.159462062	0.909824346	-0.102587436	0.867681854	-0.067045839
Q9H6Z4	Ran-binding protein 3	0.230020153	-3.484693451	0.042910535	-4.712107552	0.306372907	-2.856689497
Q9H853	Putative tubulin-like protein alpha-4B	0.528647372	0.036709646	0.262872156	1.510377196	0.659343951	-0.161979128
Q9H8Y8	Golgi reassembly-stacking protein 2	0.830267460	-0.349145366	0.835152732	-0.157935929	0.759414051	-0.141957943
Q9H910	Jupiter microtubule associated homolog 2	0.136643143	-0.248467117	0.211071998	0.620485241	0.621599031	-0.058774823
Q9H9A6	Leucine-rich repeat-containing protein 40	0.538009451	0.364233071	0.884743801	-0.100090993	0.808935107	-0.013375871
Q9H9B4	Sideroflexin-1	0.356420780	0.185195312	0.168663236	1.349797331	0.889307401	-0.036553960
Q9H9Z2	Protein lin-28 homolog A	0.217041413	0.919636290	0.064089276	1.815679346	0.409552004	-0.247202885
Q9HAV0	Guanine nucleotide-binding protein subunit beta-4	0.896387611	0.318164509	0.125368854	-0.548843861	0.155266578	0.183784959
Q9HAV4	Exportin-5	0.032060454	-2.260409822	0.079021158	-1.318610235	0.139100819	-1.266095499
Q9HB71	Calcyclin-binding protein	0.377745025	0.387386145	0.466236714	0.213531785	0.981891395	-0.011230908
Q9HC38	Glyoxalase domain-containing protein 4	0.336721552	0.553825819	0.459028376	0.494230808	0.599144273	-0.125056144
Q9HCD6	Protein TANC2	0.684717179	-0.154837240	0.691464475	0.268273776	0.232730403	-0.508299750
Q9HCM2	Plexin-A4	0.913160385	0.075413136	0.246447175	0.173268036	0.161792237	-0.212030579
Q9NP72	Ras-related protein Rab-18	0.373370232	0.411163317	0.588640900	-0.069492769	0.713481197	0.141654299
Q9NP81	Serine--tRNA ligase_ mitochondrial	0.028397542	-1.319825365	0.086941750	-0.937337186	0.003011624	-1.933856196
Q9NPH2	Inositol-3-phosphate synthase 1	0.140822272	-0.427872768	0.215789806	0.507409463	0.945254710	-0.002854587
Q9NPQ8	Synembryon-A	0.952985038	0.132155145	0.347347940	0.838724617	0.630048668	-0.745872089
Q9NQ50	39S ribosomal protein L40_ mitochondrial	0.054169271	-0.965154977	0.146945926	-0.767661045	0.062872443	-0.418320096
Q9NQA5	Transient receptor potential cation channel subfamily V member 5	0.089508124	-0.751960981	0.161943967	-0.510433237	0.881817086	0.008299381
Q9NQC3	Reticulon-4	0.369440459	-0.447045056	0.112823600	-0.712006164	0.920182259	-0.001440902

Q9NQG5	Regulation of nuclear pre-mRNA domain-containing protein 1B	0.268936165	-0.278030781	0.083019548	-0.614061670	0.914809043	0.021218382
Q9NR30	Nucleolar RNA helicase 2	0.073678775	0.802115851	0.318562142	-0.299992858	0.542377841	-0.174679066
Q9NR31	GTP-binding protein SAR1a	0.835766137	-0.014588005	0.485605218	0.108320991	0.260842552	0.234435636
Q9NRR5	Ubiquilin-4	0.313576001	-0.441554993	0.706581824	0.019228886	0.328309281	-0.370837649
Q9NRW1	Ras-related protein Rab-6B	0.028462279	-0.623856572	0.041859021	-0.601464447	0.153709255	-0.349017296
Q9NS61	Kv channel-interacting protein 2	0.026714135	-3.261912019	0.177632234	-0.750904741	0.116823024	-1.409469215
Q9NSB2	Keratin_type II cuticular Hb4	0.541157950	-0.795873696	0.591819053	-0.563353531	0.728797743	-0.344283745
Q9NTK5	Obg-like ATPase 1	0.267768561	-1.066773668	0.345334568	-0.680519502	0.555448845	-0.608230892
Q9NVA2	Septin-11	0.680054837	-0.935405152	0.585026537	-0.856608488	0.590009379	-0.213493336
Q9NVE7	Pantothenate kinase 4	0.203363195	0.732472568	0.640443056	0.307678891	0.650892433	0.309526751
Q9NVJ2	ADP-ribosylation factor-like protein 8B	0.721461921	0.721416338	0.163970013	1.273610823	0.409815159	-1.517910587
Q9NVP1	ATP-dependent RNA helicase DDX18	0.104099463	0.410148971	0.057295298	-0.697549106	0.700978666	0.546866948
Q9NWL6	Asparagine synthetase domain-containing protein 1	0.239815692	-0.443232293	0.880604337	0.002400187	0.630042174	-0.130317020
Q9NY27	Serine/threonine-protein phosphatase 4 regulatory subunit 2	0.025472232	-1.669999178	0.159765034	-0.720980841	0.068160022	0.544845497
Q9NYC9	Dynein heavy chain 9_axonemal	0.093863354	-0.839706337	0.124383872	-1.095046455	0.157794160	-0.722790402
Q9NYL9	Tropomodulin-3	0.430819330	-1.589486144	0.734173818	0.023974325	0.988842848	-0.137837760
Q9NYU2	UDP-glucose:glycoprotein glucosyltransferase 1	0.738577690	-0.091474597	0.188159818	-0.339065673	0.943652468	-0.001017896
Q9NZI8	Insulin-like growth factor 2 mRNA-binding protein 1	0.122520012	0.355786902	0.077221398	0.415901547	0.846958774	-0.022524521
Q9NZL9	Methionine adenosyltransferase 2 subunit beta	0.600307165	0.377900718	0.073476104	1.175293507	0.850016809	0.155272408
Q9P035	Very-long-chain (3R)-3-hydroxyacyl-CoA dehydratase 3	0.087102436	0.453882724	0.132179277	0.679691004	0.945772520	0.045798899
Q9P0J0	NADH dehydrogenase [ubiquinone] 1 alpha subcomplex subunit 13	0.992416658	-0.061782745	0.115148155	-0.952081249	0.838991259	-0.025287005
Q9P0L0	Vesicle-associated membrane protein-associated protein A	0.364991200	-0.350211654	0.082457781	-1.181250304	0.508595870	0.115316543
Q9P0M6	Core histone macro-H2A.2	0.262081723	0.429522769	0.768112815	-0.165124898	0.565095289	-0.223445745

Q9P1U1	Actin-related protein 3B	0.765158800	-0.012670223	0.127557548	-0.593847474	0.549906549	-0.195322054
Q9P1Z9	Coiled-coil domain-containing protein 180	0.229725465	-0.319044427	0.050987079	-1.105476495	0.882519638	0.203105511
Q9P253	Vacuolar protein sorting-associated protein 18 homolog	0.547028771	-0.318654767	0.058504769	-0.918594478	0.846397479	-0.081333885
Q9P258	Protein RCC2	0.131561299	0.723494347	0.081516992	1.421171034	0.803291384	-0.008790436
Q9P2J5	Leucine--tRNA ligase_ cytoplasmic	0.286703522	0.295046798	0.342251100	1.662127386	0.507497649	0.106305418
Q9P2S6	Ankyrin repeat and MYND domain-containing protein 1	0.243128907	0.304776966	0.109345913	-0.385725685	0.293695625	-0.425176207
Q9UBB4	Ataxin-10	0.939225079	-0.139489016	0.587383471	-0.341137950	0.675678272	-0.222499457
Q9UBE0	SUMO-activating enzyme subunit 1	0.927657033	0.021144004	0.544012715	-0.107548303	0.733982651	-0.025890490
Q9UBF2	Coatomer subunit gamma-2	0.095506043	1.859143076	0.225043631	0.647028325	0.957776625	-0.173547691
Q9UBK8	Methionine synthase reductase	0.172596117	0.770438907	0.148220824	1.424519858	0.060667681	-0.400734186
Q9UBQ5	Eukaryotic translation initiation factor 3 subunit K	0.146846937	-0.454075473	0.847328260	-0.091814114	0.474475988	-0.201151087
Q9UBQ7	Glyoxylate reductase/hydroxypyruvate reductase	0.058628139	-2.657743948	0.118153164	-2.193241434	0.628872457	-0.537425278
Q9UBT2	SUMO-activating enzyme subunit 2	0.210820963	1.087379713	0.068218953	0.650196919	0.658715712	-0.118233920
Q9UDY6	Tripartite motif-containing protein 10	0.079021181	0.816256494	0.580217376	0.098278429	0.624804618	-0.105617839
Q9UFH2	Dynein heavy chain 17_axonemal	0.003254844	-1.731556697	0.216785421	-0.453855590	0.155610571	-0.494331851
Q9UHB9	Signal recognition particle subunit SRP68	0.395337480	0.215503743	0.070582261	0.620515119	0.905294931	0.000047271
Q9UHD8	Septin-9	0.107906857	1.517863918	0.564437827	0.090807428	0.097678128	-0.215562590
Q9UHX1	Poly(U)-binding-splicing factor PUF60	0.963496393	-0.026750472	0.882267228	-0.049794424	0.570802757	0.086395594
Q9UII15	Transgelin-3	0.034055263	-0.775031436	0.238866559	-0.176132792	0.067657340	0.675538183
Q9UIW2	Plexin-A1	0.001448666	0.942935711	0.165986811	1.536883372	0.160547247	-0.356576485
Q9UJU6	Drebrin-like protein	0.010961953	-1.545137573	0.063969641	-1.193693454	0.136434216	-0.726821459
Q9UJZ1	Stomatin-like protein 2_mitochondrial	0.869362667	0.063068012	0.767282730	-0.004387528	0.172303535	0.697212953
Q9UK32	Ribosomal protein S6 kinase alpha-6	0.233068594	0.202261366	0.268967025	-0.227855275	0.915183810	0.016388222
Q9UK76	Jupiter microtubule associated homolog 1	0.657921830	-0.033245316	0.254699133	0.725533782	0.032068645	-0.480748744
Q9UKA9	Polypyrimidine tract-binding protein 2	0.300816756	0.242176931	0.128184178	1.067334682	0.977932184	0.108629293

Q9UKD2	mRNA turnover protein 4 homolog	0.372552174	0.237189687	0.702561935	0.062521446	0.887387746	-0.053511186
Q9UKK9	ADP-sugar pyrophosphatase	0.986031713	0.015352336	0.889236561	0.004769054	0.983988785	0.060779400
Q9UKM9	RNA-binding protein Raly	0.061875208	0.970505022	0.361918127	0.244071748	0.440676220	0.196018674
Q9UKV3	Apoptotic chromatin condensation inducer in the nucleus	0.859803505	0.106945454	0.074660294	0.574269043	0.152950603	-0.241621588
Q9UKX7	Nuclear pore complex protein Nup50	0.035990495	-0.495710203	0.226703861	-0.303986101	0.573212039	-0.071489473
Q9UL46	Proteasome activator complex subunit 2	0.000062675	-0.732936987	0.102425640	-0.261589942	0.296782237	-0.129493247
Q9ULH1	Arf-GAP with SH3 domain_ ANK repeat and PH domain-containing protein 1	0.421167982	0.568728607	0.469025054	-0.370747335	0.180527459	-0.678594803
Q9ULV4	Coronin-1C	0.571658707	-0.592050801	0.389602902	0.474960174	0.950249828	-0.182274459
Q9UMS4	Pre-mRNA-processing factor 19	0.051905074	0.585403518	0.312072976	0.187254329	0.203277461	0.214617402
Q9UMX0	Ubiquilin-1	0.276452800	-0.598509345	0.991377427	-0.016952757	0.986535995	-0.081297426
Q9UN86	Ras GTPase-activating protein-binding protein 2	0.199805554	-0.903500087	0.657941186	-0.251577050	0.964686362	-0.089516473
Q9UNM6	26S proteasome non-ATPase regulatory subunit 13	0.476345955	-0.315056384	0.251508396	-0.393454810	0.936789745	-0.022492194
Q9UNW9	RNA-binding protein Nova-2	0.648380230	-0.243722061	0.873383307	-0.077571763	0.063470011	0.585114750
Q9UNZ2	NSFL1 cofactor p47	0.117306770	-0.613496499	0.021501765	-0.709772676	0.450224309	-0.216143396
Q9UPW6	DNA-binding protein SATB2	0.046638318	-1.596398633	0.553185902	0.028338151	0.092371746	-1.024090465
Q9UQ80	Proliferation-associated protein 2G4	0.953179988	0.029047481	0.706698508	0.090366849	0.321045384	-0.194146360
Q9UQE7	Structural maintenance of chromosomes protein3	0.411063369	0.655398677	0.111863001	-0.994338505	0.247309184	1.689731873
Q9UQM7	Calcium/calmodulin-dependent protein kinase type II subunit alpha	0.052650615	-3.410681085	0.539561983	-0.925425733	0.064782287	-2.589465623
Q9Y224	RNA transcription_ translation and transport factor protein	0.466606364	0.112497970	0.761082593	0.136900250	0.599220369	0.049679888
Q9Y230	RuvB-like 2	0.000020911	1.668351213	0.283484872	-0.141167317	0.175653577	0.205671722
Q9Y262	Eukaryotic translation initiation factor 3 subunitL	0.161677901	-0.744864677	0.579422541	-0.060500834	0.523536102	-0.286295911
Q9Y265	RuvB-like 1	0.483353072	0.300140897	0.120725153	0.793351227	0.663150809	-0.098925531
Q9Y266	Nuclear migration protein nudC	0.607073876	-0.413241954	0.863980524	-0.093280620	0.549758270	-0.366713583

Q9Y277	Voltage-dependent anion-selective channel protein 3	0.436803645	0.209748621	0.913652269	-0.029067678	0.483761179	-0.225094539
Q9Y281	Cofilin-2	0.503496264	-0.399834608	0.549938156	0.154934055	0.498517279	-0.394836644
Q9Y295	Developmentally-regulated GTP-binding protein 1	0.097902232	-0.230478560	0.086588290	-0.615258792	0.874801682	0.106738517
Q9Y2B0	Protein canopy homolog 2	0.165428121	-0.207754228	0.672791610	0.250754791	0.184887159	-0.167397455
Q9Y2H1	Serine/threonine-protein kinase 38-like	0.442222470	0.147305036	0.461435279	-0.158173454	0.442394723	0.382970132
Q9Y2X3	Nucleolar protein 58	0.568959062	0.322375938	0.989245710	0.183887114	0.031232444	-0.481270318
Q9Y2Z0	Protein SGT1 homolog	0.523946599	-0.090340487	0.062078293	-0.354399490	0.190659351	-0.190670174
Q9Y333	U6 snRNA-associated Sm-like protein LSm2	0.004972835	-0.669736286	0.648537673	-0.046218260	0.702927865	0.102672660
Q9Y383	Putative RNA-binding protein Luc7-like 2	0.412933658	-0.634119951	0.624391016	0.356619265	0.610178446	0.339551154
Q9Y3F4	Serine-threonine kinase receptor-associated protein	0.128971519	-1.838987860	0.244694502	-1.415119707	0.411579496	-0.970567561
Q9Y3I0	tRNA-splicing ligase RtcB homolog	0.773964861	1.068980112	0.799991268	-0.018743108	0.990929108	0.272317671
Q9Y3U8	60S ribosomal protein L36	0.887789648	-0.010329306	0.341405750	-0.134845799	0.004383670	-0.470385762
Q9Y490	Talin-1	0.388995051	0.140383638	0.996169111	0.015437868	0.938935096	0.037034361
Q9Y4L1	Hypoxia up-regulated protein 1	0.716170835	-0.060102829	0.501993138	0.237308812	0.025925150	-0.348294857
Q9Y5B9	FACT complex subunit SPT16	0.022993314	0.360859487	0.118594495	0.331061765	0.295238104	-0.167116044
Q9Y5L0	Transportin-3	0.841349443	-0.218591848	0.977395798	-0.085206456	0.825048822	0.318174873
Q9Y5M8	Signal recognition particle receptor subunit beta	0.694268025	-0.166917015	0.840000027	0.071190216	0.341645783	-0.373101537
Q9Y5S2	Serine/threonine-protein kinase MRCK beta	0.254850635	-0.923086325	0.180851890	-1.288399915	0.656147198	0.066019903
Q9Y5Y2	Cytosolic Fe-S cluster assembly factor NUBP2	0.983317053	-0.067605061	0.114556979	-0.778156277	0.944163568	0.344148600
Q9Y617	Phosphoserine aminotransferase	0.874100757	0.116415381	0.583234099	0.153244711	0.261559339	-0.239350571
Q9Y678	Coatomer subunit gamma-1	0.226247774	-0.360838144	0.108700273	-0.444050755	0.764476082	0.215612181
Q9Y696	Chloride intracellular channel protein 4	0.591650768	0.109760189	0.420161008	-0.118139002	0.778873134	0.046868833
Q9Y6B6	GTP-binding protein SAR1b	0.224455182	0.580715713	0.399401155	0.239003704	0.076704067	0.605857133
Q9Y6G9	Cytoplasmic dynein 1 light intermediate chain 1	0.458881358	-0.387418686	0.150983606	-0.686930125	0.835480070	-0.023477587
Q9Y6M1	Insulin-like growth factor 2 mRNA-binding protein 2	0.129663408	0.398535982	0.106016699	0.669080840	0.834928540	0.102473263

Q9Y6N5	Sulfide:quinone oxidoreductase_ mitochondrial	0.892366086	0.113473991	0.069651171	-0.828627794	0.335202194	1.184518073
Q9Y6N7	Roundabout homolog 1	0.488855032	-1.175658232	0.264639134	-0.666211751	0.468353898	-1.077808054

Table S2. List of proteins identified, quantified, differentially regulated, upregulated, and downregulated in neurospheres infected with Br ZIKV, ZIKV 766 and DENV.

Accession	Description	Anova (p) ZIKV 766	Log FC ZIKV 766	Anova (p) Br ZIKV	Log FC Br ZIKV	Anova (p) DENV	Log FC DENV
A0A075B759	Peptidyl-prolyl cis-trans isomerase A-like 4E	0.494997846	0.521619423	0.185147932	0.738521468	0.013169586	0.934396898
A0A0B4J2D5	Glutamine amidotransferase-like class 1 domain-containing protein 3B_mitochondrial	0.00039489	-0.789807545	0.749451623	0.241662135	0.425904001	-0.101408514
A3KMH1	von Willebrand factor A domain-containing protein 8	0.793425878	0.70654282	0.124384577	0.973539564	0.791684055	0.075316547
A4UGR9	Xin actin-binding repeat-containing protein 2	0.497126312	1.501624321	0.295696523	1.583750702	0.572545868	-0.699903776
A5A3E0	POTE ankyrin domain family member F	0.748894233	0.492198323	0.032109117	0.60099669	0.439671086	-0.102320543
A6NEC2	Puromycin-sensitive aminopeptidase-like protein	0.216163594	2.161775031	0.296188997	2.006789347	0.265825297	-0.436680571
A6NHL2	Tubulin alpha chain-like 3	0.001820938	-1.333881031	0.00966097	-1.253733494	0.159050789	-0.664917756
A6NIZ1	Ras-related protein Rap-1b-like protein	0.103896424	1.246658083	0.002443189	1.277506698	0.244674824	0.417948827
A6NJ46	Homeobox protein Nkx-6.3	0.03964376	-0.437850598	0.960874463	-0.024407504	0.404516279	-0.236426569
A6NKL1	Zinc finger and SCAN domain-containing protein 5B	0.704041696	0.23800536	0.032373586	-0.410754981	0.098329252	-0.596385759
A6NNZ2	Tubulin beta-8 chain-like protein LOC260334	0.004003566	-0.684735685	0.854943173	0.047498022	0.802681487	0.021914128
B2RXH8	Heterogeneous nuclear ribonucleoprotein C-like 2	0.322337333	1.537935527	0.256928661	1.255409659	0.639302764	-0.517071252
E9PAV3	Nascent polypeptide-associated complex subunit alpha_muscle-specific form	0.752397455	0.067337777	0.553711432	-0.108618077	0.493788723	0.508298878
O00154	Cytosolic acyl coenzyme A thioester hydrolase	0.189529699	1.362044311	0.149206024	2.000642146	0.385905267	-0.354656082
O00231	26S proteasome non-ATPase regulatory subunit 11	0.076976891	-0.675514761	0.678404525	-0.128207732	0.129453777	-0.857788785
O00232	26S proteasome non-ATPase regulatory subunit 12	0.003904973	-0.912502243	0.032917408	-1.236507606	0.232161522	-0.50980892
O00264	Membrane-associated progesterone receptor component 1	0.488448942	-0.407709636	0.183864827	0.439178123	0.860610898	0.218720479
O00299	Chloride intracellular channel protein 1	0.027833684	-0.708431901	0.631360108	-0.177616877	0.205840872	-0.642486454
O00370	LINE-1 retrotransposable element ORF2 protein	0.827340546	-0.010107745	0.190476327	-0.809085784	0.856530181	0.149623109
O00410	Importin-5	0.624587484	0.895977907	0.006155111	1.110307053	0.524462356	0.160422456
O00425	Insulin-like growth factor 2 mRNA-binding protein 3	0.120716709	-0.334702243	0.586113677	-0.069611911	0.186649825	-0.228278531

O00429	Dynamin-1-like protein	0.199368548	1.309764382	0.055273845	1.15155173	0.109921133	0.462166807
O00560	Syntenin-1	0.817383632	-0.004288391	0.408979063	-0.479271936	0.682570087	-0.238019424
O00567	Nucleolar protein 56	0.269758274	-0.541803997	0.388036266	-0.124310177	0.171674678	1.041945509
O00571	ATP-dependent RNA helicase DDX3X	0.364967677	-0.205402768	0.883551047	0.009320115	0.046044462	-0.502984373
O00764	Pyridoxal kinase	0.124959017	-0.300249968	0.130950293	-0.217499946	0.4949992	0.245617841
O14531	Dihydropyrimidinase-related protein 4	0.263203367	-0.34314277	0.648902609	-0.136060689	0.078955594	-0.954783669
O14556	Glyceraldehyde-3-phosphate dehydrogenase-testis-specific	0.251329315	1.421524375	0.194567046	1.371543007	0.59978222	-0.493484732
O14579	Coatomer subunit epsilon	0.000635513	-1.509746392	0.304166342	-0.488895593	0.089491699	-1.410381944
O14737	Programmed cell death protein 5	0.926617114	-0.124929108	0.652450061	-0.479927112	0.608739153	-0.431738331
O14744	Protein arginine N-methyltransferase 5	0.277376467	0.621886454	0.05119715	1.204775065	0.881805713	0.132595129
O14782	Kinesin-like protein KIF3C	0.052576319	-0.669515413	0.080423371	-0.370889525	0.390529115	-0.265950242
O14818	Proteasome subunit alpha type-7	0.241332762	-0.492008454	0.208515754	-0.528062098	0.089725388	-0.726236769
O14936	Peripheral plasma membrane protein CASK	0.077540781	-0.436801069	0.00889922	-0.345676141	0.457691261	-0.197876182
O14950	Myosin regulatory light chain 12B	0.274057146	0.591720231	0.900399058	0.290132561	0.04663518	-0.56873934
O14979	Heterogeneous nuclear ribonucleoprotein D-like	0.395648469	1.268827845	0.095316336	1.224342599	0.739908158	-0.392523193
O14980	Exportin-1	0.688805274	-0.080353091	0.789578354	0.016316028	0.49148509	-0.172237802
O15067	Phosphoribosylformylglycinamide synthase	0.278875275	1.337562396	0.091501439	0.950148224	0.667992262	-0.290455242
O15075	Serine/threonine-protein kinase DCLK1	0.476679077	0.724903743	0.338394347	1.004556198	0.139225579	-0.81933828
O15078	Centrosomal protein of 290 kDa	0.743489555	0.524634719	0.258609215	-0.210200374	0.878088576	1.626523008
O15123	Angiopoietin-2	0.023733935	-1.023132595	0.684985903	-0.117025823	0.725034144	0.220110142
O15173	Membrane-associated progesterone receptor component 2	0.047279615	-1.367195779	0.085195021	-1.386071784	0.123304115	-1.10207956
O15260	Surfeit locus protein 4	0.900379839	0.084732244	0.019957145	0.368585326	0.010886565	0.521149877
O15305	Phosphomannomutase 2	0.873727111	0.171229086	0.07346971	8.424574216	0.193741446	2.364629164
O15347	High mobility group protein B3	0.495671719	-0.1453919	0.826479759	-0.013387083	0.102214304	-0.817461184
O15360	Fanconi anemia group A protein	0.132940611	-0.954389547	0.004384179	-1.788039504	0.049930391	-0.988369822

O15371	Eukaryotic translation initiation factor 3 subunitD	0.001413603	-1.603320131	0.093619828	-0.737725027	0.035989494	-0.866344594
O15523	ATP-dependent RNA helicase DDX3Y	0.072828487	-0.437327431	0.93944567	-0.000605957	0.924374749	0.090245769
O43143	Pre-mRNA-splicing factor ATP-dependent RNA helicase DHX15	0.171926298	-0.257987045	0.596089677	-0.099634282	0.206810113	-0.206014845
O43150	Arf-GAP with SH3 domain_ ANK repeat and PH domain-containing protein 2	0.399551097	1.657859203	0.080507105	1.813117252	0.680494988	-0.290667053
O43175	D-3-phosphoglycerate dehydrogenase	0.061812822	-0.459736126	0.743237013	-0.116899951	0.729477131	0.041289758
O43237	Cytoplasmic dynein 1 light intermediate chain 2	0.001341412	-1.231790254	0.048181542	-1.46350671	0.145908482	-1.085168099
O43242	26S proteasome non-ATPase regulatory subunit 3	0.477880502	-0.126145462	0.942850997	0.097627526	0.276762134	-0.211948111
O43347	RNA-binding protein Musashi homolog 1	0.009448327	-1.361009294	0.770548272	0.684363845	0.135878058	1.000106906
O43390	Heterogeneous nuclear ribonucleoprotein R	0.232170514	-0.288757616	0.220510977	-0.279192928	0.415653843	0.21050683
O43396	Thioredoxin-like protein 1	0.766642527	0.239191014	0.506592997	0.367485888	0.1430432	-0.807751327
O43423	Acidic leucine-rich nuclear phosphoprotein 32 family member C	0.136725214	-0.630095577	0.096635157	-0.872335584	0.212559531	-0.5638346
O43602	Neuronal migration protein doublecortin	0.96540912	0.090059413	0.877931653	-0.016910042	0.05026386	-0.882392802
O43684	Mitotic checkpoint protein BUB3	0.025605782	-0.633446317	0.853748747	0.005485294	0.556789025	0.141061304
O43707	Alpha-actinin-4	0.279000342	-0.249061203	0.053890428	-0.248633031	0.294202118	0.725401004
O43765	Small glutamine-rich tetratricopeptide repeat-containing protein alpha	0.312159375	1.326495333	0.140626072	1.35980879	0.77328509	0.013881928
O43776	Asparagine--tRNA ligase_ cytoplasmic	0.607155351	-0.019613083	0.01344257	-0.415134578	0.029240061	0.288850282
O43790	Keratin_type II cuticular Hb6	0.922454573	0.307785187	0.344091534	-0.221428086	0.62003013	0.056697256
O43809	Cleavage and polyadenylation specificity factor subunit 5	0.636803059	0.209304754	0.163584553	1.219248942	0.000522521	0.783136729
O43852	Calumenin	0.02485404	-0.558953879	0.266593284	-0.244982982	0.345200874	-0.392446208
O43866	CD5 antigen-like	0.391199449	-0.160551197	0.441691756	1.340777642	0.866473613	0.703835466
O60256	Phosphoribosyl pyrophosphate synthase-associated protein 2	0.50649823	-0.234372777	0.815513679	-0.114474314	0.124066086	-0.725192644
O60282	Kinesin heavy chain isoform 5C	0.842668957	0.601051028	0.18364152	0.754546012	0.538513454	-0.376820974
O60343	TBC1 domain family member 4	0.382734771	0.867256346	0.110220968	1.040429785	0.682669216	-0.509328046

O60361	Putative nucleoside diphosphate kinase	0.851816949	-0.041162472	0.368295835	-0.309260154	0.025070186	-0.632184986
O60506	Heterogeneous nuclear ribonucleoprotein Q	0.5707815	-0.070389395	0.947841966	0.065087712	0.139926313	0.433085991
O60522	Tudor domain-containing protein 6	0.169764526	-1.031742689	0.264948595	-0.779914977	0.151407755	-1.022917413
O60664	Perilipin-3	0.030442118	-1.343372315	0.04807065	-1.516965738	0.099252268	-1.332181024
O60684	Importin subunit alpha-7	0.16777613	-0.595314607	0.266193117	-0.412514068	0.026942389	0.395556082
O60701	UDP-glucose 6-dehydrogenase	0.756571186	-0.067658101	0.510306539	-0.173727302	0.163283614	-0.49099759
O60888	Protein CutA	0.762244549	-0.028622831	0.9242705	-0.006394494	0.001827479	-0.500059064
O75044	SLIT-ROBO Rho GTPase-activating protein 2	0.023009094	-1.427657281	0.191240459	-0.511004715	0.0504579	-0.662436968
O75051	Plexin-A2	0.105585991	-0.907993333	0.076863016	-1.802794897	0.680563273	0.197443127
O75131	Copine-3	0.375549824	1.530126447	0.06436146	1.166652089	0.467345685	-0.304603237
O75170	Serine/threonine-protein phosphatase 6 regulatory subunit 2	7.81E-05	-0.879535126	0.000219303	-0.417885906	0.212140487	-0.577538045
O75344	Inactive peptidyl-prolyl cis-trans isomerase FKBP6	0.813409914	0.364047933	0.684890292	-0.089335206	0.074035225	-1.04275427
O75347	Tubulin-specific chaperone A	0.303165007	-0.387264862	0.043213618	-0.710137134	0.073178203	-1.000748247
O75367	Core histone macro-H2A.1	0.939661264	0.030169748	0.012572474	-0.888889453	0.763768583	0.133651979
O75368	SH3 domain-binding glutamic acid-rich-like protein	0.117089961	-0.647076008	0.212011036	-0.500734545	0.055426575	-0.78015358
O75369	Filamin-B	0.410457987	-0.747111706	0.041623395	-2.303624599	0.326842022	-0.977883542
O75390	Citrate synthase_mitochondrial	0.373151674	1.856630151	0.037383524	1.645050571	0.94122322	-0.230240883
O75410	Transforming acidic coiled-coil-containing protein 1	0.431851172	1.334184276	0.137272033	1.377613722	0.648461754	-0.224936499
O75436	Vacuolar protein sorting-associated protein 26A	0.092972065	-0.700059817	0.034728231	-0.743789469	0.257172126	-0.314788707
O75448	Mediator of RNA polymerase II transcription subunit 24	0.196295652	-1.434432319	0.080688572	-2.337614431	0.105692125	-2.09053152
O75526	RNA-binding motif protein_X-linked-like-2	0.601704446	1.020132303	0.593689512	-0.321779145	0.821885543	-0.07184873
O75531	Barrier-to-autointegration factor	0.062922987	-0.746256413	0.000279385	-3.024833884	0.316118258	-0.223720686
O75533	Splicing factor 3B subunit 1	0.52000508	0.95810994	0.037390828	0.846404672	0.410967333	-0.283560671
O75569	Interferon-inducible double-stranded RNA-dependent protein kinase activator A	0.224333384	1.570907577	0.044484589	1.170578118	0.659947723	-0.122665524

O75608	Acyl-protein thioesterase 1	0.720920769	0.964355777			0.733488899	1.908345804
O75643	U5 small nuclear ribonucleoprotein 200 kDa helicase	0.496864521	0.561712113	0.254939084	0.290590383	0.143141831	-0.688300244
O75874	Isocitrate dehydrogenase [NADP] cytoplasmic	0.460499639	1.296318444	0.167956928	1.266980286	0.853275345	-0.326937036
O75937	DnaJ homolog subfamily C member 8	0.76732472	0.257773369	0.805105906	0.233474677	0.933643507	-0.112599472
O75947	ATP synthase subunit d_mitochondrial	0.191652346	-1.915553487	0.265392243	0.273565194	0.20921194	1.639208736
O76021	Ribosomal L1 domain-containing protein 1	0.748376802	-0.204973225	0.698328473	0.101063452	0.100113634	1.613162085
O76094	Signal recognition particle subunit SRP72	0.382473234	-0.257916361	0.227872048	-0.447660146	0.240860323	-0.446824365
O94887	FERM_ARHGEF and pleckstrin domain-containing protein 2	0.864811427	0.294695981	0.875578614	-0.022230318	0.275094879	-0.499626948
O95292	Vesicle-associated membrane protein-associated protein B/C	0.011904016	0.814889134	0.014962629	0.943844005	0.118462949	1.16908544
O95336	6-phosphogluconolactonase	0.255792906	-0.421671843	0.956533389	0.095284883	0.106798417	-0.53292543
O95373	Importin-7	0.675778634	-0.192967107	0.671765301	-0.158198421	0.910852463	0.045704002
O95678	Keratin_type II cytoskeletal 75	0.602681998	0.187035288	0.675041921	-0.136203287	0.387017393	-0.347049172
O95757	Heat shock 70 kDa protein 4L	0.325906625	0.987309369	0.687458901	1.283760106	0.158369318	-1.128729522
O95758	Polypyrimidine tract-binding protein 3	0.423553813	1.318334725	0.929303851	-0.027866981	0.191070401	-0.861737572
O95865	N(G)_N(G)-dimethylarginine dimethylaminohydrolase 2	0.915710312	0.100585251	0.002202801	1.505383734	0.098769786	1.618812177
P00338	L-lactate dehydrogenase A chain	0.931455379	-0.072469434	0.55026676	0.093461771	0.73889012	0.495735818
P00367	Glutamate dehydrogenase 1_mitochondrial	0.127868164	0.328508102	0.855882171	0.06423876	0.250870074	-0.297145387
P00387	NADH-cytochrome b5 reductase 3	0.025043509	0.96638798	0.10693471	0.563687062	0.006340932	1.2621397
P00441	Superoxide dismutase [Cu-Zn]	0.736663727	0.055429589	0.338260569	-0.208702816	0.084626536	-0.514120635
P00505	Aspartate aminotransferase_mitochondrial	0.055106607	0.38224479	0.316305504	0.289948951	0.335410447	-0.266631782
P00558	Phosphoglycerate kinase 1	0.349191939	-0.231312992	0.398114194	-0.141298636	0.204468225	-0.655382151
P01266	Thyroglobulin	0.946561161	-0.415636406	0.091976163	1.094149538	0.7897182	-0.211424967
P02545	Prelamin-A/C	0.224269242	-0.449550547	0.416105936	-0.219678887	0.671190365	-0.134927473
P02768	Serum albumin	0.39565895	1.526131185	0.066054351	1.52283147	0.474669126	-0.566655382
P02787	Serotransferrin	0.364110557	1.661378922	0.074945374	1.632729573	0.586721687	0.128489858

P02790	Hemopexin	0.463195506	1.960983434	0.160173098	1.593483884	0.927848921	-0.262104785
P04075	Fructose-bisphosphate aldolase A	0.974966939	0.121123889	0.51710359	-0.179384601	0.742026013	-0.087136173
P04080	Cystatin-B	0.4647435	-0.651039115	0.877924376	-0.600967056	0.274471589	-1.449186038
P04083	Annixin A1	0.668194957	0.536041448	0.752534119	0.944675214	0.076523729	-1.08369824
P04114	Apolipoprotein B-100	0.167246448	1.673682228	0.156842639	1.587817126	0.925615662	-0.155845125
P04259	Keratin_type II cytoskeletal 6B	0.177410355	-0.197609114	0.211084141	-0.337178451	0.306820492	-0.32190802
P04264	Keratin_type II cytoskeletal 1	0.29736084	0.096285834	0.743246199	0.258746016	0.82384282	-0.637610114
P04350	Tubulin beta-4A chain	0.008707954	-0.704276914	0.525556489	-0.060206747	0.046785788	-0.427194259
P04406	Glyceraldehyde-3-phosphate dehydrogenase	0.332090704	-0.24063782	0.653489174	-0.082890914	0.154495243	-0.337709581
P04632	Calpain small subunit 1	0.510049172	-0.225304749	0.899525439	-0.005162351	0.321364315	-0.392089726
P04792	Heat shock protein beta-1	0.515243047	-0.599385963	0.282950045	-1.691568045	0.817656171	-0.124323049
P04843	Dolichyl-diphosphooligosaccharide--protein glycosyltransferase subunit 1	0.98262217	0.089753398	0.613699863	-0.104406639	0.24488529	-0.408247242
P04844	Dolichyl-diphosphooligosaccharide--protein glycosyltransferase subunit 2	0.488727088	-0.113856685	0.24203835	-0.230009338	0.577344382	-0.113939886
P04899	Guanine nucleotide-binding protein G(i) subunit alpha-2	0.683918608	0.21347972	0.317194526	0.271342025	0.550290953	-0.249800252
P05023	Sodium/potassium-transporting ATPase subunit alpha-1	0.197706154	0.925585905	0.537508933	-0.252450529	0.781528166	-0.090025932
P05091	Aldehyde dehydrogenase_mitochondrial	0.216074669	0.527284325	0.05635387	-0.456664935	0.222304223	-0.352737697
P05141	ADP/ATP translocase 2	0.086951617	-0.488752844	0.038074481	-0.633970208	0.249869738	-0.406616445
P05198	Eukaryotic translation initiation factor 2 subunit 1	0.006888388	-0.832728899	0.386680704	-0.173466409	0.017256735	-0.521353907
P05386	60S acidic ribosomal protein P1	0.266498434	-0.151501657	0.574992498	-0.095154994	0.659042536	0.120171437
P05387	60S acidic ribosomal protein P2	0.277852866	-0.727517228	0.549717631	-0.562760183	0.382186104	-0.727521526
P05388	60S acidic ribosomal protein P0	0.638752485	-0.131074667	0.489998124	-0.205208438	0.256151488	0.297205977
P05455	Lupus La protein	0.478322322	-0.212324034	0.037039682	0.648009627	0.245483951	0.237232869
P05787	Keratin_type II cytoskeletal 8	0.977465113	0.098564122	0.043766154	-0.363961495	0.544477164	-0.066907638
P06396	Gelsolin	0.989539771	0.115967914	0.616011459	0.165926193	0.789525539	0.025736982
P06454	Prothymosin alpha	0.228725191	-0.748959259	0.917880331	-0.007240023	0.329775028	-0.287900953

P06576	ATP synthase subunit beta_mitochondrial	0.413870546	-0.174616073	0.479502791	-0.179505621	0.66114615	0.062931979
P06727	Apolipoprotein A-IV	0.118839307	0.550627925	0.455522951	0.608267781	0.720562665	0.222380856
P06732	Creatine kinase M-type	0.904460084	0.172504965	0.160168978	-0.36086272	0.139153772	-1.407312376
P06733	Alpha-enolase	0.77902603	-0.014379929	0.662891957	-0.088665084	0.011700252	-0.756143174
P06737	Glycogen phosphorylase_liver form	0.98482292	0.014606046	0.889851965	0.104348505	0.260071364	-0.475269038
P06744	Glucose-6-phosphate isomerase	0.238863134	-0.266995288	0.495888714	0.129514486	0.503861014	-0.188179212
P06748	Nucleophosmin	0.773391607	-0.018960393	0.50961258	0.171380137	0.041158476	0.556291116
P06753	Tropomyosin alpha-3 chain	0.576865138	0.053324976	0.063916793	-2.204680696	0.974650105	-0.36293656
P06899	Histone H2B type 1-J	0.805423534	0.068089027	0.190159193	-0.835908407	0.598772824	0.24673794
P07195	L-lactate dehydrogenase B chain	0.774509384	0.207439066	0.770870309	-0.050573638	0.005020107	-0.708896258
P07196	Neurofilament light polypeptide	0.677704172	-0.154709162	0.41437279	0.504435763	0.941792317	-0.056241019
P07197	Neurofilament medium polypeptide	0.361232905	1.602646483	0.079457285	1.403505591	0.626986619	-0.343187161
P07205	Phosphoglycerate kinase 2	0.35878659	0.772013902	0.310747621	0.79645617	0.519021685	-0.508775015
P07237	Protein disulfide-isomerase	0.346383638	-0.198279583	0.103009668	-0.285144897	0.893825346	-0.001012296
P07339	Cathepsin D	0.076123649	-0.944550769	0.179448571	-0.693844159	0.47031331	-0.308783089
P07355	Annexin A2	0.34533593	1.244112101	0.028763626	1.441916774	0.142341685	-0.930728409
P07437	Tubulin beta chain	0.002397746	-0.513501823	0.674120035	-0.073645165	0.051798074	-0.471195389
P07602	Prosaposin	0.69955388	-0.083252409	0.655728765	-0.291600717	0.542841013	-0.329132905
P07737	Profilin-1	0.002027951	-0.734657555	0.555389061	-0.143660989	0.022096365	-0.8909034
P07741	Adenine phosphoribosyltransferase	0.648497738	-0.338358427	0.533208153	-0.192186214	0.549205313	0.201905322
P07814	Bifunctional glutamate/proline-tRNA ligase	0.092548114	-0.690259581	0.236625611	-0.457891795	0.00022848	1.29622579
P07864	L-lactate dehydrogenase C chain	0.164146862	0.301934857	0.447353229	0.689855301	0.294646686	-0.995285649
P07900	Heat shock protein HSP 90-alpha	0.062289138	-0.406161097	0.920325941	0.015764697	0.161911268	-0.367545834
P07910	Heterogeneous nuclear ribonucleoproteins C1/C2	0.932396543	0.217649021	0.247831118	0.372598359	0.234178405	0.434430168
P07954	Fumarate hydratase_mitochondrial	0.861735524	0.112768728	0.698013187	-0.197775686	0.093099908	-0.712800038
P08133	Annexin A6	0.702844331	0.653243422	0.974443638	0.313954075	0.262679817	-0.97454971
P08134	Rho-related GTP-binding protein RhoC	0.536419629	0.308005365	0.640279151	-0.142302918	0.146423365	-0.460336505

P08237	ATP-dependent 6-phosphofructokinase_ muscle type	0.482927816	0.54874107	0.369927771	-0.176723347	0.002461022	0.529964786
P08238	Heat shock protein HSP 90-beta	0.130822054	-0.348317463	0.941453683	0.016783122	0.09264507	-0.58796865
P08559	Pyruvate dehydrogenase E1 component subunit alpha_ somatic form_ mitochondrial	0.34206064	-0.286572698	0.003513883	-1.343609668	0.357663891	-0.320599403
P08621	U1 small nuclear ribonucleoprotein 70 kDa	0.424933174	-0.147973414	0.894962108	0.191978754	0.020117972	0.423028199
P08670	Vimentin	0.856776248	-0.100407034	0.780397931	0.007714623	0.365341201	0.381299523
P08708	40S ribosomal protein S17	0.171203434	-0.534058985	0.844394295	-0.096966306	0.938005389	-0.046359782
P08729	Keratin_ type II cytoskeletal 7	0.835415342	0.66536913	0.395559103	0.275768292	0.155756	-0.910474814
P08754	Guanine nucleotide-binding protein G(i) subunit alpha	0.203830085	-0.532723012	0.174239075	-0.825211063	0.926653354	-0.039089119
P08758	Annexin A5	0.714788623	0.083324716	0.734353777	-0.036566978	0.002571507	-0.472466043
P08865	40S ribosomal protein SA	0.389631795	-0.253490316	0.549911353	-0.220332386	0.323597789	-0.365102008
P09104	Gamma-endolase	0.668639103	0.161464137	0.0193533	-0.662738236	0.545379314	-0.103051481
P09211	Glutathione S-transferase P	0.006237727	-0.643487478	0.431814833	-0.264156835	0.012566023	-1.051584449
P09429	High mobility group protein B1	0.160055913	-0.435876832	0.203745888	-0.503104138	0.041562695	-0.839263078
P09471	Guanine nucleotide-binding protein G(o) subunit alpha	0.517097623	-0.133970178	0.946190389	0.141370915	0.631561007	0.19152305
P09493	Tropomyosin alpha-1 chain	0.236130392	-0.766043424	0.514597353	-0.293336113	0.430661661	-0.597579648
P09496	Clathrin light chain A	0.762623944	-0.028992001	0.309937933	0.467449864	0.685593429	0.705717456
P09622	Dihydrolipoyl dehydrogenase_ mitochondrial	0.849117436	0.93455433	0.947312007	-0.112369951	0.729911517	0.05113495
P09651	Heterogeneous nuclear ribonucleoprotein A1	0.480310816	-0.149712507	0.764352754	-0.009339398	0.1017265	0.354662678
P09661	U2 small nuclear ribonucleoprotein A'	0.381852363	0.801132421	0.428752399	-0.271198232	0.89090593	0.016590045
P09874	Poly [ADP-ribose] polymerase 1	0.456931507	1.347962532	0.060249727	1.302842213	0.427028485	-0.294417099
P09936	Ubiquitin carboxyl-terminal hydrolase isozymeL1	0.019356439	-0.934219882	0.0849115	-0.609475376	0.031664793	-0.837930263
P09960	Leukotriene A-4 hydrolase	0.060720509	-0.470761579	0.22861855	-0.274549702	0.008534083	-0.45556545
P09972	Fructose-bisphosphate aldolase C	0.050954134	-1.309196906	0.012380418	-2.026225035	8.84855E-06	-3.731692334
P0CG38	POTE ankyrin domain family member I	0.353219129	0.666477859	0.457303199	0.005147628	0.329046723	-1.061193016

P0CG47	Polyubiquitin-B	0.74939268	-0.011065472	0.959815274	0.009805609	0.199812733	-0.626605581
P0DMV9	Heat shock 70 kDa protein 1B	0.596389189	-0.006272365	0.909585646	0.050238696	0.356043726	-0.305495808
P0DN79	Cystathione beta-synthase-like protein	0.837277235	0.183766415	0.001450272	0.927865483	0.05787097	1.105897168
P0DP24	Calmodulin-2	0.626890827	0.060318264	0.14969034	-0.223097242	0.004585409	-0.598020372
P0DPH8	Tubulin alpha-3D chain	0.957983107	0.64268629	0.121351973	-1.017798989	0.291846257	-0.684556343
P10155	60 kDa SS-A/Ro ribonucleoprotein	0.19868832	-0.56187097	0.359430026	-0.452539959	0.126916228	-0.821996563
P10253	Lysosomal alpha-glucosidase	0.642052425	-0.085158969	0.203560164	-0.647488474	0.142172088	-0.725168966
P10412	Histone H1.4	0.294132242	0.26648683	0.642912826	-0.166978006	0.024519634	0.907974682
P10588	Nuclear receptor subfamily 2 group F member 6	0.461249209	-0.374253403	0.841090218	-0.272198887	0.414654116	-0.846810044
P10599	Thioredoxin	0.80383381	0.012664996	0.903986079	0.162675431	0.502451564	-0.198291764
P10768	S-formylglutathione hydrolase	0.122722549	0.871899626	0.146097746	0.676512707	0.82462737	-0.044254676
P10809	60 kDa heat shock protein_mitochondrial	0.100297875	-0.395674974	0.039204115	-0.475454264	0.876439707	-0.015763789
P10909	Clusterin	0.994175588	-0.141956152	0.115375062	-1.799329228	0.357788107	-1.183334936
P11021	Endoplasmic reticulum chaperone BiP	0.754230403	0.001070983	0.950873772	0.013987677	0.118574653	0.244710102
P11137	Microtubule-associated protein 2	0.346301611	1.348652087	0.100750599	1.296281749	0.782174403	-0.327014404
P11142	Heat shock cognate 71 kDa protein	0.478760088	-0.186472345	0.788351058	0.041751295	0.143028422	-0.40357405
P11216	Glycogen phosphorylase_brain form	0.582277893	0.180363684	0.49087081	-0.22528246	0.056093039	-0.627472191
P11279	Lysosome-associated membrane glycoprotein 1	0.085322486	-0.497869091	0.233978583	-0.45724841	0.045242459	-0.69575014
P11310	Medium-chain specific acyl-CoA dehydrogenase_mitochondrial	0.383338079	1.886885193	0.051216215	1.911291935	0.855112566	-0.188507607
P11413	Glucose-6-phosphate 1-dehydrogenase	0.164933288	0.408708078	0.731212701	0.325339326	0.043853947	1.032833155
P11488	Guanine nucleotide-binding protein G(t) subunit alpha-1	0.528410805	-0.421141844	0.309243685	-0.602247042	0.18347089	-1.145752393
P11586	C-1-tetrahydrofolate synthase_cytoplasmic	0.020494552	-0.491113921	0.040533258	-0.573230238	0.08388472	-0.394481487
P11766	Alcohol dehydrogenase class-3	0.241270528	-0.411738322	0.764550294	-0.144531162	0.106304011	-0.784182807
P11940	Polyadenylate-binding protein 1	0.011358385	2.217122451	0.015700312	1.784569918	0.304682328	1.019520279
P12004	Proliferating cell nuclear antigen	0.854060759	0.180681997	0.408339139	0.343548351	0.134430116	-0.617265984
P12036	Neurofilament heavy polypeptide	0.645306952	-0.040600546	0.223999227	-0.221283074	0.773912597	0.388256203

P12081	Histidine--tRNA ligase_ cytoplasmic	0.976286483	0.132469923	0.318246876	-0.540922919	0.240119186	-0.635205174
P12236	ADP/ATP translocase 3	0.82280289	0.390674346	0.929523419	0.077700482	0.034815343	1.171915288
P12270	Nucleoprotein TPR	0.367191804	1.611903788	0.140333536	1.436001579	0.955629624	-0.161485646
P12277	Creatine kinase B-type	0.659359727	0.119284838	0.430758631	0.118189316	0.022401352	-0.258323314
P12814	Alpha-actinin-1	0.167047158	-0.216120127	0.384340939	-0.130894068	0.086463344	-0.570867943
P12956	X-ray repair cross-complementing protein 6	0.53989714	0.450745243	0.003013699	0.791497889	0.068947782	0.434891777
P13010	X-ray repair cross-complementing protein 5	0.254560575	-0.372580706	0.269667748	0.468687237	0.016707923	0.431107926
P13056	Nuclear receptor subfamily 2 group C member 1	0.506095186	-1.149825552	0.163502398	-2.142834049	0.782448264	1.504771164
P13473	Lysosome-associated membrane glycoprotein 2	0.263740976	-0.478910702	0.171166145	-0.544059728	0.088453704	-0.704359437
P13489	Ribonuclease inhibitor	0.172570592	-0.594887997	0.261305831	-0.387596232	0.069827589	0.356776055
P13637	Sodium/potassium-transporting ATPase subunit alpha-3	0.105085312	-1.182608558	0.232514611	-1.069856085	0.522696213	1.900501458
P13639	Elongation factor 2	0.033932605	-0.175974953	0.524264692	-0.084436405	0.500144721	0.339518231
P13645	Keratin_type I cytoskeletal 10	0.014948523	1.013029115	0.035689379	0.975091886	0.525576034	0.340112857
P13646	Keratin_type I cytoskeletal 13	0.524860918	1.272523521	0.041125019	1.234722692	0.349452094	-0.499226024
P13647	Keratin_type II cytoskeletal 5	0.117845708	-0.440586581	0.388041683	-0.203401714	0.512269633	0.165254061
P13667	Protein disulfide-isomerase A4	0.73474287	0.108962959	0.003965828	-1.020809697	0.000539405	-0.652427734
P13797	Plastin-3	0.770913904	0.468752757	0.00073769	-1.192315796	0.800963265	0.102571325
P13804	Electron transfer flavoprotein subunit alpha_mitochondrial	0.09636589	0.181453854	0.857212253	0.071235374	0.218419748	0.302559043
P13929	Beta-enolase	0.997994518	0.021605429	0.957515342	0.013797961	0.64586012	0.733195142
P14136	Glial fibrillary acidic protein	0.667463001	0.111352758	0.520956186	2.46886482	0.531307118	-1.445079932
P14314	Glucosidase 2 subunit beta	0.009602945	-0.770883042	0.831048141	0.054429234	0.123117558	-0.602024246
P14324	Farnesyl pyrophosphate synthase	0.124153733	-0.361177069	0.279656107	-0.315788081	0.08786739	-0.613703137
P14550	Aldo-keto reductase family 1 member A1	0.169559738	-0.47621355	0.078523864	-0.593294699	0.046940221	-0.812341235
P14618	Pyruvate kinase PKM	0.117435519	-0.631781425	0.293816977	-0.515294967	0.094995924	-0.814812954
P14625	Endoplasmin	0.234076571	0.321098898	0.21100842	-0.565343844	0.143647808	-0.71134686
P14866	Heterogeneous nuclear ribonucleoprotein L	0.685358259	0.158957638	0.001765123	0.705453807	0.094405657	0.898769992

P14868	Aspartate--tRNA ligase_ cytoplasmic	0.956055647	-1.960291766	0.818410767	-2.512622644	0.61622281	-3.966765963
P15121	Aldo-keto reductase family 1 member B1	0.269768468	-0.361936662	0.447702641	0.12966107	0.143059939	-0.344461133
P15153	Ras-related C3 botulinum toxin substrate 2	0.275408778	-0.178159787	0.484314757	-0.155958334	0.141977372	-0.356392941
P15259	Phosphoglycerate mutase 2	0.571726675	0.102956371	0.488706244	-0.333766528	0.521789609	-0.257247424
P15311	Ezrin	0.18884083	1.331885307	0.066116493	1.058788113	0.543887479	0.103861063
P15531	Nucleoside diphosphate kinase A	0.339376893	-0.323259972	0.48307736	-0.232699541	0.039948664	-0.876990624
P15586	N-acetylglucosamine-6-sulfatase	0.928996221	0.126735788	0.765290756	-0.099071314	0.180376514	-0.483532014
P15880	40S ribosomal protein S2	0.84427866	-0.013794104	0.111620473	0.172578345	0.780385065	0.039020933
P15927	Replication protein A 32 kDa subunit	0.178657701	-0.680396638	0.966973544	0.159786884	0.96712419	-0.103034098
P16104	Histone H2AX	0.086421896	0.771355867	0.969522198	1.077317839	0.01624554	1.979177351
P16152	Carbonyl reductase [NADPH] 1	0.018843065	2.237184367	0.018337053	2.134678959	0.05414031	1.122323623
P16401	Histone H1.5	0.98046173	0.064070905	0.780894426	-0.030373302	0.321128612	0.626034113
P16403	Histone H1.2	0.294132025	0.26648683	0.642912277	-0.166978006	0.024519759	0.907974682
P16435	NADPH--cytochrome P450 reductase	0.1111433803	-1.988646167	0.198533881	-1.997385959	0.750490498	-0.933480758
P16615	Sarcoplasmic/endoplasmic reticulum calcium ATPase 2	0.115723443	0.935811753	0.281188654	1.236579907	0.139054766	-0.448865987
P16949	Stathmin	0.21053207	-0.31687188	0.602774427	0.135979307	0.030990821	-0.670012784
P17066	Heat shock 70 kDa protein 6	0.174179625	-0.611647358	0.247031278	-0.535287924	0.104283072	-1.306995675
P17174	Aspartate aminotransferase_ cytoplasmic	0.163004947	0.307606164	0.726074702	-0.028812195	0.559124479	-0.075633468
P17661	Desmin	0.621632805	-0.400265105	0.957910708	0.093979653	0.278569909	-0.813219442
P17677	Neuromodulin	0.127328597	-0.862859452	0.130095404	-1.016059908	0.208239335	-0.901801093
P17844	Probable ATP-dependent RNA helicase DDX5	0.084970529	1.097273085	0.558685593	-0.220608819	0.182551711	-0.590048268
P17858	ATP-dependent 6-phosphofructokinase_ liver type	0.10671661	-0.649547896	0.230526093	-0.509162008	0.073925343	-0.612715758
P17948	Vascular endothelial growth factor receptor 1	0.261779874	-3.027755082	0.346637584	3.41122609	0.745425636	1.114857773
P17980	26S proteasome regulatory subunit 6A	0.128903167	-0.441663273	0.700028919	-0.1512583	0.146320569	-0.530719873
P17987	T-complex protein 1 subunit alpha	0.639061029	0.147383426	0.76600479	-0.042522443	0.76588672	0.199502968
P18085	ADP-ribosylation factor 4	0.085273071	-0.39520518	0.010877592	-0.566830239	0.013716417	-0.430138163

P18124	60S ribosomal protein L7	0.346526839	0.350170145	0.289434831	0.189503673	0.837981631	-0.058020913
P18206	Vinculin	0.620215439	-0.068584123	0.030253543	-0.549710899	0.742868718	0.079178527
P18621	60S ribosomal protein L17	0.790026272	0.091240761	0.726463353	0.207177869	0.885579211	-0.076745953
P18669	Phosphoglycerate mutase 1	0.560909785	-0.004230422	0.261138505	-0.301022402	0.00434637	-0.723397938
P18754	Regulator of chromosome condensation	0.698335668	0.254432116	0.615279988	0.213547571	0.755628316	0.306094744
P18859	ATP synthase-coupling factor 6_mitochondrial	0.59372176	0.216132794	0.852073555	0.18297763	0.462974054	-0.436898714
P19022	Cadherin-2	0.249355376	-0.240497943	0.182093657	-0.348905095	0.191922224	-0.678614659
P19338	Nucleolin	0.558706527	0.130171334	0.063927804	0.169945777	0.022093281	0.254066281
P19404	NADH dehydrogenase [ubiquinone] flavoprotein 2_mitochondrial	0.858786991	0.18872577	0.019500453	1.195158653	0.849179057	0.984541617
P20290	Transcription factor BTF3	0.275373498	-0.408924507	0.497375954	-0.293160051	0.675465912	0.37283043
P20338	Ras-related protein Rab-4A	0.966455652	0.647178092	0.022452952	1.658300711	0.35728896	2.564817919
P20340	Ras-related protein Rab-6A	0.027115255	3.261660253	0.083245702	1.65072045	0.130378174	0.365441082
P20591	Interferon-induced GTP-binding protein Mx1	0.148068309	0.352738997	0.04203714	0.658902729	0.08824643	1.129055796
P20618	Proteasome subunit beta type-1	0.356812042	-0.269507132	0.417693871	-0.156445	0.062394659	-1.070370594
P20674	Cytochrome c oxidase subunit 5A_mitochondrial	0.336833103	0.31717011	0.556557084	0.200605764	0.324616293	0.838447804
P20700	Lamin-B1	0.258978724	0.220128664	0.781554145	0.159725194	0.000126893	0.926063968
P20962	Parathymosin	0.483213543	-0.1287478	0.966526264	0.117696748	0.225394768	-1.253674082
P21281	V-type proton ATPase subunit B_brain isoform	0.032833835	-0.993959313	0.187488751	-0.435501285	0.877599534	0.009914749
P21333	Filamin-A	0.112079223	0.176671387	0.432698537	0.391684395	0.222125248	0.167617372
P21796	Voltage-dependent anion-selective channel protein 1	0.1752603	-0.280658465	0.292216029	-0.288675564	0.072311171	-0.551403457
P22061	Protein-L-isoaspartate(D-aspartate) O-methyltransferase	0.672586567	1.729609266	0.066487575	1.503856971	0.366489669	-0.776076137
P22102	Trifunctional purine biosynthetic protein adenosine-3	0.485734756	0.659935194	0.240019592	-0.328353758	0.984355029	0.016398747
P22234	Multifunctional protein ADE2	0.358088796	1.393294429	0.351083081	1.248034359	0.595799705	-0.312018433
P22314	Ubiquitin-like modifier-activating enzyme 1	0.296379861	0.34045103	0.462307667	0.108469027	0.948407612	0.124092457
P22392	Nucleoside diphosphate kinase B	0.401143678	-0.247723751	0.34954991	-0.319299148	0.008761211	-0.953476028

P22492	Histone H1t	0.265230203	0.249699839	0.846509262	0.009609203	0.014314594	0.875159759
P22570	NADPH:adrenodoxin oxidoreductase_mitochondrial	0.43842397	1.413394568	0.07585198	1.411137926	0.442830411	-0.545329115
P22626	Heterogeneous nuclear ribonucleoproteins A2/B1	0.641150896	-0.059930546	0.793715645	0.100475077	0.139422302	0.45941336
P22695	Cytochrome b-c1 complex subunit 2_mitochondrial	0.167654554	-0.649406257	0.513002072	-0.118474579	0.72826527	0.325610505
P23193	Transcription elongation factor A protein 1	0.110329974	3.69004395	0.014940167	3.1836089	0.775768457	0.796197208
P23246	Splicing factor_proline- and glutamine-rich	0.69817242	0.027909207	0.620287327	0.580736015	0.212974271	0.427928266
P23258	Tubulin gamma-1 chain	0.709376598	1.025343262	0.029572172	3.810064216	0.003364291	2.668982074
P23284	Peptidyl-prolyl cis-trans isomerase B	0.715849338	0.131203563	0.673083509	0.102499853	0.389046317	0.159518203
P23381	Tryptophanyl-tRNA ligase_cytoplasmic	0.553806327	0.181611691	0.27615053	1.727493081	0.926211795	-0.8610819
P23396	40S ribosomal protein S3	0.049696282	-0.597581079	0.036643027	-0.491868337	0.085937999	-0.392319476
P23526	Adenosylhomocysteinase	0.25843827	-0.268222685	0.688758985	-0.106562627	0.08189884	-0.586860399
P23528	Cofilin-1	0.064451791	-0.536973228	0.474907358	-0.234350404	0.035368428	-0.691860147
P23588	Eukaryotic translation initiation factor 4B	0.642054577	-0.033565207	0.020498349	-0.721164328	0.04917798	-0.690377552
P23786	Carnitine O-palmitoyltransferase 2_mitochondrial	0.464900861	1.85783288	0.289548607	1.843572136	0.463478569	-0.243206258
P23921	Ribonucleoside-diphosphate reductase large subunit	0.44421564	0.206214604	0.783306271	0.170351096	0.272696069	0.45894856
P24534	Elongation factor 1-beta	0.23337211	-0.329502958	0.385081231	0.201520775	0.211953708	-0.428103247
P24539	ATP synthase F(0) complex subunit B1_mitochondrial	0.036374685	-0.785036503	0.035243445	-0.893494199	0.001389079	-0.457451084
P24666	Low molecular weight phosphotyrosine protein phosphatase	0.071624922	-0.682136952	0.224089102	-0.313829295	0.781110859	-0.029359408
P24752	Acetyl-CoA acetyltransferase_mitochondrial	0.84955757	-0.24297744	0.686784987	0.00908552	0.759633885	-0.164079505
P25205	DNA replication licensing factor MCM3	0.209334929	0.629170812	0.006057241	1.220462453	0.425203878	0.219043255
P25398	40S ribosomal protein S12	0.6394033	-0.167191799	0.824398223	-0.110278663	0.505401771	-0.253479523
P25705	ATP synthase subunit alpha_mitochondrial	0.183697899	0.951829197	0.025285877	0.726136192	0.627180974	0.100361041
P25786	Proteasome subunit alpha type-1	0.227606791	-0.476611015	0.030499837	-0.700188125	0.113711631	-0.573816024
P25787	Proteasome subunit alpha type-2	0.998209383	0.058000373	0.102398654	-0.13976416	0.003384687	-0.415738532

P25788	Proteasome subunit alpha type-3	0.370267926	-0.354225572	0.294030688	-0.173508924	0.101902985	-1.047548978
P25789	Proteasome subunit alpha type-4	0.891168504	0.014517219	0.029476972	0.751402772	0.275073057	1.333750732
P26038	Moesin	0.687564652	-0.049942339	0.012844353	-0.539149195	0.6096863	-0.102942018
P26196	Probable ATP-dependent RNA helicase DDX6	0.298004956	1.965777426	0.058750239	1.595925027	0.634866448	-0.405960218
P26232	Catenin alpha-2	0.214640174	0.950369525	0.143561504	1.193988641	0.902278135	0.190519033
P26368	Splicing factor U2AF 65 kDa subunit	0.32152752	-0.264870334	0.123989173	0.705552143	0.021277734	0.807562203
P26373	60S ribosomal protein L13	0.183400225	-0.518186653	0.370208547	-0.306325569	0.591161501	-0.193459276
P26583	High mobility group protein B2	0.549117224	-0.144518388	0.327500391	-0.378138241	0.146549159	-0.620991533
P26599	Polypyrimidine tract-binding protein 1	0.873517469	0.014202166	0.686727211	0.136364509	0.017191284	0.502237901
P26640	Valine-tRNA ligase	0.600861914	0.146516866	0.690902172	0.907632724	0.341566985	1.093781766
P26641	Elongation factor 1-gamma	0.399225826	-0.130155263	0.835760596	0.040632129	0.559558811	0.068325829
P27348	14-3-3 protein theta	0.655774563	-0.051995003	0.584317134	-0.042174678	0.357812245	-0.262574489
P27635	60S ribosomal protein L10	0.162310535	-0.307381689	0.484823272	-0.124024627	0.469419565	-0.202065985
P27695	DNA-(apurinic or apyrimidinic site) lyase	0.404459816	0.579352388	0.189616409	0.775131606	0.321394676	-0.510184371
P27708	CAD protein	0.642481124	0.122193815	0.888279606	0.012147967	0.91914017	-0.060043863
P27797	Calreticulin	0.521359296	0.206999938	0.89623373	0.082732512	0.024245584	-0.318288721
P27816	Microtubule-associated protein 4	0.555784574	0.085955806	0.967096486	-0.111455635	0.655566065	0.14597551
P27824	Calnexin	0.392400518	0.941118684	0.180277565	0.806020111	0.545646109	-0.185107357
P28066	Proteasome subunit alpha type-5	0.291224116	-0.277126477	0.621735842	-0.074782267	0.05160776	-0.810669954
P28070	Proteasome subunit beta type-4	0.158340103	-0.588172026	0.306874927	-0.436426069	0.708890063	0.027260431
P28072	Proteasome subunit beta type-6	0.844149602	0.003232631	0.011625324	-0.275834166	0.801509523	-0.014928079
P28074	Proteasome subunit beta type-5	0.289146498	-0.298469693	0.049682009	-0.397884994	0.19871208	-0.313037291
P28161	Glutathione S-transferase Mu 2	0.053655763	-2.504076924	0.374086252	-0.2411001	0.384740281	-0.535441465
P28331	NADH-ubiquinone oxidoreductase 75 kDa subunit_mitochondrial	0.505226228	-0.100277123	0.743610084	-0.106404589	0.899944101	-0.044419662
P28799	Progranulin	0.397571739	-0.487707008	0.184053697	-0.932083368	0.404032608	-0.553033416
P28838	Cytosol aminopeptidase	0.930568304	0.085642644	0.374736266	-0.185900763	0.19955112	0.798669689

P29373	Cellular retinoic acid-binding protein 2	0.435374676	-0.191785187	0.224949512	-0.325654447	0.3436673	-0.356576744
P29401	Transketolase	0.80801379	0.062992973	0.303223858	-0.175687661	0.005383326	-0.661358957
P29692	Elongation factor 1-delta	0.879019273	-0.050293846	0.091653072	0.544846932	0.154782968	-0.931282304
P29762	Cellular retinoic acid-binding protein 1	0.027994376	-0.913593741	0.091934255	-0.694864927	0.277636711	-0.459212179
P29966	Myristoylated alanine-rich C-kinase substrate	0.467880761	-0.297206491	0.959678303	0.059023912	0.087016484	-1.375932659
P29992	Guanine nucleotide-binding protein subunit alpha-11	0.734103866	-0.182020777	0.875231295	0.435028495	0.320445931	0.921051938
P30040	Endoplasmic reticulum resident protein 29	0.178641197	1.707431564	0.082355868	1.409287638	0.707171849	-0.328228057
P30041	Peroxiredoxin-6	0.070465927	-0.30749405	0.038731283	-0.61170661	0.5698277	-0.127471135
P30044	Peroxiredoxin-5_mitochondrial	0.20644154	-0.163855409	0.038838477	-0.373400668	0.280311098	-0.177162609
P30046	D-dopachrome decarboxylase	0.183407238	-0.469047065	0.021636754	-0.904095402	0.018500944	-0.842526463
P30048	Thioredoxin-dependent peroxide reductase_mitochondrial	0.754797211	0.042421865	0.255676577	-0.182015502	0.842100562	0.035567847
P30050	60S ribosomal protein L12	0.952167471	-0.059674198	0.674310726	0.020706297	0.365082224	0.422677945
P30084	Enoyl-CoA hydratase_mitochondrial	0.092047006	1.307924426	0.054583126	1.104690882	0.237375723	0.341788114
P30085	UMP-CMP kinase	0.417908641	0.159728457	0.195913233	-0.45007646	0.054754964	0.576537857
P30086	Phosphatidylethanolamine-binding protein 1	0.581213345	-0.064235145	0.641558107	-0.110851202	0.00556211	-0.787676918
P30101	Protein disulfide-isomerase A3	0.012288993	-0.624611774	0.068142386	-0.429483955	0.067522695	-1.042492852
P30153	Serine/threonine-protein phosphatase 2A 65 kDa regulatory subunit A alpha isoform	0.816458213	-0.082570385	0.317427997	0.674573573	0.629980442	-0.159135608
P30154	Serine/threonine-protein phosphatase 2A 65 kDa regulatory subunit A beta isoform	0.517389272	0.69843818	0.161573231	-0.73504046	0.237453395	-0.561228006
P30419	Glycylpeptide N-tetradecanoyltransferase 1	0.019373489	0.663371243	0.007363138	0.87002205	0.018354845	0.573362648
P30613	Pyruvate kinase PKLR	0.877357938	0.67647668	0.370005168	-0.235073079	0.024859517	-0.74440806
P30626	Sorcin	0.011260978	-1.256103424	0.025347782	-0.651129884	0.122087011	-0.500675131
P30837	Aldehyde dehydrogenase X_mitochondrial	0.154655444	-1.293852852	0.582643727	1.717343774	0.101758921	2.054647888
P31150	Rab GDP dissociation inhibitor alpha	0.016438276	-0.361964791	0.102870657	-0.146024857	0.000399062	-0.421473567
P31689	DnaJ homolog subfamily A member 1	0.226162465	-0.248912876	0.17016126	-0.64871084	0.10571433	0.356614208

P31930	Cytochrome b-c1 complex subunit 1_mitochondrial	0.441949385	-0.21087234	0.605667588	-0.152177849	0.484581021	-0.237951839
P31939	Bifunctional purine biosynthesis protein PURH	0.715231498	0.183924668	0.782685607	-0.012691488	0.118632149	-0.1312142
P31942	Heterogeneous nuclear ribonucleoprotein H3	0.303182061	2.079615258	0.103076176	2.401257962	0.668316917	-0.189513598
P31943	Heterogeneous nuclear ribonucleoprotein H	0.454267399	0.8756426	0.105775741	0.757384144	0.58185207	0.011911581
P31946	14-3-3 protein beta/alpha	0.006939269	-0.770800932	0.041413227	-0.347269763	0.020356751	-0.605894617
P31948	Stress-induced-phosphoprotein 1	0.09900932	1.893469178	0.026521489	1.850132552	0.459175597	0.544708198
P32119	Peroxiredoxin-2	0.930190621	0.035423199	0.679899482	-0.093935953	0.028942198	-0.76708273
P32969	60S ribosomal protein L9	0.08376304	-0.626892975	0.13991826	-0.610348537	0.907822546	0.273091986
P33176	Kinesin-1 heavy chain	0.734441839	0.080899929	0.842495296	-0.282466106	0.625477494	0.046540104
P33991	DNA replication licensing factor MCM4	0.76398721	-0.078643651	0.654713461	0.49062191	0.202907891	-0.70057084
P33993	DNA replication licensing factor MCM7	0.325481918	0.202448784	0.555910896	0.523520659	0.343177852	-0.320745567
P34897	Serine hydroxymethyltransferase_ mitochondrial	0.986028806	0.034832523	0.019315452	-0.410725736	0.043983761	1.233607099
P34931	Heat shock 70 kDa protein 1-like	0.11188157	-1.438676229	0.028981858	-2.039279113	0.624511482	-0.578777843
P34932	Heat shock 70 kDa protein 4	0.46199904	1.214369841	0.147409936	1.398392365	0.487921565	-0.415671286
P35221	Catenin alpha-1	0.774338462	0.182084107	0.418790747	0.105552693	0.752295848	-0.04640616
P35222	Catenin beta-1	0.211379247	0.752817811	0.097729057	0.689356385	0.3220391	-0.43949987
P35232	Prohibitin	0.998897991	0.010597106	0.076538895	0.494748558	0.630679307	0.159111865
P35241	Radixin	0.053280668	1.329871403	0.123287976	0.825487199	0.706395097	0.071423221
P35268	60S ribosomal protein L22	0.068264313	-0.498776773	0.315970202	-0.382656028	0.558744803	0.110636262
P35579	Myosin-9	0.520058206	0.204179614	0.457696441	0.259056555	0.286023002	-0.351038807
P35580	Myosin-10	0.125607025	-0.554630035	0.506296093	-0.226360788	0.027345834	-0.745484448
P35606	Coatomer subunit beta'	0.546639182	1.108307023	0.22184305	1.272109089	0.84928075	0.156865243
P35609	Alpha-actinin-2	0.072727943	-0.609555601	0.306991195	-0.3772215	0.660961957	0.014057212
P35611	Alpha-adducin	0.065150794	-1.227985133	0.035957135	-2.039802819	0.599856194	-0.173534223
P35613	Basigin	0.34711944	-0.342306795	0.151181144	-1.163992065	0.718715626	-0.157537129
P35637	RNA-binding protein FUS	0.303731016	-0.253548964	0.32529928	-0.229498623	0.432150883	-0.245281304

P35659	Protein DEK	0.901245871	0.383633399	0.625162006	1.529218774	0.639922492	0.720662469
P35749	Myosin-11	0.749375349	0.111518357	0.021374924	-0.883290766	0.791509858	0.39286976
P35908	Keratin_type II cytoskeletal 2 epidermal	0.574370526	-0.098729375	0.789256063	0.467470913	0.632267509	-0.86516458
P35998	26S proteasome regulatory subunit 7	0.303333429	-0.204191026	0.010588511	-1.019733822	0.42773756	-0.230496854
P36405	ADP-ribosylation factor-like protein 3	0.442031774	-0.160203227	0.082249563	-0.453267175	0.130743209	-0.442452931
P36578	60S ribosomal protein L4	0.346663057	1.292947483	0.189859869	0.795906615	0.924371011	-0.111158423
P36873	Serine/threonine-protein phosphatase PP1-gamma catalytic subunit	0.748880681	0.035618428	0.955100264	0.14763684	0.167915771	0.29972565
P37108	Signal recognition particle 14 kDa protein	0.867332847	-0.00196927	0.19430497	0.09618084	0.01997869	0.18331441
P37235	Hippocalcin-like protein 1	0.255622942	-0.289323954	0.902310874	0.127133684	0.924474565	0.032447996
P37268	Squalene synthase	0.905099328	-0.131963318	0.26600108	0.755771646	0.368710109	-0.823049947
P37802	Transgelin-2	0.010456215	-2.072714829	0.030702055	-1.603721543	0.297156657	-0.697610149
P37837	Transaldolase	0.009532164	-1.047450158	0.586400027	-0.18781477	0.290644567	-0.400914675
P38159	RNA-binding motif protein_X chromosome	0.302745344	1.33700425	0.179071423	1.72416386	0.463469903	-0.362527783
P38405	Guanine nucleotide-binding protein G(olf) subunit alpha	0.83378013	0.118933386	0.592167091	-0.100461952	0.745714958	-0.046095634
P38606	V-type proton ATPase catalytic subunit A	0.790626858	0.423345464	0.169732452	0.424627205	0.175047682	-0.472067469
P38646	Stress-70 protein_mitochondrial	0.921767188	-0.032939687	0.561145296	0.279976857	0.870745383	-0.151167085
P38919	Eukaryotic initiation factor 4A-III	0.945703766	0.165744069	0.748252531	0.856683554	0.000955721	1.552893711
P39019	40S ribosomal protein S19	0.062488636	-0.315577646	0.006626697	-0.453417572	0.066296012	-0.435754522
P39023	60S ribosomal protein L3	0.395435268	-0.173889011	0.092079443	-0.458163609	0.081949228	-0.656512972
P39656	Dolichyl-diphosphooligosaccharide--protein glycosyltransferase 48 kDa subunit	0.008622531	-0.715061548	0.001948463	-0.832785237	0.707527851	0.300361252
P39687	Acidic leucine-rich nuclear phosphoprotein 32 family member A	0.806873707	0.088096601	0.792459533	0.222423334	0.062231113	-0.596704124
P39748	Flap endonuclease 1	0.207828532	-0.429062099	0.331982257	-0.409129724	0.481957261	-0.301488049
P40123	Adenylyl cyclase-associated protein 2	0.056447981	-0.572449226	0.306953835	-0.406154483	0.330468701	-0.336470766
P40227	T-complex protein 1 subunit zeta	0.330301775	1.277985507	0.037788268	1.087111061	0.512793842	-0.218825656
P40925	Malate dehydrogenase_cytoplasmic	0.362718323	-0.199235697	0.849482124	-0.046711213	0.45569038	-0.144150112

P40926	Malate dehydrogenase_mitochondrial	0.753588334	0.187246594	0.485024333	-0.119039605	0.239652429	-0.271383963
P40939	Trifunctional enzyme subunit alpha_mitochondrial	0.652135794	0.676234061	0.087933138	1.225445151	0.000633338	1.292417347
P41091	Eukaryotic translation initiation factor 2 subunit 3	0.101180545	-0.381982791	0.027269719	-1.272872463	0.524389205	-0.14839392
P41219	Peripherin	0.245093637	-0.294618961	0.182637825	-0.169081449	0.191561487	-0.711031233
P41225	Transcription factor SOX-3	0.026361982	-0.644275742	0.753157397	0.392857119	0.114876929	0.603294843
P41250	Glycine-tRNA ligase	0.063389825	0.441131851	0.649259056	0.218002559	0.861155163	-0.106985547
P42166	Lamina-associated polypeptide 2_isoform alpha	0.087514071	-0.445999	0.001836301	-0.37397212	0.072668648	-0.60367882
P42167	Lamina-associated polypeptide 2_isoforms beta/gamma	0.063766156	-0.742765385	0.049894819	-0.627825604	0.092223029	-0.904415787
P42224	Signal transducer and activator of transcription 1-alpha/beta	0.259471779	-0.939098024	0.845107088	4.329912395	0.917697087	6.112031115
P42356	Phosphatidylinositol 4-kinase alpha	0.985070214	0.309266424	0.367051261	-0.360509225	0.175021571	-0.612666491
P42704	Leucine-rich PPR motif-containing protein_mitochondrial	0.531908723	0.40071974	0.493145517	-0.126615238	0.101549404	-0.647751261
P42766	60S ribosomal protein L35	0.754080306	0.053989366	0.876386537	-0.072761248	0.509010294	0.136514537
P42785	Lysosomal Pro-X carboxypeptidase	0.773124499	1.414471391	0.867084211	0.303652445	0.029734825	-1.644417325
P43034	Platelet-activating factor acetylhydrolase IB subunit alpha	0.975015497	0.134573618	0.492943404	-0.132585834	0.388228199	-0.151580075
P43243	Matrin-3	0.07073885	0.380247039	0.356853437	1.34429262	0.000549747	1.431164529
P43487	Ran-specific GTPase-activating protein	0.202169064	-0.4804788	0.430862007	-0.28085292	0.157632601	-1.048063573
P43686	26S proteasome regulatory subunit 6B	0.100577653	-0.680226519	0.877186555	0.075999132	0.580840777	-0.109609397
P45880	Voltage-dependent anion-selective channel protein 2	0.038376312	-2.569480059	0.045767766	-2.753506948	0.091426799	-2.282434957
P45973	Chromobox protein homolog 5	0.854564025	0.603358136	0.726721746	-0.047647496	0.884951353	0.14462172
P45974	Ubiquitin carboxyl-terminal hydrolase 5	0.063015688	1.540642302	0.178609607	1.482733083	0.731441732	0.102899099
P46109	Crk-like protein	0.286658788	1.96598167	0.08652331	-2.115274373	0.173017115	-1.600827637
P46459	Vesicle-fusing ATPase	0.157881668	1.275596931	0.058197731	0.914123601	0.486443477	-0.290093838
P46776	60S ribosomal protein L27a	0.149593952	-0.95493308	0.057027781	-1.685837827	0.69698892	-0.466500261
P46777	60S ribosomal protein L5	0.200273444	-0.303213982	0.202840943	-0.33136127	0.22722063	-0.316413178

P46778	60S ribosomal protein L21	0.220496402	-0.216448612	0.681150914	-0.07977521	0.152871095	-0.305367775
P46779	60S ribosomal protein L28	0.045481605	-0.637795812	0.86002384	-0.087238642	0.102445111	-0.763200849
P46781	40S ribosomal protein S9	0.666999447	0.225647807	0.314210847	0.497324145	0.62450281	-0.229890242
P46782	40S ribosomal protein S5	0.680765526	-0.47298036	0.795863233	-0.43626581	0.284666582	-1.768871888
P46783	40S ribosomal protein S10	0.070134569	-0.32532143	0.627479366	-0.10423326	0.037525473	-0.714297536
P46821	Microtubule-associated protein 1B	0.174167685	-0.313881307	0.891395671	-0.046390097	0.145964791	-0.40065083
P46926	Glucosamine-6-phosphate isomerase 1	0.152786979	-0.456565144	0.151569356	-0.408558884	0.267183235	-0.358804955
P46940	Ras GTPase-activating-like protein IQGAP1	0.174044075	-0.732865688	0.115195312	-0.934707649	0.530289183	-0.357881605
P47755	F-actin-capping protein subunit alpha-2	0.000368672	-0.834009317	0.126359521	-0.634605195	0.006715579	-1.086947299
P47756	F-actin-capping protein subunit beta	0.862437433	0.216463423	0.965391505	0.531970109	0.472965469	0.480353372
P47897	Glutamine--tRNA ligase	0.806283765	0.071268201	0.608359592	-0.101694683	0.528581751	0.202692228
P48047	ATP synthase subunit O_ mitochondrial	0.352175869	-0.162807306	0.826732202	0.160451731	0.831642469	0.014394263
P48147	Prolyl endopeptidase	0.122538669	0.546877081	0.036349323	0.351018272	0.886229718	0.260564103
P48643	T-complex protein 1 subunit epsilon	0.001579839	-0.903762275	0.085049048	-0.398158978	0.482263552	-0.159402783
P48681	Nestin	0.883638442	0.012929511	0.746586236	-0.027756115	0.003673683	0.697073961
P48735	Isocitrate dehydrogenase [NADP]_ mitochondrial	0.185168438	-0.407455437	0.21140459	-0.509641181	0.171318251	-0.632207408
P48739	Phosphatidylinositol transfer protein beta isoform	0.278185987	0.962705454	0.211554145	0.573739099	0.887005832	-0.672512303
P49006	MARCKS-related protein	0.499778336	-0.156642387	0.769778281	-0.093584464	0.179610626	-1.678904636
P49207	60S ribosomal protein L34	0.479910873	-0.412589368	0.04843803	-7.326358181	0.655110792	1.823763469
P49321	Nuclear autoantigenic sperm protein	0.158909479	0.541073126	0.177896647	1.186520488	0.274556415	0.579513124
P49327	Fatty acid synthase	0.718615635	-0.035448098	0.383007316	-0.277348532	0.005907916	-0.816809929
P49368	T-complex protein 1 subunit gamma	0.088388298	-0.329027857	0.669325729	0.05530138	0.483174967	-0.186019997
P49411	Elongation factor Tu_ mitochondrial	0.47055334	0.304679806	0.161130388	0.496361276	0.707408069	0.043472232
P49419	Alpha-amino adipic semialdehyde dehydrogenase	0.224256245	-0.402935118	0.074053333	-0.816605239	0.124021973	-0.73513779
P49448	Glutamate dehydrogenase 2_ mitochondrial	0.280967564	-0.318808737	0.98213684	0.004130566	0.637740265	0.200562443
P49588	Alanine--tRNA ligase_ cytoplasmic	0.184568798	-0.520075346	0.419072514	-0.158829779	0.493837801	0.143009469
P49591	Serine--tRNA ligase_ cytoplasmic	0.209233056	-0.465167159	0.07031728	-0.643609471	0.134574741	-0.848945907

P49720	Proteasome subunit beta type-3	0.662902044	-0.030845261	0.006269807	-0.712378423	0.042373388	-0.800938149
P49721	Proteasome subunit beta type-2	0.38913272	1.509437813	2.0208E-06	2.43126278	0.503834935	-0.160468376
P49736	DNA replication licensing factor MCM2	0.182824137	-2.020704426	0.160612024	-2.378801893	0.311539446	-1.951225987
P49755	Transmembrane emp24 domain-containing protein 10	0.041372846	-0.483554471	0.711932808	0.065253859	0.492165103	-0.16240932
P49773	Histidine triad nucleotide-binding protein 1	0.273460387	0.534646139	0.30371339	1.303013417	0.13544603	-0.887187093
P49840	Glycogen synthase kinase-3 alpha	0.1217284	-1.701949694	0.100785309	-1.550945327	0.017472953	-2.674847954
P49903	Selenide_water dikinase 1	0.049704591	-2.663010724	0.012412912	-4.106231677	0.054366689	-3.398998043
P49915	GMP synthase [glutamine-hydrolyzing]	0.041584617	-0.159654648	0.347217604	-0.105948738	0.076387462	-0.218449741
P50148	Guanine nucleotide-binding protein G(q) subunit alpha	0.094340367	-1.996349925	0.200131468	-1.341745772	0.538582791	0.264749382
P50395	Rab GDP dissociation inhibitor beta	0.020271991	-0.367750276	0.325743598	0.210853923	0.096075787	-0.347781354
P50454	Serpin H1	0.772038264	0.139174883	0.640527584	-0.080343572	0.249661676	0.888140728
P50502	Hsc70-interacting protein	0.002899416	-0.544863128	0.056152258	-0.271442211	0.03358763	-0.661918318
P50897	Palmitoyl-protein thioesterase 1	0.526316522	-0.116133888	0.704331679	0.271781624	0.346532372	-0.229625397
P50914	60S ribosomal protein L14	0.351858466	-0.251199976	0.515508125	-0.193222675	0.63357712	0.253238494
P50990	T-complex protein 1 subunit theta	0.256083419	-0.404290879	0.338825725	0.394802628	0.142118073	-0.622894097
P50991	T-complex protein 1 subunit delta	0.008146963	-0.66373899	0.288698106	-0.352911834	0.130104374	-0.610322965
P51148	Ras-related protein Rab-5C	0.079789732	-0.742867122	0.066569071	-0.379692439	0.034260916	-0.623681496
P51149	Ras-related protein Rab-7a	0.148357891	-0.379291704	0.70282561	0.177702611	0.014458906	0.575292264
P51659	Peroxisomal multifunctional enzyme type 2	0.606881183	0.296965832	0.946936973	0.062352857	0.409364156	-0.241993625
P51805	Plexin-A3	0.002120469	1.245872303	0.103679378	0.394300894	0.861889272	-0.059425978
P51858	Hepatoma-derived growth factor	0.379647689	-0.161584591	0.155016054	0.27960881	0.016446747	-0.383765956
P51991	Heterogeneous nuclear ribonucleoprotein A3	0.209102227	-0.281971418	0.253791997	-0.288988076	0.806984502	0.115865238
P52209	6-phosphogluconate dehydrogenase_decarboxylating	0.695621753	0.450174407	0.43760483	0.62871429	0.291834206	-0.581716836
P52272	Heterogeneous nuclear ribonucleoprotein M	0.849913855	1.034057311	0.161060414	1.14691177	0.621877646	-0.337237967
P52292	Importin subunit alpha-1	0.773521128	1.090263064	0.145427273	0.544684707	0.159958722	-0.973658536

P52306	Rap1 GTPase-GDP dissociation stimulator 1	0.603153009	0.238921076	0.744346454	1.644915	0.245476298	1.059003708
P52565	Rho GDP-dissociation inhibitor 1	0.972955662	0.077167845	0.006760484	-0.562200661	0.161633714	-0.314644215
P52597	Heterogeneous nuclear ribonucleoprotein F	0.207540638	1.509821574	0.100585778	1.48642618	0.931573251	-0.093634908
P52788	Spermine synthase	0.432337491	-0.27840883	0.076381138	-0.813065449	0.515888241	-0.260573262
P52907	F-actin-capping protein subunit alpha-1	0.027292465	-0.667097501	0.619668993	-0.180962465	0.07361528	-0.663420268
P52926	High mobility group protein HMGI-C	0.87031955	0.313765835	0.765976975	0.682749676	0.451437434	0.973854577
P52943	Cysteine-rich protein 2	0.062290919	-2.125951408	0.142383804	-1.755564198	0.285145643	-1.189792005
P53396	ATP-citrate synthase	0.139779448	-0.765667373	0.023652956	-1.310858429	0.043577189	-1.416294222
P53618	Coatomer subunit beta	0.022027345	-0.685367025	0.124232122	-0.417139451	0.008665663	-0.443471594
P53621	Coatomer subunit alpha	0.017752396	-0.405014852	0.069388574	-0.29007914	0.497679151	0.402521477
P53675	Clathrin heavy chain 2	0.391066434	0.961578466	0.121068893	0.658296978	0.551744024	-0.291895724
P53999	Activated RNA polymerase II transcriptional coactivator p15	0.635063182	0.123541804	0.589546597	-0.01910621	0.217430947	-0.595644826
P54136	Arginine--tRNA ligase_ cytoplasmic	0.029878916	-1.216927373	0.890503377	-0.051559241	0.620589159	0.367058578
P54198	Protein HIRA	0.433056926	-0.158492222	0.15507302	-0.743478107	0.039774392	-1.424670728
P54687	Branched-chain-amino-acid aminotransferase_cytosolic	0.322545891	0.181932401	0.284066038	0.334682262	0.451471416	-0.477666845
P54725	UV excision repair protein RAD23 homolog A	0.328608234	3.887336461	0.010513442	3.407678787	0.88984436	1.0223505
P54727	UV excision repair protein RAD23 homolog B	0.725623565	-0.023762168	0.334368924	0.511586482	0.194669375	0.343566974
P54819	Adenylate kinase 2_mitochondrial	0.417865433	-0.212402932	0.061811328	-1.018520116	0.610553892	-0.148648068
P54920	Alpha-soluble NSF attachment protein	0.549676517	1.028406579	0.20668512	1.07381636	0.318892817	-0.744124678
P55010	Eukaryotic translation initiation factor 5	0.25543578	-0.537945253	0.603799009	-0.366050811	0.268082696	-0.63190356
P55060	Exportin-2	0.021665181	-0.391381549	0.79191143	-0.051118639	0.769355091	-0.067789548
P55072	Transitional endoplasmic reticulum ATPase	0.676701428	-0.041052425	0.778353469	-0.014206794	0.898251287	0.060552391
P55145	Mesencephalic astrocyte-derived neurotrophic factor	0.87876207	0.02118846	0.064947001	0.147705643	0.328303716	-0.112728451
P55209	Nucleosome assembly protein 1-like 1	0.292997719	-0.199911399	0.11496937	-0.228110913	0.109025438	-0.442320485
P55289	Cadherin-12	0.273140168	-0.477520756	0.866396165	0.1564296	0.15538948	0.518240701

P55786	Puromycin-sensitive aminopeptidase	0.787208146	-0.092099656	0.268409062	0.555849063	0.138126029	-0.675702874
P55795	Heterogeneous nuclear ribonucleoprotein H2	0.525984644	1.527896207	0.138939773	1.594230227	0.306136858	-0.795174069
P55884	Eukaryotic translation initiation factor 3 subunitB	0.210257199	-0.500921511	0.922436924	-0.047193234	0.702339867	-0.220802028
P56192	Methionine-tRNA ligase_ cytoplasmic	0.82616843	0.020099771	0.846919012	0.228644113	0.019097639	0.69246321
P56537	Eukaryotic translation initiation factor 6	0.135024207	1.362528266	0.330077008	1.382949914	0.579874495	-0.089807319
P56545	C-terminal-binding protein 2	0.322087173	-0.195094508	0.231044658	-0.156570487	0.502875173	-0.144072813
P57721	Poly(rC)-binding protein 3	0.498258468	0.526722502	0.602956067	-0.072131731	0.231876533	-0.391796724
P58546	Myotrophin	0.126242619	-0.664833438	0.167216578	-0.624705255	0.074418705	-0.981278665
P59047	NACHT_ LRR and PYD domains-containing protein 5	0.425948423	-0.245444712	0.117984001	-0.488322528	0.31825962	-0.357038714
P59190	Ras-related protein Rab-15	0.942417446	3.02408819	0.842873566	0.710889252	0.174154492	-2.636952692
P60174	Triosephosphate isomerase	0.814456413	0.32173177	0.848749607	-0.040342947	0.010131365	-0.569116152
P60228	Eukaryotic translation initiation factor 3 subunit E	0.011180767	-1.108876191	0.662495091	0.058781892	0.661249586	0.163970868
P60660	Myosin light polypeptide 6	0.957959874	0.162214324	0.197293258	0.504192815	0.92257987	0.103064563
P60842	Eukaryotic initiation factor 4A-I	0.973337182	0.03603002	0.578198639	0.555677247	0.754190052	-0.288447353
P60866	40S ribosomal protein S20	0.044199505	-0.329692096	0.874049335	-0.032575876	0.289906756	-0.245003946
P60900	Proteasome subunit alpha type-6	0.565717956	0.149270433	0.969681803	0.044771452	0.133933175	-0.590743806
P60953	Cell division control protein 42 homolog	0.601218972	0.041332066	0.85358969	0.0162128	0.920291756	0.015076368
P60981	Destrin	0.75089099	-0.040791589	0.095094606	-0.790277701	0.706012564	-0.083855139
P61006	Ras-related protein Rab-8A	0.981539357	0.024800051	0.358490941	-0.32157604	0.180096025	0.502014106
P61018	Ras-related protein Rab-4B	0.401237686	1.247395486	0.173248949	-1.401793143	0.879356434	0.171757671
P61019	Ras-related protein Rab-2A	0.329444945	1.495663904	0.957677184	-0.117057542	0.061745194	-0.974950769
P61026	Ras-related protein Rab-10	0.053515743	0.104894367	0.126828544	-0.144764077	0.016172664	-0.22817891
P61077	Ubiquitin-conjugating enzyme E2 D3	0.730826806	0.062332546	0.584054598	0.409481328	0.22159258	0.803651712
P61081	NEDD8-conjugating enzyme Ubc12	0.174848639	-0.217943101	0.702331204	0.255880615	0.051287555	0.385544752
P61088	Ubiquitin-conjugating enzyme E2 N	0.001433719	-0.818352406	0.721622956	-0.065093243	0.037190119	-0.491566255
P61158	Actin-related protein 3	0.166444269	-0.704090907	0.157194909	-0.762704694	0.044829946	-1.048519938

P61160	Actin-related protein 2	0.47504418	1.168899637	0.498759473	0.36045976	0.249890293	-0.495453543
P61163	Alpha-centractin	0.005155201	-0.805815215	0.520176419	-0.162768452	0.011583563	-0.678246399
P61204	ADP-ribosylation factor 3	0.087153398	-0.539522215	0.001315	-0.644138816	0.044216915	-0.346607543
P61221	ATP-binding cassette sub-family E member 1	0.786589835	-0.110792829	0.004118285	-1.752597191	0.859083815	0.205004721
P61247	40S ribosomal protein S3a	0.078847857	-0.854142207	0.163811185	-0.818916237	0.067507637	-1.314184736
P61313	60S ribosomal protein L15	0.071957575	-0.716540407	0.11041206	-0.571745794	0.059387826	-0.645450565
P61326	Protein mago nashi homolog	0.831767158	0.000240412	0.825980146	-0.067462774	0.75776794	1.089837948
P61353	60S ribosomal protein L27	0.491951937	0.657762051	0.352756753	0.786515708	0.322838712	-0.606200476
P61586	Transforming protein RhoA	0.774011443	0.017363763	0.842490127	-0.051204189	0.341420551	-0.22643468
P61604	10 kDa heat shock protein_ mitochondrial	0.545818838	0.198822812	0.809318835	0.024137354	0.024760604	-0.737168198
P61758	Prefoldin subunit 3	0.558038159	-0.094541805	0.197614805	-0.357400311	0.174938976	-0.463802305
P61916	NPC intracellular cholesterol transporter 2	0.926917418	-0.03266218	0.621554096	-0.11784293	0.828611953	0.204514049
P61970	Nuclear transport factor 2	0.740152488	1.545456983	0.474386698	1.70813684	0.358609779	-1.10549379
P61978	Heterogeneous nuclear ribonucleoprotein K	0.789869886	0.006307742	0.357278646	0.214301813	0.121357099	0.297873946
P61981	14-3-3 protein gamma	0.034701589	-0.387609686	0.489544262	0.234202176	0.056668723	-0.910584223
P62081	40S ribosomal protein S7	0.268853201	-0.249655073	0.144897739	-0.447139531	0.561861176	0.073973273
P62136	Serine/threonine-protein phosphatase PP1-alpha catalytic subunit	0.91058199	-0.0133797	0.577906259	0.410806435	0.091232889	0.687941268
P62140	Serine/threonine-protein phosphatase PP1-beta catalytic subunit	0.063453748	0.748676669	0.001887718	1.050916746	0.031549692	0.471944629
P62191	26S proteasome regulatory subunit 4	0.783390155	0.304675295	0.00590023	0.683293444	0.007101663	1.335785044
P62195	26S proteasome regulatory subunit 8	0.035283371	-0.782216795	0.166668138	-0.35997427	0.045474556	-0.641585034
P62241	40S ribosomal protein S8	0.297332843	-0.351028599	0.202647568	-0.399068351	0.073897658	-0.969297428
P62244	40S ribosomal protein S15a	0.001879812	-0.549607391	0.143642273	-0.468678905	0.119087211	-0.291531193
P62249	40S ribosomal protein S16	0.077449	-0.519088505	0.090737527	-0.778397166	0.138535255	-0.776420552
P62258	14-3-3 protein epsilon	0.082393123	-0.369406202	0.181744183	-0.485825631	0.011412718	-0.945698731
P62263	40S ribosomal protein S14	0.156779583	-0.314193104	0.198012881	-0.238179217	0.315820927	-0.43908066
P62266	40S ribosomal protein S23	0.004365068	-0.596628941	0.316525304	-0.2153001	0.594090367	-0.123398912

P62269	40S ribosomal protein S18	0.018084982	-0.556210571	0.484113008	-0.204313778	0.918550267	0.064880707
P62277	40S ribosomal protein S13	0.10212563	-0.480324699	0.046717201	-0.557690248	0.171893639	-0.71313976
P62280	40S ribosomal protein S11	0.722392554	-0.047907063	0.328682697	-0.336649782	0.374897861	0.312286247
P62304	Small nuclear ribonucleoprotein E	0.231144524	-0.321975774	0.55570605	0.259261775	0.212298744	-0.547508206
P62310	U6 snRNA-associated Sm-like protein LSm3	0.482273458	3.421375756	0.73225848	1.703713463	0.795274316	-0.531517391
P62314	Small nuclear ribonucleoprotein Sm D1	0.750693718	0.155454761	0.802097731	0.444142855	0.249791598	0.766166174
P62316	Small nuclear ribonucleoprotein Sm D2	0.431389129	-0.127622181	0.377925713	-0.090623022	0.988607691	0.005816976
P62318	Small nuclear ribonucleoprotein Sm D3	0.224109078	-0.304294093	0.907807069	0.08472968	0.159640484	-0.763600363
P62328	Thymosin beta-4	0.278013091	-0.60689395	0.14121412	-0.924863924	0.160744444	-1.255257683
P62333	26S proteasome regulatory subunit 10B	0.005259601	-1.100338225	0.311466236	-0.355121383	0.040732125	-0.664085691
P62424	60S ribosomal protein L7a	0.557439889	-0.170875515	0.27560438	-0.336410311	0.438426582	-0.268080562
P62495	Eukaryotic peptide chain release factor subunit 1	0.416401824	-0.168015389	0.006795739	-0.546014774	0.128286585	-0.8077127
P62701	40S ribosomal protein S4_X isoform	0.876075132	0.259202861	0.313575036	-0.124026843	0.057795803	-0.364806651
P62714	Serine/threonine-protein phosphatase 2A catalytic subunit beta isoform	0.74931	0.351738293	0.943203001	-0.009914602	0.992453001	1.217238028
P62750	60S ribosomal protein L23a	0.457523241	0.117310323	0.461364506	-0.169293532	0.490225494	0.150789045
P62753	40S ribosomal protein S6	0.026734042	-0.732374143	0.110482678	-0.505569802	0.16212134	-0.47147033
P62805	Histone H4	0.819188751	0.112676247	0.550079416	-0.015356688	0.372172068	0.461157583
P62820	Ras-related protein Rab-1A	0.036241157	-0.451252926	0.812336469	-0.058001355	0.066608284	-0.41356848
P62826	GTP-binding nuclear protein Ran	0.689184417	-0.080026885	0.925452319	0.019657788	0.053308468	-0.854101798
P62829	60S ribosomal protein L23	0.911758585	0.018162318	0.830608712	0.096596015	0.930713328	0.111902995
P62841	40S ribosomal protein S15	0.210839572	-0.579686726	0.372604139	0.180468166	0.254227983	0.335095434
P62851	40S ribosomal protein S25	0.943528541	0.077093233	0.052091507	0.480053507	0.731799383	-0.0547643
P62873	Guanine nucleotide-binding protein G(I)/G(S)/G(T) subunit beta-1	0.560429093	0.537268632	0.007227229	0.545168372	0.714582166	0.059254741
P62879	Guanine nucleotide-binding protein G(I)/G(S)/G(T) subunit beta-2	0.077452466	-0.251992247	0.189698866	-0.207275365	0.227989222	-0.308453224
P62888	60S ribosomal protein L30	0.048060784	-0.272479108	0.002609792	-0.474536945	0.033112654	-0.455538437

P62899	60S ribosomal protein L31	0.440193493	1.768336028	0.32024845	1.8845117	0.885829745	-0.344898638
P62906	60S ribosomal protein L10a	0.134500762	-0.861364891	0.102863791	-1.199988122	0.091149255	-1.22729676
P62910	60S ribosomal protein L32	0.136997174	-0.357634362	0.199069055	-0.433513649	0.185392906	0.28800509
P62913	60S ribosomal protein L11	0.230683412	-0.307992616	0.247873589	-0.313061158	0.077255642	-0.623935513
P62917	60S ribosomal protein L8	0.04714747	-0.416247086	0.09630751	-0.422889062	0.992912339	0.079816279
P62937	Peptidyl-prolyl cis-trans isomerase A	0.282579534	-0.198559745	0.583299934	0.06851699	0.210845922	-0.234959809
P62979	Ubiquitin-40S ribosomal protein S27a	0.74308743	-0.032364005	0.999124735	0.029538965	0.189139109	-0.642369455
P62995	Transformer-2 protein homolog beta	0.901697722	2.068483385	0.012146338	1.523906579	0.254687354	-0.09709522
P63000	Ras-related C3 botulinum toxin substrate 1	0.730322988	-0.068923026	0.498572282	-0.150035205	0.082084705	-0.388173675
P63010	AP-2 complex subunit beta	0.704770833	1.317156486	0.565040699	0.67812742	0.190598774	0.603639336
P63096	Guanine nucleotide-binding protein G(i) subunit alpha-1	0.814705941	0.673894278	0.152977932	1.814319762	0.183944552	2.79178094
P63104	14-3-3 protein zeta/delta	0.206658699	-0.186364324	0.004378156	0.551704534	0.042474194	-0.332657645
P63151	Serine/threonine-protein phosphatase 2A 55 kDa regulatory subunit B alpha isoform	0.935134811	1.438907455	0.057463158	1.661976488	0.178250775	-0.659642765
P63162	Small nuclear ribonucleoprotein-associated protein N	0.053404142	-0.521998521	0.098407522	-0.721649734	0.126374333	-0.688180474
P63167	Dynein light chain 1_ cytoplasmic	0.820965554	0.23153624	0.753660699	0.152926294	0.086108908	-1.233981896
P63241	Eukaryotic translation initiation factor 5A-1	0.158355903	-0.415748318	0.397403501	-0.231675273	0.166074488	-0.704785783
P63244	Receptor of activated protein C kinase 1	0.577379141	-0.325064133	0.705662014	-0.277982866	0.210861961	-0.732219943
P63261	Actin_ cytoplasmic 2	0.289425643	-0.388712857	0.895702027	-0.069237469	0.273361524	-0.432665706
P67809	Nuclease-sensitive element-binding protein 1	0.002172653	-0.96746368	0.024933061	-0.662438484	0.245414992	-0.455513255
P67936	Tropomyosin alpha-4 chain	0.362267372	-0.257479778	0.00919078	-0.777161607	0.013927392	-0.931959336
P68032	Actin_ alpha cardiac muscle 1	0.034706286	-0.743174693	0.776645728	-0.057888692	0.094611097	-0.34570298
P68036	Ubiquitin-conjugating enzyme E2 L3	0.014114846	-0.572459774	0.87072038	-0.069888964	0.163999247	-0.414723114
P68366	Tubulin alpha-4A chain	0.600473768	-0.022546157	0.432459782	-0.719959075	0.405655165	-0.725823994
P68371	Tubulin beta-4B chain	0.008698427	-0.668624915	0.097977715	-0.178149592	0.080477992	-0.505018147
P68402	Platelet-activating factor acetylhydrolase IB subunit beta	0.685177294	-0.00625403	0.299448256	-0.297877536	0.673279866	0.117481425

P68431	Histone H3.1	0.297455378	0.417619159	0.878256786	0.014011475	0.164017344	0.732739732
P78310	Coxsackievirus and adenovirus receptor	0.281480952	-0.540109209	0.217576616	-0.736941883	0.167456979	-0.702191142
P78344	Eukaryotic translation initiation factor 4 gamma 2	0.292958787	-0.721744587	0.102093192	-2.236495571	0.144655186	-1.82328732
P78347	General transcription factor II-I	0.234699345	0.572468317	0.302313423	0.195358531	0.061476313	-0.790796826
P78371	T-complex protein 1 subunit beta	0.385825888	-0.231179141	0.563084226	0.090992325	0.483362542	-0.229963196
P78386	Keratin_type II cuticular Hb5	0.253203889	-0.260704711	0.256457235	-0.162452767	0.371877477	0.175879074
P78527	DNA-dependent protein kinase catalytic subunit	0.754715631	0.890473208	0.055039227	0.612733002	0.261014544	-0.24660185
P78559	Microtubule-associated protein 1A	0.894371554	1.131747692	0.143884027	1.466785214	0.033852054	-1.798062901
P80192	Mitogen-activated protein kinase kinase kinase 9	0.286141324	-0.818482298	0.631678266	0.62691917	0.57807896	-0.668131596
P80404	4-aminobutyrate aminotransferase_mitochondrial	0.211045865	1.837439872	0.169140075	1.519030217	0.492215998	0.168845695
P80723	Brain acid soluble protein 1	0.915606473	0.290564382	0.017056081	-0.45296265	0.107010089	-0.963924706
P83731	60S ribosomal protein L24	0.082803839	-0.748450031	0.292654692	-0.421921429	0.229976997	-0.686051639
P83916	Chromobox protein homolog 1	0.053936757	0.677641509	0.476967678	0.658243368	0.010889318	0.743441393
P84085	ADP-ribosylation factor 5	0.115798401	-0.395196859	0.022713787	-0.423466456	0.009721331	-0.488258685
P84098	60S ribosomal protein L19	0.23017383	-0.24911683	0.039593498	-0.415466209	0.339173693	-0.235656127
P84103	Serine/arginine-rich splicing factor 3	0.383990743	-0.118564441	0.04014367	-0.501365016	0.470445337	-0.157097727
P84243	Histone H3.3	0.191880102	0.425589386	0.776825337	0.033029901	0.265381998	0.606715192
Q00005	Serine/threonine-protein phosphatase 2A 55 kDa regulatory subunit B beta isoform	0.011804805	-1.455970216	0.077770361	-1.137115286	0.017912257	-1.091206897
Q00169	Phosphatidylinositol transfer protein alpha isoform	0.357006791	1.51440195	0.064614363	1.320524705	0.382690489	-0.590687861
Q00325	Phosphate carrier protein_mitochondrial	0.306702912	0.474019761	0.644956356	0.455180214	0.90913556	-0.030587826
Q00610	Clathrin heavy chain 1	0.308187523	0.405301336	0.253220455	0.387722737	0.330891254	0.370110986
Q00688	Peptidyl-prolyl cis-trans isomerase FKBP3	0.456269093	-0.268947908	0.412037101	-0.274808152	0.159761821	-0.736358192
Q00839	Heterogeneous nuclear ribonucleoprotein U	0.313631536	1.266494602	0.136577354	1.269643639	0.887937692	-0.072839866
Q01082	Spectrin beta chain_non-erythrocytic 1	0.275137127	0.2722464	0.686459764	-0.138525956	0.962338569	0.034180747
Q01105	Protein SET	0.491178414	-0.116600691	0.039650503	-0.584894503	0.019224698	-0.714488311
Q01130	Serine/arginine-rich splicing factor 2	0.095549802	-0.833285486	0.052572583	-1.009086206	0.309402467	-0.507926713

Q01469	Fatty acid-binding protein 5	0.627504033	-0.234607547	0.660373994	0.122521731	0.121816502	-0.773787699
Q01518	Adenylyl cyclase-associated protein 1	0.105586119	-0.381316087	0.614621666	-0.165270448	0.076740234	-0.586523632
Q01546	Keratin_ type II cytoskeletal 2 oral	0.570270786	0.212468744	0.69373238	-0.063301905	0.299421893	-0.40484751
Q01581	Hydroxymethylglutaryl-CoA synthase_cytoplasmic	0.334778249	0.303351038	0.272591963	0.730587786	0.168898735	0.764409399
Q01844	RNA-binding protein EWS	0.531806378	1.456068533	0.150934262	1.528153611	0.353118962	-0.844386794
Q02218	2-oxoglutarate dehydrogenase_ mitochondrial	0.195875784	-0.477621445	0.493251431	0.318473637	0.53326536	0.813074385
Q02224	Centromere-associated protein E	0.063688388	-2.133004694	0.068823723	-2.526423778	0.388503674	-0.66152893
Q02543	60S ribosomal protein L18a	0.088805715	-0.441861407	0.026620229	-0.557400189	0.253925668	-0.401014161
Q02790	Peptidyl-prolyl cis-trans isomerase FKBP4	0.300753972	-0.462201505	0.03732404	-0.455501414	0.044805232	-1.486412571
Q02878	60S ribosomal protein L6	0.423063721	-0.121000407	0.979207932	0.001571561	0.688530865	-0.06075303
Q03113	Guanine nucleotide-binding protein subunit alpha-12	0.445163729	0.290688039	0.053458287	0.930738417	0.797825895	0.295217657
Q03181	Peroxisome proliferator-activated receptor delta	0.521869184	2.17118198	0.091212687	1.833128469	0.361794277	-0.41291415
Q03252	Lamin-B2	0.099641502	-0.800003233	0.389594637	-0.231493456	0.628722385	-0.000406981
Q04721	Neurogenic locus notch homolog protein 2	0.69158257	0.292344077	0.030466041	0.537859677	0.091333219	-1.463768852
Q04760	Lactoylglutathione lyase	0.084911092	-0.574199733	0.022181188	-0.578409136	0.011754308	-0.804685585
Q04837	Single-stranded DNA-binding protein_mitochondrial	0.992334191	0.031550932	0.49421329	-0.256074621	0.353176982	0.65826384
Q04917	14-3-3 protein eta	0.03316905	-1.209859971	0.477276546	-0.32958271	0.075107372	-1.062815593
Q05639	Elongation factor 1-alpha 2	0.00241307	-0.724344298	0.136550692	-0.39948926	0.075010659	-0.378267776
Q06830	Peroxiredoxin-1	0.36955352	-0.192268892	0.395070677	-0.204026963	0.017917278	-0.693026394
Q07020	60S ribosomal protein L18	0.298158299	-0.354526068	0.405342822	-0.268700438	0.416954424	0.862202055
Q07065	Cytoskeleton-associated protein 4	0.025512851	1.665300382	0.164256264	0.98743192	0.688294491	-0.256415484
Q07666	KH domain-containing_ RNA-binding_ signal transduction-associated protein 1	0.693207754	-0.042193943	0.211534908	0.514167393	0.00011207	0.802573718
Q07812	Apoptosis regulator BAX	0.049851905	-1.646507439	0.210325874	-0.657089182	0.152766145	-1.197593292
Q07955	Serine/arginine-rich splicing factor 1	0.515244744	-0.106816646	0.688835657	-0.027527091	0.013216807	0.407320822
Q08170	Serine/arginine-rich splicing factor 4	0.347466779	-0.179779744	0.043925423	-0.332576502	0.384057895	-0.306906228

Q08211	ATP-dependent RNA helicase A	0.194709163	0.703395204	0.188407954	0.661322306	0.420196006	0.2159014
Q08289	Voltage-dependent L-type calcium channel subunit beta-2	0.582650186	-0.31934017	0.24799655	-1.39145754	0.017775457	-3.536755015
Q08623	Pseudouridine-5'-phosphatase	0.461709671	1.623084463	0.822212047	-0.025619132	0.144419368	1.673714213
Q08945	FACT complex subunit SSRP1	0.661594921	0.005847594	0.367393032	-0.304103645	0.0465838	0.92991141
Q09028	Histone-binding protein RBBP4	0.447239928	-0.235179372	0.970119332	-0.013514288	0.246248933	-0.398960801
Q0P6D6	Coiled-coil domain-containing protein 15	0.236082188	0.986556421	0.003937532	1.813174048	0.478323914	2.226900353
Q12765	Secernin-1	0.369287843	0.1759362	0.517640374	-0.314707052	0.929405634	-0.006429679
Q12840	Kinesin heavy chain isoform 5A	0.88094337	0.013976613	0.483846278	-0.209427513	0.134088675	-0.368178301
Q12888	TP53-binding protein 1	0.719743781	0.400492753	0.918791029	0.164771497	0.876428102	-0.081683363
Q12905	Interleukin enhancer-binding factor 2	0.285555147	-0.265101016	0.02579624	-0.66422119	0.560419955	-0.095498272
Q12906	Interleukin enhancer-binding factor 3	0.468749047	0.441464032	0.596356549	0.865229723	0.466048084	-0.360951531
Q12931	Heat shock protein 75 kDa_mitochondrial	0.385531142	0.491130681	0.013048693	1.411803494	0.43589751	0.804067138
Q13011	Delta(3_5)-Delta(2_4)-dienoyl-CoA isomerase_mitochondrial	0.375781413	2.400861939	0.265937546	-0.466147679	0.096973496	-1.523072608
Q13126	S-methyl-5'-thioadenosine phosphorylase	0.73847975	0.141620792	0.76752542	-0.153356989	0.107992071	1.770378841
Q13148	TAR DNA-binding protein 43	0.93032635	0.480854039	0.813602708	0.085236059	0.292994847	-0.404852882
Q13151	Heterogeneous nuclear ribonucleoprotein A0	0.575930866	-0.13233988	0.261344455	-0.405723488	0.56076583	0.409839969
Q13162	Peroxiredoxin-4	0.326683794	0.552242698	0.80091908	0.164683149	0.556915914	-0.139561665
Q13177	Serine/threonine-protein kinase PAK 2	0.117929832	-0.743555669	0.000476139	-1.471605244	0.001566909	-1.037698349
Q13185	Chromobox protein homolog 3	0.448826658	0.221533154	0.062424599	0.48807995	0.001907597	0.669722857
Q13200	26S proteasome non-ATPase regulatory subunit 2	0.337531492	-0.307820707	0.442291795	-0.294036853	0.035617344	-0.74761876
Q13242	Serine/arginine-rich splicing factor 9	0.070595317	-1.165544869	0.050546856	-1.16552932	0.849949519	0.383680849
Q13247	Serine/arginine-rich splicing factor 6	0.3234821	0.536633188	0.349463876	0.346154112	0.374188973	-0.365983525
Q13263	Transcription intermediary factor 1-beta	0.455375683	1.122703298	0.089824047	1.195702475	0.810053939	-0.462168727
Q13283	Ras GTPase-activating protein-binding protein 1	0.513442068	0.12701204	6.31644E-07	-1.324862379	0.037802569	-1.451172187
Q13310	Polyadenylate-binding protein 4	0.076585743	-0.310592616	0.056688472	-0.418264996	0.28227797	-0.513695793
Q13347	Eukaryotic translation initiation factor 3 subunit I	0.124716698	-0.617616757	0.073343005	-0.309811137	0.122264845	-1.006380592

Q13363	C-terminal-binding protein 1	0.668371657	0.065612443	0.83451866	0.513741161	0.2267952	0.921885512
Q13367	AP-3 complex subunit beta-2	0.633847649	0.26884455	0.062190457	-2.467650092	0.38979065	-1.149598762
Q13404	Ubiquitin-conjugating enzyme E2 variant 1	0.235455663	-0.266539601	0.351756887	-0.262001943	0.884716866	0.137255092
Q13409	Cytoplasmic dynein 1 intermediate chain 2	0.097212125	-2.162022232	0.231387322	-1.915837516	0.889554654	-0.705099451
Q13435	Splicing factor 3B subunit 2	0.42084902	0.333485575	0.415948064	0.809897451	0.604804153	-0.450811573
Q13509	Tubulin beta-3 chain	0.005767034	-0.565311629	0.726789815	-0.04503515	0.049738327	-0.755890051
Q13535	Serine/threonine-protein kinase ATR	0.196678524	-0.730489559	0.993684693	0.673465889	0.248305872	-0.467050054
Q13561	Dynactin subunit 2	0.118268546	-0.573734446	0.990287241	-0.079161316	0.682155435	-0.164679298
Q13564	NEDD8-activating enzyme E1 regulatory subunit	0.088513076	-1.591238844	0.010915222	-0.750902686	0.157435426	-0.395310131
Q13642	Four and a half LIM domains protein 1	0.339363744	-0.246321822	0.042668088	-0.61019689	0.121948319	-0.479639206
Q13813	Spectrin alpha chain_non-erythrocytic 1	0.048408108	0.478153193	0.45432943	0.393725282	0.101806419	-0.749381049
Q13838	Spliceosome RNA helicase DDX39B	0.160297669	1.118841658	0.160542657	0.875307462	0.639682849	0.114691335
Q13867	Bleomycin hydrolase	0.783642246	0.422143367	0.074459482	0.755883943	0.030859527	-0.821456898
Q13885	Tubulin beta-2A chain	0.000861475	-0.550905538	0.097955049	-0.10371836	0.030567164	-0.535923359
Q13907	Isopentenyl-diphosphate Delta-isomerase 1	0.699852564	0.807015889	0.517918354	-0.031880868	0.906160312	-0.025383389
Q14019	Coactosin-like protein	0.077738238	0.278487912	0.526416696	0.219574718	0.388091992	0.22070786
Q14103	Heterogeneous nuclear ribonucleoprotein D0	0.519963512	-0.121456753	0.805205941	0.351998623	0.567532324	0.554164114
Q14141	Septin-6	0.349103197	-0.222452279	0.978671344	0.008812151	0.499314918	0.156106883
Q14152	Eukaryotic translation initiation factor 3 subunitA	0.498501055	1.517010804	0.142584971	1.698922886	0.264787731	-0.891033817
Q14194	Dihydropyrimidinase-related protein 1	0.31311968	0.570419765	0.085678047	0.848713801	0.157159488	-0.470343909
Q14195	Dihydropyrimidinase-related protein 3	0.0380704	-0.61518338	0.27545107	-0.161488265	0.021655955	-0.785792268
Q14204	Cytoplasmic dynein 1 heavy chain 1	0.082301083	1.236657515	0.040075988	1.183311007	0.098576599	0.777707512
Q14240	Eukaryotic initiation factor 4A-II	0.001169146	-1.173468384	0.000263869	-1.119830288	0.00286638	-0.968027192
Q14257	Reticulocalbin-2	0.32800658	-0.530278333	0.851032549	1.014870309	0.102333938	1.305408369
Q14344	Guanine nucleotide-binding protein subunit alpha-13	0.903719919	-0.0704763	0.143576983	-0.777537912	0.941782594	0.307115096
Q14376	UDP-glucose 4-epimerase	0.610179789	0.972998119	0.454957644	-0.175742973	0.775351648	0.697964525

Q14444	Caprin-1	0.402757169	0.264314641	0.626607705	-0.110821383	0.15645376	-0.367294018
Q14498	RNA-binding protein 39	0.73225502	0.062626556	0.802715841	0.141176259	0.426416969	-0.247140784
Q14566	DNA replication licensing factor MCM6	0.000119542	-0.762944681	0.107414041	-0.273474216	0.996091146	0.038846845
Q14568	Heat shock protein HSP 90-alpha A2	0.245905237	0.930393919	0.933044113	-0.034371238	0.767675248	0.30838853
Q14571	Inositol 1_4_5-trisphosphate receptor type 2	0.076344366	1.274927759	0.476717848	0.470941436	0.717797541	0.454660079
Q14643	Inositol 1_4_5-trisphosphate receptor type 1	0.282113684	0.186613109	0.815835054	-0.028660646	0.915770122	0.18837105
Q14669	E3 ubiquitin-protein ligase TRIP12	0.491168124	0.585547355	0.708796029	0.071690822	0.244310604	-0.422892993
Q14697	Neutral alpha-glucosidase AB	0.052459025	-0.646480898	0.231962112	-0.574389438	0.089615839	-0.922284499
Q14738	Serine/threonine-protein phosphatase 2A 56 kDa regulatory subunit delta isoform	0.716599496	-0.236371478	0.057550158	2.161916986	0.781446516	-0.153894717
Q14839	Chromodomain-helicase-DNA-binding protein 4	0.571683591	0.263199701	0.38497999	1.15819397	0.022250204	1.539373871
Q14964	Ras-related protein Rab-39A	0.066756769	1.318108894	0.001023061	1.802782325	0.031831142	0.811349105
Q14974	Importin subunit beta-1	0.847444246	0.043882622	0.355935207	0.329123056	0.20603356	0.474891593
Q14980	Nuclear mitotic apparatus protein 1	0.964760019	0.022015905	0.644169618	-0.228550133	0.949258983	0.087862848
Q15019	Septin-2	0.470683743	-0.118442379	0.63584177	-0.092552211	0.498163213	-0.157760951
Q15029	116 kDa U5 small nuclear ribonucleoprotein component	0.65054663	1.404822229	0.572882643	2.023363972	0.202713259	1.825153874
Q15056	Eukaryotic translation initiation factor 4H	0.497326988	1.095403223	0.220658598	0.627694364	0.219515598	-0.30824149
Q15084	Protein disulfide-isomerase A6	0.723356793	-0.019299433	0.001618048	-0.443221879	0.340615521	-0.089429396
Q15102	Platelet-activating factor acetylhydrolase IB subunit gamma	0.392124715	-0.201563311	0.001568588	-0.547942904	0.053631005	-0.935529907
Q15165	Serum paraoxonase/arylesterase 2	0.698072259	0.225433389	0.279219809	-0.205350853	0.090418191	-1.058148358
Q15181	Inorganic pyrophosphatase	0.195999356	-0.3292679	0.049379062	-0.657003572	0.03867669	-0.853452598
Q15233	Non-POU domain-containing octamer-binding protein	0.18180437	-0.271981903	0.535382741	0.143116376	0.380701903	-0.182714007
Q15257	Serine/threonine-protein phosphatase 2A activator	0.171265682	-0.227180841	8.46896E-06	0.433808343	0.742225023	0.248444079
Q15274	Nicotinate-nucleotide pyrophosphorylase [carboxylating]	0.526009293	-0.224379775	0.782396966	0.481162305	0.792401649	0.016591204
Q15286	Ras-related protein Rab-35	0.26504809	0.697155173	0.597812179	0.149528924	0.00054702	1.003537521

Q15293	Reticulocalbin-1	0.034237026	-0.745476081	0.022371017	-0.467512703	0.033366478	-0.442747535
Q15349	Ribosomal protein S6 kinase alpha-2	0.695694736	0.242101727	0.672905596	0.093889495	0.390209107	0.362498639
Q15365	Poly(rC)-binding protein 1	0.133244587	-0.350241845	0.486140833	-0.077106506	0.260927367	-0.174389057
Q15366	Poly(rC)-binding protein 2	0.027964036	-0.489386274	0.880313543	0.011705681	0.101248121	-0.448275781
Q15369	Elongin-C	0.805001856	-0.203617233	0.598630746	0.070751657	0.496495506	-0.445804492
Q15393	Splicing factor 3B subunit 3	0.345202314	1.563134575	0.056338809	1.468101433	0.509705775	-0.538847859
Q15417	Calponin-3	0.00212582	-0.865035505	0.067466008	-0.515805575	0.346786488	-0.272271288
Q15424	Scaffold attachment factor B1	0.561988617	-0.121487653	0.685524562	0.092827323	0.130960205	0.303156046
Q15435	Protein phosphatase 1 regulatory subunit 7	0.412627828	1.037732418	0.114847763	1.136895683	0.412609663	-0.532950788
Q15436	Protein transport protein Sec23A	0.204853312	-0.215733546	0.02060946	2.012166426	0.004992419	-3.909541476
Q15459	Splicing factor 3A subunit 1	0.75285435	-0.14512464	0.131317222	0.518236058	0.148597971	0.694541488
Q15637	Splicing factor 1	0.383244822	-0.336808913	0.302977955	0.251398142	0.195397913	-0.612716533
Q15643	Thyroid receptor-interacting protein 11	0.119457975	1.903848224	0.107303642	1.461447183	0.826924009	-0.059923371
Q15691	Microtubule-associated protein RP/EB family member 1	0.962836529	0.100701929	0.807506977	-0.054125236	0.090117674	-0.546891104
Q15717	ELAV-like protein 1	0.440545951	-0.106514699	0.241619816	0.280557422	0.730414333	0.093280695
Q15771	Ras-related protein Rab-30	0.534474675	0.289537293	0.373746899	-0.307960801	0.633158111	0.129622119
Q15772	Striated muscle preferentially expressed protein kinase	0.373977522	1.383226527	0.803963276	0.435032581	0.079842681	1.302211702
Q16181	Septin-7	0.333883691	-0.234288655	0.016294114	-1.01240617	0.015249559	-1.402286375
Q16352	Alpha-internexin	0.091673667	0.238587746	0.008022979	0.956992483	0.259746929	0.378476648
Q16543	Hsp90 co-chaperone Cdc37	0.004626572	-0.623024206	0.559015541	-0.147710304	0.6499083	-0.119854357
Q16555	Dihydropyrimidinase-related protein 2	0.627278357	0.403336708	0.072709207	0.545574828	0.20412436	-0.643779651
Q16576	Histone-binding protein RBBP7	0.827980279	0.35290998	0.365122379	0.179941477	0.193098704	-0.393997676
Q16629	Serine/arginine-rich splicing factor 7	0.337175244	-0.131651929	0.003285198	-0.942156141	0.524800641	-0.101215423
Q16630	Cleavage and polyadenylation specificity factor subunit 6	0.642708718	-0.093975988	0.853586032	0.453134424	0.241816503	0.429232872
Q16643	Drebrin	0.26907684	-0.209638835	0.514910877	0.073276519	0.466219832	0.135820509

Q16658	Fascin	0.239190735	-0.69088363	0.712774534	-0.341658143	0.164066293	-1.011544707
Q16659	Mitogen-activated protein kinase 6	0.612613572	2.164973914	0.119003479	1.840368332	0.409990788	-0.372746525
Q16695	Histone H3.1t	0.303329872	0.279755273	0.629638561	-0.081120137	0.539679321	0.608489041
Q16698	2_4-dienoyl-CoA reductase_mitochondrial	0.332513595	1.480115926	0.01470649	1.178553712	0.974373707	0.306541621
Q16787	Laminin subunit alpha-3	0.010198361	1.528171212	0.142706225	0.569592638	0.429533513	-0.242147202
Q16836	Hydroxyacyl-coenzyme A dehydrogenase_mitochondrial	0.253039021	2.679779794	0.167927255	2.173745176	0.584272807	0.055013975
Q16881	Thioredoxin reductase 1_cytoplasmic	0.543601412	-0.575169915	0.628032449	-0.275158079	0.596550145	0.198082998
Q16891	MICOS complex subunit MIC60	0.80305244	0.39099444	0.215916414	-0.43931378	0.700874663	0.061226883
Q1KMD3	Heterogeneous nuclear ribonucleoprotein U-like protein 2	0.531310278	-0.141103302	0.265827732	-0.235770609	0.898058724	0.095664573
Q32P51	Heterogeneous nuclear ribonucleoprotein A1-like2	0.182454397	-0.535070751	0.001804999	-0.628644203	0.131783962	-0.832843421
Q3MII6	TBC1 domain family member 25	0.212948065	0.97093721	0.150360424	0.464574737	0.507450589	0.145972739
Q3SXM5	Inactive hydroxysteroid dehydrogenase-like protein 1	0.862890406	0.185663502	0.175695063	0.911433947	0.265146563	0.609027784
Q3V6T2	Girdin	0.937010092	-0.516171705	0.166418699	0.726560854	0.138703479	1.375764179
Q3ZCM7	Tubulin beta-8 chain	0.008516377	-0.611393093	0.39531293	0.252538858	0.41298849	-0.236768124
Q4VXU2	Polyadenylate-binding protein 1-like	0.207111009	-0.378242396	0.45572594	-0.15340299	0.405053588	0.149360172
Q52LJ0	Protein FAM98B	0.539261775	0.871892639	0.827980465	1.250893355	0.249314776	-0.767382317
Q53GQ0	Very-long-chain 3-oxoacyl-CoA reductase	0.320346966	-0.263773083	0.013955827	-0.913344428	0.876387496	0.073069436
Q53GS9	U4/U6.U5 tri-snRNP-associated protein 2	0.336938939	0.279106643	0.2309889	1.98458679	0.001221402	1.860684869
Q562R1	Beta-actin-like protein 2	0.295092481	-0.24587912	0.188982118	-0.313064139	0.259475851	-0.557001384
Q58FF3	Putative endoplasmin-like protein	0.407301832	1.803907447	0.104282415	1.95040081	0.800773969	-0.198131998
Q58FF6	Putative heat shock protein HSP 90-beta 4	0.078956807	1.056798706	0.464517159	0.800427241	0.841335055	-0.057566412
Q58FF8	Putative heat shock protein HSP 90-beta 2	0.091398205	-0.296085648	0.302570557	-0.22707166	0.704660835	-0.084384776
Q58FG0	Putative heat shock protein HSP 90-alpha A5	0.352597497	0.879054291	0.129646059	0.988123062	0.31140056	-0.462031699
Q58FG1	Putative heat shock protein HSP 90-alpha A4	0.482031271	1.501420224	0.134793714	1.436317705	0.806810767	-0.107167186
Q5JQF8	Polyadenylate-binding protein 1-like 2	0.107013533	-0.61750173	0.163174301	-0.392211483	0.119802922	-0.547338791

Q5JWF2	Guanine nucleotide-binding protein G(s) subunit alpha isoforms XLas	0.682513951	0.708559951	0.755787475	0.27276658	0.325899698	-0.446267119
Q5JXB2	Putative ubiquitin-conjugating enzyme E2 N-like	0.122306393	1.126147508	0.287344024	1.237167192	0.891591917	-0.017138298
Q5QNW6	Histone H2B type 2-F	0.498532674	0.145459264	0.68441513	-0.023428795	0.0472519	0.816721712
Q5SSJ5	Heterochromatin protein 1-binding protein 3	0.189781225	-0.618434615	0.255978465	-0.621254271	0.941144845	-0.068627247
Q5T7P8	Synaptotagmin-6	0.246158953	0.389504952	0.549371187	0.725778416	0.765650201	0.954384883
Q5TCY1	Tau-tubulin kinase 1	0.283206666	1.041043721	0.038683672	0.853358457	0.389101016	-0.210284841
Q5VTE0	Putative elongation factor 1-alpha-like 3	0.10600562	-0.389651463	0.933431979	-0.012200278	0.600763003	-0.130328732
Q5VZ46	Uncharacterized protein KIAA1614	0.548365871	1.964907121	0.243070374	1.860105506	0.598729211	-0.6827287
Q5XKE5	Keratin_type II cytoskeletal 79	0.830577257	0.029343506	0.00541869	-0.422259657	0.419782391	-0.140349474
Q66LE6	Serine/threonine-protein phosphatase 2A 55 kDa regulatory subunit B delta isoform	0.04716728	-1.175147662	0.027652044	-1.342061034	0.023431157	-1.636409309
Q674X7	Kazrin	0.356407819	-0.357655905	0.293371962	-0.404841575	0.15566185	-0.859800118
Q687X5	Metalloreductase STEAP4	0.015845315	2.535197484	0.145578796	-1.058726078	0.123041604	-1.139182892
Q68CZ1	Protein fantom	0.321501707	-0.767827706	0.486036841	-0.545589588	0.309173272	-0.949599448
Q6BDS2	UHRF1-binding protein 1	0.789508841	0.13909599	0.668104823	0.828998377	0.667052797	0.592558416
Q6DKJ4	Nucleoredoxin	0.546264504	0.353785687	0.738059292	-0.03240043	0.543894953	0.210618005
Q6FI81	Anamorsin	0.128062445	1.615351681	0.12368343	1.822579278	0.317256476	0.873645278
Q6NUK1	Calcium-binding mitochondrial carrier protein SCaMC-1	0.441591237	-0.147627411	0.159598286	-0.860562344	0.693919744	-0.194185319
Q6NW34	Nucleolus and neural progenitor protein	0.95332878	-1.096302725	0.294409088	-0.136052833	0.341257377	-0.015638716
Q6P2Q9	Pre-mRNA-processing-splicing factor 8	0.392368042	0.252578808	0.550197714	0.262832293	0.268863164	-0.355618839
Q6S8J3	POTE ankyrin domain family member E	0.457825303	1.063337538	0.665003672	0.249438676	0.43046856	-0.640321952
Q6SA08	Testis-specific serine/threonine-protein kinase 4	0.504365607	2.254149374	0.072474494	1.893480906	0.318957071	-0.338506399
Q6UB98	Ankyrin repeat domain-containing protein 12	0.301128858	-0.793139033	0.012637365	-2.49281758	0.685078183	-0.397606186
Q6UB99	Ankyrin repeat domain-containing protein 11	0.342748509	-0.302711319	0.02665524	-0.384551853	0.166384584	-0.553672374
Q6ZU80	Centrosomal protein of 128 kDa	0.824959474	1.203535376	0.020043673	0.997076276	0.173825995	-0.540527772
Q71DI3	Histone H3.2	0.397591646	0.411330394	0.659669564	-0.215504437	0.287167593	0.538294717

Q71UI9	Histone H2A.V	0.588489327	0.081257661	0.296099754	-0.540293975	0.208870442	0.827757305
Q7KZF4	Staphylococcal nuclease domain-containing protein 1	0.802698775	0.092560025	0.157233809	-0.479086176	0.527123497	-0.115522903
Q7L1Q6	Basic leucine zipper and W2 domain-containing protein 1	0.469451766	-0.145198173	0.020166161	0.3726835	0.165998548	0.441735402
Q7RTS9	Dymeclin	0.65532183	-0.016881766	0.500558274	-0.164223494	0.772786179	-0.075988367
Q7Z5M8	Protein ABHD12B	0.602130303	1.667830786	0.055599724	1.743421912	0.627585955	-0.404393015
Q7Z6Z7	E3 ubiquitin-protein ligase HUWE1	0.309025251	-0.271412453	0.817530006	0.222909278	0.354995641	0.325832008
Q7Z7K6	Centromere protein V	0.525212079	0.499096365	0.402024971	0.453217606	0.94954398	0.256935264
Q86SE5	RNA-binding Raly-like protein	0.319947083	1.663231915	0.134745749	1.073572899	0.626317632	-0.307291508
Q86UQ4	ATP-binding cassette sub-family A member 13	0.480266116	0.386294177	0.116861533	0.585395141	0.409940318	-0.224820202
Q86V81	THO complex subunit 4	0.638244356	0.231242992	0.228761246	-0.258955329	0.90047984	0.176045728
Q86VP6	Cullin-associated NEDD8-dissociated protein 1	0.03034812	-0.680058627	0.105645785	-0.406538998	0.039007952	-0.990255076
Q86W56	Poly(ADP-ribose) glycohydrolase	0.903271702	0.264615797	0.763165975	-0.021990265	0.368405802	-0.354461032
Q86XT4	E3 ubiquitin-protein ligase TRIM50	0.114445156	1.580915057	0.009779447	1.797421886	0.552033707	-0.405389099
Q86YS6	Ras-related protein Rab-43	0.784396723	2.280995909	0.198942114	2.90776132	0.239354376	1.736916084
Q8IUE6	Histone H2A type 2-B	0.094905624	0.802559562	0.930328129	1.257218011	0.019192218	2.087860446
Q8IV08	Phospholipase D3	0.599998352	-0.160517027	0.915053849	0.030285685	0.171667688	-1.310469699
Q8IVF4	Dynein heavy chain 10_axonemal	0.113067625	5.700098707	0.025524642	4.763244996	0.662159517	0.414374215
Q8IWJ2	GRIP and coiled-coil domain-containing protein2	0.083182295	-0.809185641	0.003541573	-1.75565548	0.231273801	-1.32040207
Q8IWS0	PHD finger protein 6	0.621268856	0.036073859	0.498102957	-0.227438323	0.725197109	-0.01837704
Q8IWZ3	Ankyrin repeat and KH domain-containing protein 1	0.252176868	0.673920555	0.560140376	-0.247981536	0.785013291	0.177781645
Q8IX03	Protein KIBRA	0.694565751	0.680885524	0.642602876	0.770492413	0.510667705	1.161790811
Q8IYB3	Serine/arginine repetitive matrix protein 1	0.799318996	-0.015834825	0.972802913	0.354053936	0.016235522	0.934582366
Q8IYT4	Katanin p60 ATPase-containing subunit A-like 2	0.069137028	-0.580401973	0.08175328	-1.040194923	0.574214515	-0.070383327
Q8IZS8	Voltage-dependent calcium channel subunit alpha-2/delta-3	0.194575489	-0.477071482	0.023137499	-0.355975263	0.362597637	-0.378944314

Q8IZU2	WD repeat-containing protein 17	0.65516568	-0.052953978	0.007626911	0.445716948	0.351877151	-0.287190984
Q8N0Y7	Probable phosphoglycerate mutase 4	0.028108668	-1.087114346	0.002274361	-1.337008514	0.050748207	-0.895228652
Q8N158	Glypican-2	0.181239481	0.387000864	0.863845122	0.342985208	0.16045295	0.79386627
Q8N163	Cell cycle and apoptosis regulator protein 2	0.117777348	-0.537857243	0.203005376	-0.445922694	0.079813926	-0.94822574
Q8N1F7	Nuclear pore complex protein Nup93	0.785279628	1.382778088	0.055577158	-1.563742386	0.428850389	-0.24599524
Q8N1G4	Leucine-rich repeat-containing protein 47	0.488286659	0.571894727	0.921741857	0.101874693	0.523592385	-0.171600583
Q8N1N4	Keratin_type II cytoskeletal 78	0.33968785	-0.16215474	0.197247094	-0.921227799	0.771657259	0.546169544
Q8N3P4	Vacuolar protein sorting-associated protein 8 homolog	0.485905337	1.28338358	0.143800764	1.501978314	0.41675577	-0.818622245
Q8N568	Serine/threonine-protein kinase DCLK2	0.089565847	-0.679068261	0.396184474	-0.294883331	0.058403692	-0.616155436
Q8N7X1	RNA-binding motif protein_X-linked-like-3	0.023671211	2.103898624	0.010758022	3.356993739	0.421150687	-0.806401028
Q8N859	Zinc finger protein 713	0.925303375	1.801523744	0.042695734	1.600171903	0.23119212	-0.404541745
Q8NBS9	Thioredoxin domain-containing protein 5	0.166607828	-0.410444081	0.649581258	-0.059768537	0.836894265	0.927284967
Q8NC51	Plasminogen activator inhibitor 1 RNA-binding protein	0.248544063	-0.211251264	0.266069149	-0.307136156	0.612304074	-0.069036735
Q8NCI6	Beta-galactosidase-1-like protein 3	0.17033627	-1.873384663	0.333831933	0.219444162	0.920169755	-0.420984643
Q8NCM8	Cytoplasmic dynein 2 heavy chain 1	0.157939762	1.627876295	0.106434186	1.441655736	0.830170079	-0.278621276
Q8TAA3	Proteasome subunit alpha-type 8	0.607426696	-0.17308057	0.049179137	-1.063000845	0.045257981	-0.964305027
Q8TD26	Chromodomain-helicase-DNA-binding protein 6	0.292759114	1.413868751	0.362099821	1.598027461	0.349886395	-0.815931393
Q8TD43	Transient receptor potential cation channel subfamily M member 4	0.62474134	0.51330757	0.236682604	-0.543115037	0.101046978	-0.87000762
Q8TD57	Dynein heavy chain 3_axonemal	0.754884003	0.036563462	0.574264774	-0.114781545	0.117866047	-0.391067033
Q8TEX9	Importin-4	0.174303616	1.27790029	0.023178472	0.823780144	0.484550514	0.215369461
Q8WUD1	Ras-related protein Rab-2B	0.213162899	1.343725486	0.261342016	1.007823811	0.457087924	-0.312900404
Q8WUM4	Programmed cell death 6-interacting protein	0.523785889	-0.028663688	0.039147733	-0.954101567	0.125816246	0.615675421
Q8WVV9	Heterogeneous nuclear ribonucleoprotein L-like	0.372498212	0.189804529	0.914477754	-0.087423018	0.226609674	-0.491147454
Q8WWY3	U4/U6 small nuclear ribonucleoprotein Prp31	0.505614904	0.469892866	0.77487965	-0.068681313	0.033905824	1.223151371
Q8WXF1	Paraspeckle component 1	0.08765324	-0.445477084	0.598431519	-0.052812267	0.164929162	0.287979073

Q92499	ATP-dependent RNA helicase DDX1	0.182399081	-0.613883767	0.783108194	-0.266780813	0.395969907	-0.507819712
Q92522	Histone H1x	0.026199396	-0.326237782	0.283532651	-0.239736601	0.386599052	0.429595056
Q92598	Heat shock protein 105 kDa	0.236187099	1.626857632	4.06729E-06	1.325891443	0.726701352	0.148010246
Q92618	Zinc finger protein 516	0.644404682	0.402624877	0.010674175	0.652230109	0.284693887	-0.406875331
Q92622	Run domain Beclin-1-interacting and cysteine-rich domain-containing protein	0.562406171	0.994856494	0.945980714	1.464097736	0.466619788	-0.297869586
Q92688	Acidic leucine-rich nuclear phosphoprotein 32 family member B	0.079216947	-0.823303981	0.082039913	-0.6676449	0.016116308	-1.030122613
Q92769	Histone deacetylase 2	0.964785892	0.344519572	0.019801513	0.546743902	0.613055583	0.116616726
Q92841	Probable ATP-dependent RNA helicase DDX17	0.602351149	0.901109127	0.03187544	0.997487131	0.554451414	-0.151512673
Q92928	Putative Ras-related protein Rab-1C	0.308464355	0.917872118	0.325425802	1.052993358	0.757946582	-0.202869786
Q92930	Ras-related protein Rab-8B	0.797876505	0.775539706	0.481037047	0.178868507	0.22323278	-0.568019272
Q92945	Far upstream element-binding protein 2	0.852980584	0.197163167	0.327815201	0.711371412	0.25794498	-0.433738061
Q92973	Transportin-1	0.503757212	-0.119078887	0.181206631	-0.190569144	0.593076441	-0.089849864
Q93009	Ubiquitin carboxyl-terminal hydrolase 7	0.375405034	1.861047053	0.063948881	1.521092089	0.46079654	0.110617877
Q96A08	Histone H2B type 1-A	0.123929028	1.372741505	0.815986513	0.159871679	0.388696216	2.660334233
Q96AB3	Isochorismatase domain-containing protein 2	0.084974478	-0.824975844	0.127603009	-1.02641693	0.437969976	0.933310544
Q96AE4	Far upstream element-binding protein 1	0.511829	-0.288354195	0.670044661	0.207792533	0.41918253	-0.392151843
Q96AG4	Leucine-rich repeat-containing protein 59	0.509521747	-0.3270164	0.239359544	0.459899935	0.035667971	0.878944556
Q96AY3	Peptidyl-prolyl cis-trans isomerase FKBP10	0.356949218	1.167183426	0.20067445	1.285762869	0.478246321	-0.475104712
Q96B54	Zinc finger protein 428	0.047824375	-1.483222077	0.021197949	-1.560153709	0.167633551	-0.985414575
Q96BM9	ADP-ribosylation factor-like protein 8A	0.115906246	0.294781706	0.530119725	-0.13189207	0.053570087	0.647915102
Q96C45	Serine/threonine-protein kinase ULK4	0.226417746	-1.321096318	0.86772734	1.400377771	0.228561121	1.478959349
Q96CS3	FAS-associated factor 2	0.071998806	-0.662013107	0.749009137	0.004833825	0.11553278	1.53833963
Q96DA2	Ras-related protein Rab-39B	0.556838511	0.909225099	0.206726968	1.102932823	0.385024641	-0.489570811
Q96DH6	RNA-binding protein Musashi homolog 2	0.16490241	0.913966976	0.075808263	0.699368264	0.011786541	1.602573324
Q96E39	RNA binding motif protein_X-linked-like-1	0.280582381	1.398110619	0.221460601	1.791137442	0.604685116	-0.440796846
Q96FW1	Ubiquitin thioesterase OTUB1	0.387122078	0.215617004	0.310659537	-0.25076735	0.099068335	-0.407863508

Q96G03	Phosphoglucomutase-2	0.436850457	-0.191481906	0.382593055	-0.225501585	0.092391187	-0.340723951
Q96HN2	Adenosylhomocysteinase 3	0.152849017	-0.813527107	0.185609184	-1.2271838	0.294780504	-0.848633457
Q96I24	Far upstream element-binding protein 3	0.155957076	0.991097066	0.009678282	1.151275278	0.196949457	0.93618526
Q96KP4	Cytosolic non-specific dipeptidase	0.567376675	0.35912788	0.224627448	0.558827541	0.507422768	-0.229181529
Q96L21	60S ribosomal protein L10-like	0.162310543	-0.307381689	0.484823258	-0.124024627	0.469419823	-0.202065985
Q96M83	Coiled-coil domain-containing protein 7	0.905855867	-0.167211218	0.315386438	-1.09452111	0.60536876	0.679403806
Q96N46	Tetratricopeptide repeat protein 14	0.943348064	3.274832599	0.758184651	0.675391389	0.239867501	0.29258584
Q96P70	Importin-9	0.522992142	-0.118459516	0.597650247	-0.108058195	0.123728447	-0.309146773
Q96PK6	RNA-binding protein 14	0.053277715	-1.362581351	0.643773419	0.918842994	0.033878783	1.661201296
Q96Q15	Serine/threonine-protein kinase SMG1	0.22920432	0.303517403	0.975317862	-5.01646662	0.25630967	-1.227606794
Q96QK1	Vacuolar protein sorting-associated protein 35	0.15455664	-1.786065081	0.129547026	-1.74782876	0.676731001	-0.609326985
Q96SI9	Spermatid perinuclear RNA-binding protein	0.611545397	-0.076147638	0.024452497	-0.387145173	0.705460606	1.203039102
Q99426	Tubulin-folding cofactor B	1.14E-05	-1.957730425	0.017100155	-1.06725589	0.419112322	-0.165093989
Q99436	Proteasome subunit beta type-7	0.398068012	0.890385611	0.886540333	0.136439195	0.203767958	0.457849186
Q99439	Calponin-2	0.517814582	-0.202587738	0.034235652	0.821026504	0.024543128	0.938512823
Q99460	26S proteasome non-ATPase regulatory subunit 1	0.050288069	-0.597868258	0.623597723	-0.163079396	0.203310318	-0.562502343
Q99497	Protein/nucleic acid deglycase DJ-1	0.857262992	0.086578665	0.404545607	-0.218138867	0.008605901	-1.354530638
Q99536	Synaptic vesicle membrane protein VAT-1 homolog	0.06646699	-0.832475812	0.976465824	-0.058923992	0.129206198	-0.850242657
Q99623	Prohibitin-2	0.718994874	-0.045665045	0.570223787	-0.082368897	0.966909146	0.092830743
Q99706	Killer cell immunoglobulin-like receptor 2DL4	0.088067581	-0.347681693	0.515628927	-0.164336993	0.05356432	-0.76793198
Q99714	3-hydroxyacyl-CoA dehydrogenase type-2	0.038693032	-0.951390143	0.954906915	0.14197831	0.911406609	-0.152657437
Q99729	Heterogeneous nuclear ribonucleoprotein A/B	0.678185163	-0.063633687	0.020829907	-0.59915863	0.707037574	0.358469492
Q99733	Nucleosome assembly protein 1-like 4	0.1370412	-1.342338531	0.228733664	-0.494880226	0.219321649	-1.556471465
Q99798	Aconitate hydratase_ mitochondrial	0.959874246	-0.041126753	0.510531394	0.140343719	0.869169113	0.0623954
Q99829	Copine-1	0.893074079	0.186444551	0.526727214	-0.348948902	0.706949225	0.489033614
Q99832	T-complex protein 1 subunit eta	0.063426053	0.151323068	0.027326595	0.295285131	0.245531438	0.241891437

Q99873	Protein arginine N-methyltransferase 1	0.241614502	1.244670551	0.05429506	0.926130891	0.362881693	-0.362984279
Q99878	Histone H2A type 1-J	0.045363762	0.501401498	0.139946532	-0.796243963	0.041344863	1.128016034
Q9BPU6	Dihydropyrimidinase-related protein 5	0.105289834	-0.507881239	0.182765163	0.579422352	0.055842271	-0.241137109
Q9BPW8	Protein NipSnap homolog 1	0.054593377	-0.441606346	0.170766912	-0.265771182	0.60831645	-0.091849029
Q9BQE3	Tubulin alpha-1C chain	0.005867681	-0.732665138	0.04385125	-0.348553753	0.103121038	-0.752480943
Q9BRA2	Thioredoxin domain-containing protein 17	0.008196948	-0.765880273	0.072037655	-0.619835859	0.018388716	-0.421601597
Q9BRL6	Serine/arginine-rich splicing factor 8	0.258777829	-0.401739396	0.216905526	-0.314175585	0.121731532	-0.957906288
Q9BRX8	Peroxiredoxin-like 2A	0.26656646	-0.394469915	0.421139428	0.214165061	0.674661069	0.042335995
Q9BT78	COP9 signalosome complex subunit 4	0.10125972	-8.084353369	0.242952749	-6.292815029	0.666614947	-1.776647809
Q9BTT0	Acidic leucine-rich nuclear phosphoprotein 32 family member E	0.211595196	-0.598612621	0.466270402	0.142617989	0.590860309	-0.227766924
Q9BU02	Thiamine-triphosphatase	0.338141528	1.375155615	0.097520893	1.113416402	0.862995759	-0.254435758
Q9BUF5	Tubulin beta-6 chain	0.067719889	-0.632770414	0.038700724	-0.180830734	0.139391616	-0.908186095
Q9BUJ2	Heterogeneous nuclear ribonucleoprotein U-like protein 1	0.83391518	-0.008829725	0.742904224	0.24332407	0.962892458	0.255079495
Q9BV20	Methylthioribose-1-phosphate isomerase	0.357024944	-0.603292166	0.906801325	0.065819768	0.126034871	-1.197981499
Q9BVA1	Tubulin beta-2B chain	0.000483082	-0.477951227	0.639104941	-0.047756705	0.006772938	-0.397224598
Q9BWD1	Acetyl-CoA acetyltransferase_cytosolic	0.375732718	0.955710457	0.734741498	0.026363372	0.374017691	0.333743595
Q9BWF3	RNA-binding protein 4	0.546126638	0.456348405	0.423151784	0.21452171	0.292326114	0.300964144
Q9BX97	Plasmalemma vesicle-associated protein	0.043195357	0.676581873	0.983901495	0.156080808	0.458265923	0.443855993
Q9BXF9	Tekton-3	0.851874684	0.706515437	0.685587999	-0.072124605	0.004416096	5.176035497
Q9BXK5	Bcl-2-like protein 13	0.000751862	-1.333122574	0.002851746	-1.179216027	0.179317094	-0.696702977
Q9BXS5	AP-1 complex subunit mu-1	0.325921913	-0.247894042	0.660629817	-0.091868437	0.840783484	0.388378358
Q9BXT5	Testis-expressed protein 15	0.802971338	-0.041613877	0.344572205	0.14555753	0.005259313	1.390999429
Q9BY65	Nasopharyngeal carcinoma down-regulated gene protein 1	0.441040602	-1.718957794	0.288421181	-1.934374987	0.624869142	-0.458414679
Q9BYD6	39S ribosomal protein L1_mitochondrial	0.450093266	-2.058004892	0.995053309	2.426883155	0.255241572	0.893763399
Q9BYZ2	L-lactate dehydrogenase A-like 6B	0.030741752	-2.008218021	0.294383548	-0.066307967	0.470387461	0.530259756

Q9BZ23	Pantothenate kinase 2_mitochondrial	0.335890112	1.635159754	0.241046579	1.487187565	0.336058601	-0.647864067
Q9BZZ5	Apoptosis inhibitor 5	0.368879934	0.313761521	0.128958442	1.258702621	0.001216336	0.822157972
Q9C005	Protein dpy-30 homolog	0.287219183	0.551433077	0.074175986	1.711497654	0.625973685	0.368317014
Q9C0A0	Contactin-associated protein-like 4	0.180027613	0.942769227	0.383579333	0.854701846	0.256723607	-0.540286022
Q9C0K3	Actin-related protein 3C	0.217510044	-1.281518573	0.586811337	0.012792292	0.545352267	1.145774858
Q9GZT4	Serine racemase	0.248550884	-0.477030609	0.177569371	-0.920849201	0.188843895	1.678111831
Q9GZV4	Eukaryotic translation initiation factor 5A-2	0.105108857	-0.631414484	0.137029039	-0.542499647	0.175156711	-0.754939381
Q9H0A0	RNA cytidine acetyltransferase	0.358593844	0.491418998	0.233621146	1.347180661	0.042203986	2.20446288
Q9H0C2	ADP/ATP translocase 4	0.017397947	-0.870734199	0.253460174	-0.529434715	0.330673684	-0.402311633
Q9H0W9	Ester hydrolase C11orf54	0.52579195	-0.083968777	0.03687764	-0.610717378	0.067973227	-1.14564584
Q9H173	Nucleotide exchange factor SIL1	0.197636387	-0.389933468	0.001038274	-1.399822883	0.202875762	-0.664304703
Q9H1E3	Nuclear ubiquitous casein and cyclin-dependent kinase substrate 1	0.982310548	1.587044231	0.092300675	0.644717653	0.642221934	0.755329902
Q9H2C0	Gigaxonin	0.338734326	-0.395846811	0.332967373	-0.601241949	0.260028484	-0.894502411
Q9H2M9	Rab3 GTPase-activating protein non-catalytic subunit	0.000458848	1.612321966	0.271144362	0.309538408	0.929042169	0.054731999
Q9H361	Polyadenylate-binding protein 3	0.134782633	0.465621387	0.085825574	0.548252755	0.874444927	0.376634843
Q9H3N1	Thioredoxin-related transmembrane protein 1	0.295767586	-0.284859456	0.425105898	-0.172212489	0.945420751	0.074240814
Q9H4B7	Tubulin beta-1 chain	0.276993926	-0.277007807	0.723201524	0.12901084	0.60771795	-0.071195634
Q9H6N6	Putative uncharacterized protein MYH16	0.659967487	0.970643015	0.076610258	-0.543367664	0.236621292	0.402037116
Q9H6T0	Epithelial splicing regulatory protein 2	0.320114854	2.069133427	0.043566757	1.701687407	0.715257865	-0.46843676
Q9H9I0	Jupiter microtubule associated homolog 2	0.460730233	2.150017529	3.90942E-05	3.204299023	0.025381532	-0.928574105
Q9H9A6	Leucine-rich repeat-containing protein 40	0.11265429	1.754336338	0.066642278	1.781078596	0.426538583	-0.638301516
Q9H9B4	Sideroflexin-1	0.478899269	0.213852224	0.092505513	0.355819642	0.012381917	0.82403012
Q9H9Z2	Protein lin-28 homolog A	0.11414362	0.7055314	0.872894478	0.232582371	0.451028882	-0.32986545
Q9HAV0	Guanine nucleotide-binding protein subunit beta-4	0.404395769	1.030158981	0.000569962	1.155668114	0.239513431	0.240596811
Q9HB71	Calcyclin-binding protein	0.074225332	-0.835531215	0.053755853	-0.76701482	0.255909115	-0.503592455

Q9HC77	Centromere protein J	0.221474598	-0.310940059	0.677659041	0.063279315	0.299389219	0.536014339
Q9HCD6	Protein TANC2	0.005012944	0.360874269	0.0577723	0.179196062	0.529398161	-0.130336299
Q9HCM2	Plexin-A4	0.483076116	1.46853472	0.241237463	1.554053024	0.531827217	-0.649614715
Q9HDC9	Adipocyte plasma membrane-associated protein	0.291041063	1.259866934	0.239127235	0.735888526	0.540817424	0.085329598
Q9NPH2	Inositol-3-phosphate synthase 1	0.500734214	-0.167411386	0.606660125	0.1541154	0.791646272	-0.022417001
Q9NQ75	Cas scaffolding protein family member 4	0.230649151	1.48185739	0.053005285	1.343145448	0.533664228	-0.368336159
Q9NQA5	Transient receptor potential cation channel subfamily V member 5	0.666972597	0.761418341	0.972279556	0.269514004	0.690988432	-0.26217016
Q9NQC3	Reticulon-4	0.0355858	-0.764550377	0.576837154	-0.08981359	0.135740189	-0.281071391
Q9NQG5	Regulation of nuclear pre-mRNA domain-containing protein 1B	0.228081804	-0.538826971	0.841876804	0.34197831	0.16637016	0.535911698
Q9NR22	Protein arginine N-methyltransferase 8	0.502027964	1.185915935	0.999306383	2.586210169	0.18597622	1.597491033
Q9NR30	Nucleolar RNA helicase 2	0.098293218	-0.846156074	0.456652219	-0.261406399	0.265983789	1.194401995
Q9NR31	GTP-binding protein SAR1a	0.024383132	-0.772309495	0.256448867	-0.351686282	0.915885798	0.062705472
Q9NRF8	CTP synthase 2	0.925306216	0.114094459	0.614744087	2.787789313	0.032817935	-1.889111437
Q9NSB2	Keratin_type II cuticular Hb4	0.118288627	-0.462856879	0.109135505	-0.2971376	0.354230486	1.247916781
Q9NSD9	Phenylalanine-tRNA ligase beta subunit	0.899138771	-0.008689124	0.382195581	-0.267665319	0.130879263	0.278481585
Q9NTK5	Obg-like ATPase 1	0.407874011	0.456774456	0.973493382	0.213049306	0.119768752	1.073786217
Q9NVA2	Septin-11	0.517637934	-0.257732047	0.20587281	-0.83006354	0.252250487	-0.850236971
Q9NVJ2	ADP-ribosylation factor-like protein 8B	0.608204084	0.66064194	0.030046889	1.939043444	0.944215669	0.447188211
Q9NWL6	Asparagine synthetase domain-containing protein 1	0.739132435	0.974257881	0.876184304	2.619325622	0.088756364	2.961959902
Q9NYK6	Protein EURL homolog	0.168689809	-0.616726718	0.067539657	-0.433252275	0.319826268	0.317094101
Q9NYL9	Tropomodulin-3	0.284814104	-3.482840317	0.687217421	0.30757088	0.993463764	0.031263215
Q9NYU2	UDP-glucose:glycoprotein glucosyltransferase 1	0.222314316	1.032638633	0.259132084	0.717171359	0.888614076	-0.110895231
Q9NZI8	Insulin-like growth factor 2 mRNA-binding protein 1	0.371680147	0.767189178	0.968787843	0.061215074	0.72506992	-0.058969675
Q9NZL9	Methionine adenosyltransferase 2 subunit beta	0.450785278	-0.195423351	0.33474699	-0.273241657	0.130404463	-0.603374546

Q9P035	Very-long-chain (3R)-3-hydroxyacyl-CoA dehydratase 3	0.975155522	-0.071405681	0.047669512	0.602851102	0.652604279	-0.169574864
Q9P0L0	Vesicle-associated membrane protein-associated protein A	0.74629671	-0.079159346	0.868969648	-0.052632685	0.116100298	-0.385556054
Q9P0M6	Core histone macro-H2A.2	0.760314054	-0.080793468	0.321952028	-0.660310427	0.114450427	1.3663423
Q9P1Z9	Coiled-coil domain-containing protein 180	0.685061367	0.380832588	0.742091263	0.232005047	0.024783534	1.55158776
Q9P258	Protein RCC2	0.107871297	-0.757533633	0.049483288	-0.766984634	0.029725072	-0.621180829
Q9P2D1	Chromodomain-helicase-DNA-binding protein 7	0.56723988	1.555054399	0.02619861	1.719188034	0.751679814	-0.289220399
Q9P2J5	Leucine-tRNA ligase_cytoplasmic	0.031894221	0.865507781	0.905863257	0.425808073	0.896960728	0.792639079
Q9UBB4	Ataxin-10	0.45380967	2.644019358	0.000354668	2.669367092	0.873068641	0.106792478
Q9UBE0	SUMO-activating enzyme subunit 1	0.196710389	-0.404578898	0.42537465	-0.219057418	0.286915481	0.411861368
Q9UBF2	Coatomer subunit gamma-2	0.308009652	-0.252910642	0.540095706	0.243872739	0.546035177	-0.10043666
Q9UBQ7	Glyoxylate reductase/hydroxypyruvate reductase	0.472514363	1.165319105	0.258479804	1.178330532	0.264224598	-0.920150524
Q9UBT2	SUMO-activating enzyme subunit 2	0.32384351	-0.299539095	0.420558441	0.327299132	0.193523953	-0.322839273
Q9UHB9	Signal recognition particle subunit SRP68	0.549916618	0.396925797	0.4170686	-0.242590292	0.895209757	0.353245171
Q9UHD8	Septin-9	0.601342552	0.287490732	0.100353911	-0.456012302	0.227038488	-0.309091334
Q9UHV9	Prefoldin subunit 2	0.833200607	-0.186052032	0.46846596	0.173444653	0.386208171	-0.55429417
Q9UHX1	Poly(U)-binding-splicing factor PUF60	0.010341495	-0.414776206	0.091550458	-0.484121551	0.017375803	-0.402167232
Q9UI15	Transgelin-3	0.068024488	-0.798142901	0.049174272	-0.434512819	0.185145045	-0.424170347
Q9UIW2	Plexin-A1	0.684524665	0.572663093	0.458462203	0.383782479	0.713577393	0.350593862
Q9UJZ1	Stomatin-like protein 2_mitochondrial	0.377141975	-0.220885866	0.80615243	0.146140565	0.12904538	1.186486744
Q9UK76	Jupiter microtubule associated homolog 1	0.562629451	1.373924614	0.338381039	0.987507818	0.296051199	-0.760042633
Q9UKA9	Polypyrimidine tract-binding protein 2	0.025226071	-0.716064362	0.648976708	-0.102908211	0.219737027	-0.502971954
Q9UKD2	mRNA turnover protein 4 homolog	0.489219255	0.200590248	0.481640716	-0.145925222	0.534612138	0.706718755
Q9UKK9	ADP-sugar pyrophosphatase	0.33471234	-0.382152318	0.343014294	-0.415666378	0.378913596	1.072155424
Q9UKL3	CASP8-associated protein 2	0.388272672	-0.263028589	0.155959183	-0.792907344	0.390418835	0.624415891
Q9UKM9	RNA-binding protein Raly	0.003598924	-0.916274067	0.017114501	-0.916082434	0.283802399	-0.285520348
Q9UKX7	Nuclear pore complex protein Nup50	0.266969728	-0.368358172	0.079312997	-0.546538796	0.593090452	0.496960803

Q9UL46	Proteasome activator complex subunit 2	0.35218824	0.378681154	0.013911147	1.033765496	0.021680795	0.708115151
Q9ULU8	Calcium-dependent secretion activator 1	0.026658086	-1.079620413	0.000163956	-1.155373662	0.32796144	-0.375172632
Q9ULV4	Coronin-1C	0.093295636	0.296814659	0.881619071	0.130572751	0.569038548	0.165911706
Q9UMS4	Pre-mRNA-processing factor 19	0.290573933	-0.335323843	0.044495744	-0.642778646	0.271200252	-0.317009907
Q9UMX0	Ubiquilin-1	0.371248956	1.181181879	0.345957329	1.722006078	0.688329525	0.091519453
Q9UN86	Ras GTPase-activating protein-binding protein 2	0.003379915	-1.46672055	0.051021792	-0.648464899	0.065387855	-1.039302248
Q9UNM6	26S proteasome non-ATPase regulatory subunit13	0.017586006	-0.437444903	0.064760601	-0.412184312	0.133841986	-0.370432467
Q9UNW9	RNA-binding protein Nova-2	0.778029962	-0.146297206	0.159807384	1.333898469	0.176574819	0.778977664
Q9UNZ2	NSFL1 cofactor p47	0.123838471	1.139810394	0.18780633	1.483373612	0.534057393	-0.575615275
Q9UPG8	Zinc finger protein PLAGL2	0.477625285	1.187756815	0.159111418	1.37819178	0.496571931	-0.498454013
Q9UQ80	Proliferation-associated protein 2G4	0.476232912	1.356763681	0.159450363	1.117760606	0.57389567	-0.293821495
Q9Y224	RNA transcription_translation and transport factor protein	0.912984225	0.043224561	0.030854627	-0.42122424	0.024799335	0.474483479
Q9Y230	RuvB-like 2	0.384346774	1.406179971	0.132345019	1.256158966	0.450769192	-0.605382455
Q9Y265	RuvB-like 1	0.618037774	-0.173757049	0.529363088	0.115463591	0.714473168	-0.026363272
Q9Y266	Nuclear migration protein nudC	0.00503163	-0.661679477	0.431361754	-0.1718336	0.430973632	-0.1837697
Q9Y277	Voltage-dependent anion-selective channel protein 3	0.33981988	-0.309031359	0.628049948	-0.141557809	0.188646029	0.38702961
Q9Y281	Cofilin-2	0.064642175	-0.728567149	0.005009261	-1.266439558	0.087193293	-0.859224658
Q9Y2B0	Protein canopy homolog 2	0.836129186	0.136869817	0.820024853	0.455233287	0.454868562	-0.163462519
Q9Y2X3	Nucleolar protein 58	0.311122412	-0.2238968	0.119628091	0.60640362	0.001866866	0.80981809
Q9Y2Z0	Protein SGT1 homolog	0.884887588	0.279375301	0.389094074	0.429393658	0.194510617	-0.377312815
Q9Y333	U6 snRNA-associated Sm-like protein LSm2	0.203927162	-0.491572199	0.293208959	-0.33482579	0.005328076	-0.759557842
Q9Y3F4	Serine-threonine kinase receptor-associated protein	0.069684081	-0.647141955	0.132890688	-0.48063405	0.197688647	-0.327907972
Q9Y3I0	tRNA-splicing ligase RtcB homolog	0.233774247	-0.704226176	0.828608575	0.028404285	0.779754767	-0.176259832
Q9Y3U8	60S ribosomal protein L36	0.844956397	0.50836041	0.024611215	-1.103667677	0.034583599	0.722964414
Q9Y426	C2 domain-containing protein 2	0.741709753	-0.68592302	0.592690573	-0.055552855	0.424494212	0.248001018

Q9Y490	Talin-1	0.893936808	0.190590973	0.804077178	-0.200073163	0.495376692	1.25458989
Q9Y4E1	WASH complex subunit 2C	0.031340997	-2.696066357	0.010918458	-4.650425704	0.074733202	-2.054343234
Q9Y4L1	Hypoxia up-regulated protein 1	0.840638496	0.225700675	0.08593797	-0.45146963	0.828372211	-0.069787393
Q9Y5B9	FACT complex subunit SPT16	0.270111879	0.648807693	0.120903966	0.424049887	0.864216287	0.144112671
Q9Y5S9	RNA-binding protein 8A	0.679900544	-0.05853837	0.548410523	0.375074096	0.950451641	0.062702035
Q9Y5T5	Ubiquitin carboxyl-terminal hydrolase 16	0.325637012	0.601889835	0.032799831	-0.339353383	0.562425187	0.12775575
Q9Y5Y2	Cytosolic Fe-S cluster assembly factor NUBP2	0.38297524	-0.506237582	0.750711392	0.531871713	0.291293943	0.628282442
Q9Y605	MORF4 family-associated protein 1	0.282441091	0.66198931	0.121886595	0.259446381	0.149628819	0.196287531
Q9Y617	Phosphoserine aminotransferase	0.655899811	-0.072779954	0.422569481	-0.176641047	0.866014841	-0.037021106
Q9Y678	Coatomer subunit gamma-1	0.88294893	-0.184297808	0.980148534	0.184627712	0.252576037	1.236782615
Q9Y696	Chloride intracellular channel protein 4	0.27028424	-0.228693439	0.761934925	-0.01263838	0.469050292	-0.141362599
Q9Y6E2	Basic leucine zipper and W2 domain-containing protein 2	0.625523201	0.406001369	0.741607611	0.015519922	0.025869217	1.479637155
Q9Y6G9	Cytoplasmic dynein 1 light intermediate chain 1	0.036148714	-0.528733244	0.123788567	-0.587872748	0.042660637	-0.735372458
Q9Y6M1	Insulin-like growth factor 2 mRNA-binding protein 2	0.41059905	0.402358914	0.109589131	-0.287430689	0.247602023	0.744393034
Q9Y6N7	Roundabout homolog 1	0.656727416	-0.068453065	0.140454833	0.554741272	0.064371203	-0.594085548

8 ANEXOS

8.1 DECLARAÇÃO DE BIOÉTICA E BIOSSEGURANÇA



COORDENADORIA DE PÓS-GRADUAÇÃO
INSTITUTO DE BIOLOGIA
Universidade Estadual de Campinas
Caixa Postal 6109. 13083-970, Campinas, SP, Brasil
Fone (19) 3521-6378. email: cpgib@unicamp.br



DECLARAÇÃO

Em observância ao **§5º do Artigo 1º da Informação CCPG-UNICAMP/001/15**, referente a Bioética e Biossegurança, declaro que o conteúdo de minha Dissertação de Mestrado, intitulada "***Perfil proteômico de células progenitoras neurais e neuroesferas infectadas com cepas de Zika vírus e Dengue vírus***", desenvolvida no Programa de Pós-Graduação em Biologia Funcional e Molecular do Instituto de Biologia da Unicamp, não versa sobre pesquisa envolvendo seres humanos, animais ou temas afetos a Biossegurança.

Assinatura: Danielle Gouveia Junqueira
Nome do(a) aluno(a): Danielle Gouvêa Junqueira

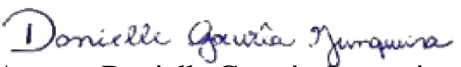
Assinatura: _____
Nome do(a) orientador(a): Daniel Martins de Souza

Data: 05/06/2021

8.2 DECLARAÇÃO DE DIREITOS AUTORAIS

As cópias de artigos de minha autoria ou de minha co-autoria, já publicados ou submetidos para publicação em revistas científicas ou anais de congressos sujeitos a arbitragem, que constam na minha dissertação de mestrado intitulada “**Perfil proteômico de células progenitoras neurais e neuroesferas infectadas com cepas de Zika vírus e Dengue vírus**”, não infringem os dispositivos da lei nº 9.610/98, nem o direito autoral de qualquer editora.

Campinas, 05 de junho de 2021


Danielle Gouvêa Junqueira
Autora: Danielle Gouvêa Junqueira

RG: 50.875.944-4 – SSP/SP


Orientador: Daniel Martins de Souza
RG: 32.431.379-2 – SSP/SP